FORSCHUNGSZENTRUM JÜLICH GmbH

KFA

Projektträger Biologie, Energie, Ökologie (BEO)
International Energy Agency IEA

Implementing Agreement for a Programme of Research and Development on Wind Energy Conversion Systems – Annex XI

25th Meeting of Experts – Increased Loads in Wind Power Stations, "Wind Farms"

Gothenburg, May 3-4, 1993

Organized by:
Project Management for Biology, Energy, Ecology (BEO)
Research Centre Jülich (KFA)

On behalf of the
Federal Ministry of Research and Technology,
The Fluid Mechanics Department
of the Technical University of Denmark

Scientific Coordination:
M. Pedersen (Techn. Univ. of Denmark)
R. Windheim (BEO-KFA Jülich)

Implementing Agreement for a Programme of Research and Development on Wind Energy Conversion Systems – Annex XI

25th Meeting of Experts – Increased Loads in Wind Power Stations, "Wind Farms"

Gothenburg, May 3-4, 1993

Organized by:
Project Management for Biology, Energy, Ecology (BEO)
Research Centre Jülich (KFA)

On behalf of the
Federal Ministry of Research and Technology,
The Fluid Mechanics Department
of the Technical University of Denmark

Scientific Coordination:
M. Pedersen (Techn. Univ. of Denmark)
R. Windheim (BEO-KFA Jülich)

CONTENTS

INTRODUCTORY NOTE - IEA EXPERT MEETING ON:

INCREASED LOADS IN WIND POWER STATIONS

"WIND FARMS"

Gothenburg, Sweden 3-4 may 1993

S. E. Thor

INTRODUCTION

Harnessing the wind for utility bulk power production often requires that wind turbines are located in clusters (usually called wind farms), primarily due to land shortage. Operation of wind turbines in clusters shows that the loading situation is different from operation of a single turbine in the free wind. A number of authors have reported increased loads in the WECS when the turbine is operating in a wake of another turbine, [1], [2], [3], [4] and [5].

The increased loading on the turbines is a result of a different wind situation in the wake of another turbine. Increased turbulence and wind speed deficit are factors influencing the loading situation. The operation in a partial wake is also resulting in increased loads.

It has for example been reported [2] that the turbulence intensity of the wind increases by a factor of 3 at a point 5 diameters downstream of a turbine. It was also seen that the vertical wind shear was decreased at wake operation.

Measurements on three bladed rigid hub turbines, [4], have shown that increased turbulence intensity in the ambient flow increases the loadcycling (flap bending moment) on a single turbine. However, increased turbulence intensity in the ambient flow will, in some cases, decrease the loads for a turbine operating in the wake of another turbine. This is contrary to what is experienced for the single turbine. The maximum load cycles occur when a turbine operates partly in the wake of another turbine. During one turbine revolution the blades will experience undisturbed air flow outside the wake as well as decelerated air flow inside the wake. The high loads are not caused by the increased turbulence intensity inside the wake but by the deterministic velocity deficit in the flow.

Measurements clearly indicate that there is a change in the wind situation behind a turbine. The cluster wind situation gives higher loads in different parts of the downstream turbine.

One important question is, how will turbines with different design concepts (rigid, teeter, flap, pitch-, stall-, yaw controlled....) experience the flow conditions prevailing in a wind farm.

ANALYSIS OF LOAD SITUATIONS IN WIND FARMS

There seems to be no unified way of designing/analysing wind turbines for operation in wind farms. Informal information seems to indicate that some people tries to adjust the turbulence intensity in order to account for these effects. But usually wind farm operation is not accounted for when designing turbines. The effect of wakes is supposed to be covered by the safety factors.

The latter approach will probably not be sufficient when building larger machines. Efficient designs are becoming more crucial. Better and validated methods to analyse these effects are required.

Some limited calculations of loads in wind farms have been published. The approach till now have been directed towards verifying special situations. Analytical tools are available for such analysis in the time domain. A unified approach to the total load situation is required to obtain a cost-effective design. This approach probably has to include both operational statistics as well as characteristics of the wind at different types of operation.

NORMS AND STANDARDS

Presently there is a number of norms and standards which applies to the design of wind turbine systems. Guide lines for designing wind turbines operating in a farm are very rare. If there is any recommendation they generally state that wind farm operation has to be accounted for, but no rules are given of how to analyse the effect.

Some rules recommend the addition of a specific fatigue damage to account for the wake operation. This method is considered to be too coarse for this purpose. It also violates the background theory for calculating fatigue damage in materials.

The measurements mentioned above clearly indicate that the designer has to account for cluster operation. Is it a realistic requirement to have guidelines in standards presently?

RECOMMENDED TOPICS FOR THE EXPERT MEETING

I suggest to have presentations/discussions on the following topics at the expert meeting:

- The necessity to account for increased loads in the design
- Better guidelines that account for loads in wind farms
- Wind farm layout to minimise loads
- Concept: how to minimise loads by using relevant design solutions
- Computational methods, tools and philosophy
- Meteorological description of wakes, relevant for wind turbine design
- Presentation of new measurements, preferably on comparisons on flexible and rigid turbines

REFERENCES

1 Vølund, P.
Loads on a horizontal axis wind turbine operating in wake.
EWEC, October 14-18 1991

2 Schepers, J.G., Bulder B.H.
Load prediction and fatigue evaluation of the WPS-30 wind turbine
European Wind Energy Association Special Topic Conf '92
The Potentials of Wind Farms. 8-11 September 1992.

3 Thomsen, K., Petersen S.M., Lading P., Sangill, O.
Analysis of loads on wind turbines in complex terrain wind farms.
European Wind Energy Association Special Topic Conf '92
The Potentials of Wind Farms. 8-11 September 1992.

4 Dahlberg, J.Å., Poppen M., Thor, S.E.
Wind farm load spectra based on measurements.
European Wind Energy Association Special Topic Conf '92
The Potentials of Wind Farms. 8-11 September 1992.

5 Christensen, C. J., Courtney, M.S., Højstrup, J.
Turbulence and turbine dynamics in a wind farm.
European Wind Energy Association Special Topic Conf '92
The Potentials of Wind Farms. 8-11 September 1992.

INFLOW CHARACTERISTICS ASSOCIATED WITH HIGH-BLADE-LOADING EVENTS IN A WIND FARM

N.D. Kelley
Wind Technology Division
National Renewable Energy Laboratory
Golden, Colorado U.S.A.

Introduction

The stochastic characteristics of the turbulent inflow have been shown to be of major significance in the accumulation of fatigue in wind turbines. Because most of the wind turbine installations in the United States have taken place in multi-turbine or wind farm configurations, the fatigue damage associated with the higher turbulence levels within such arrangements must be taken into account when making estimates of component service lifetimes. The simultaneous monitoring of two adjacent wind turbines over a wide range of turbulent inflow conditions has given us more confidence in describing the structural load distributions that can be expected in such an environment.

The adjacent testing of the two turbines allowed us to postulate that observed similarities in the response dynamics and load distributions could be considered "quasi-universal," while the dissimilarities could be considered to result from the differing design of the rotors. The format has also allowed us to begin to define appropriate statistical load distribution models for many of the critical components in which fatigue is a major driver of the design. In addition to the adjacent turbine measurements, we also briefly discuss load distributions measured on a teetered-hub turbine.

Approach

Two adjacent Micon 65/13 turbines, installed in a very large wind farm in San Gorgonio Pass, California, were used for the measurements. These rigid-hub turbines were identical except for the rotor blades. The rotor of one turbine consisted of blades based on the NREL (SERI) thin-airfoil family, and the other had refurbished, original-equipment AeroStar blades. Each turbine was extensively instrumented. A wide range of turbine dynamics was rainflow counted. A total of 67.5 hours of operational data over a wide range of inflow conditions is available for analysis from the two Micons. Figure 1 summarizes the distributions of the mean wind speed, wind-speed standard deviation, turbulence intensity, and time of day for the 405, 10-minute records available. A total of 70.1 hours of similar data is available for limited comparison from the prototype NPS100 turbine that incorporated a two-bladed, teetered rotor.

Statistical Load Distribution Models

Our analysis has shown that all of the alternating (range or peak-to-peak) load distributions, can be described using a *mixture of three statistical models*. While the first and second models in the mixture

appear to be well defined by the Gaussian and lognormal distributions, respectively, the third appears to be a function of the turbine dynamic being described. Figure 2 schematically describes the linear summation of the individual model distributions. The p-p root flapwise bending moment distribution is pictured in Figure 3 with each of the contributions to the mixture highlighted. We hypothesize that the three-distribution mixture is a direct result of a similar mixture describing the cyclic content of the wind. The cyclic distributions of the hub-elevation horizontal and vertical wind speeds are plotted in Figure 4. We believe that the infrequent or low-cycle, high-amplitude loads seen by the wind turbines are a consequence of the non-Gaussian characteristics of the turbulent inflow. These are indicated by the shaded areas of Figure 4.

Comparisons of Turbine Dynamic Load Distributions

We present graphic comparisons of the mixed process, cyclic load distributions associated with several turbine dynamics measured on each of the machines under test. Figure 5 plots the summary of observed range or p-p cycles of the root flapwise and edgewise bending moments for the three blades on each turbine. While the flapwise loads are nearly identical, the edgewise loads reflect the greater mass of the AeroStar blades. The low-speed shaft bending and torque distributions are displayed in Figure 6. Again, while the bending distributions are the same, the greater weight of the AeroStar blades appears to be responsible for the higher loading cycles in the high- and mid-frequency cycle range. Figure 7 plots the distributions associated with axial and inplane components of the thrust vector. The NREL rotor exhibits slightly higher low-cycle range axial loads while the AeroStar-equipped rotor displays the same for the inplane component. We believe that the former is a result of a greater swept area and the greater mass of the latter. The identical yaw drive torque distributions are plotted in Figure 8. These results suggest that, when variations in inertia and swept areas are considered, the underlying statistical distributions are identical for both turbines. Also, the striking similarity between the mid- and low-frequency range gust distributions of Figure 4 and the turbine dynamic distributions of Figures 5 through 8 suggests that the latter are the result of the former.

Cycle Counting of Rigid- and Teetered-Hub Turbines

Recently, we compared the sample populations of cyclic load distributions of the flap and edgewise root bending moments from the two rigid-hub Micons and the teetered NPS100 prototype. It was fortunate that the size and weight of the rotor blades for these turbines were similar. A total of 67.5 hours of data in 10-minute records is available for the Micons, and 70.1 hours in 11-minute records is available for the NPS100. The Micon records were rainflow counted individually and as a single record. This process confirmed that, for the flapwise loads, the important low-cycle, high-amplitude range above 15 kNm can be described by an *exponential distribution*. While further work is needed for confirmation, the edgewise loads appear to be more appropriately fitted by an *extreme value distribution* (Type I). Figure 9 plots the flapwise load distributions for the Micons and the NPS100. A decaying exponential has been fitted to each above 15 kNm. This diagram suggests that the teetered hub provides load relief over the rigid hub in the mid-frequency cycle range. It also indicates that little, if any, relief is gained from the most damaging infrequent or low-cycle, high-amplitude excursions.

This leads us to hypothesize an overall model for the statistical load structure as a result of turbulence excitation on wind turbines. Figure 10 schematically describes this hypothesis. We suggest that the overall statistical distribution is a summation of at least four component processes. These components include a high-cycle, low-amplitude Gaussian distribution; what we believe to be a *transition* lognormal distribution; a parameter-dependent low-cycle, high-amplitude distribution; and some form of a *rare* event distribution. The last two are of the most concern. We believe that the low-cycle, high-load range

(about once per operating hour to one in 10,000 hours) results from encountering *coherent turbulent structures* in the turbine inflow and is responsible for a major portion of component fatigue damage. The rare event distribution is primarily related to matters of turbine survivability as a result of violent atmospheric phenomena such as hurricanes, tornadoes, etc., that may occur during the machine's lifetime.

Coherent turbulence load excitation

We analyzed the 405, 10-minute records available from the two Micons and identified the peak loading events [both positive (tension) and negative (compression) peaks], which, when paired, formed the 25 largest and most damaging fatigue cycles. We found the following:

- *All of the tension peaks associated with the largest stress cycles occurred during slightly stable flows emerging from a deep canyon southwest of the wind park.*
- *The most common time of occurrence was 22 h local standard time.*
- *The negative (compression) peaks of these cycles occurred during* ***slightly more stable*** *conditions centered near 04 h.*

The previous year, we made extensive turbulence measurements up- and downwind of the large wind farm in the San Gorgonio, California, wind farm in which the Micons were located. These measurements indicated that a minimum of at least *three distinct flow regimes* are present in the turbine inflows. The regimes appear to be the result of circulations derived from the surrrounding complex terrain features, transient induced shears resulting from nonlinear atmospheric phenomena such as waves, and (within the wind farm) decaying wakes from upstream turbines. The characteristic times for each are 300, 10, and 1 seconds, respectively. We used the data collected to develop empirical models of three component velocity spectra, spatial coherence, and local cross-axis correlations. As an example, Figure 11 compares the 12 m/s spectra of the crosswind (v) component for unstable, near-neutral, and stable flow conditions up- and downwind of the wind farm and over homogeneous or smooth terrain.

In Figure 12, we present an example of the NREL-equipped rotor meeting a coherent turbulent structure. This encounter produced the largest positive (tension) flapwise moment seen in the Micon 65 data set on this turbine. From the figure, one can see the interaction of each blade with the structure over about a 2-second period. The plots show that Blade No. 3 receives the largest transient tension load while, at the same time, the other two are undergoing compression. This suggests that the entire rotor was concurrently involved. The associated hub-elevation, estimated vorticity/helicity time series has been aligned with the peak on Blade No.3 and is plotted in Figure 13. It also covers a period of about 2 seconds, suggesting a strong correlation of the two events.

Conclusions

There is significant evidence that the largest loads in the low-cycle frequency range are produced by the rotor interacting with a coherent turbulent structure. These interactions produced a coherent (phase specific) response in the turbine's rotor and other components as a result of the simultaneous excitement of multiple structural modes. The period of these excursions (at least in the root flapwise bending

moment) is much less than the period of one rotor revolution. The most damaging tension peaks occur during atmospheric conditions likely to support wave motions and extended wakes.

Acknowledgement

This work has been supported by the U.S. Department of Energy under contract DE-AC02-83CH10093.

References

Kelley, N.D., "Full Vector (3-D) Inflow Simulation in Natural and Wind Farm Environments Using an Expanded Version of the SNLWIND (Veers) Turbulence Code," NREL TP-442-5225, National Renewable Energy Laboratory, November 1992.

Olesen, H.R., S.E. Larsen, and J. Højstrup, "Modeling Velocity Spectra in the Lower Part of the Planetary Boundary Layer," *Boundary-Layer Meteorology*, Vol. 29, 1984.

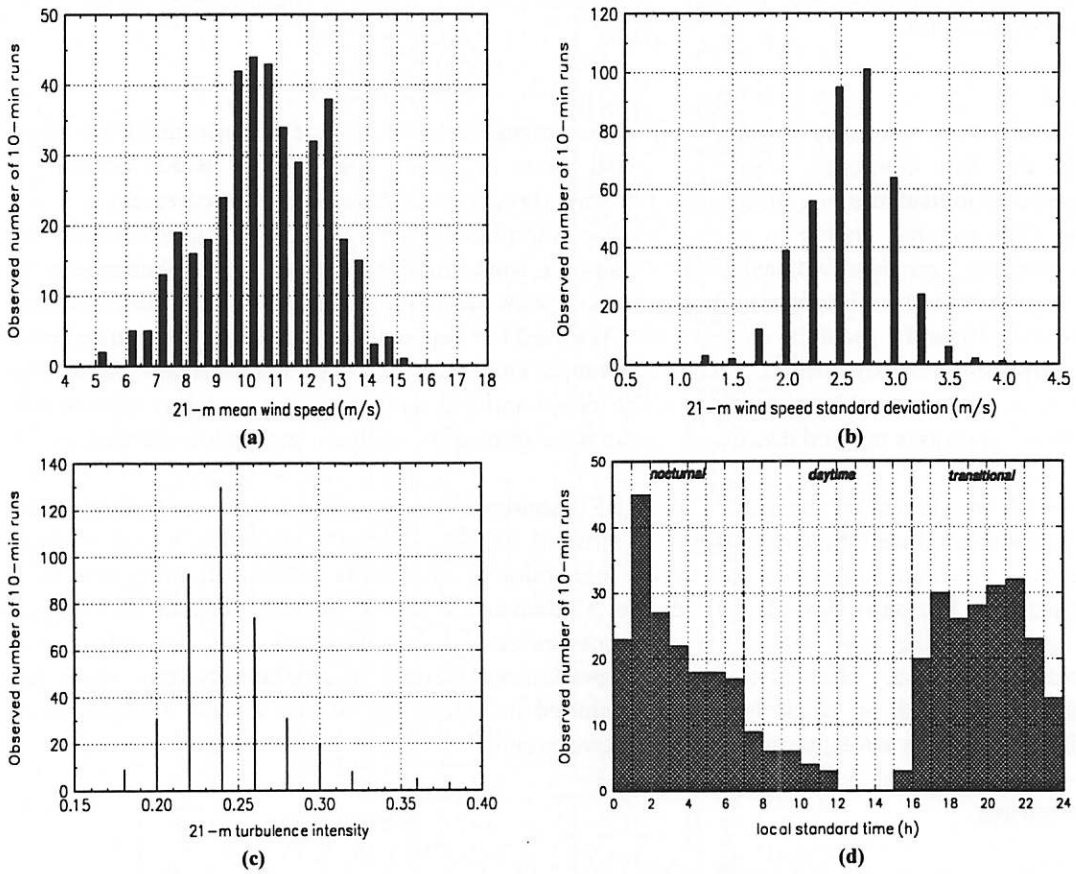

Figure 1. Histogram summaries at 21m: (a) mean wind speed, (b) wind-speed standard deviation, (c) turbulence intensity, and (d) time of day for the 405 data records used in the Micon 65 study

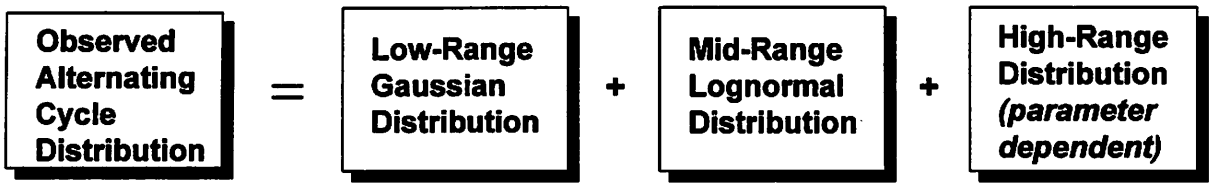

Figure 2. Suggested components of a mixed distribution model to explain observed alternating loads

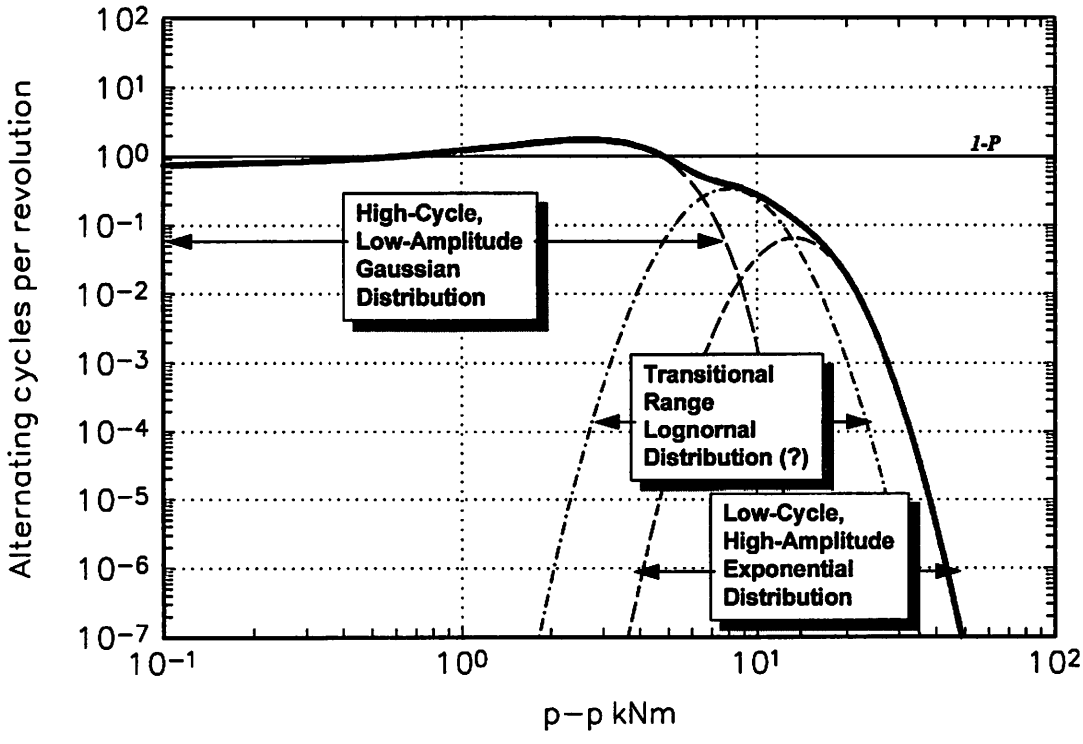

Figure 3. An example of the the mixed distribution model for the p-p root flapwise bending

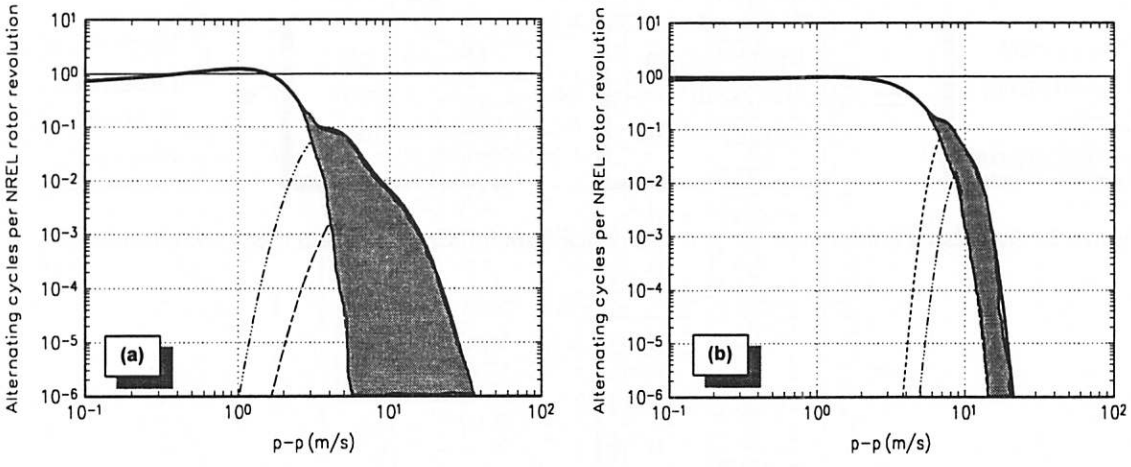

Figure 4. Observed wind speed component alternating cycle distributions: (a) horizontal wind speed (b) vertical wind speed

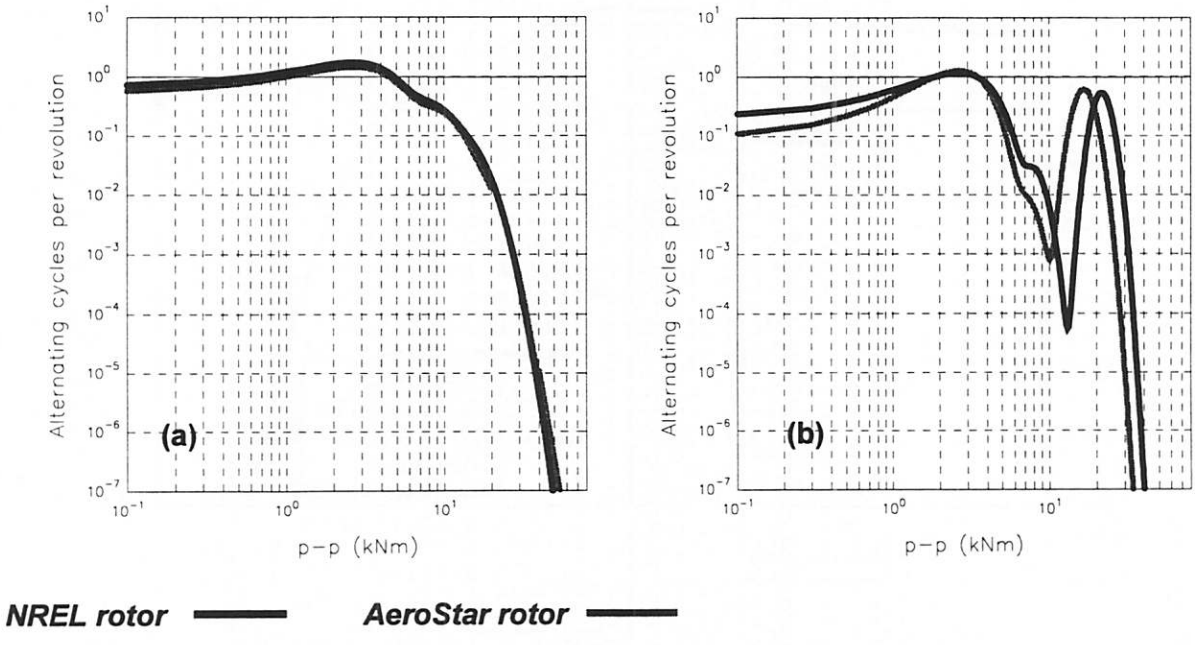

Figure 5. Three-blade flapwise (a) and edgewise (b) root bending alternating cycle distributions

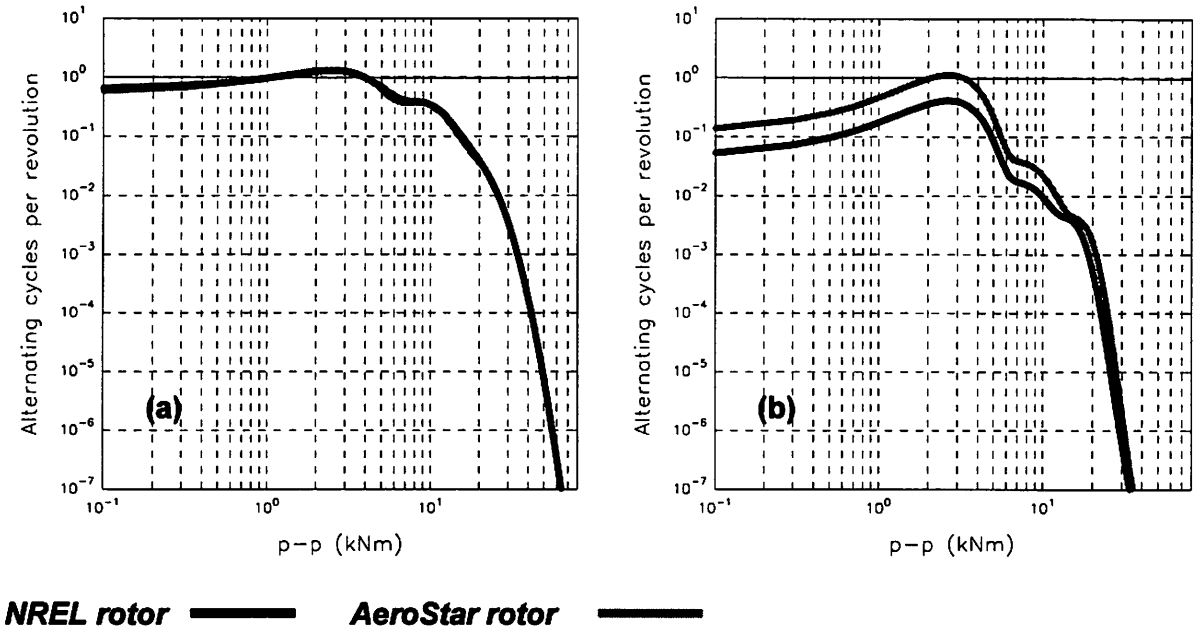

Figure 6. Low-speed shaft bending (a) and torque (b) cyclic distributions

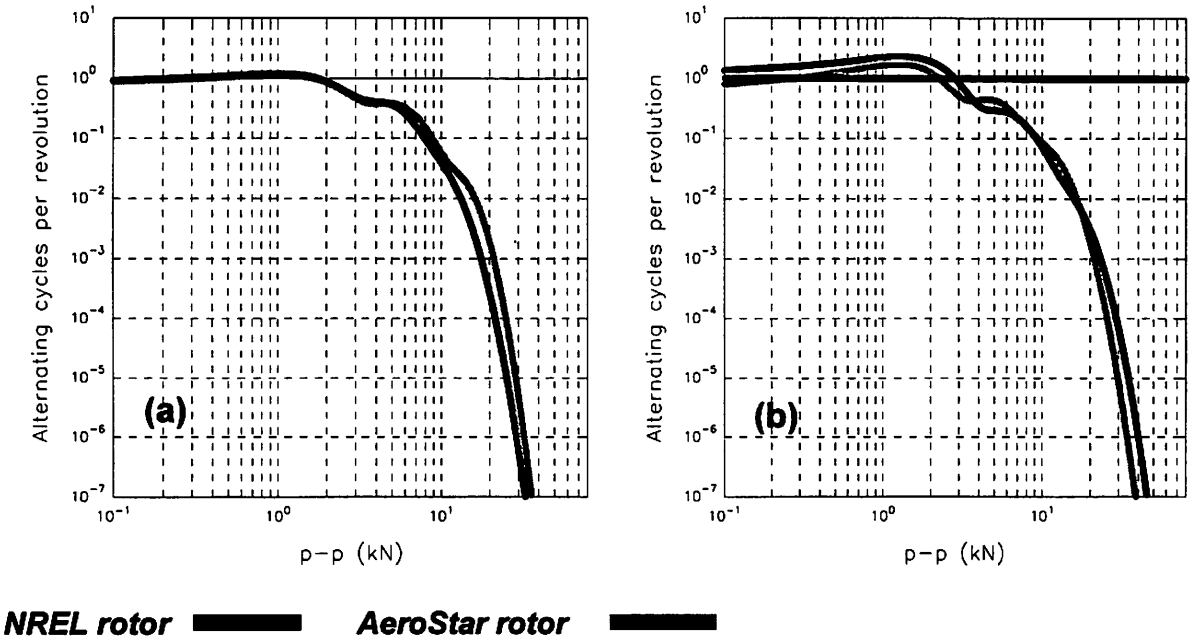

Figure 7. Axial (a) and inplane (b) thrust component cyclic distributions

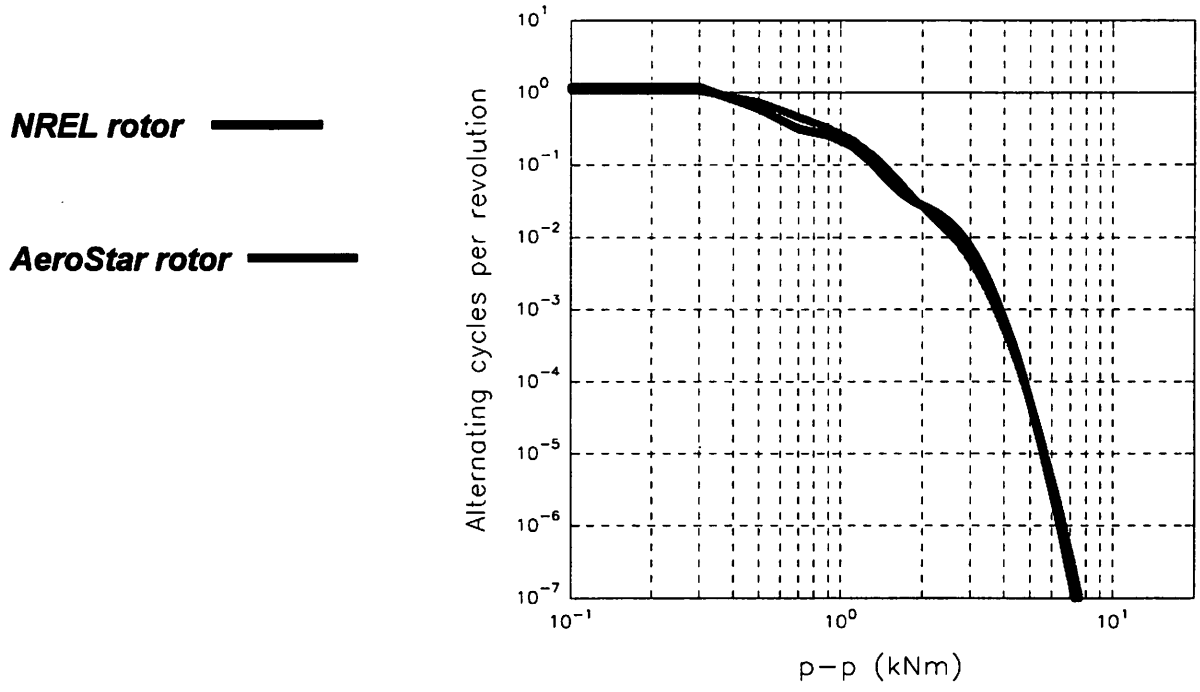

Figure 8. Yaw drive torque cyclic distributions

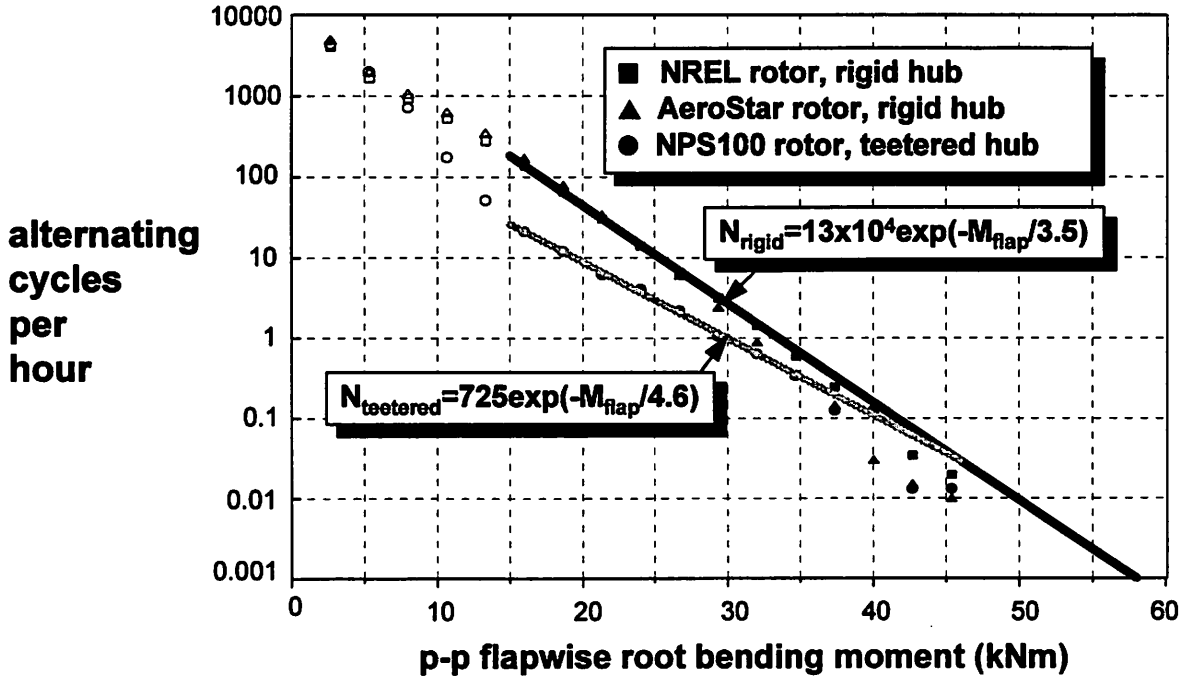

Figure 9. Comparison of rigid- versus teetered-hub low-cycle alternating flapwise loads

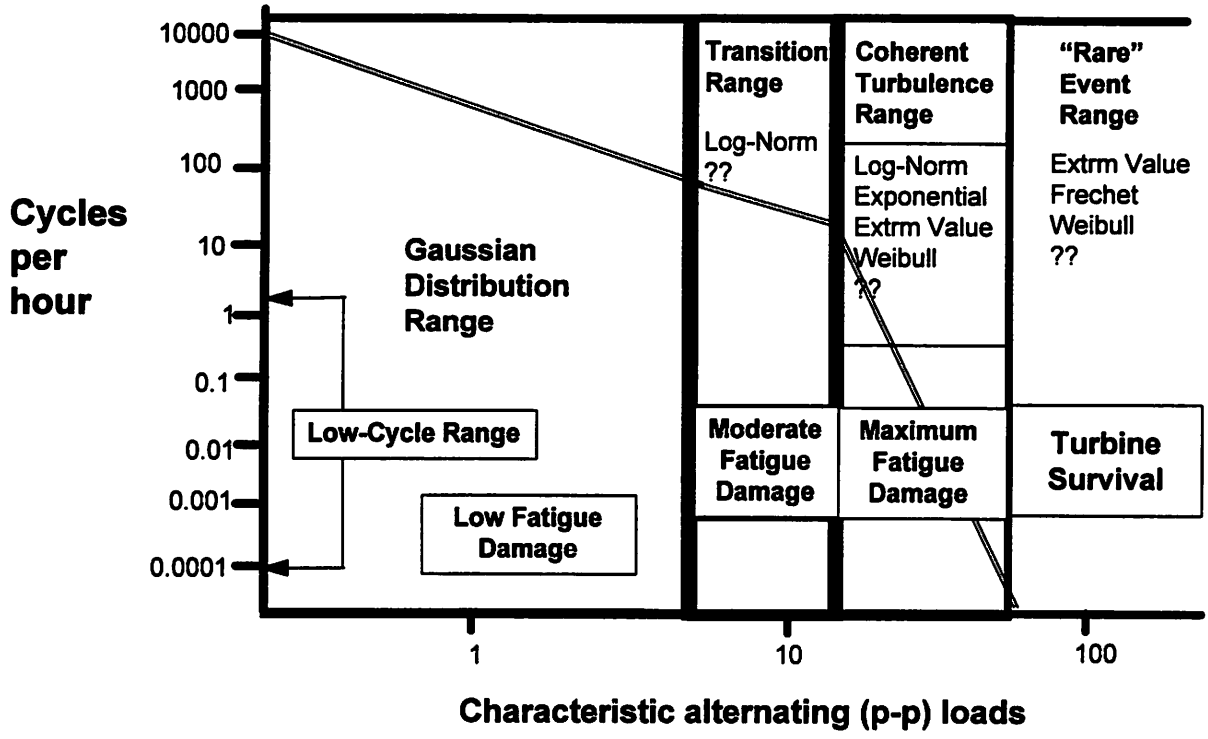

Figure 10. Hypothesized turbulence-loading statistical structure

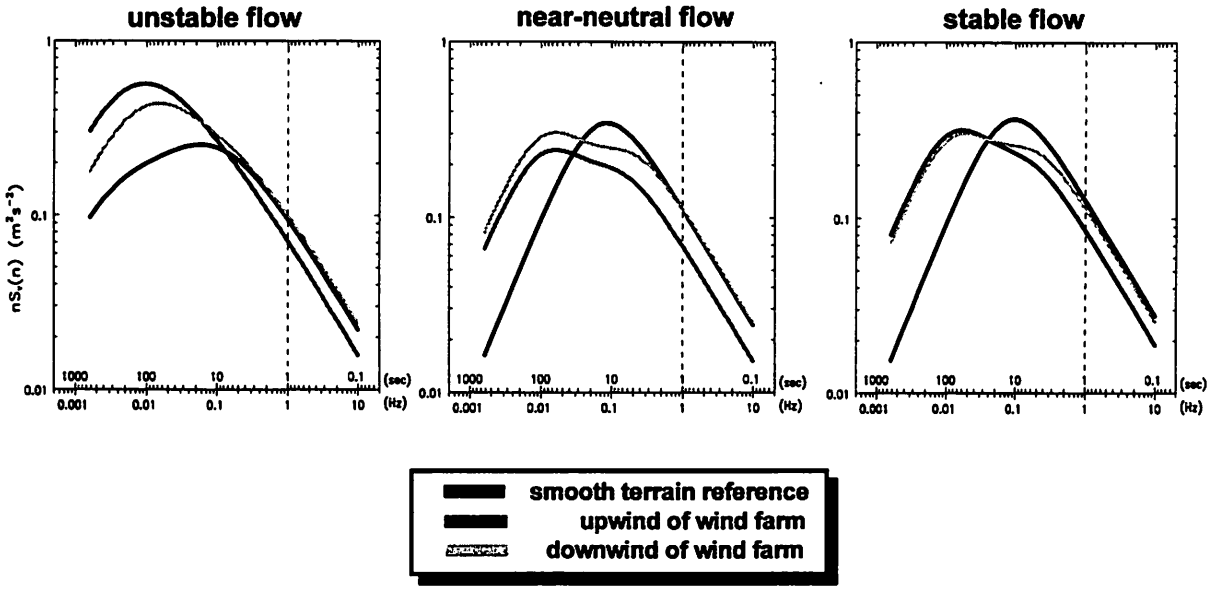

Figure 11. Comparison of predicted crosswind (v) velocity spectra for 12 m/s mean wind speed

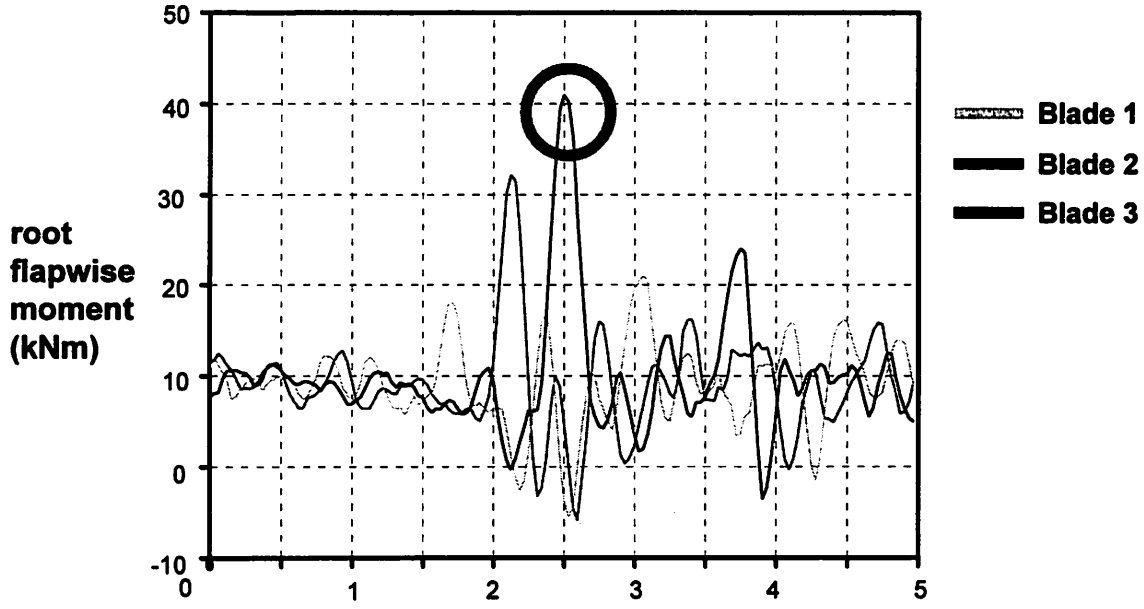

Figure 12. Largest positive (tension) peak stress cycle observed for the NREL rotor

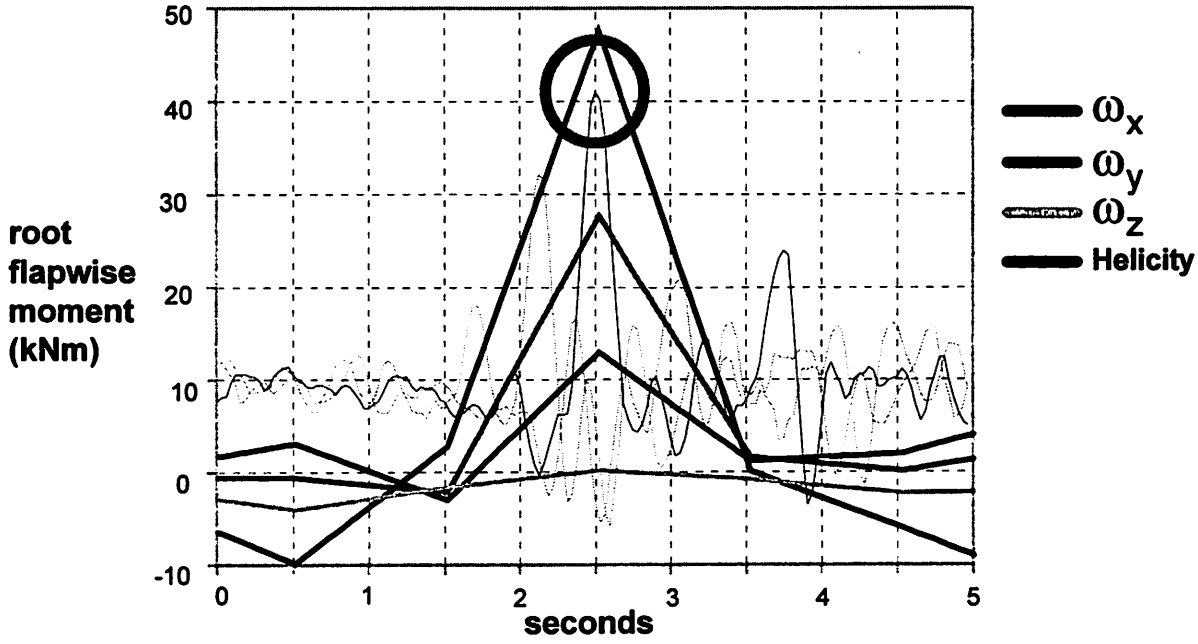

Figure 13. Hub-height vorticity/helicity estimates aligned with peak flapwise moment

Loads on Wind Turbines in Complex Terrain Wind Farms

Kenneth Thomsen
The Test Station for Wind Turbines
Risø National Laboratory

Danish wind turbines are often installed outside of Denmark where the wind energy potential is found in connection with terrain-induced concentration effects in complicated or even mountainous terrain. Examples are California, India or Southern Europe. Whereas the wind potential in terms of average wind speeds routinely is investigated prior to wind turbine projects, the short-term behaviour or the load-generating characteristics of the wind under such terrain conditions are less well-known.

Two Danwin 23 machines that were installed in the Alta Mesa wind farm site in San Gorgonio near Palm Springs were instrumented and tested as part of a previous measurement project. The Danwin machine is well known from a comprehensive test programme which was carried out at The Test station for Wind Turbines at Risø National Laboratory in Denmark. The site in San Gorgonio has primarily been chosen because the general operational experience with wind farm operation in California shows that the wind load conditions in this area are among the most severe.

Only few data are available from sites in severely complicated terrain which can be used to investigate the dynamic load-generating mechanisms such as turbulence, horizontal and vertical wind shear, changes in the wind direction or possibly wake effects from other machines. Data that illustrates the wind loading under these conditions are scarce, and the new dataset with simultaneous measurements of the wind in-flow and the wind turbine response carried out in connection with this project will significantly improve the rational basis for the design of wind turbines.

Thus, this analysis has the objective to quantify the wind inflow conditions and corresponding dynamic loads for wind turbines, which have been installed in wind farms in severely complicated terrain. The analysis are to some extend based on the full amount of collected data, but to identify and investigate the different load-generating mechanisms and corresponding response in detail some of the collected data series have been selected for further analysis. In the analysis, data series have been selected at two wind speeds, below and above rated wind speed respectively.

The first part of the presentation concentrate on the wind and turbulence characteristics. The different load generating mechanisms are separated and analyzed. The second part of the presentation is concentrated on the response of the turbine. The relative importance of the deterministic and the stochastic part of the loads are investigated and the fatigue loads are analyzed.

Wind and turbulence characteristics

The analysis of the short-term wind climate has the aim to clarify the differences between the wind inflow to the turbine at the edge of the wind farm and inside the wind farm. Furthermore the characteristics of the wind inflow are compared to the wind inflow to a turbine in a homogeneous terrain. These objectives are satisfied by identifying and separating the different load-generating mechanisms and then afterwards investigating the influence of these mechanisms to the structural response of the turbines. The wind climate is investigated in this chapter and the parameters in focus are: the wind shear, vertical wind speeds, the changes in wind direction and final, the characteristics

of the three-dimensional turbulence.

The analysis of the wind and turbulence characteristics is performed in two ways. First all the collected data are analyzed for high statistical precision and afterwards selected measurement from both turbines are analyzed in detail. For the detailed investigation measurements are selected at two wind speeds; above and below rated wind speed respectively. Due to different measurement periods for the two turbines there is a lack of high wind speed data for the turbine inside the wind farm, E33.

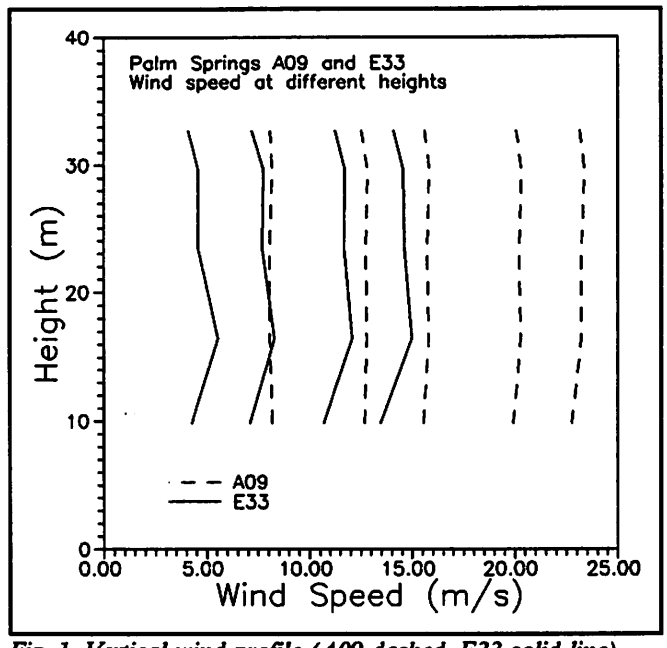

Fig. 1. Vertical wind profile (A09 dashed, E33 solid line)

From Fig. 1 it is obvious that the traditional used logarithmic wind profile do not fit the measured wind profiles very well. In both cases the observed wind profile upstream each wind turbine is seen to be constant, although there is a tendency of a minor difference in the two lowest stations inside the wind farm (E33). Since this particular meteorology mast is observing the turbulence created by the turbines in front of it in combination with the natural turbulence the wind profile is expected to diminish. Concerning the turbine in the front row no dependency of height is observed in the almost constant wind profile. This is the combined effects of wind shear and speed-up phenomenon from the terrain slope in front of the wind mast. The slope of the terrain causes acceleration of the flow, which diminishes the usual wind shear. The wind profiles are very different from what is measured in wind farms in homogeneous terrain.

The vertical component of the wind speed (w-component) were measured by sonic anemometers and data from the height 32.7 m are analyzed here. The data are represented as 10 minute averages and in Fig. 2 the vertical wind speeds at the edge of the farm and inside the wind farm are compared. The vertical wind speeds are illustrated as function of the 23 m horizontal cup anemometer wind speed.

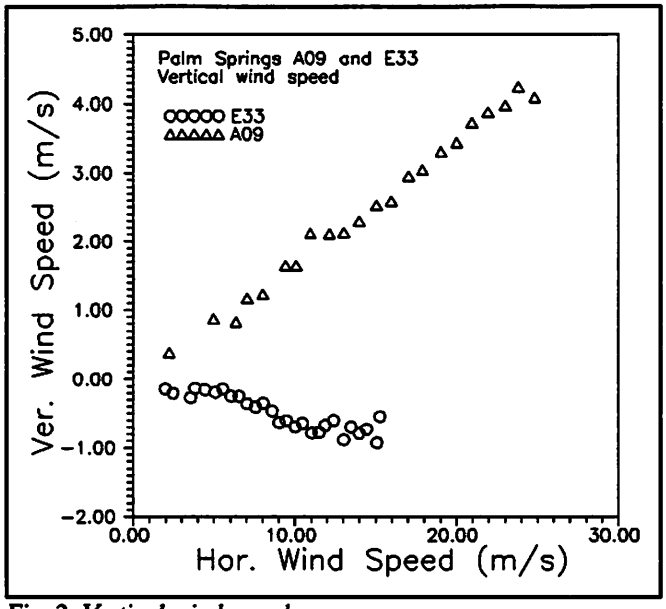

Fig. 2. Vertical wind speeds.

From Fig. 3 a clear difference in standard deviation of the wind direction is observed. At the edge of the wind farm (A09) the standard deviation is almost independent of the horizontal wind speed at 23 m and has values in the range of 5° to 15°. Inside the wind farm the standard deviation is strongly increased to values of 10° to 30°. This is due to the turbines in front of the E33 turbine which contributes heavily to an increased level of turbulence.

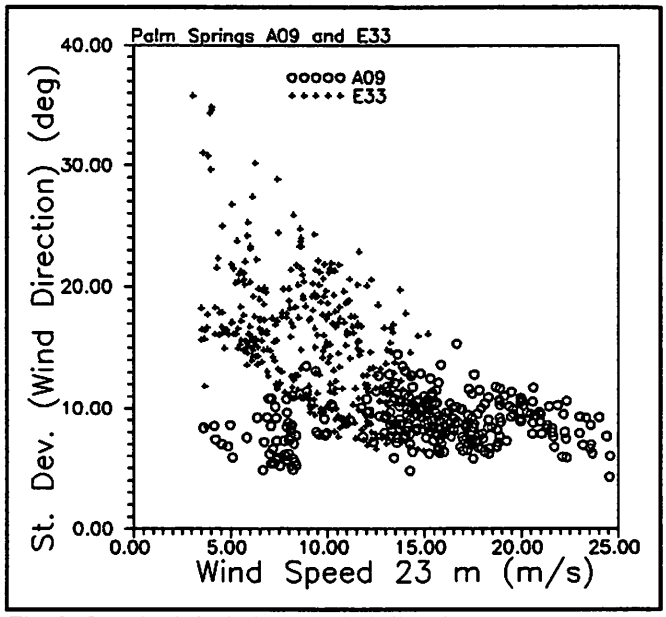

Fig. 3. Standard deviation of wind direction.

To some extent the different effects treated so far influence the wind turbine loadings in a deterministical way. The only mentioned parameter that has a stochastical influence on the loadings

are the wind direction changes in the previous paragraph. In this paragraph a full stochastical load-generating effect will be treated, namely the wind turbulence. From several previously investigations the conclusion have been that the most important wind inflow parameter causing fatigue loads to turbines are the longitudinal turbulence component (u component). This has been the conclusion from analysis of measurements from stand alone wind turbines in homogeneous terrain and from measurements from wind farms in homogeneous terrain. In this project the phenomenon to some extent are mixed together since the turbines are placed in a wind farm in a inhomogeneous and very complex terrain. Due to this the characteristics of the wind turbulence is expected to be very different from the characteristics in homogeneous terrain and especially the longitudinal component of the turbulence is investigated in detail. The transverse and vertical velocity components will be analyzed for a few of the measurements.

To illustrate the variation of the basic descriptor of the turbulence, the turbulence intensity (I_u = σ_u/U), the hub height (23 m) wind speeds at the two meteorology masts are averaged in 10 minute periods and the intensities are calculated. In Fig. 4 the results are illustrated as function of the mean hub height wind speed. It should be noted that the wind speed treated here are the cup anemometer wind speed, i.e. the vector sum of the longitudinal and the transverse components (u and v components).

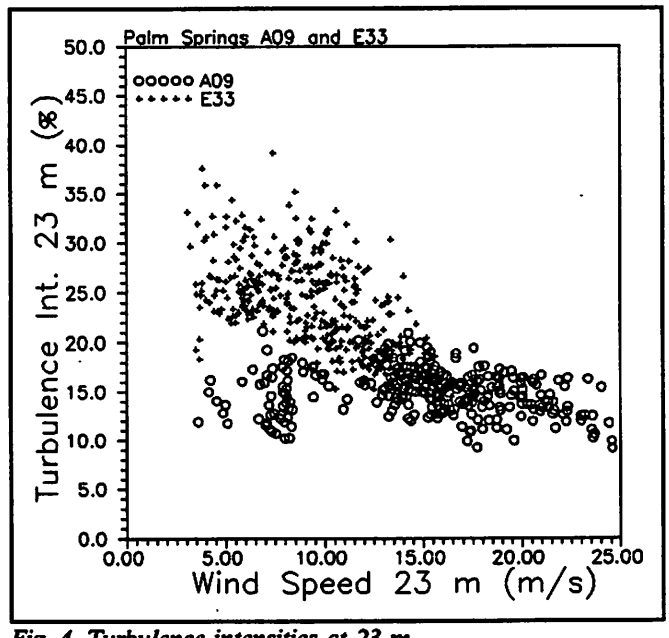

Fig. 4. Turbulence intensities at 23 m.

Based on a comparison between the measured wind turbulence spectra and the theoretical Kaimal expression the length scale of the turbulence in the selected time series is calculated. Although the method is not stringent in a meteorological way it reveals the possibility to quantify the spectra from the two sites relative to each other.

In Fig. 5 an example of two measured spectra is shown. The time series are with a mean wind speed of approximately 15 m/s and turbulence intensities of approximately 15 %. The fitted theoretical spectra are also shown in the figure and this is fitted to the measurements in the frequency range 0.1 - 0.7 Hz.

The tendency seen is very typical for all the analyzed time series. A large difference in length scale

estimate between the two sites is observed, at the edge of the wind farm the length scale is approximately 800 m while it decreases to a value of approximately 300 m inside the wind farm. Typical values of length scales in homogeneous terrain in Denmark are 600-800 m but since these values could depend of the method of which they are calculated care should be taken in a comparison.

The horizontal turbulence eddies seems to be compressed to a radical lower extension when they pass the first row of wind turbines. This is seen for all the selected time series and a minor dependency of the mean wind speed is also observed. In Table 1 the average of the calculated turbulence length scale is listed.

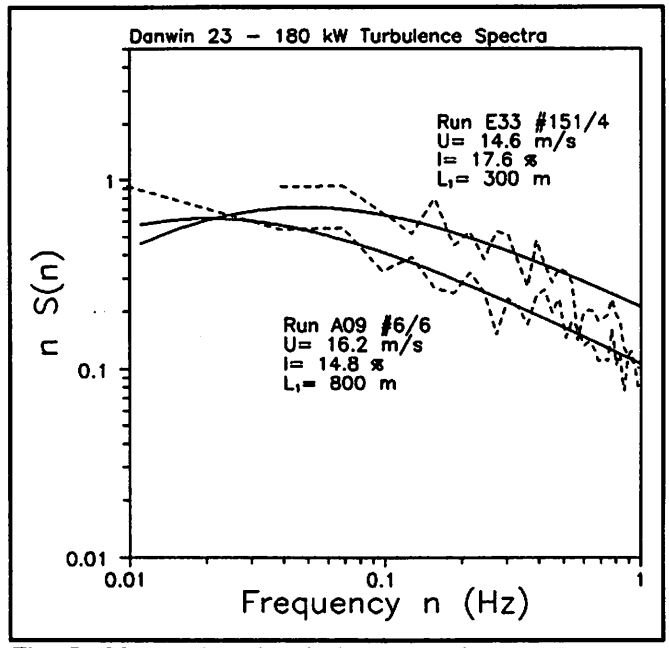

Fig. 5. Measured and calculated turbulence spectra, cup anemometer.

Table 1. Calculated length scales inside and outside the wind farm.

	wind speed	Length scale
At the edge of the wind farm A09 site	8.1 m/s	533 m
	16.3 m/s	690 m
Inside the wind farm E33 site	8.4 m/s	217 m
	14.7 m/s	320 m

The inflow to the two selected turbine are analyzed and the different load-generating mechanisms are separated into deterministic and stochastic parts.

One characteristic phenomenon observed at the site is that the vertical wind profiles differs significantly from the traditional logarithmic wind profile. In both cases an almost constant mean wind speed is observed across the rotor plane. A clear correlation between the topography and the vertical

mean wind speeds is seen, with resulting wind speed aligned respectively 9° and slightly negative relative to a horizontal plane.

The stochastic wind inflow is analyzed partially as standard deviations of wind speed and direction and partially in a spectral form. The variations in wind direction and turbulence intensity observed inside the wind farm is typical at a level of a factor of two relative to what is observed at the edge of the wind farm, and concerning the turbulence intensity no significantly variation with height above ground is observed. The cup anemometer measurements are compared to theoretical Kaimal wind spectra and using the spectral length scale as a fitting parameter a difference of a factor of two is observed between the two sites. At the edge of the wind farm a noteworthy amount of energy is found in the transverse and vertical wind speed components. Inside the wind farm these two components are profound reduced compared to the longitudinal component.

Fatigue load response.

In order to quantify the structural response in a proper way with regard to a design process it is necessary to establish a measure for the fatigue damage. This is performed by using the Rainflow counting method for all the collected data. The Rainflow counting results in a load spectrum with information of a number of cycles in a certain load range. The information is this load spectrum is afterwards characterized by a single quantity, the equivalent load. Based on the equivalent loads at different operational conditions it is possible to create a life time load spectrum which is used in the design process.

In Fig. 6 the Rainflow Counting spectra are converted to equivalent loads, based on a fixed number of cycles. This means that R_{eq} is a direct expression for the fatigue damage.

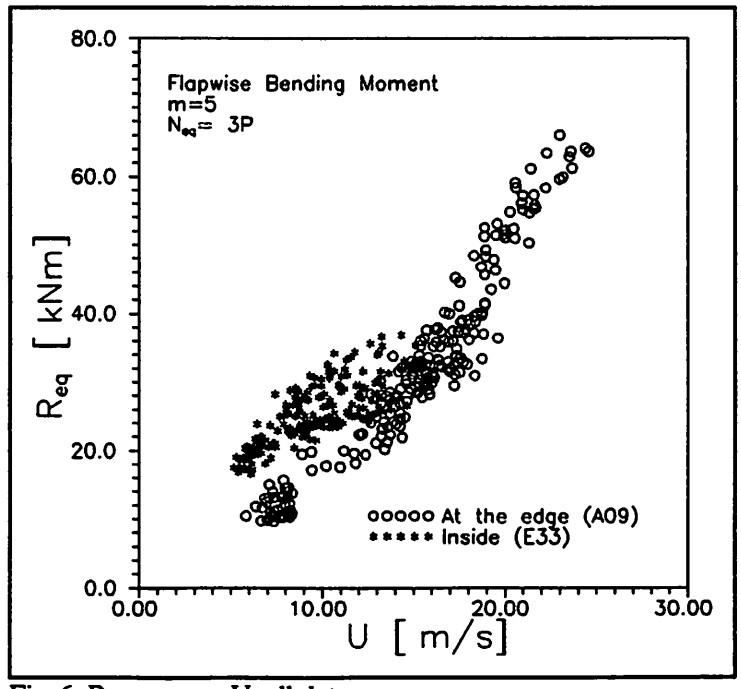

Fig. 6. $R_{eq,fl}$ versus U, all data.

Due to different turbulence intensities and yaw errors a large amount of scatter exist in the overall statistics of the equivalent loads versus wind speed. For the flapwise blade moment the equivalent loads from the turbine inside the wind farm are seen to be significantly higher than the loads experienced by the turbine at the front row of the wind farm. This is naturally due to the turbulence created by the wind farm.

Another way of representing the data is to select a small range of wind speeds and see how the fatigue loads changes with turbulence intensity. Representing the turbulence intensity by the wind speed standard deviation the relation is illustrated in Fig. 7 for the flapwise blade bending moment.

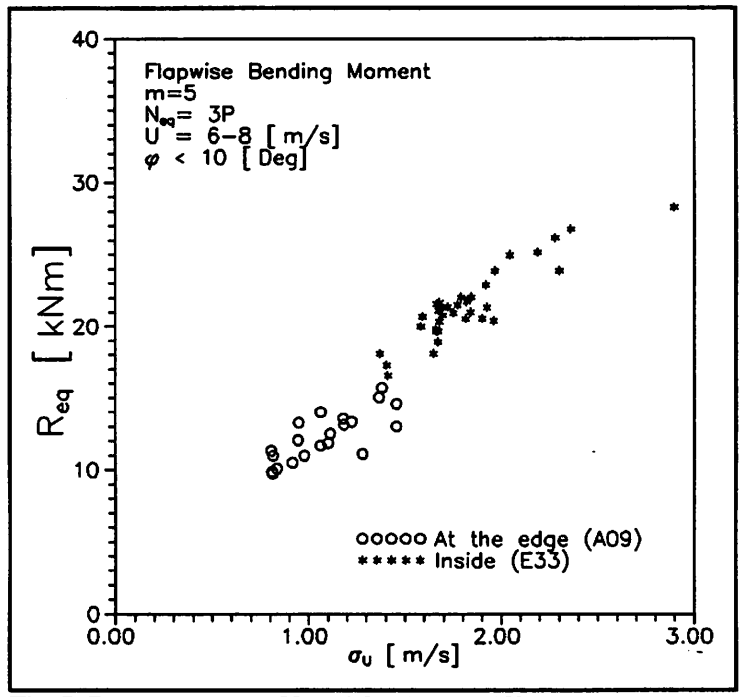

Fig. 7. $R_{eq,fl}$ versus σ_U, U = 6-8 m/s, $\phi < 10°$.

The sensitivity to turbulence is seen to be highly dependent on mean wind speed, and again no significant differences between the two turbines are observed. Due to the narrow ranges of operational conditions of the selected data only relatively few data are shown. In spite of this it seems convincing that the equivalent fatigue load ranges depends primarily on the mean wind speed and the turbulence intensity.

The life time fatigue loads can be evaluated as a load spectrum by collecting the individual counted spectra at each operational condition, and to place these in an overall range reference. It has the advantage that the result consists of a spectrum with detailed information of the distribution of load cycles. Furthermore it is possible to calculate a life time fatigue load represented by a single number from the fatigue load spectrum. This provides the possibility to make an overall comparison with e.g. design codes.

To obtain information on the distribution of the ranges, life time load spectra are constructed by combining the measured countings at each wind speed. At a given wind speed the counted spectra are averaged and weighted according to a prescribed wind speed distribution.

To see how the differences in loads influences the life time fatigue loads, 20 years load spectra are calculated for the two turbines. Due to the difference in wind speeds during the two measurements periods only data up to 16 m/s are used in this first comparison. Minimum wind speed is selected to 5 m/s and only data with yaw errors less than 15° are used. The wind speed distribution is selected as a Weibull distribution with scale parameter 7.47 [m/s] and shape parameter 1.9. Based on the averaged Rainflow Countings, 20 year life time load spectra are calculated, Fig. 8 and 9. In the figures a life time equivalent load based on 10^7 cycles are listed.

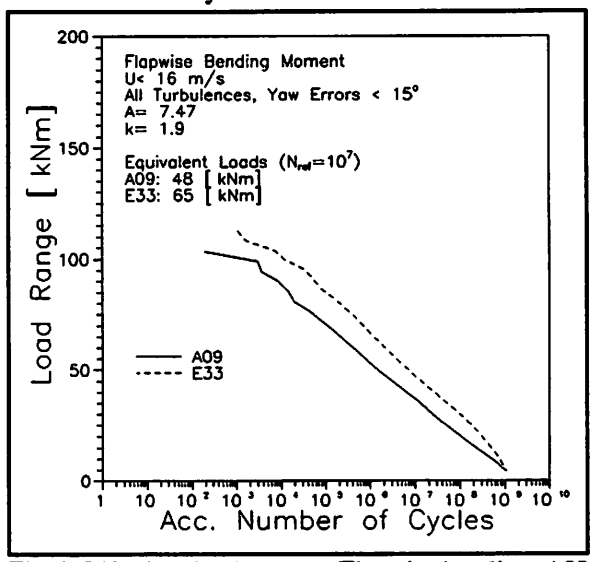

Fig. 8. Life time load spectra. Flapwise bending, A09 and E33. U<16 m/s.

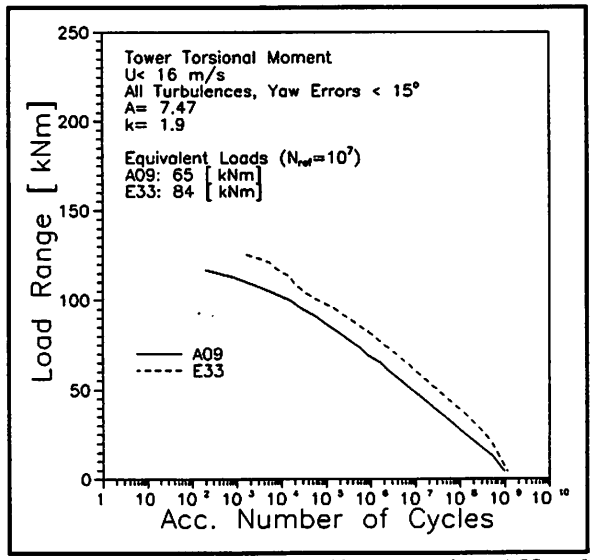

Fig. 9. Life time load spectra. Tower torsion, A09 and E33. U<16 m/s.

Figs. 8 and 9 represent a direct comparison of the life time equivalent loads on the two turbines with the restriction that only wind speeds below 16 m/s are used.

The major part of the fatigue analysis is based on the equivalent load approach, which characterize a Rainflow counting spectrum at a given operational condition by two numbers; the equivalent load range referred to an equivalent number of load cycles. By selecting the equivalent number of load cycles as constant the relative fatigue damage observed by a given component is described by the equivalent load range only. The equivalent load ranges are observed to depend highly on the turbulence intensity, the yaw error and the mean wind speed. This influence the comparison of loads observed by the wind turbine inside the wind farm and at the edge of the wind farm in a way that makes a direct comparison difficult concerning the full operational wind speed range. A comparison is carried out for wind speeds up to 16 m/s for all turbulence intensities. The differences in total life time fatigue load spectrum of the two turbines are believed to be solely dependent on the differences in turbulence intensities. This conclusion is supported by the investigation based on equivalent moments, and it means that differences in vertical wind speeds, longitudinal component length scale and wind shear all are to be dealt with as secondary effects compared to the longitudinal component turbulence intensity.

References

Reports

Rasmussen, F. et al. Investigations of Aerodynamics, Structural Dynamics and Fatigue on Danwin 180 kW. Risø-M-2727. Risø National Laboratory 1988.

Pedersen, T.F., S.M. Petersen, K. Thomsen, P.H. Madsen, J. Højstrup. Loads for Wind Turbines in Inhomogeneous Terrain Measurement Report, Risø-M-2922, Risø National Laboratory, July 1991

Thomsen, K., S. M. Petersen, O. Sangill, P. Lading. Analysis of Loads for Wind Turbines in Inhomogeneous Terrain. To be published (Sept.-Oct. 93).

Papers

Petersen, S.M, K. Thomsen, P. Lading. Measurements of Wind Conditions and Loads on a Wind turbine in Inhomogeneous and Complex Terrain. Paper presented at the ASME conference, Houston 1992.

Madsen, P.H. Wind Loads in Complex Terrain. Wind Power in Icing Conditions, Finland 1992.

Thomsen, K., S. M. Petersen, O. Sangill, P. Lading. Analysis of loads on Wind turbines in complex terrain wind farms. Proc. EWEA 1992, Herning, Denmark, September 1992, paper D2.

ON TURBULENCE AND LOAD IN WIND FARMS; MEASUREMENTS IN NØRREKÆR ENGE II

Sten Frandsen
Risø National Laboratory
DK-4000 Roskilde, Denmark

ABSTRACT. A key question concerning wind farms is of cource whether effectively the special flow conditions cause increased and/or more frequent loads inside wind farms. A fair number of experiments have been carried out, providing several different conclusions on the subject. The experiments cover most terrain conditions: flat and homogeneous terrain, complex terrain and studies of narrowly spaced single and double row clusters of wind turbines. In this paper measurements from the Nørrekær Enge II wind farm are presented. Also, an attemp is made to compare the recorded data with a model of the "global" flow inside a large cluster of wind turbines.

BACKGROUND

The flow environment of the interior of a wind farm is in any given point effected by both the individual wakes of the neighbouring machines, and the global flow generated by the air's passage through the "forrest" of wind turbines. To determine the significance of the individual wakes relative to the global flow with respect to wind speed reduction and dynamic loads on the wind turbines is an unsettled question. However, experience tend to indicate that for distancies downsteam of a wind turbine larger than 6-8D the contours of the wake have become little distinct. For smaller downstream distancies the wake shape is more intact, but since also the wind speed deficit increases sharply the machine separations in larger wind turbine arrays - at least in Denmark - is rarely less than 5D.

In fairly flat homogeneous terrain boundary layer similarity theory tells that in neutral atmospheric stratefication the change of wind speed (u) with height (z) is logaritmic:

$$\frac{u}{u_*} = \frac{1}{\kappa} \ln\left(\frac{z}{z_o}\right)$$

where u_* is the socalled friction velocity and κ the von Karman contant (measured to be 0.4). With neutrally stratefication is meant that the air temperature variation with height is such that mixing of air is only generated mechanically. Under these circumstances the shear stress ($\tau_* = \rho u_*^2$) in the flow is constrant though the boundary layer zone and so is the turbulence level, which by measurements have been evaluated to be

$$\sigma_u \approx 2.5 u_* = \frac{u}{\ln(z/z_o)}$$

In [1] the presense of the wind turbines is modelled by assuming that the impact of the turbines on the flow is a discrete-layer, horizontally evenly distributed shear stress at hub height (h):

$$t = \rho c_t u_h^2$$

where u_h is the wind speed at hub height, and the term c_t is the average drag from the wind turbines per m^2 occupied land:

$$c_t = \pi C_T / (8 s^2)$$

where C_T is the wind turbine drag coefficient and s is the average number of rotor diameters separation. And finally, assuming the vertical wind profile logaritmic over and under the shear jump at hub height and continuity of the profile also at hubheight, the apparent roughness of the layer over hub height can be determined:

$$z_{o,outer} = h \cdot \exp\left[-\frac{\kappa}{\sqrt{c_t + \left(\frac{\kappa}{\ln(h/z_o)} \right)^2}} \right]$$

It is seen that if the drag from the wind turbines, c_t, is small then $z_{o,outer}$ approaches z_o.

This simple model (for further details see ref. [1] or [2]) provides and estimate of the reduction of mean wind speed at hub height (illustrated in fig. 2 and 3), and the increase in turbulence above hub height (see fig. 4) and a corresponding decrease below hub height. The decrease in turbulence below hub may be disputed (single, multible wake models), but data from Nørrekær Enge II indicate that the turbulence level (in absolute terms) is more or less unchanged relative to free-flow conditions.

In order to seek verification for the above global wind farm model, the present presentation probes the load levels inside the wind farm simply by comparing power output characteristics of the two instrumented machines. Power output is used because it is easier and more reliable and because it is assumed that an important structural load such as flapwise bending of the blades - which is actually measured - over a range of wind speeds is propotional to power. So for an preliminary evaluation of *changes* in dynamic loading we assume that standard deviations of power and flapwise bending moment are proportional:

$$\sigma_{flap} \sim \sigma_{power}$$

If this relation holds - at least for wind speed below stall - the ratio $(\sigma_{p,A1}/\sigma_{p,F6})$ as a function of wind direction (wd) should give some indication of the change of load from a free stream

location to a position "in the middle of a wind farm".

THE TEST SITE

Figure 1 shows the layout of the wind farm. The machines are numbered A1 through F7, with the instrumented machines being A1 and F6. Meteorological towers, 58m of height, are placed close to these two machines.

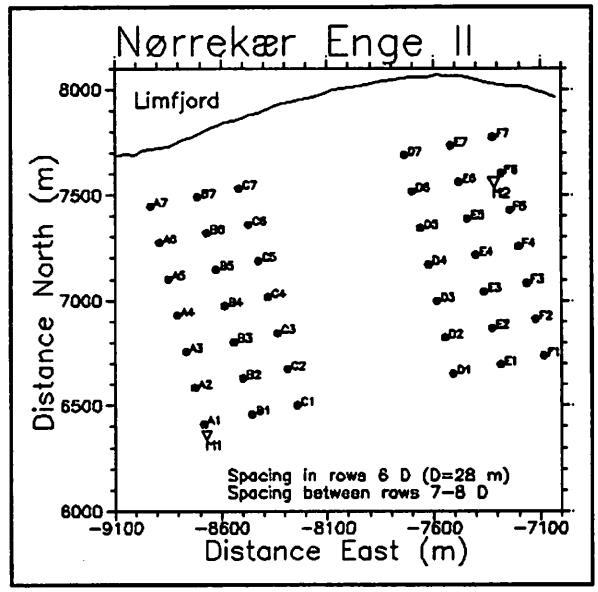

Figure 1 *Layout of the Nørrekær Enge II. East-West spacing between the machines is 8D, South-North 6D. The precise orientation of South-North rows is 166.9° and East-West 78.5°.*

Figure 5 shows the ratio of 30 min. mean power from the two instrumented machines for wind speeds between 10 and 12 m/s. As expected, F6 produces more power in northerly to easterly wds (0-90 deg), while for wds between 180 and 270 deg A1 produces the most. The sectors 180 to 300 deg. are best covered with data.

Figures 6-9 show various ratios of wind speeds. Fig. 10 shows ratio of standard deviation of power of the two turbines A1 and F6 and ratio of relative standard diviation of the same quantity. It is seen that the variation in the ratio of relative standard deviations is much larger than the direct ratio, indicating that looking separate at a wind turbine inside a wind farm the dynamic loading *seems* to have increased, but in reality it is unchanged compared to the machine placed in the free flow field.

Conclusion: There are certain indications already that data support the global wind farm flow model presented in [1]. As for turbulence the model points toward unchanged standard deviation of wind speed.

Fig. 2. Wind profiles inside and outside a wind farm according to model , [1].

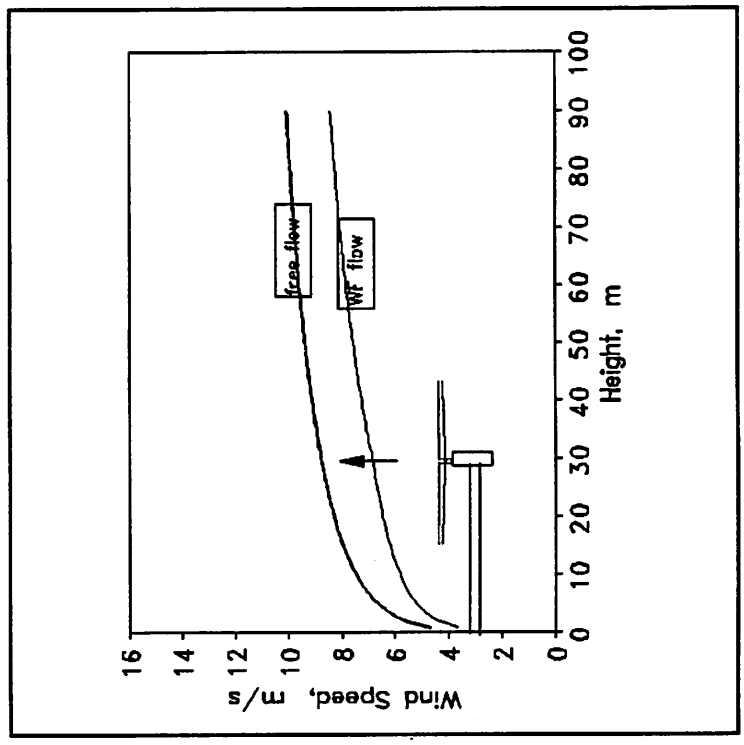

Fig. 3. Apparent surfase roughness and wind speed reduction at hub height as a function of wt separation (h=D=30m, C_T=0.5).

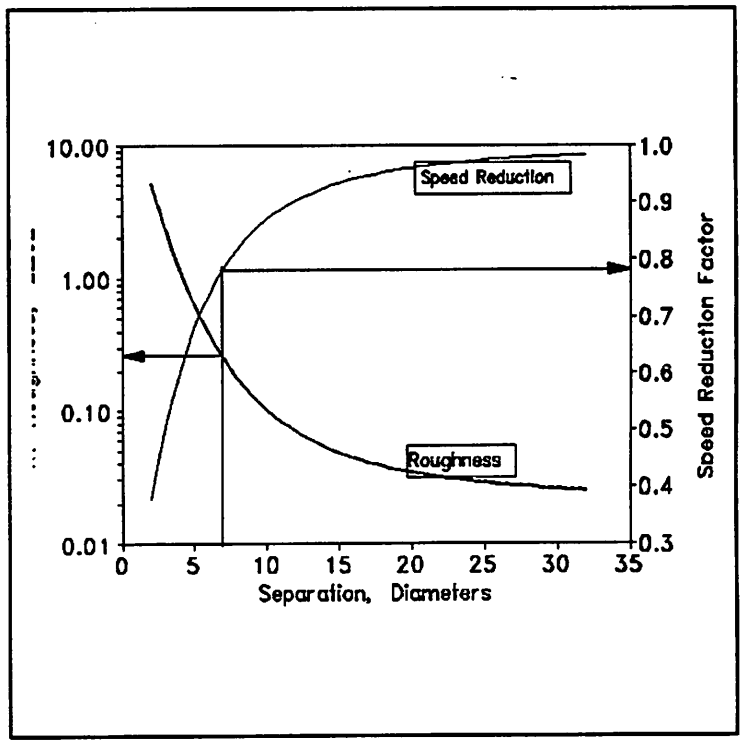

Fig. 4. Increased turbulence above the wind farm as a function of wt separation.

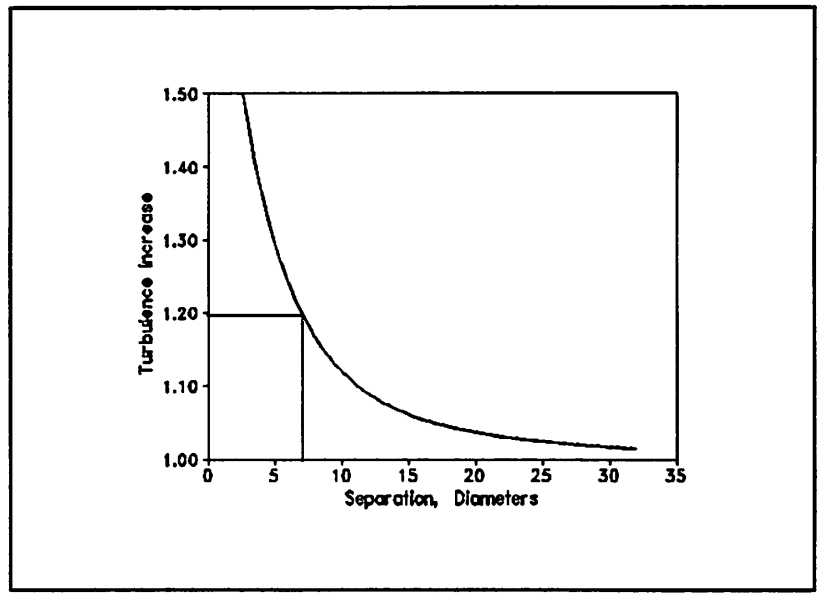

Figure No. 5. *8-10 m/s; Ratio between power output from WT F6 and A1 and number of scan in each wind direction bin.*

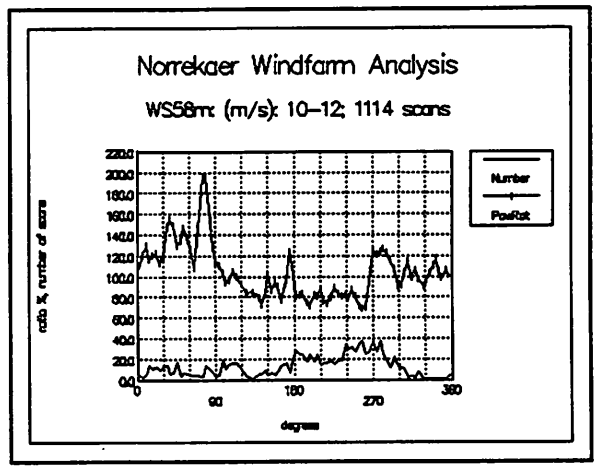

Figure 6. *Ratios of wind speeds and turbulence (σ_u) measured at 58m in the meteorological masts.*

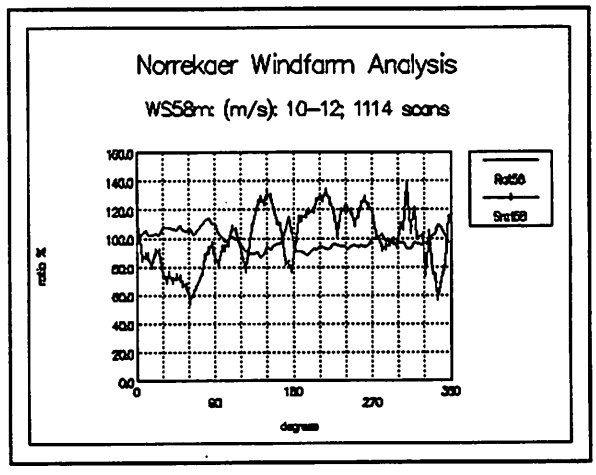

Figure No. 7. *8-10 m/s; Ratio of RMS ($\sigma_{p,F6}/\sigma_{p,A1}$) and relative RMS ($(P_{A1}\sigma_{p,F6})/(P_{F6}\sigma_{p,A1})$) of power from machines F6 and A1.*

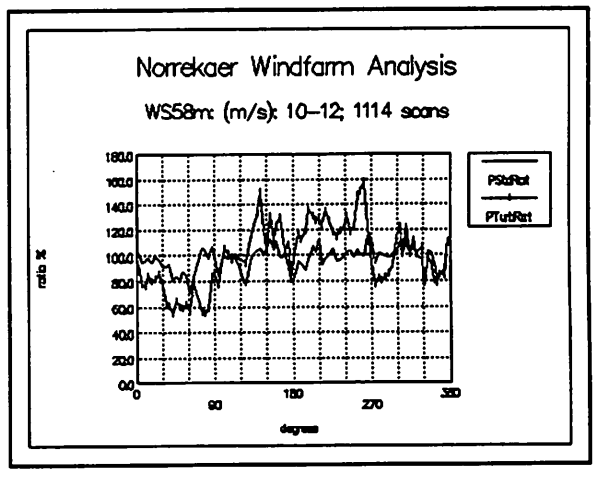

Figure 8. *As figure 2, but for wind speeds between 8 and 10 m/s.*

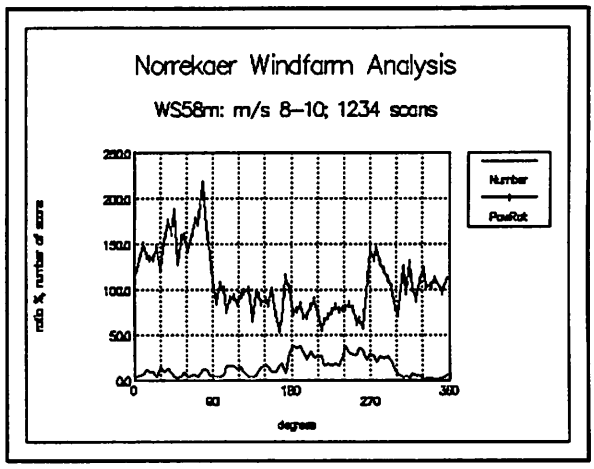

Figure 9. *As figure 3, but for wind speeds between 8 and 10 m/s.*

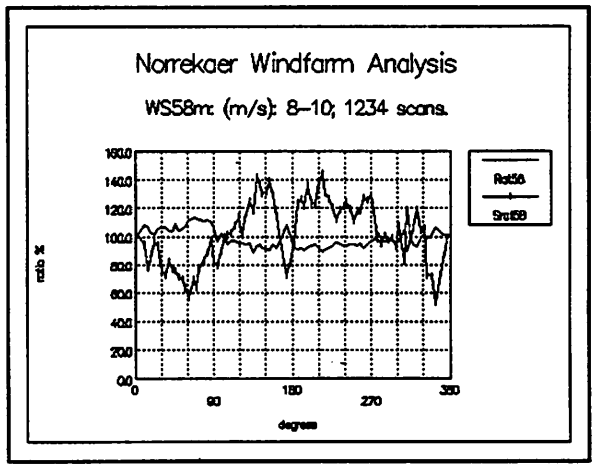

Figure 10. *As figure 4, but for wind speeds between 8 and 10 m/s.*

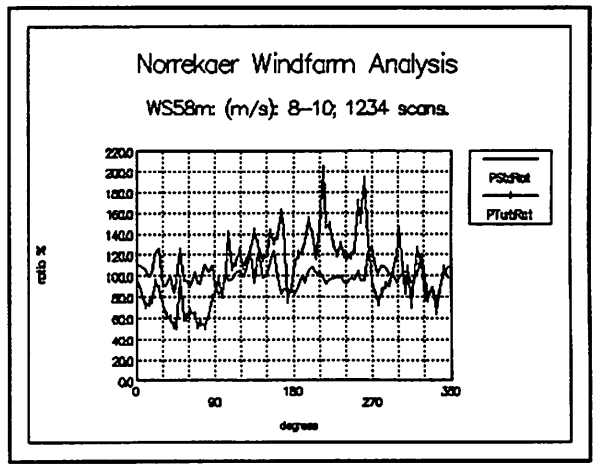

REFERENCES:

[1] Frandsen, S., *On the Wind Speed Reduction in the Center of Large Clusters of Wind Turbines*; Jour. of Wind Engineering and Industrial Aerodynamics, 39 (1992) 251-265

[2] Emeis, S. and Sten Frandsen, *Reduction of horizontal wind speed in a boundary layer with obstacles*, Jour. of Boundary Layer Meteorology 64, 297-305, 1993.

Continuous Measurements of the Sexbierum Experimental Wind Farm

B.H. Bulder
Netherlands Energy Research Foundation ECN
Unit Renewable Energy
P.O. Box 1, 1755 ZG Petten

May 1993

1 INTRODUCTION

A joint research project was set up in The Netherlands between KEMA (project management and measurements), ECN (load calculations and analyses) and TNO (supply of wind data), to investigate the influence of upstream wind turbines on the loads on a wind turbine.
The experimental wind farm "Sexbierum" in the north of The Netherlands has been used as the project wind farm. Sexbierum consists of 18 HOLEC WPS–30 wind turbines. This wind turbine (rated power 300 kW) is designed in the beginning of the 1980's and has a variable speed, full span pitch power control. The hub height is 35 m and the upwind rotor has a diameter of 30 m with steel blades.

The wind farm has a relatively simple layout of 3 * 6 wind turbines with a variable spacing and is surrounded by flat simple terrain, see figure 1. The prevailing wind direction at Sexbierum is south westerly. See table 2 with wind speed and wind rose distribution. Turbine 36 is extensively instrumented with strain gauges and other measuring devices.

The project concerns mainly the analyses of loads and the influences of the wake situation on the loads. Part of the results has been reported in [1]. The array losses in the wind farm are not analysed.

The project is strongly related to the CEC JOULE–I project 'Dynamic Loads in Wind Farms' coordinated by Garrad and Hassan (UK) [2].

The wake influences are categorized in 6 wind speed classes and 4 wake classes, see table 1. This gives 24 different wake and wind speed bins.

The blade load are measured at two radial positions. For the continuous measurements only the blade root loads at 3.5 m are recorded. The shaft torque is measured at the slow shaft.

2 MEASUREMENTS

The following continuous measurements are discussed in this presentation.

- For 69 different wind directions and 6 wind speed classes the azimuthal (60 azimuth positions) binned value, the standard deviation, mean and the minimum and maximum value of the flatwise bending moment are stored. The 69 different wind directions have an in-

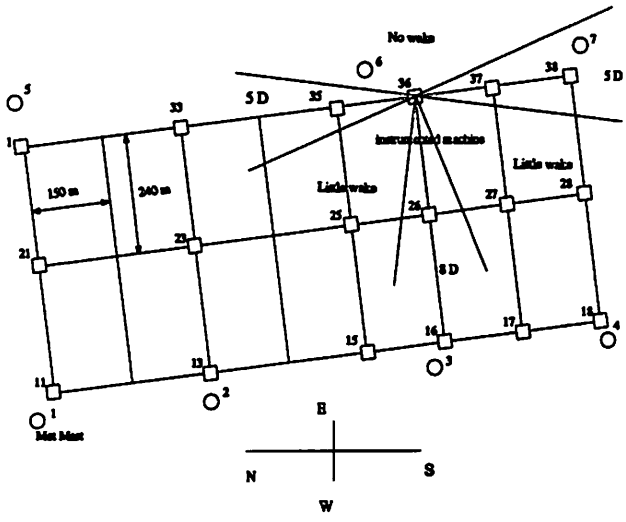

Figure 1: Lay-out of the Sexbierum wind farm

terval of 2.5° in those directions where it is necessary to have a high resolution. In other directions the intervals are quite large, see table 3. The results are transferred every 180 seconds in a wind speed direction and wind speed bin matrix. Each week this matrix is saved to tape and then refreshed. The measurements took place in the weeks 14, 20 – 23, 50, 51, 52 and 53 of 1992 and the weeks 1 – 4 of 1993. Because of this short period of measurement not all wind direction and wind speed bins contain a transaction, see number of transaction(s) per wind speed and wind direction in table 3;

- Rain flow cycles of blade flatwise moment and shaft torque moment for the 4 wake and 6 wind speed bins which are mentioned above. The rain flow cycles are transfered every 600 seconds in a From – To rain flow matrix for the average wake and wind speed bin of the period. Each week these rain flow matrices are saved to tape and refreshed. The measurements of the rain flow matrices took place between week 14 of 1992 and week 4 of 1993. All wake and wind speed bins contain 1 or more transaction(s), see table 4 & 5.

The wind speed and wind direction which determines in which bin the transaction should be added is measured at one of the mast outside the wind farm and never in the wake of the wind farm.

3 PROCESSING AND PRESENTATION OF RESULTS

3.1 Azimuthal binned flatwise moment

The processing of the measurements is done according to the following manner:

- Standard deviation
  The azimuthal binned standard deviation of the flatwise moment is averaged over all azimuth positions and then averaged over all transfers made into each wind direction and wind speed bin. See figure 2;

- Range
  The maximum range is determined by sorting the largest range within each week per wind direction and wind speed interval. Then the maximum range over all weeks is determined. See figure 3.

The results are presented in a polar graph with straight lines between the different angles where results are measured. These results are further denoted as the 1 P averaged measurements.

3.2 Rain flow cycles of the blade loads and shaft torque

The rain flow matrices are converted into:

- Load range - accumulated number of cycles figures for a 1000 hr of operation for each wind speed and wake bin. The measurements within one wind speed and wake bin are always shorter than 1000 hr's. The measured cycles are multiplied with a factor to come to a 1000 hr of operation. This is not a true extrapolation as reported by [3]. See figures 4 – 9. Also the load spectrum for a stand alone turbine and for the turbine 36 in the wind farm are calculated, these results are shown in the figures 10 & 11;

- The 1 Hz equivalent load cycle is determined for each wake and wind speed bin for the flatwise- and shaft torque moment using a log - log description of the S-N curve. This equivalent load cycle is the constant amplitude load cycle which, multiplied with the number of seconds the spectrum is good for results in the same fatigue damage as the actual variable amplitude load spectrum. This is the equivalence of the 1 - P load cycle which is used for constant rotor speed wind turbines. The method is previously reported by [4]. The ratio's of the 1 Hz equivalent load cycles have been calculated for each wake class divided by the free stream load cycle for each wind speed class.
  The blade flatwise equivalent load is calculated for a slope of 10 and 14 which could be used for glass fibre reinforced plastic or laminated wood. The shaft torque equivalent load is calculated for a slope of 3 and 5 which is applicable for steel. See tables 6, 7. The equivalent load cycles are calculated for turbine 36 with the actual wind speed and direction distribution and assuming a wind farm operation and for a stand alone wind turbine with the same wind speed distribution. The ratio's of the wind farm configuration compared to the stand alone configuration of the 1 Hz equivalent cycle is for both loads (the flatwise moment with a power of 10 S – N curve and for the shaft torque moment and a S – N curve with a power of 3) 0.96 .

4 DISCUSSION

4.1 1 P averaged signals

Standard deviation The standard deviation of the flatwise moments is increased up to a factor of 1.5 in the 5 D single & 5 D double wake (5 DD) situation. Unfortunately there is no data for the two highest wind speed intervals for the easterly direction. This causes the lines to cross the lower wind speed intervals. The most probable value of these directions will be around 15 kNm. It appears that the highest standard deviations are always shifted a few degrees to the right of the direct line of the array of turbines. This can be caused by partial wake which gives a higher horizontal shear but may also be caused by a shift to the right of the wake. This is shown for all wake situations.

Maximum range The maximum ranges show a good correlation with the standard deviation. Hence the same as mentioned above will also be relevant for the maximum ranges.

It can also be seen that the maximum ranges found in these measurements are higher ($\approx$ 20 %) than the maximum ranges in the rain flow cycle measurements. This means that by rain flow counting 10 minute time series the maximum range are under estimated by at least 20 %.

4.2 Rain flow data

The accumulated cycles The accumulated cycles graphs show that the wake in-

fluence is evident, although the measured maximum ranges are not always in the same order. It also shows that the more transactions in one bin are measured the higher the highest cycles are. The derivatives of the curves do not tend to flatten off (on a lin log plot) for the cycles with a low probability of occurence. This property can probably be used to extrapolate more accurately to a life time load spectrum for the flatwise moment [3].

The 1 Hz equivalent load cycle The 1 Hz equivalent load cycles of the flatwise moment show that for the wake class 2 (little wake) there is hardly any effect on the loads and if there is an effect it is a decrease in loads. The wake class 3 (8 D & 8 DD) shows a mixed results, however it seems that only the wind speed below V_{rated} have a ratio larger than 1. The wake class 4 (5 D & 5 DD) shows an increase in loading up to 22 % only for the wind speed intervals below V_{rated}. Above V_{rated} the ratio's are near 1.
The 1 Hz equivalent load cycles of the shaft torque moment show for all wake classes with wind speed below V_{rated} a ratio below 1. or only just above 1.0. For above V_{rated} the influence seems to be quit large in an unfavourable way. These results however might not be very reliable because for the free stream and wind intervals 5 and 6 case only a few transactions are recorded, respectively 18 and 1. The overall results for turbine 36 compared to a stand alone wind turbine in the same ambient conditions show a slightly lower 1 Hz equivalent load cycle for both the flatwise moment and the shaft torque moment.

5 CONCLUSIONS

The effect of wind farm operation of the WPS – 30 wind turbine on the fatigue damage is only for some wind directions and wind speed intervals unfavourable. The effect on mechanical loads when the wind turbines are positioned more than 8 D upstream is neglectable.
The lay-out of the Sexbierum wind farm and the wind rose results in low array losses (in the order of 5 %). Thus fatigue life consumption per generated power for turbine 36 will be almost equal to the life consumption for a stand alone wind turbine.

However when the turbines are spaced closer together, e.g. 5 D spacing in both directions, the loads will increase and the array losses will be much larger. In view of the difficulties of getting permits to use land for wind farms it is a trend to build them with 5 D or even less distance apart. This will lead to shorter life times and a higher fatigue life consumption per generated power compared to stand alone operation.

References

[1] Schepers J.G. and Bulder B.H. "Load prediction and fatigue evaluation of the WPS–30 wind turbine in the Sexbierum Wind Farm.". In *Proceedings of the EWEA special topic conference "The Potential of Wind Farms" held at Herning 8 – 11 September 1992*, pages D1–1 – D1–10, September 1992.

[2] Tindal A. et. al. "Dynamic Loads in Wind Farms.". In *Proceedings of the ECWEC conference held at Travemunde 8 – 12 March 1993*, March 1993.

[3] Seifert H. "Monitoring fatigue loads using cycle counting field computer". In *Proceedings of the European Community Wind Energy Conference 1993*, March 1993.

[4] Wastling M.A. and Tindal A.J. "The fatigue life of wind turbines within windfarms"

Table 1: The wind speed and wake class bins of the rainflow cycle measurements

	V_1 [m/s]	V_2 [m/s]	V_3 [m/s]	V_4 [m/s]	V_5 [m/s]	V_6 [m/s]
	6 - 8	8 - 10	10 - 12	12 - 14	14 - 16	16 - 20
W_1	Free stream					
W_2	Little wake ≡ upstream turbine more than 8 D away					
W_3	8 D and 8 D double wake					
W_4	5 D and 5 D double wake					

Table 2: The wind speed and wake class distribution of turbine 36

	V_1 [m/s]	V_2 [m/s]	V_3 [m/s]	V_4 [m/s]	V_5 [m/s]	V_6 [m/s]
	6 - 8	8 - 10	10 - 12	12 - 14	14 - 16	16 - 20
W_1 [hr]	623	357	136	56	26	20
W_2 [hr]	768	719	533	333	203	180
W_3 [hr]	181	151	119	87	61	77
W_4 [hr]	393	275	164	88	42	25
total [hr]	1966	1501	951	563	333	303

Table 3: The number of transactions and direction intervals for the azimuthal binned measurements

D_{class}	ϕ_1	ϕ_2	W_{class}	V_1	V_2	V_3	V_4	V_5	V_6
1	0.0	2.5	4	2	4	3	0	0	0
2	2.5	5.0	4	77	23	6	0	0	0
3	5.0	7.5	4	76	31	6	2	0	0
4	7.5	10.0	1	55	36	8	0	0	0
5	10.0	12.5	1	64	49	7	1	0	0
6	12.5	152.5	1	3839	2684	766	396	68	10
7	152.5	155.0	1	30	21	1	0	0	0
8	155.0	157.5	1	30	39	5	3	0	0
9	157.5	160.0	4	12	28	8	4	0	0
10	160.0	162.5	4	11	15	13	13	3	0
11	162.5	165.0	4	4	24	35	45	4	0
12	165.0	167.5	4	3	19	29	44	7	0
13	167.5	170.0	4	0	5	30	34	3	1
14	170.0	172.5	4	1	18	11	13	4	4
15	172.5	175.0	4	2	13	6	10	9	1
16	175.0	177.5	4	6	9	8	5	2	1
17	177.5	180.0	4	13	16	9	12	10	1
18	180.0	182.5	4	18	32	18	27	23	4
19	182.5	185.0	4	35	34	28	33	19	6
20	185.0	187.5	4	31	46	17	7	47	7
21	187.5	190.0	2	35	54	11	4	44	2
22	190.0	192.5	2	39	70	19	6	17	11
23	192.5	195.0	2	29	49	34	11	46	25
24	195.0	197.5	2	42	43	32	11	41	11
25	197.5	200.0	2	45	37	27	9	23	7
26	200.0	202.5	2	34	42	19	10	23	3
27	202.5	205.0	2	21	60	18	20	23	32
28	205.0	207.5	2	14	75	55	43	27	38
29	207.5	210.0	2	6	71	46	46	35	26
30	210.0	212.5	2	7	60	66	52	63	27
31	212.5	215.0	2	14	61	108	44	42	24
32	215.0	217.5	2	14	70	46	22	46	13
33	217.5	220.0	2	18	58	59	32	59	10
34	220.0	222.5	2	25	73	54	48	34	24
35	222.5	225.0	2	20	79	37	26	11	89
36	225.0	227.5	2	12	65	46	25	27	128
37	227.5	230.0	2	8	45	42	29	31	132
38	230.0	232.5	2	15	48	16	36	35	216
39	232.5	235.0	2	16	30	28	35	82	196
40	235.0	237.5	2	35	55	41	51	116	218
41	237.5	240.0	2	37	80	57	79	61	103
42	240.0	242.5	2	45	115	82	74	53	113
43	242.5	245.0	2	20	75	53	36	51	51
44	245.0	247.5	2	14	105	52	57	24	29
45	247.5	250.0	3	38	98	106	100	29	4
46	250.0	252.5	3	36	94	100	77	25	23
47	252.5	257.5	3	87	217	141	118	110	87
48	257.5	260.0	3	39	99	81	77	61	50
49	260.0	262.5	3	18	79	54	27	43	84
50	262.5	265.0	3	24	87	46	17	39	53
51	265.0	267.5	3	23	82	11	20	35	31
52	267.5	270.0	3	28	81	9	18	51	31
53	270.0	272.5	3	26	45	19	40	80	39
54	272.5	275.0	3	36	47	35	21	56	40
55	275.0	277.5	3	17	34	40	32	93	56
56	277.5	280.0	2	23	24	32	32	126	108
57	280.0	282.5	2	23	25	28	19	28	37
58	282.5	332.5	2	263	390	470	251	129	180
59	332.5	335.0	2	9	12	5	3	5	13
60	335.0	337.5	2	8	8	4	3	5	5
61	337.5	340.0	4	6	13	5	6	12	2
62	340.0	342.5	4	3	12	5	1	6	5
63	342.5	345.0	4	2	17	5	0	3	5
64	345.0	347.5	4	4	16	5	0	2	3
65	347.5	350.0	4	9	10	5	0	1	0
66	350.0	352.5	4	15	11	16	1	0	1
67	352.5	355.0	4	23	9	7	0	0	0
68	355.0	357.5	4	11	7	3	0	0	0
69	357.5	360.0	4	1	2	0	0	0	0

Table 4: Number of 10 minute transactions of rainflow cycles of the flatwise moment

	W_1	W_2	W_3	W_4
V_1	1519	825	260	432
V_2	1026	1368	744	406
V_3	554	1353	527	247
V_4	201	651	323	232
V_5	81	539	225	98
V_6	18	544	243	118

Table 5: Number of 10 minute transactions of rainflow cycles of the shaft torque moment

	W_1	W_2	W_3	W_4
V_1	672	926	384	437
V_2	341	1281	777	329
V_3	229	1391	582	240
V_4	86	833	416	253
V_5	1	610	289	127
V_6	6	592	278	128

Table 6: Ratio's of 1 Hz equivalent flatwise moments

	S - N curve with a slope of 10				S - N curve with a slope of 14			
	W_1	W_2	W_3	W_4	W_1	W_2	W_3	W_4
V_1	1.000	0.962	0.930	1.118	1.000	0.947	0.900	1.115
V_2	1.000	0.983	1.026	1.152	1.000	0.849	0.915	1.062
V_3	1.000	1.100	1.104	1.219	1.000	1.079	1.073	1.146
V_4	1.000	0.965	0.963	1.070	1.000	0.951	0.956	1.080
V_5	1.000	0.990	1.009	1.023	1.000	0.963	0.989	0.998
V_6	1.000	0.926	0.928	0.954	1.000	0.895	0.869	0.937

Table 7: Ratio's of 1 Hz equivalent shaft torque moments

	S - N curve with a slope of 3				S - N curve with a slope of 5			
	W_1	W_2	W_3	W_4	W_1	W_2	W_3	W_4
V_1	1.000	1.048	1.002	1.132	1.000	1.009	0.954	1.073
V_2	1.000	0.800	0.886	0.674	1.000	1.055	1.059	0.980
V_3	1.000	0.914	0.876	0.890	1.000	1.071	1.046	1.039
V_4	1.000	0.760	0.903	0.775	1.000	0.957	1.003	1.035
V_5	1.000	1.617	2.128	1.948	1.000	2.456	2.841	3.009
V_6	1.000	1.276	1.581	1.448	1.000	1.439	1.679	1.660

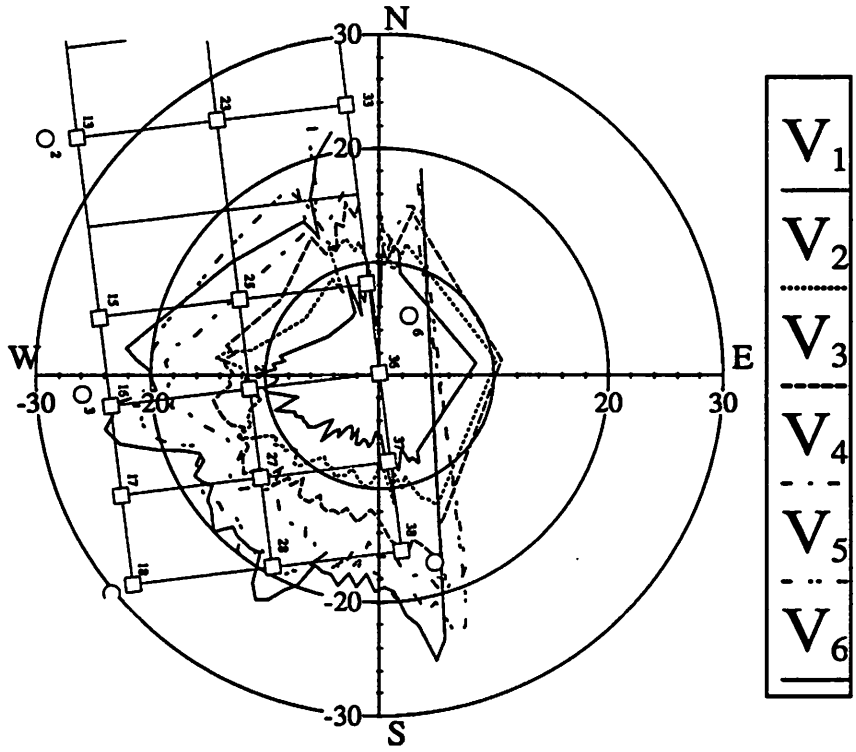

Figure 2: Standard deviation of the flatwise moment [kNm]

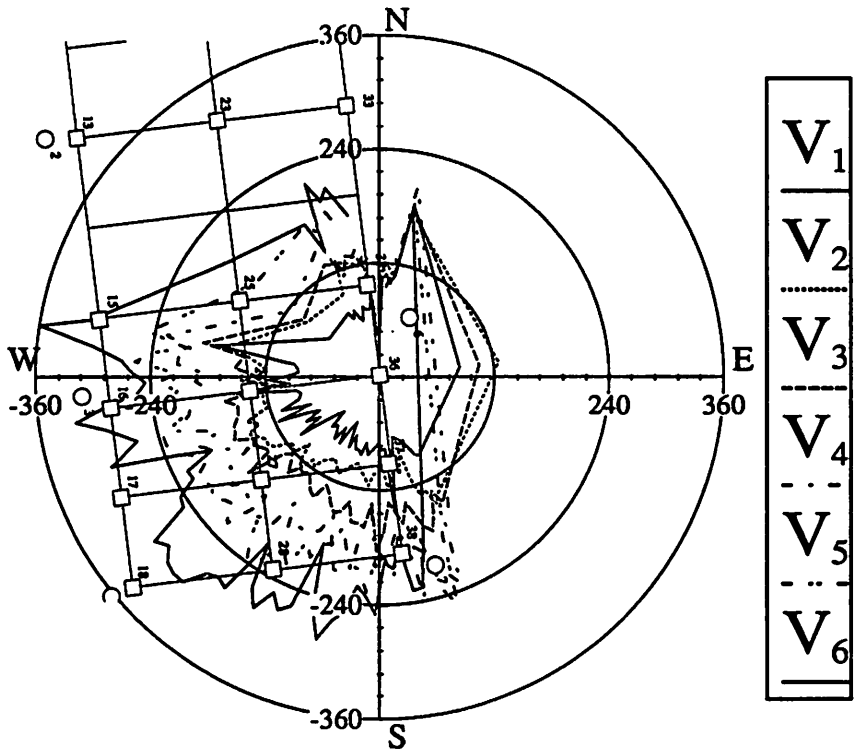

Figure 3: Maximum range of the flatwise moment [kNm]

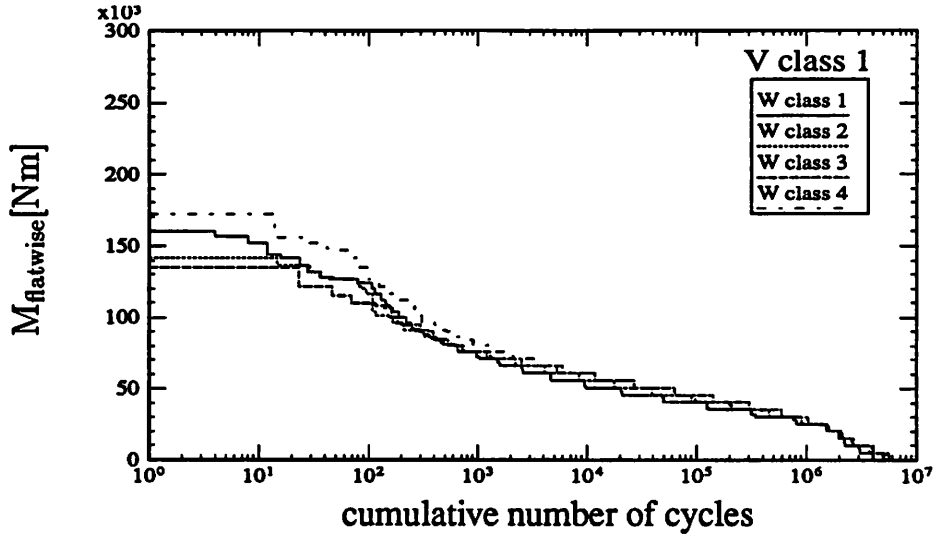

Figure 4: 1000 hr range spectrum for wind class 1 (6 - 8 m/s)

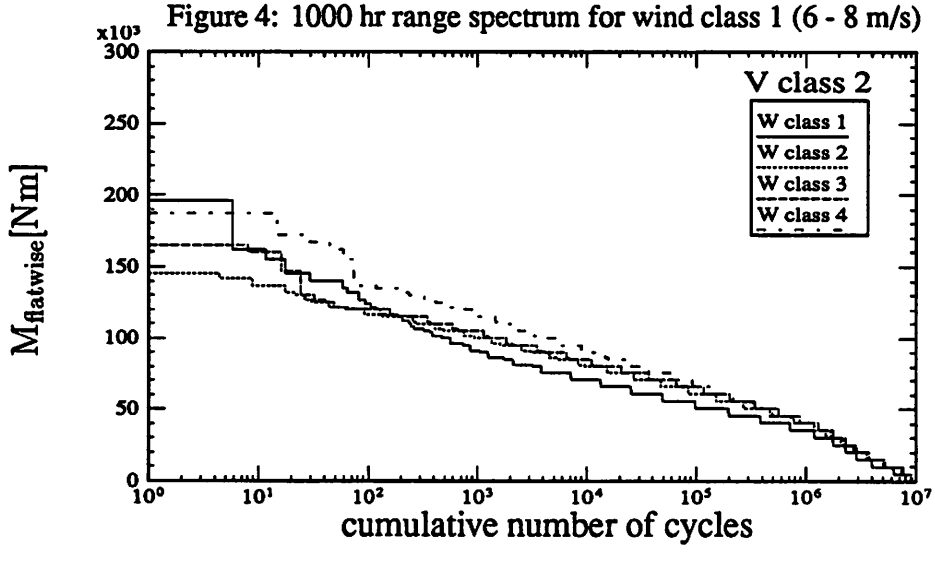

Figure 5: 1000 hr range spectrum for wind class 2 (8 - 10 m/s)

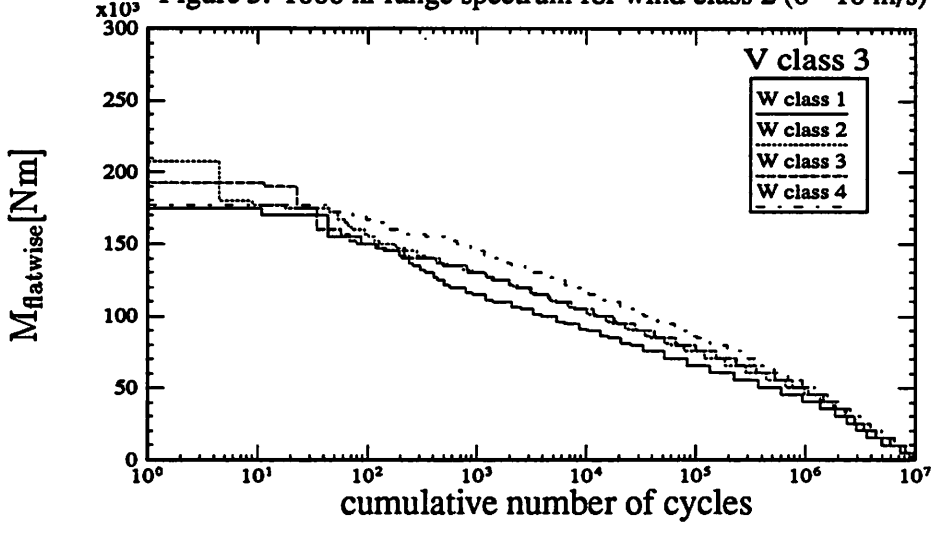

Figure 6: 1000 hr range spectrum for wind class 3 (10 - 12 m/s)

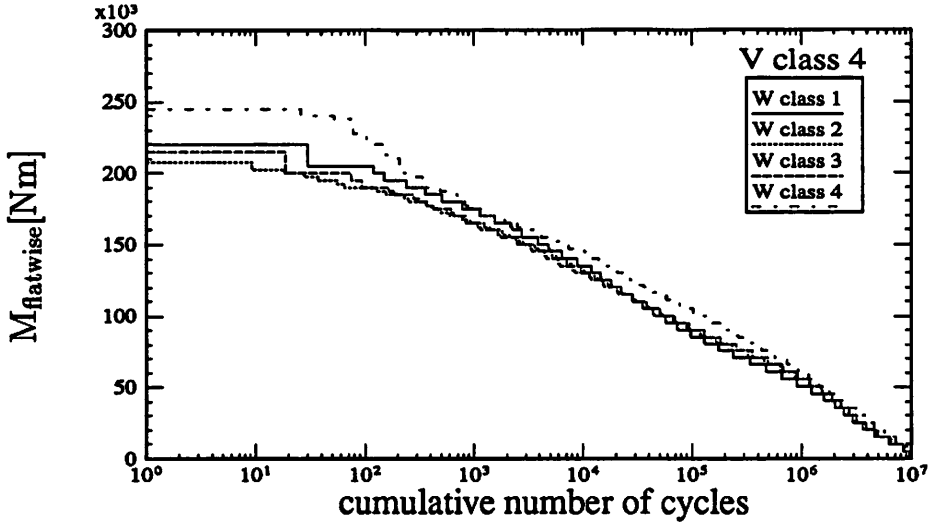

Figure 7: 1000 hr range spectrum for wind class 4 (12 - 14 m/s)

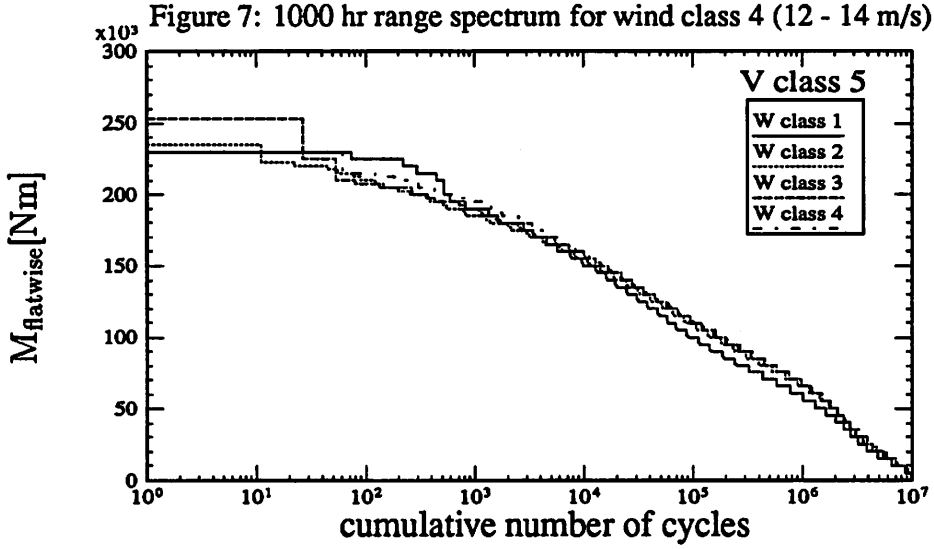

Figure 8: 1000 hr range spectrum for wind class 5 (14 - 16 m/s)

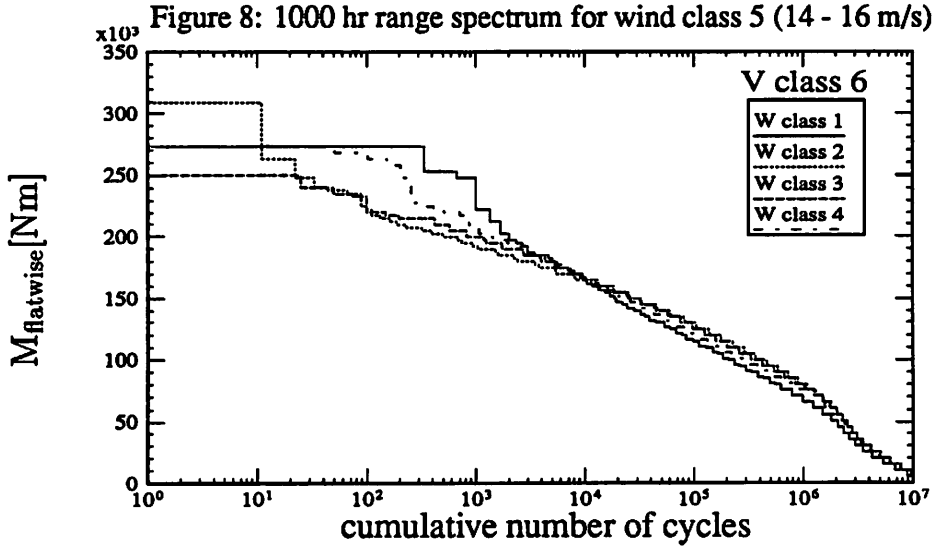

Figure 9: 1000 hr range spectrum for wind class 6 (16 - 30 m/s)

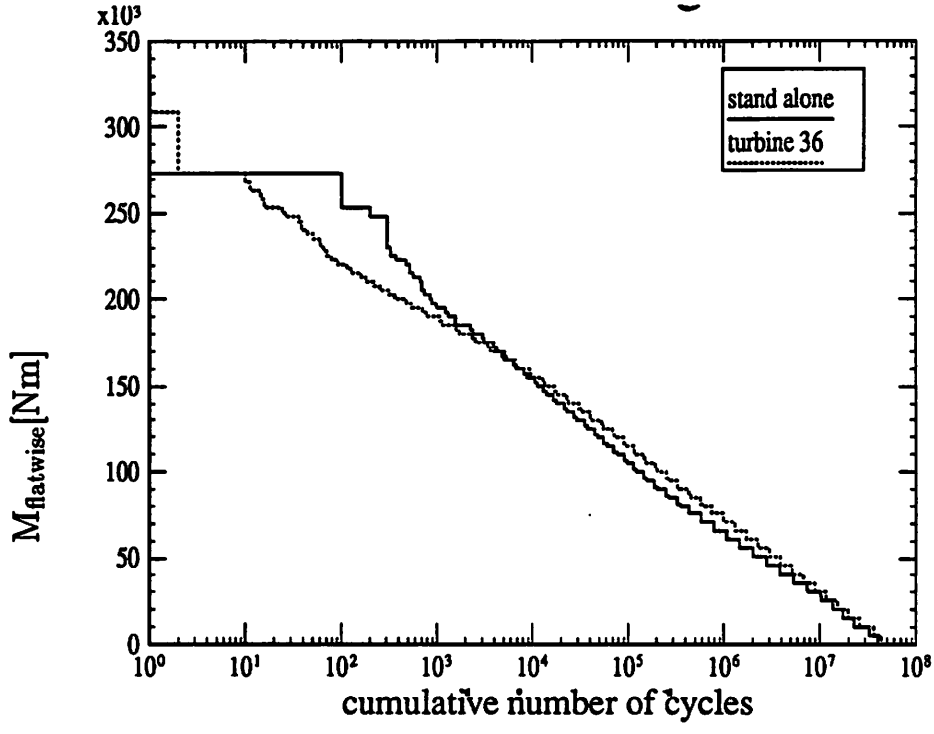

Figure 10: Flatwise moment spectrum for 1 year of operation for turbine 36 compared to a stand alone turbine

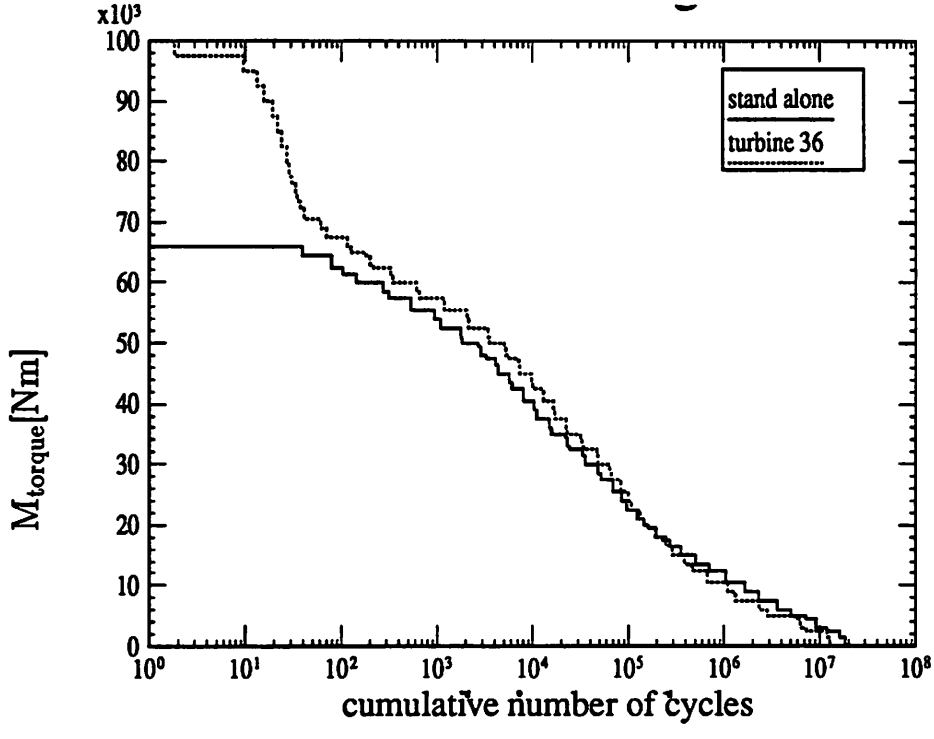

Figure 11: Torque moment spectrum for 1 year of operation for turbine 36 compared to a stand alone turbine

1

Dynamic Loads in Wind Farms

Garrad Hassan and Partners
ECN TNO
KEMA

Joule 1 Project

2

Participants

- *Garrad Hassan*
  - *Coordination*
  - *Wind tunnel modelling*
  - *Numerical modelling*
- *ECN*
  - *Machine response*
- *TNO*
  - *Wake modelling*
- *KEMA*
  - *Full scale measurements*

3

Project Aims

- *To quantify the increase in loading of machines in wind farms*
- *To estimate how the increase varies with spacing and position*
- *To assess the maturity of the combined wind farm and machine behaviour models*

4

Three pronged attack

- *Full scale measurements*
- *Wind tunnel measurements*
- *Numerical modelling*

5

Full scale measurements in simple terrain

- *Sexbierum*
  - *18 x 300 kW machines*
  - *Steel blads*
  - *Variable speed*
  - *Pitch control*
- *Norrekaer Enge II*
  - *42 x 300 kW machines*
  - *GRP blades*
  - *Fixed speed*
  - *Stall regulated*

6

Spectrum of wind speed

Freestream and wake measurements

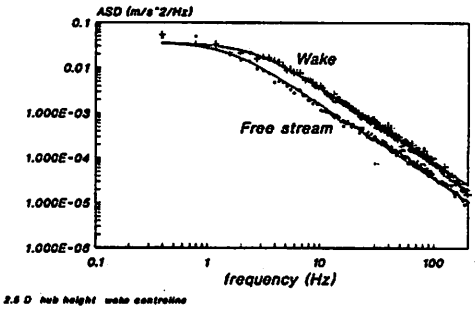

2.5 D hub height wake centreline

7

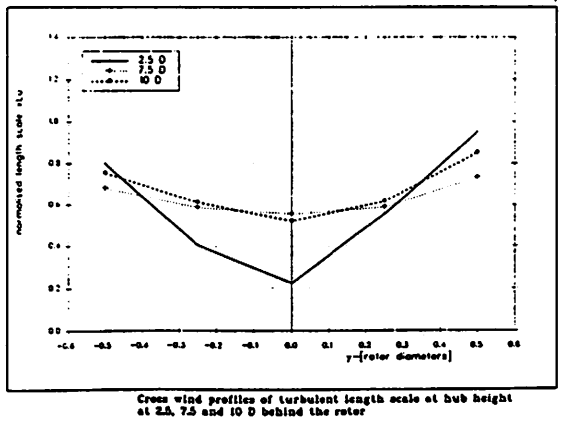

Cross wind profiles of turbulent length scale at hub height at 2.5, 7.5 and 10 D behind the rotor

8

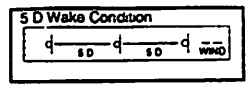

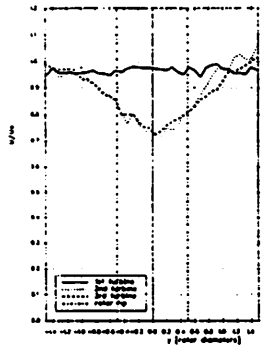

Cross wind profiles

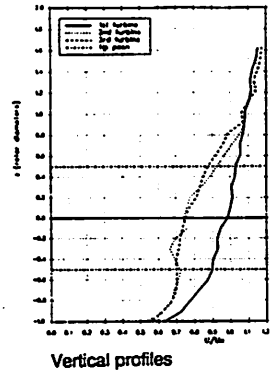

Vertical profiles

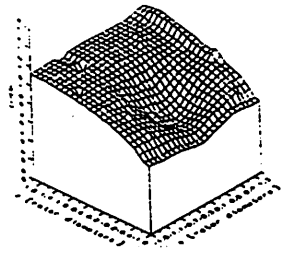

Second machine position

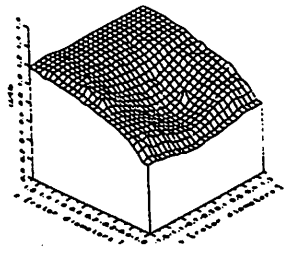

Third machine position

Velocity Ratio

9

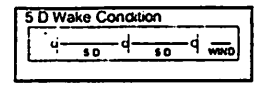

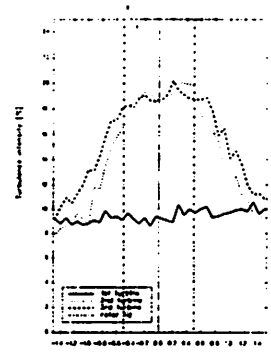

Cross wind profiles

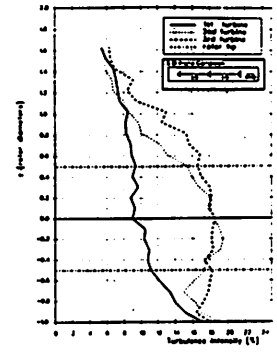

Vertical profiles

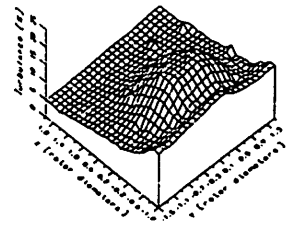

Second machine position

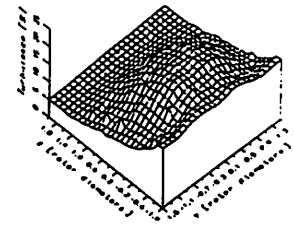

Third machine position

Turbulence Intensity

10

Norrekaer Enge II Simple terrain

Regular layout, multiple wakes

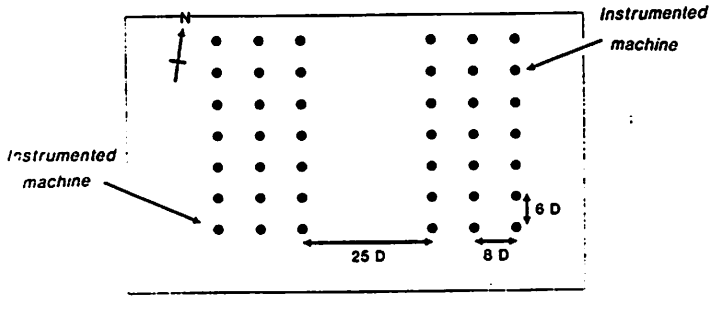

11

Norrekaer Enge II machine power Predictions and measurements

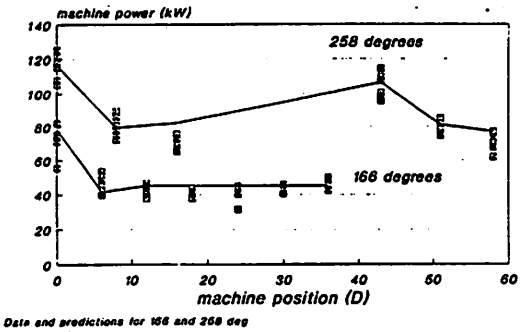

Data and predictions for 166 and 258 deg

12

Wind speed class		Wind speed range (m/s)
Class 1		5 to 8
Class 2		8 to 10
Class 3		10 to 12
Class 4		12 to 14
Class 5		14 to 16
Class 6		16 to 20
Wake class	Description	Direction range (degrees)
Case 1	Free stream	7 – 157
Case 2	Little Wake	187 – 247 & 277 – 337
Case 3	8 D Wake	247 – 277
Case 4	5 D Wake	157 – 187 & 337 – 7

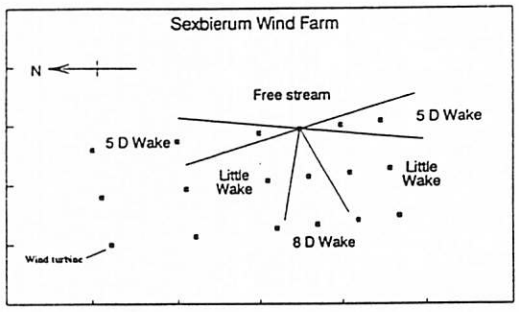

Definitions of wind speed and wake classes for continuous rainflow cycle count measurements of blade loads

13

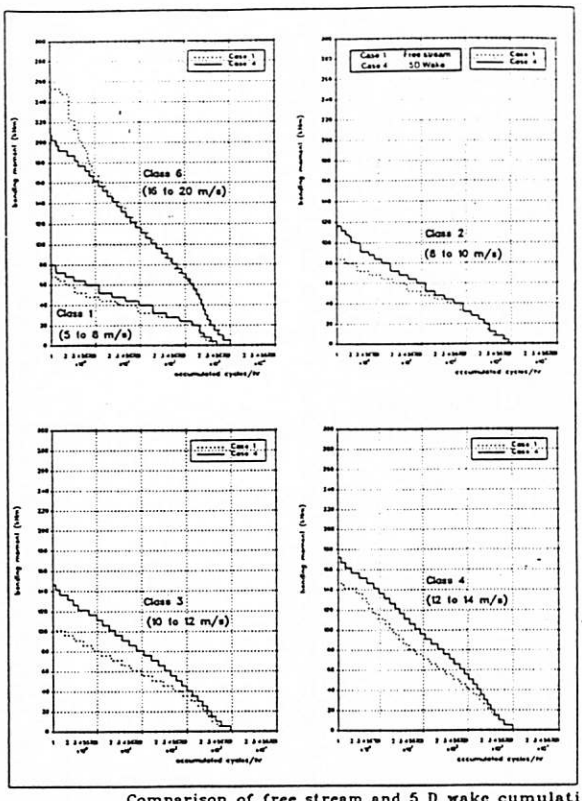

Comparison of free stream and 5 D wake cumulative load spectra over a range of wind speeds derived from long term continuous measurements

14

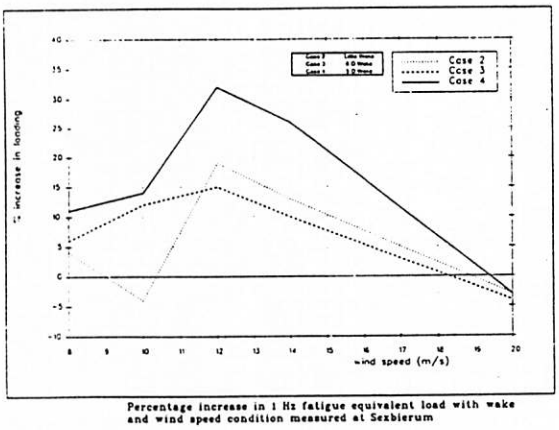

Percentage increase in 1 Hz fatigue equivalent load with wake and wind speed condition measured at Sexbierum

15

Fatigue loading within wind farm

- *The wind conditions at each machine were calculated for all ambient wind speeds and directions*
- *The loading experienced by each machine for the wind conditions evaluated above have been calculated*
- *Total fatigue loading for each machine was evaluated by combining above tables with wind speed direction frequency table*
- *The process was repeated for an isolated machine*

16

% increase in 1 Hz equivalent load summed over wind rose at Sexbierum

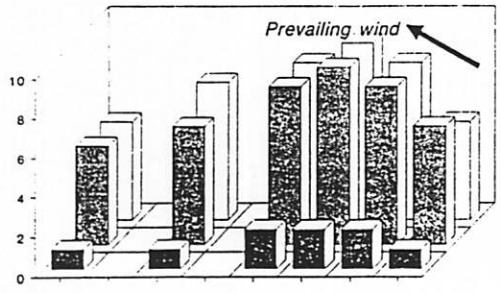

17

1 Hz load normalised to load seen by isolated machine with 18 % turbulence

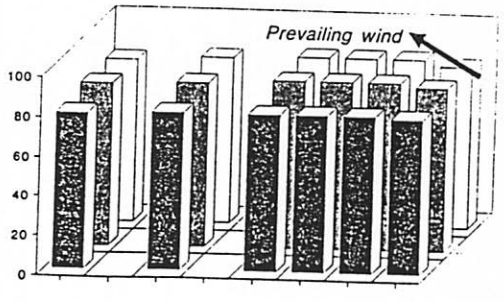

Expressed as percentage

18

Conclusions

- *Computational models work well in simple terrain for single wakes*
- *Large increases in fatigue equivalent loads (30%) are likely but integrated effect is modest (10%)*
- *von Karman shape is preserved in the wake Measurements have confirmed changes in length scale*
- *Wind tunnel measurements agree well with full scale*
- *Joule II*
  - *Simple terrain guidelines*
  - *Complex terrain*
  - *Multiple wakes*

DYNAMIC LOADS IN WIND FARMS

A J Tindal and A D Garrad Garrad Hassan & Partners Ltd., UK
G Schepers and B Bulder ECN, The Netherlands
H Hutting KEMA, The Netherlands
F Verheij TNO, The Netherlands

Abstract: This paper describes the Joule I project (JOUR 0084). Measured data from two wind farms in simple terrain - Sexbierum in the Netherlands and Nørrekær Enge II in Denmark have been used to validate and improve combined wind farm and machine behaviour models. A detailed study of wind conditions in the wake has also been investigated using wind turbine models in a wind tunnel. The main aims of the study are:

- To quantify the level of increase in loading of machines in wind farms.
- To estimate how the loading varies with spacing and position.
- To assess the maturity of the combined wind farm and machine behaviour models.

1 Introduction

This work has been funded by the CEC and the national programmes of the UK, through the DTI, and The Netherlands. In previous work funded by these sources, the description of wind turbine wakes and the dynamic response of the machines have been considered separately. The purpose of this project is to bring together those two areas of work into a single project, aimed at describing the dynamic response of a wind turbine in a wind farm. For this project it was decided that it was important to have very simple topography in order to remove its influence from the response. The Sexbierum site in northern Netherlands is very flat and it is used as the main source of data in this project. In addition to using full scale measurements wind tunnel measurements have also been made. The two experimental approaches are complemented by numerical models of the machine behaviour and the wind flow. Towards the end of the project the numerical tools developed and validated with data recorded at Sexbierum and in the wind tunnel have been applied to the Nørrekær Enge II wind farm. The Nørrekær Enge II comparison acts as a check on the general validity of the tools developed for Sexbierum.

2 Data sources

Measured data from three different sources has been used in this project. A summary is given below:

- **The Sexbierum wind farm in the Netherlands**
  18 Holec 300 kW wind turbines
  Variable speed
  Pitch regulated
  Steel blades
  One instrumented machine

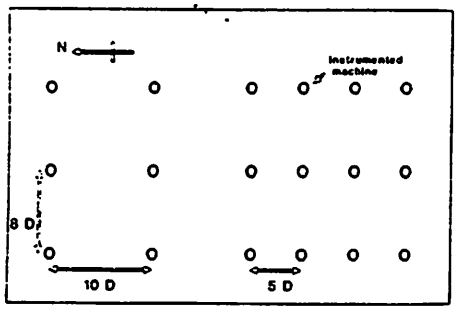

Figure 1 Layout of the Sexbierum wind farm

- **Wind tunnel tests carried out in UK and the Netherlands**
  Atmospheric boundary layer tunnel
  1:300 scale wind turbine models

- **Nørrekær Enge II wind farm in Denmark**
  42 Nordtank 300 kW wind turbines
  Fixed speed
  Stall regulated
  GRP blades
  Two instrumented machines

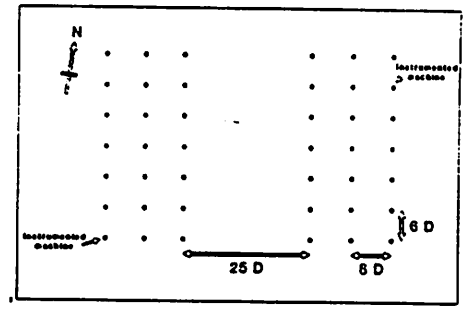

Figure 2 Layout of the Nørrekær Enge II wind farm

3 Wind structure in the wake

In order to simulate the applied loading of a wind turbine in a turbulent wind field it is necessary to use a model of the wind which has the correct representation of both the temporal and spatial structure of the longitudinal wind speed fluctuations. The wind simulation methods adopted by Garrad Hassan and ECN are based on that described by Veers [1]. The time series generated may have any user-specified auto-spectral density and coherence properties. For simulations of the operation of isolated wind turbines it is common to assume von Karman properties for the wind.

One of the aims of this project has been to investigate the structure of the wind in the wake in order to evaluate the wind input required to simulate satisfactorily the applied loading of a wind turbine operating in a wind farm. Figure 3 presents the auto-spectral density of the wind recorded in the free stream and 2.5 D behind an operational wind turbine on the machine centre line at hub height. ESDU spectra fitted to the measured data are also presented. The measurements were made in an atmospheric boundary layer wind tunnel using a 1:300 scale simulation. Experimental details are given in [2]. It is clear that the wind in

the wake has the same structure as the ambient wind, there is, however, a marked reduction in the longitudinal turbulence length scale - $^{x}L_u$. Measurements were made at 2.5, 7.5 and 10 D downstream at a range of lateral positions at machine hub-height. The resulting length scale profiles are presented in Figure 4. The greatest reduction in length scale is seen at 2.5 D on the wake centre line where the length scale has reduced to a quarter of the free stream value. The length scale profile is generally seen to broaden and recover in similar manner to velocity profile. The results show the length scale at 10 D to be smaller than that at 7.5 D which is a surprising result. It was observed that the ambient length scale with which the 7.5 D results were normalised was approximately 10 % lower than the 2.5 D and 10 D results. If the 7.5 D results were normalised to the same ambient levels as 2.5 D and 10 D the trend described above would be reversed.

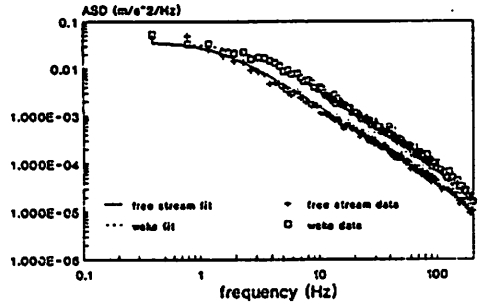

Figure 3 Spectrum of wind speed in free stream conditions and on the wake centre line at hub height 2.5 D behind the rotor

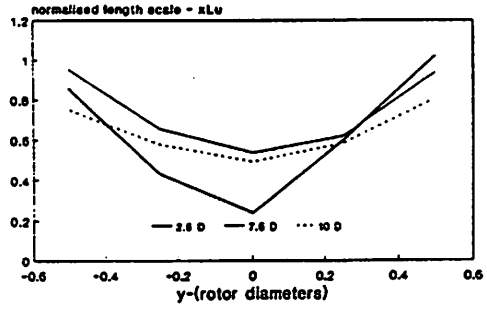

Figure 4 Cross wind profiles of turbulent length scale at hub height at 2.5, 7.5 and 10 D behind the rotor

Measurements made in the ambient wind and in the wake at downstream positions of 4 and 7 D have been recorded at Sexbierum. These data have been analysed by TNO in a fashion similar to that used for the wind tunnel data. The results have also shown that no significant alteration is seen in the structure of the wind in the wake except for change in length scale. Reduction in the longitudinal turbulence length scale to between 20 and 40 % of the free stream value on the wake centre line at hub height are seen at a downstream distance of 4 D. This result is broadly in agreement with the results from the wind tunnel, although, the estimate of length scale from the full scale data is more difficult than from the wind tunnel data.

The results from the two data sources described above lead to the important conclusion that the structure of the wind in a wake is well represented by a von Karman spectrum. In addition an indication is given of the likely variation of longitudinal length scale with wake position. This allows the applied loading of a wind turbine in a wind farm to be simulated with confidence using a von Karman model of the wind, with an appropriately reduced length scale.

A data base of mean and turbulent wind conditions in the 5 D and 8 D single and multiple wake situations which occur in the Sexbierum wind farm was generated. These conditions have also been replicated in the wind tunnel by TNO and GH. Replication of a part of the full scale wind farm in the wind tunnel allows more detailed wind measurements to be made than are practical in the field. Figure 5 presents surface plots of the wind speed at the second and third machine positions for a westerly wind direction at Sexbierum. These results were measured in the wind tunnel by removing the second and third turbines in turn and making wake traverses in their place. The results show that the centre line deficit at the third machine position is not significantly greater than at the second machine position. This observation is important and is further discussed in Section 4. The wake is, however, wider and extends to a greater height at the third machine position than at the second.

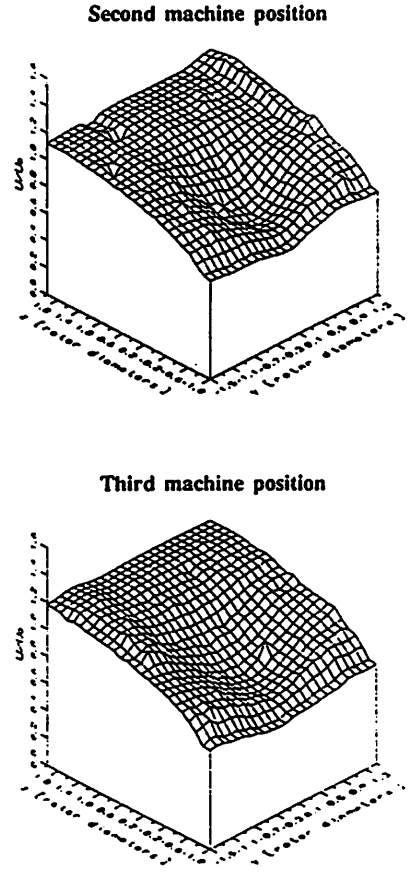

Figure 5 Surface plots of wind speed at 2nd and 3rd machine positions for 3 wind turbines with 5 D spacing

4 Dynamic loads and fatigue damage in wind farms

Accurate computer models of the wind turbines have been created. The ability of GH and ECN to predict the behaviour of the machines for free stream conditions has been confirmed through detailed analysis and comparison with measured data.

Measurements of individual machine power at Sexbierum and Nørrekær Enge II have been used to validate the wind farm models. Figure 6 presents the measured mean power for each wind turbine in the wind farm for two wind directions. Predictions from the GH proprietary code EVFARM are also included on the figure. Results from Sexbierum show similar trends and levels of agreement to those presented above. It is considered from these results that the ability of the code to predict the wind conditions within the wind farm is good. This allows the task of predicting wind farm machine loading to be tackled with confidence. The TNO code FARMS has also been shown to replicate measured wind farm behaviour well.

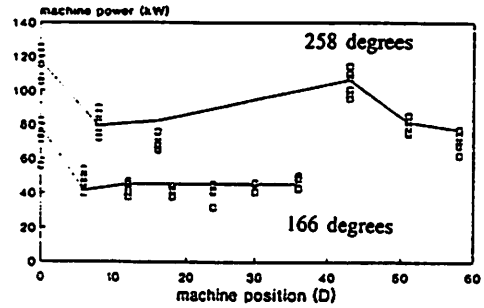

Figure 6 Measurements and predictions of individual mean machine power for two wind directions at Nørrekær Enge II

4.1 Campaign data

Two wake cases have been considered at the Sexbierum wind farm: the operation of the instrumented machine behind a wind turbine 8D upstream and behind a wind turbine 5D upstream. An example of the level of agreement achieved between GH and ECN predictions and measurements for an 8 D wake case is given in Figure 7 which presents the auto-spectral density of blade flatwise bending moment at a radial station of 3.5 m. The level of agreement of the predictions with measurements is similar to that achieved for free stream conditions. The data in Figure 7 is presented as just one example result. Flatwise and edgewise blade bending moment at two radial stations, slow speed shaft torque and tower bending moments have also been considered for a range of wake and wind speed conditions. In addition to single wake conditions a limited number of multiple wake conditions have been investigated.

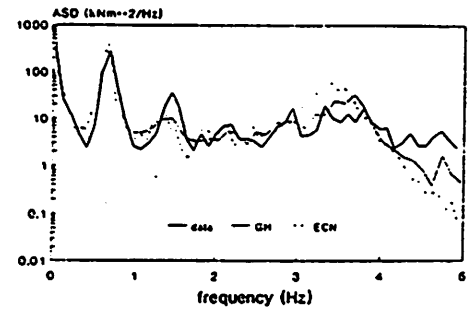

Figure 7 ASD of flatwise blade bending moment at 3.5 m for Holec WPS-30 during wake operation

Data from Nørrekær Enge II has been used towards the end of the project to confirm the results from Sexbierum. For machine loading only a westerly wind direction and one blade radial station have been considered. The presence of two instrumented machines in the wind farm allows the behaviour of a machine at the front of the wind farm to be compared directly with that of a machine at the back of the wind farm. An example result which shows the auto-spectral density of flatwise bending moment near the root is presented in Figure 8. The predictions agree well with measurements.

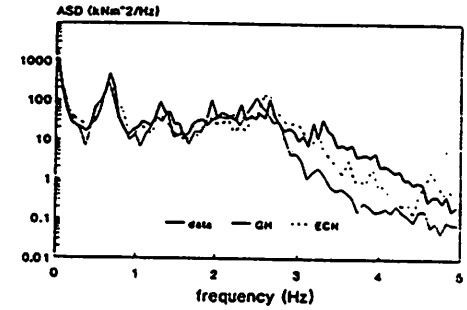

Figure 8 ASD of flatwise blade bending moment at the root for Nordtank 300 kW machine during wake operation

In order to assess the ability of GH and ECN to predict the loading of the wind turbines in free stream and wake conditions a parametric representation of the severity of loading is used. For this purpose the "1 Hz fatigue equivalent bending moment" is evaluated. This load is defined as the amplitude of sinusoidal bending moment which, if applied to the blade at 1 Hz, results in the same fatigue damage as the actual complex bending load time history. This approach allows simple comparisons to be made between predictions and measurements and different wind speeds and wake situations. Table 1 presents example comparisons of measured and predicted 1 Hz fatigue equivalent bending moment results for specific ten minute data campaigns recorded at Sexbierum and Nørrekær Enge II. The results indicate that GH and ECN can predict free stream and wake conditions in a wind farm in flat terrain with reasonable accuracy.

Campaign Description	Data	GH	ECN
Sexbierum Free stream 14.1 m/s	1.0	1.06	1.07
5 D single wake 9.3 m/s	1.0	1.07	0.95
8 D single wake 9.5 m/s	1.0	1.0	1.11
Nørrekær Enge II Free stream 9.8 m/s	1.0	0.93	1.0
8 D multiple wake 9.8 m/s	1.0	0.93	0.92

Table 1 1 Hz fatigue equivalent load predicted by GH and ECN for a range of measured campaign data sets normalised to the measured value - SN slope of 3 assumed.

4.2 Continuous data

Continuous load data has been recorded for the instrumented machine at Sexbierum. This has been binned automatically into one of six wind speed bins and four wake classes, and rainflow cycle counted. It provides a data base which allows the relative severity of different wind speed and wake conditions to be assessed. The cycle count data has been normalised to one hour's operation and the 1 Hz fatigue equivalent load has been calculated. The results are presented, normalised to the free stream class, in Figure 9. The cumulative load spectra for each wake and wind speed condition have been presented graphically by ECN in [3]. The most severe wake condition is the 5 D separation at all wind speeds. The wind speed at which the wake effects are at their greatest is the 10 to 12 m/s bin. The greatest increase in wake loading is just over 30 %.

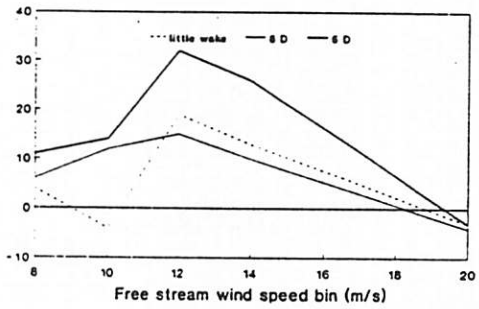

Figure 9 Percentage increase in 1 Hz fatigue equivalent load with wake and wind speed conditions measured at Sexbierum.

4.3 Fatigue loading within the wind farm

In order to assess the increase in loading in a wind farm the following approach has been used:

- The wind speed at each machine in the wind farm for all wind directions and wind speeds between cut-in and cut-out has been predicted.
- The loading experienced by each machine for the wind conditions evaluated above have been calculated.
- The total fatigue loading each machine in the wind farm will experience has been estimated by combining the above two predictions with the wind speed direction frequency for the site.
- The process is repeated for one isolated machine in place of the wind farm.

The results of this procedure allow the fatigue damage of each of the machines within the wind farm to be compared with the damage which an isolated machine on the same site would have seen. Clearly this task is onerous. Some simplifying assumptions have been made in order to make it practicable. Most notably the influence of partial wake immersion and changes in turbulence length scale have been neglected. Figure 10 presents 1 Hz fatigue equivalent flatwise blade load at 50 % span normalised to the isolated machine result. The greatest increase in fatigue loading is 9 %. The wind farm results have also been normalised to the severity of fatigue loading experienced by an isolated wind turbine operating the same wind regime but with a continuous turbulence level of 18 %. This figure is close to the 17 % assumed in the TC 88 standard [4]. The most severely loaded machine in the wind farm experiences a 1 Hz fatigue equivalent load which is 14 % lower than the isolated machine with 18 % turbulence. This indicates that if the WPS-30 were designed to this standard there is a little scope for closer machine spacing at Sexbierum wind farm without reducing the design life of the machines.

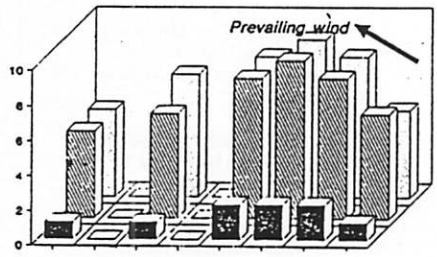

Figure 10 Predicted percentage increase in 1 Hz fatigue equivalent load for each machine in the Sexbierum wind farm

The above results are specific to the Sexbierum wind farm. From this project, however, results indicate that the reduction in energy capture and severity of machine loading deep within a large wind farm is not likely to greatly increased over that experienced by the machines in the second or third row. Machines within large, closely packed, wind farms would therefore be expected to experience greater increases in fatigue loading than found at Sexbierum due to the greater proportion of time spent in wake conditions rather than the greater severity of wake conditions themselves.

5 Conclusions

The project described is nearing completion. The following conclusions are drawn from the work.

- The structure of the wind in the wake is well represented by the von Karman spectrum. A significant reduction in turbulent length scale is seen in the wake.
- The ability of the combined wind farm and machine behaviour model to predict loading of wind turbines in wind farms in simple terrain is shown to be good.
- Measured results from Sexbierum indicate that the greatest increase in loading in the wind farm is approximately 30 %. This occurs for westerly or easterly winds of speed 10 to 12 m/s with machines at their closest spacing of 5 D
- Predictions indicate that over the lifetime of the wind farm the greatest increase in loading due to wind farm operation is likely to be in the order of 10 % for the Sexbierum wind farm. The increase in loading is seen to be sensitive to wind turbine spacing and position.

Multiple wakes and the effects of topography are still not well understood and will be addressed in the Joule II project "Dynamic loads in wind farms II".

6 References

1 Veers, P S "Three dimensional wind simulation" SAND88 -0152, Sandia National Laboratories, March 1988.

2 Hassan U "A wind tunnel investigation of the wake structure within small wind turbine arrays" Final report on Department of Energy contract E/5A/CON/5113/1890, June 1992.

3 Schepers J G and Bulder B H " Load prediction and evaluation of the WPS-30 wind turbine in the Sexbierum wind farm" Proceedings of EWEA conference, Denmark, September 1992

4 "Draft standard on the safety of wind turbine generators" IEC TC88 Issue 21 B

Production of guidelines for the increase in loading in a wind farm

J.G. Schepers
Netherlands Energy Research Foundation ECN
and
A.T. Tindal
Garrad Hassan and Partners

May 1993

1 INTRODUCTION

One of tasks in the Joule 2 project 'Dynamic Loads in Wind Farms 2', is to produce guidelines which give the increase in loading in a wind farm. The wind farm is located in simple (flat) terrain.

This report contains a description of the procedure to produce these guidelines. The document is intended to be a food for discussion for the IEA meeting 'Increased loads in Wind Farm Power stations "Wind Farms"' and for the project group 'Dynamic Loads in Wind Farms 2'

The guidelines will be based on dynamic load calculations for several wind turbines and several wind farms. Validated calculational tools will be applied. Validation takes place by comparison with measurements from different wind farms.

A thorough approach for this kind of calculations has been formulated in the Joule 1 project 'Dynamic Loads in Wind Farms 1', see [1] and section 2. However the computational time which is required to follow this approach is excessive. This is due to the dependancy of the loading on the wind direction and the fact that all the wind turbines in the farm should be considered.

Therefore an approach with some simplifying assumptions has been used in the Joule 1 project. One of the main assumptions was the neglect of partial wake effects. In section 2.4 an additional approach is sketched which does take into account the effect of partial wake effects. It is evident that the complexity and the computational time of this approach will be larger, however they are still considered to be acceptable.

Even if a reliable calculational method exists, it will be obvious that the guidelines should supply the designer direct information about the increase in loads for his particular wind farm, without the necessity of doing complex computations. Then the guidelines should consist of a table which gives an indication for the increase in loading for all kind of wind farms, ambient wind conditions, and types of wind turbines (size, control, material, fixed/teetered hub etc.). Clearly, this is a very ambitious task and within the present project the guidelines will be based on calculations of three different wind farm con-

figurations with two different turbines and two wind roses and one wind speed distribution. The outcome of the calculations will be stored in a data base, which is organized such that the increase in loading for more wind farms, wind roses and wind speed distributions can be found relatively easy. The loads will be compared with calculations for conditions similar to the conditions which are stated in the IEC TC 88 standard for the design of wind turbines. These matters will be adressed in the sections 3 and 5 .

2 CALCULATIONAL METHOD AND ASSUMPTIONS

The calculational tools which will be applied are:

- ECN: UPMWAKE [2] - SWIFT - PHATAS [3]
- GH: EVFARM-BLADED [1]

These tools will not be described in this paper, but it is assumed that they give reliable loads on a wind turbine in a wind farm from the ambient wind speed and turbulence intensity. From [1, 3, 2] this may indeed be expected for single wake conditions. The performance of the models for multiple wake conditions will be investigated within the present project.

Then the increase in fatigue damage for each of the machines in a wind farm, compared to the damage of an isolated machine can be found with the following procedure (from [1]):

- The wind conditions at each machine in the wind farm for all ambient wind directions and wind speeds between cut-in and cut-out will be predicted.
- The loading experienced by each machine for the wind conditions evaluated above will be calculated.
- The total fatigue loading each machine in the wind farm will experience will be estimated by combining the above two predictions with the wind speed direction frequency table appropriate at the site.
- The process is then repeated for one isolated machine in place of the wind farm.

If load calculations are performed for $\frac{360}{2.5}$ ambient wind direction bins and 6 ambient wind speed bins, this will result in 864 load calculations per wind turbine. Usually these load calculations are performed as 10 minutes time series with calculational times (for the ECN-method) of 5 to 10 hours. Although in reality the number of load cases will be less (due to the fact that not all ambient wind directions should be considered) this would probably lead to calculational times which are in the order of 1 year for one wind farm. In the Joule 1 project an enormous saving of computational time was reached by binning the wind conditions experienced by a wind turbine in only 6 wind speed intervals and 6 turbulence intensity intervals (at and above ambient conditions). For all of these 36 conditions load calculations and rain flow cycle counts are performed. If the effects of partial wake, change in turbulence length scale and variation of the turbulence intensity over the rotor plane are neglected then these 36 load calculations cover the loading of all wind turbines.

In the following subsections the main assumptions from the Joule 1 project are evaluated.

2.1 Turbulence intensity

A rotor averaged turbulence intensity was assumed. It is known that in wake operation

the turbulence intensity is a function of the rotor position. However the validations carried out in the Joule 1 project showed that acceptable results could be obtained with a rotor averaged turbulence intensity.

2.2 Turbulence length scale

The change in turbulence length scale was neglected because at the time of the Joule 1 project, no information was available about this subject. At present it is known that the turbulence length scale changes roughly by some 30% in 5D wake operation. For 8D spacing the change in length scale was less. Most likely the 6 turbulence levels can be related to a certain turbine spacing, so they can be associated with a turbulence length scale. Then the turbulence length scale can be taken into account without any increase in computational time.

2.3 Wake profiles

In [4] an analytical study is performed on the effect of different wake profiles on the loading. It is shown that, by assessing all 1P components, the effect of wake profiles may be limited. This is supported by the PHATAS calculations which are shown in figure 1. Calculations of the flatwise moment for the WPS-30 turbine are presented with no horizontal shear, and with a positive and negative horizontal shear (equal in magnitude). The positive shear increases the 1P periodic component, while the negative shear decreases this component. During the wind turbine lifetime, both positive and negative shear will occur and (partly) compensate each other. For this reason the effect of wake profiles was neglected in the Joule 1 project.

Although in the sequel a method is proposed which does take into account the effect of wake profiles, the method from the Joule 1 project is still preferred, because it requires a minimum of computational time and data handling. Therefore the severity of partial wake effects on the loads will be assessed: Calculations for one wind speed bin and the whole range of wind directions, with and without the effect of partial wake will be performed for the intrumented turbine in the Alsvik wind farm. The calculations will be compared with the FFA measurements. If partial wake operation has a limited effect on the fatigue damage then the method from the Joule 1 project will be applied.

In figure 2 the relative horizontal shear for the Sexbierum wind farm is presented as function of wind direction. The horizontal shear is derived from wind measurements at 0.7R left and 0.7R right from the centreline of the measurement mast. The high magnitudes of the shears which are shown in this figure, clearly throw some doubt on the assumption that they have a minor influence on the loads. If it appears that these effects cannot be neglected, then it is proposed to divide the loads into a stochastic and a deterministic part. The stochastic part can be associated to the turbulence level, while the deterministic part can be associated to a certain wake profile, see also section 2.4. Since the calculation of the deterministic part only takes a few minutes, this offers the opportunity to save a large amount of computational time.

It must be noted that the division in stochastic and deterministic loads is based on a linear approach. A similar approach is applied in the dynamic load codes in frequency domain. In [5] it is found that these models perform similarly to time domain programs, although some (limited) discrepancies may be expected at above rated conditions for stall controlled wind turbines. From the Joule 1 project, it is known that the increase in fatigue damage is greatest at rated wind speeds and decreases rapidly for above rated wind speeds. Since the time, a wind turbine spends

at above rated wind conditions will be limited, the expected deviations will not be too large.

2.4 PROPOSED METHODS

In section 2.3 it has been made clear that the method which will be applied depends upon the question whether partial wake effects have a significant effect on the increase in fatigue damage. This question will be answered from the FFA measurements.

Partial wake effects have no significant effect:

The procedure from the Joule 1 project will be applied where ten minutes times series will be calculated at 6 wind speed bins and 6 turbulence intensities. The only modification will be that each turbulence intensity is associated to a certain turbulence length scale.

Partial wake effects do have a significant effect:

- Again ten minutes time series will be calculated for 6 wind speeds and 6 turbulence intensities, which provides the stochastic part of the loads ($M_{stoch}(t, \phi_r)$) (t from 0 to 10 minutes). A rotor averaged turbulence intensity is assumed.

- The deterministic part ($M_{det}(\phi_r)$) is calculated from the known wake profile at given ambient wind conditions.

- The total load ($M_{tot}(t, \phi_r)$) follows from superposition of both signals: $M_{tot}(t, \phi_r) = M_{det}(\phi_r) + M_{stoch}(t, \phi_r)$

3 DEFINITION OF GUIDELINES

According to the project proposal the guidelines should give the increase in loading in a wind farm, with an indication for the influence of wind turbine spacing, wind rose and mode of operation.

Although the increase in loading might also be represented by an increase in wind loading (increase in turbulence and wind shear), the present project concentrates on mechanical loading. Therefore it is proposed that the guidelines should give a direct measure for the increase in fatigue damage, compared to free stream operation. Similar to the Joule 1 project, tables will be supplied which give the increase in 1P equivalent loading for the rotorshaft torque and for the flatwise and edgewise loading at blade root, 50% R and 90% R for a particular wind farm configuration, calculated with one of the procedures described in section 2.4. It will be investigated whether the resulting loads are covered by the IEC TC 88 standard. Thereto a comparison will be made with calculations for a machine which experiences the same ambient wind speed distribution and a continuous turbulence intensity of 18%. This condition is similar to that stated in the IEC TC 88 standard.

It is obvious that the number of possible wind farm configurations is infinite and that not all of them can be evaluated. Therefore a restriction will be made to rectangular 5x5 wind farms with 5D spacing, 7.5D spacing and 10D spacing. The wind farms are supposed to consist from WPS-30 turbines and Danwin 23 turbines. The WPS-30 turbine is the type which is placed in the Sexbierum wind farm, while the Danwin 23 is placed in the Alsvik farm. The actual wind speed distributions will be taken. Two wind roses will be considered:

- A wind rose with the prevailing wind direction along the main axis of the wind farm;
- A wind rose with the prevailing wind direction under an angle of 45 degrees with the main axis

The worst case will be selected for the particular wind farm and this number will be supplied to the table. The calculations will be performed for a low ambient turbulence intensity. It is supposed that wake effects will be more extreme for lower turbulence intensities, since turbulent mixing increases with the turbulence level.

Of course most wind farms will be different from the wind farms which have been calculated. Then an indication of the increase in fatigue damage may be obtained from the wind farm in the table which compares best.

It is realized that the fact that only a few wind farm configurations and ambient wind conditions are considered, is a limitation. However with a minimum of effort the increase in fatigue damage can be derived for all possible wind roses, wind speed distributions and a large number of wind farm configurations, see section 5.

4 COMPUTATIONAL TIME

A 5x5 wind farm with 5D spacing will be evaluated (figure 3). Due to the axes of symmetry in the farm, calculations for ambient wind directions between $-\phi_{y1}$ and $+\phi_{y5}$ cover the whole loading. I.e., from figure 4, it is clear that turbine 23 at a wind direction of ϕ_y - 90° is exposed to the same loading as turbine 32 at a wind direction of ϕ_y. Note that distances of 15 D and more are assumed to have a negligible wake effect.

Then the following calculations have to be performed:

- 5D (multiple) wake;
  $(-\phi_{y1} < \phi_y < +\phi_{y1})$:

  Wake calculations:

  Wake calculations should be performed at all wind speed bins for turbine 25, 35, 45 and 55. Note that turbine 25 is representative for all turbines at the second row, turbine 35 for all turbines at the third row etc. This leads to 4 wake calculations per wind speed bin.

  Deterministic load calculations:

  From the wake calculations, the deterministic wind field can be derived for all wind directions between $-\phi_{y1} < \phi_y < +\phi_{y1}$. If the wake growth is neglected then $\phi_{y1} \approx 12°$. Taking a wind direction bin of 2.5° this yields 10 deterministic single wake load calculations per wind speed bin. For multiple wake loadings, the range in possible wind directions will be much narrower, leading to less calculations (i.e. for wind direction ϕ'_y, turbine 51 is exposed to single wake loading). However for the sake of simplicity, the same wind direction range is assumed for multiple wake loading. Then the total number of deterministic load calculations per wind speed bin, will be 40.

- $\sqrt{(125)}D$ (multiple) wake;
  $(\phi_{y2} < \phi_y < \phi_{y3})$:

  Wake calculations:

  Wake calculations should be performed at each wind speed bins for turbine 34 and 54. This leads to 2 wake calculations per wind speed bin.

Deterministic load calculations:

With $\phi_{y2} \approx 21°$ and $\phi_{y3} \approx 31°$, and assuming that the wind direction range for multiple wake loading is equal to the range for single wake loading, this yields 8 deterministic load calculations per wind speed bin.

- $\sqrt{(50)}D$ (multiple) wake; $(\phi_{y4} < \phi_y < \phi_{y5})$:

  Wake calculations:

  Wake calculations should be performed at all wind speed bins for turbine 22, 33, 44 and 55. This leads to 4 wake calculations per wind speed bin.

  Deterministic load calculations:

  With $\phi_{y4} \approx 38°$ and $\phi_{y5} \approx 52°$, this yields 24 deterministic load calculations per wind speed bin.

- Total:
  60 wake calculations and 432 deterministic load calculations per wind farm (with 6 ambient wind speed bins).

Since calculations will be performed for 3 wind farm configurations (5D, 7.5D and 10D) and for a farm with WPS-30 as well as Danwin 23 turbines the total number of wake calculations will be 360 and the total number of deterministic load calculations will be 2600. This will take some days on a SUN SPARC station.

Finally 10 minutes time series have to be calculated for 6 wind speed bins and 6 turbulence intensity bins, both for the WPS-30 and the Danwin 23 machine. These calculations will take some weeks on a SUN SPARC station.

5 CALCULATION OF FATIGUE LOADING

5.1 DIFFERENT AMBIENT WIND CONDITIONS

The rain flow cycle counts for all ten minutes series which have been evaluated are stored in a database (i.e. on floppy discs). Then all cycle counts are known for every wind turbine in the farm at each wind direction and wind speed, for a period of 10 minutes. It is evident that the total cycle counts for all kind of wind roses and wind speed distributions can be calculated easily from these data by multiplying the cycle counts with the time that the corresponding wind direction will occur.

5.2 DIFFERENT WIND FARMS

- In figure 5, a 4x1 wind farm is sketched with 5D spacing.
  - $-\phi_{y1} < \phi_y < +\phi_{y1}$: Cycle counts for the turbines 2, 3 and 4 can be found from the '5D cycle counts' in the data base at the same wind directions for ten minutes periods. A similar procedure can be applied for the turbines 1, 2 and 3 at wind directions:
    $180° - \phi_{y1} < \phi_y < 180° + \phi_{y1}$.
  - For all other wind directions the turbines are exposed to free stream conditions.
  - From the wind rose and the wind speed distribution, the total number of cycles can be determined, by multiplying the cycle counts with the time that the corresponding wind conditions will occur.
- In figure 6, a 3x3 wind farm is sketched with 5D and 7.5 D spacing.

- $-\phi_{y1} < \phi_y < +\phi_{y1}$ and $180^o - \phi_{y1} < \phi_y < 180^o + \phi_{y1}$: The turbines are exposed to 7.5D wake spacing. The cycle counts can be found from the '7.5D cycle counts'
- $\phi_{y2} < \phi_y < \phi_{y3}$: The 'diagonal spacing' is about 9 D. The loading can be estimated from the 7.5 D data or from the 10 D data. It is proposed to take the '7.5 D cycle counts', since this will give the most conservative loads.
- $\phi_{y4} < \phi_y < \phi_{y5}$ and $180^o - \phi_{y4} < \phi_y < 180^o + \phi_{y5}$: The turbines are exposed to 5D wake spacing. The cycle counts can be found from the '5D cycle counts'.
- From the wind rose and the wind speed distribution, the total number of cycles can be determined, by multiplying the cycle counts with the time that the corresponding wind conditions will occur.

6 CONCLUSIONS

- Guidelines will be produced which give the increase in 1P equivalent loads for 5x5 wind farms with 5D, 7.5D and 10 D spacing and with WPS-30 and Danwin 23 turbines. The data will be stored in a data base from which the loading for a large number of other wind farms can be found relatively easy.
- It will be investigated whether the resulting loads are covered by the IEC TC 88 standard.
- If necessary the effects of partial wake can be taken into account.
- The resulting computational time will be in the order of several weeks. This is not considered to be a great problem.
- The extreme loads will also be supplied to the guidelines. The procedure will be similar as the one which is used in the Dynamic Loads in Wind Farms 1 project, and will not be described here.

References

[1] Tindal A. et. al. "Dynamic Loads in Wind Farms.". In *Proceedings of the ECWEC conference held at Travemunde 8 – 12 March 1993*, March 1993.

[2] Crespo A. et. al. "Numerical Analysis of wind turbine wakes". In *Proceedings of Delphi Workshop on "Wind turbine applications"*, 1985.

[3] Schepers J.G. and Bulder B.H. "Load prediction and fatigue evaluation of the WPS–30 wind turbine in the Sexbierum Wind Farm.". In *Proceedings of the EWEA special topic conference "The Potential of Wind Farms" held at Herning 8 – 11 September 1992*, pages D1–1 – D1–10, September 1992.

[4] Wastling M.A. and Tindal A.J. "The fatigue life of wind turbines within windfarms". In *Proceedings of the British Wind Energy Association Conference 1991*, pages 231 – 235, 1991.

[5] Grol, H.J., Snel H., and Schepers J.G. "Wind Turbine Benchmark Exercise on Mechanical loads. Volume 1, part A & B. A state of the art report.". Unclassified ECN-C–91 -031, ECN, MAY 1991.

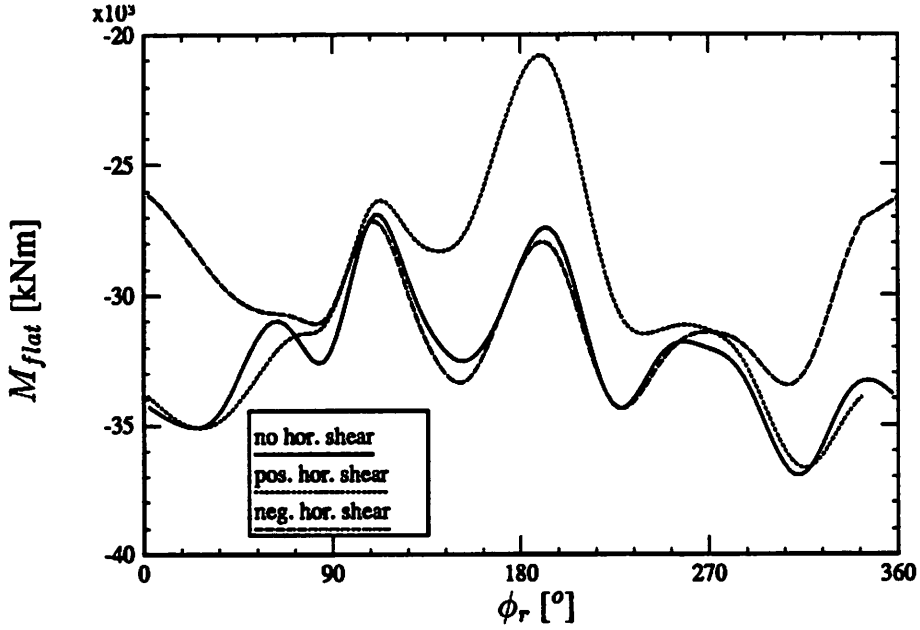

Figure 1: Effect of horizontal wind shear on deterministic flatwise moment

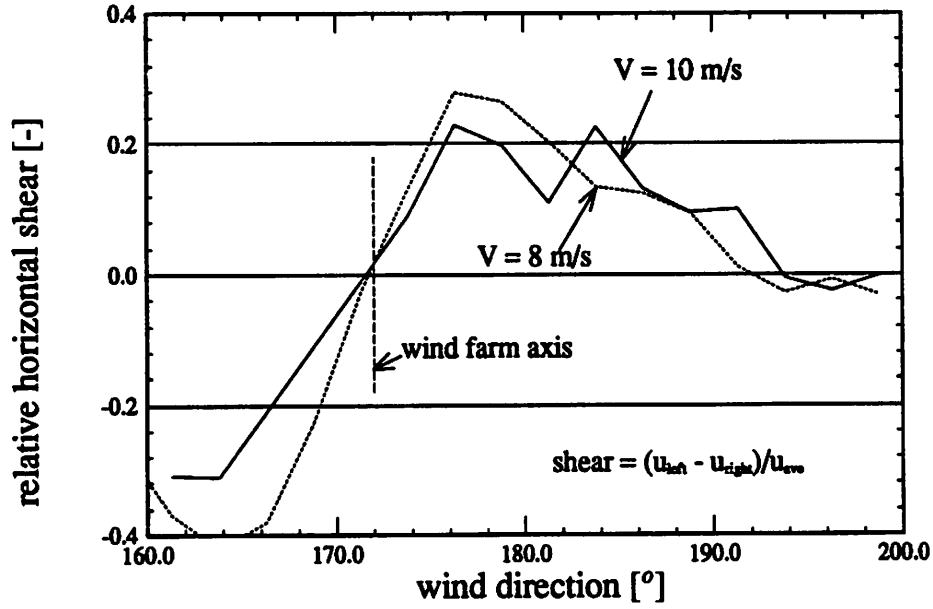

Figure 2: Measured relative horizontal shear in Sexbierum; 5D

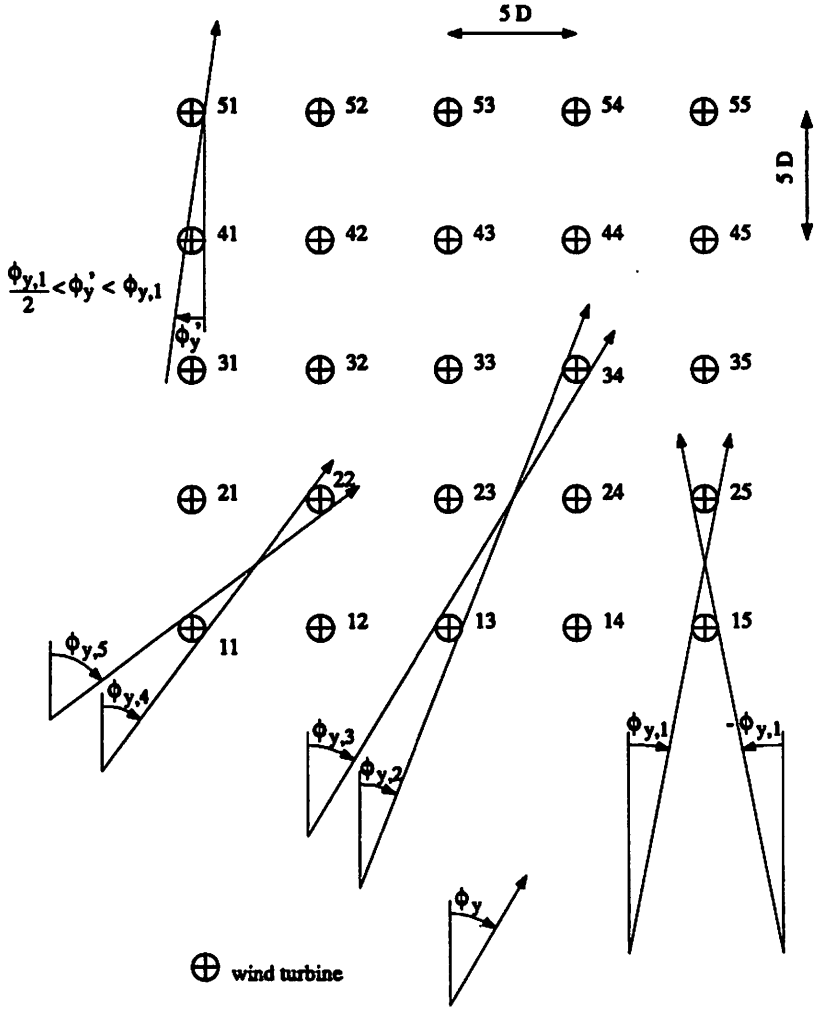

Figure 3: 5x5 wind farm with 5D spacing

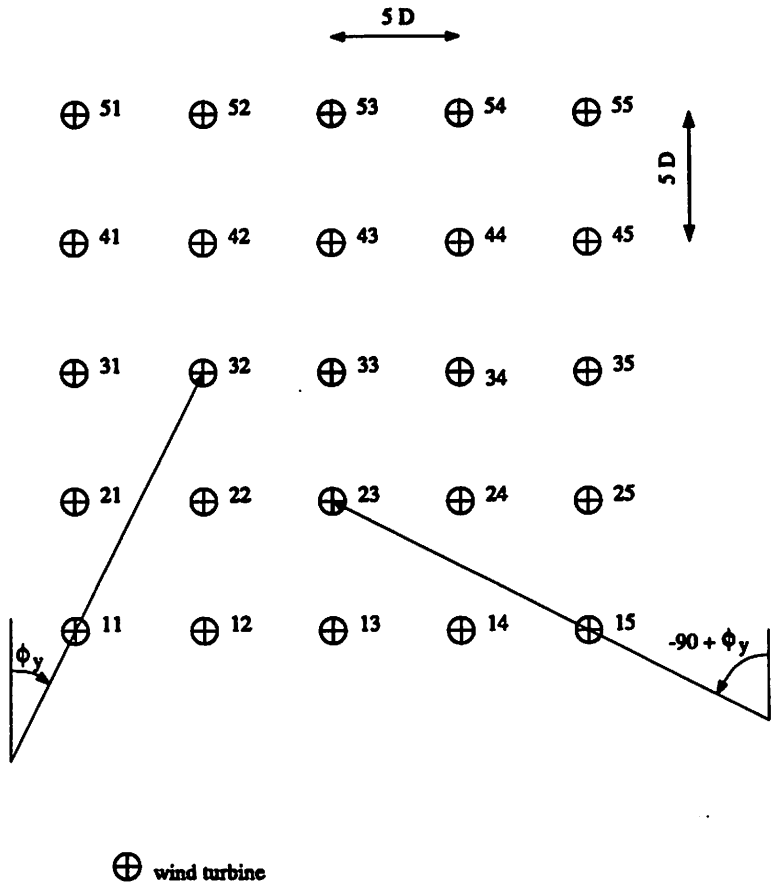

Figure 4: Symmetry in the wind farm

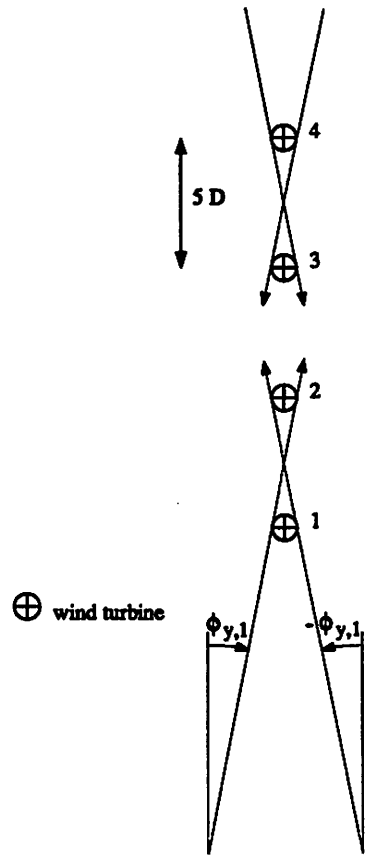

Figure 5: 4x1 wind farm with 5D spacing

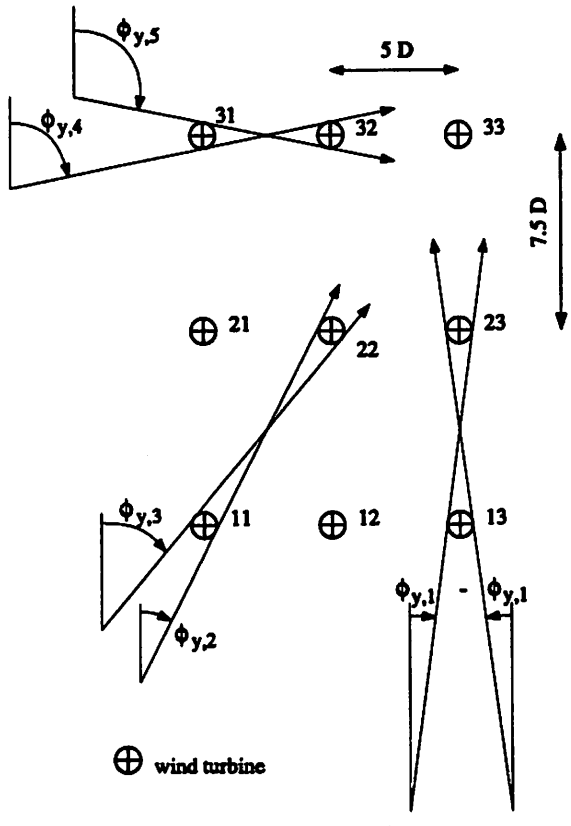

Figure 6: Wind farm with 5D and 7.5D spacing

WAKE WIND DATA ANALYSIS

Measurements from the Dutch experimental wind farm at Sexbierum

F.J. Verheij and J.W. Cleijne
TNO Environmental and Energy Research
P.O. Box 342, 7300 AH Apeldoorn, The Netherlands

IEA Expert Meeting, Gothenburg Sweden, 3 - 4 May 1993

Introduction

Both wind measurements and wind turbine power and load measurements have been performed in the Dutch experimental Wind Farm at Sexbierum. The aim of the measurements is to provide data for the validation of wake and wind farm models and to provide input data for wind turbine load calculation programmes. The Department of Fluid Dynamics of TNO Environmental and Energy Research has analyzed the wind data.

The wind has been measured at 3 heights at several positions inside and just outside the wind farm. The analysis contains horizontal and vertical profiles of the:
- U-, V- and W-component of the wind;
- turbulence intensities in three directions and turbulent kinetic energy;
- shear stresses u'v', u'w' and v'w'.

Besides power spectral densities, integral turbulence length scales and coherence functions has been determined from the data.

Some of the results of single wake measurements are shown in graphs. They concern measurement campaigns with masts at 2.5, 5.5 and 8 D behind turbine T18 and at 4D behind turbine T37 (turbine T38 out of operation and with blades in feathered position). The lay-out of the Sexbierum wind farm including the turbine numbers are shown in figure 1. Detailed information and results of other campaigns are to be found in Cleijne 1992, Cleijne 1993 and Verheij 1993.

Wind Farm Lay-out

The Dutch Experimental Wind Farm at Sexbierum is located in the Northern part of the Netherlands at approximately 4 km distance of the seashore. The wind farm is located in flat homogeneous terrain, mainly grassland used by farmers for the grazing of cows. In the direct vicinity of the wind farm only a few scattered farms are found.

The wind farm has a total of 5.4 MW installed capacity consisting of 18 turbines of 300 kW rated power each. The rotor diameter is 30.1 m, the hub height is 35 m. The wind turbines (T1 to T38) are placed in a semi-rectangular grid of 3 x 6 rows at inter-distances of 5 rotor diameters along one major grid line and at an inter-distance of 8 diameters perpendicular to this grid line (see figure 1*).

* missing

The direction of the rows is at 353° with the North. Turbine T36 has been instrumented to study the wake effects on the wind turbine loads.

Around the wind farm there are 7 meteorological masts (M1 to M7), which enables the measurement of the undisturbed wind conditions for every wind direction. Masts 4 and 6 are parallel to the prevailing wind direction and have wind sensors at 3 heights, i.e. 20, 35 and 50 m. The other 5 masts have sensors at hub height. The signals from the meteorological tower are sampled at a rate of 1 Hz.

There are three mobile masts in the wind farm for detailed wake measurements. It is possible to install the masts at any place inside the wind farm enabling detailed wind measurements of the wake structure. One mast is equipped with 3-component propeller anemometers at 47 m (b1), 35 m (b2) and 23 m (b3), respectively. At heights of 41 m (b2h) and 29 m (b2l) two extra cup anemometers have been mounted. The other two masts contain 3-component propeller anemometers at 35 m (a2 and c2). The signals from the mobile masts are sampled at a 4 Hz sampling rate. The 3-component propeller anemometer consists of three light-weight carbon fibre propellers mounted on a pyramid-shaped rig at angles of 30° relative to each other. Combination of the three anemometer signals gives the X, Y and Z components of the wind. The sensor was calibrated in a wind tunnel and yields reliable results within a cone of approximately 30° relative to the sensor centre-line.

The prevailing wind direction in the wind farm is along the line T18 to T36. The wind climate at hub height is given by Weibull frequency distribution with scale factor a=8.6 m/s and shape factor k=2.1. The average wind speed is 7.6 m/s.

Time averaging

Before the data base was further analyzed, the samples were combined to obtain 3 minute averaged quantities. Considerations for selecting a period of 3 minutes were the following:
- stationarity of the data;
- coherence between undisturbed wind signal and wake signal;
- effect of slow wind direction variations;
- number of available records;
- effect on wind turbines.

For the determination for the power spectral densities and the integral turbulence length scales and the coherence functions an averaging period of 256 s have been used for FFT-calculation purposes.

The turbulence intensity at height z, I(z) or σ_u/U (z), has been calculated according to Beljaars 1987:

$$I(z) = 2.2\ \kappa\ \ln(z/z_0)$$

in which $\kappa = 0.4$. For the V-component of the wind the constant is 1.8.
Panofsky & Dutton use the same formula, but with the constants 2.4 and 1.9 for the U- and V-component respectively.

Based on a terrain roughness length z_0=0.05 m the turbulence intensity I = 0.134, corresponding to an averaging period of 1 hour. ESDU 1983 gives expressions for the transformation of turbulence intensities obtained using shorter averaging periods into turbulence intensities based on 1-hour averaging period. For periods of 3 minutes to 256 seconds the corresponding turbulence intensity is about 0.10.
This value is in very good agreement with the measured data of the undisturbed wind speed.

Bin-sorting

The 3-minute (and 256 s respectively) samples were sorted into different bands of undisturbed wind speed and wind direction. Between 5 m/s and 12 m/s a bin width of 1 m/s was used; above 12 m/s the bin width was taken equal to 2 m/s. The selected wind direction bin width was 2.5°.

For each bin the mean value, variance, minimum and maximum values of the measured quantities were determined and saved in separate files. Together with these quantities the number of samples in the bin, the average undisturbed wind speed and the average wind direction were saved.

Since the wind turbines operate at constant tip speed ratio in the interval 6-10 m/s, it was expected that the wake effects would not vary much over this speed range. The data analysis confirmed this statement.

Wake deficit

Figure 2 shows the wind speed ratio U/U_0 at several sensors at 4 D as a function of the undisturbed wind direction for the wind speed classes between 6 m/s and 12 m/s.

Figure 3 shows the wind speed ratio U/U_0 at 2.5, 5.5 and 8 D. The measurements have been compared with calculations carried out with a wind farm code developed by CRES (Greece) and LIMSI (France). A wind direction of 0 degrees here corresponds with the direction along the line T18-T27. The calculations show good agreement.

Turbulence intensity

Figure 4 shows the turbulence intensity (non-dimensionalized with U_0) of the horizontal wind component U at 2.5, 5.5 and 8 D as a function of the undisturbed wind direction. In the 2.5 D case the turbulence intensity profile shows peaks at a wind direction of approximately ± 12 degrees, which corresponds with the locus of the maximum wind speed gradient (see figure 3). This is supposed to correspond with maximum turbulence production.

The shape of the profile differs strongly if the local mean wind speed U is used (figure 5). Figure 6 shows the results of the turbulence intensity of the V-component. The shape of the profile is more peaked than that of the U-component, but the maximum values are about equal.

Turbulent kinetic energy

The turbulent kinetic energy k is defined as half of the sum of the variances of the three wind components:

$$k = 0.5\ (u'^2 + v'^2 + w'^2)$$

Figure 7 shows the turbulent kinetic energy k (non-dimensionalized with U_0^2) as a function of the wind direction. The behaviour of k is roughly the same as that of the U-component of the turbulence. Non-dimensionalized with the local wind speed k varies much more smoothly with the wind direction.
The results derived from the measurements at 2.5 D have been compared with the aforementioned wind farm code. This code has also been used in combination with a model developed by UPM (Spain). Preliminary results are shown in figure 8. The agreement between calculations and measurements is striking.

Shear stress

The Reynolds-stress u'v' is the turbulent shear stress which is the driving force for the recovery of the wake deficit in horizontal direction. Figure 9 shows the shear stress u'v' non-dimensionalized with the undisturbed wind speed U_0 against the undisturbed wind.
Eddy-viscosity theory for turbulence assumes that the turbulent shear stress is proportional to the local shear. This is clearly reflected in the curves of figure 9. Outside the wake no horizontal wake effect is present and hence the horizontal wind gradient is zero. At the maximum gradient dU/dy shear stress reaches a maximum, after which it decreases to zero, where the wind speed shows a minimum, i.e. at the wake centre. For larger wind directions the shear shows a similar behaviour but of an opposite sign. The fact that the curves return to zero at the edge of the wake, and that they cross the x-axis at 0° wind directions gives confidence in the quality of the data. Scaling of the data with U_0 seems to be successful.

The u'w'-component at the 3 different heights at 2.5 D is given in figure 10. Apparently there is hardly a u'w'-component at hub height (35 m). This can be explained by the fact that sensor is at the symmetry plane of the wake.
Indeed the sensors at different positions show a significant u'w'-component variation over the wind directions. This can be explained as follows (see also figure 11). The shear stress u'w' is proportional to the vertical wind speed gradient dU/dz. Outside the wake the u'w' is negative corresponding the shear stress in the atmospheric boundary layer. Traversing the wake at the top sensor (47 m), the vertical gradient increases with the increasing wake effect and so u'w' becomes more negative. At the bottom sensor (23 m) the situation is different. When the wind direction changes the wake effect becomes stronger; the wind gradient and hence u'w' changes sign.

Power spectral density

The time series have been processed and transformed into power spectral density functions (PSD's). The measured PSD's have been compared with the theory. To this end the ESDU spectrum, based on the von Karman spectral equations (ESDU 1985), has been used. In neutral atmospheric wind conditions, which appears among others during periods of wind speeds higher than about 6 to 8 m/s, PSD's can be

described with one single expression for each wind speed component:

$$n \times S_u(n)/\sigma_u^2 = 4 \times n'/(1+70.8 \times n'^2)^{5/6}$$

$$n \times S_v(n)/\sigma_v^2 = 4 \times n' \times (1+755.2 \times n'^2)/(1+283.2 \times n'^2)^{11/6}$$

in which $n' = n\ {}^xL_i/U$, n being the frequency, U the mean wind speed and ${}^xL_i$ the integral turbulence length scale in x-direction for i=u and i=v respectively. The PSD's are presented in these non-dimensional parameters.

The shape of the PSD in the undisturbed flow is in very good agreement with the one of ESDU (signal U72 in figure 12). The increase of the energy at the highest frequencies is caused by aliasing: the energy in the frequencies above the sampling rate is folded into the measured frequency rate. This is due to the transformation routine.

In spite of the small number of blocks still no difference could be found between the shape of the PSD's of the single wake data and those of ESDU. This holds for all positions in the wake. Some examples of the PSD's are given in figures 13 and 14 (signals A2 and C2 respectively). The difference between ESDU and measured PSD's at the higher frequencies is due to the response function of the anemometers.

Integral turbulence length scale

According to ESDU 1975 the integral turbulence length scale for the U- and the V-component are:

$${}^xL_u = 25 * z^{0.35}/z_0{}^{0.063}$$

$${}^xL_v = 5.1 * z^{0.48}/z_0{}^{0.086}$$

For z = 35 m (hub height) and z_0 = 0.05 m the results are 105 and 36 m respectively. For z = 20 and z = 50 m the results are 86 and 119 m for the U-component and 28 and 43 m for the V-component.

Panofsky & Dutton 1984 (p.176) state that the derivation of the length scales from atmospheric data can not be well defined. Besides the methods to derive the length scales differ very much. At last we would like to remark that the number of blocks is very low and thus the results, as far as the length scales are involved, are not very reliable from a statistical point of view.

The method we used to derive the length scales is to fit the resulting data on the high frequency part of the theoretical PSD, i.e. frequencies above the frequency where the PSD has its maximum value. Due to the small number of blocks (in most bins) and the relatively short length of the blocks it is difficult to detect the maximum value of the measured PSD. Apart from the reliability of the method and the number of data deviations of 10 to 20% in the individual results are possible.

The determination of the length scales has only been carried out in case the number of blocks in a bin is at least 2. For the undisturbed wind (signal U72) we found values between 50 and 140 m (figure 15). Although these values do not deviate more than about 50% of the theoretical values from ESDU, the results endorse the opinion of Panofsky & Dutton. However, if the length scales of the 4D single wake data are divided by the corresponding length scales of U72, the wake shape is quite clear. This length scale ratio is shown in figure 16 as a function of the wind direction. At the centerline this ratio is about 0.25, which is about twice as small as the wind speed ratio at that point.

Conclusions

The measurement campaigns in the Dutch Experimental Wind Farm at Sexbierum have resulted in a useful data base for the validation of wake and wind farm models and for input to wind turbine load calculation programs. The data base has been analyzed with respect to the undisturbed wind conditions, i.e. with respect to wind speed and wind direction outside the wind farm.

The undisturbed wind conditions have been determined. The upstream roughness length was derived from the turbulence intensity.

The turbulence profile strongly depends on scaling parameter U_0 or U_w. If U_0 is used the u-component of the turbulence intensity shows peaks at the maximum wind speed gradient. This also holds for the turbulent kinetic energy. The other components lack such a peaked shape and have a much more smooth course.

The shear stresses have been measured successfully. The course of the individual shear stresses can be explained qualitatively by making some simple assumptions about the wind speed gradient in the wake.

The shape of the PSD, expressed in non-dimensional terms, does not change in wake situations. The integral length scale of the turbulence can easily be derived by fitting measured PSD's on a theoretical function of the PSD. This seems independent of the lateral or vertical position in the wake.

The length scale ratio equals one at the edge of the wake and reaches its smallest value at the centerline. This ratio decreases moving from the upstream wind turbine in the wind speed direction.

A length scale ratio has been defined, i.e. the length scale derived from measured data in the wake divided by the length scale simultaneously derived from measured data in the undisturbed wind. The shape of this length scale ratio is similar to the one from the wind speed ratio. The 'deficit' however is larger. The smallest value (at the centerline of the wake) is about 0.25 which is about 0.50 times the smallest value of the wind speed ratio.

Large data sets are required to give reliable results, especially for the PSD's, the integral length scale of the turbulence and most of all the coherence functions.

References

Beljaars, A.C.M.;
The measurements of gustiness at routine wind stations - A review;
WMO instruments and observing methods, report no. 31, Genève, 1987.

Bendat, J.S. and Piersol, A.G.;
Random data - Analysis and Measurement procedures; 2nd edition;
J. Wiley & Sons, New York, 1986.

Cleijne, J.W.;
Results of Sexbierum Wind Farm - double wake measurements;
TNO Environmental and Energy Research, 92-388, Apeldoorn, November 1992.

Cleijne, J.W.;
Results of Sexbierum Wind Farm - single wake measurements;
TNO Environmental and Energy Research, 93-082, Apeldoorn, March 1993.

ESDU;
Characteristics of atmospheric turbulence near the ground. Part III: variations in space and time for strong winds (neutral atmosphere);
Engineering Sciences Data Item 75001, July 1975.

ESDU;
Strong winds in the atmospheric boundary layer. Part 2: discrete gust speeds;
Engineering Sciences Data Item 83045, November 1983.

ESDU;
Characteristics of atmospheric turbulence near the ground. Part II: single point data for strong winds (neutral atmosphere);
Engineering Sciences Data Item 85020, October 1985.

Panofsky, H.A. and Dutton, J.A.;
Atmospheric Turbulence - Models and Methods for Engineering Applications;
J. Wiley & Sons, New York, 1984.

Verheij, F.J.;
Dynamic Loads in Wind Farms. Analysis of wind spectra, coherence functions and integral length scales of the turbulence;
TNO Environmental and Energy Research, 93-.., Apeldoorn, May 1993.

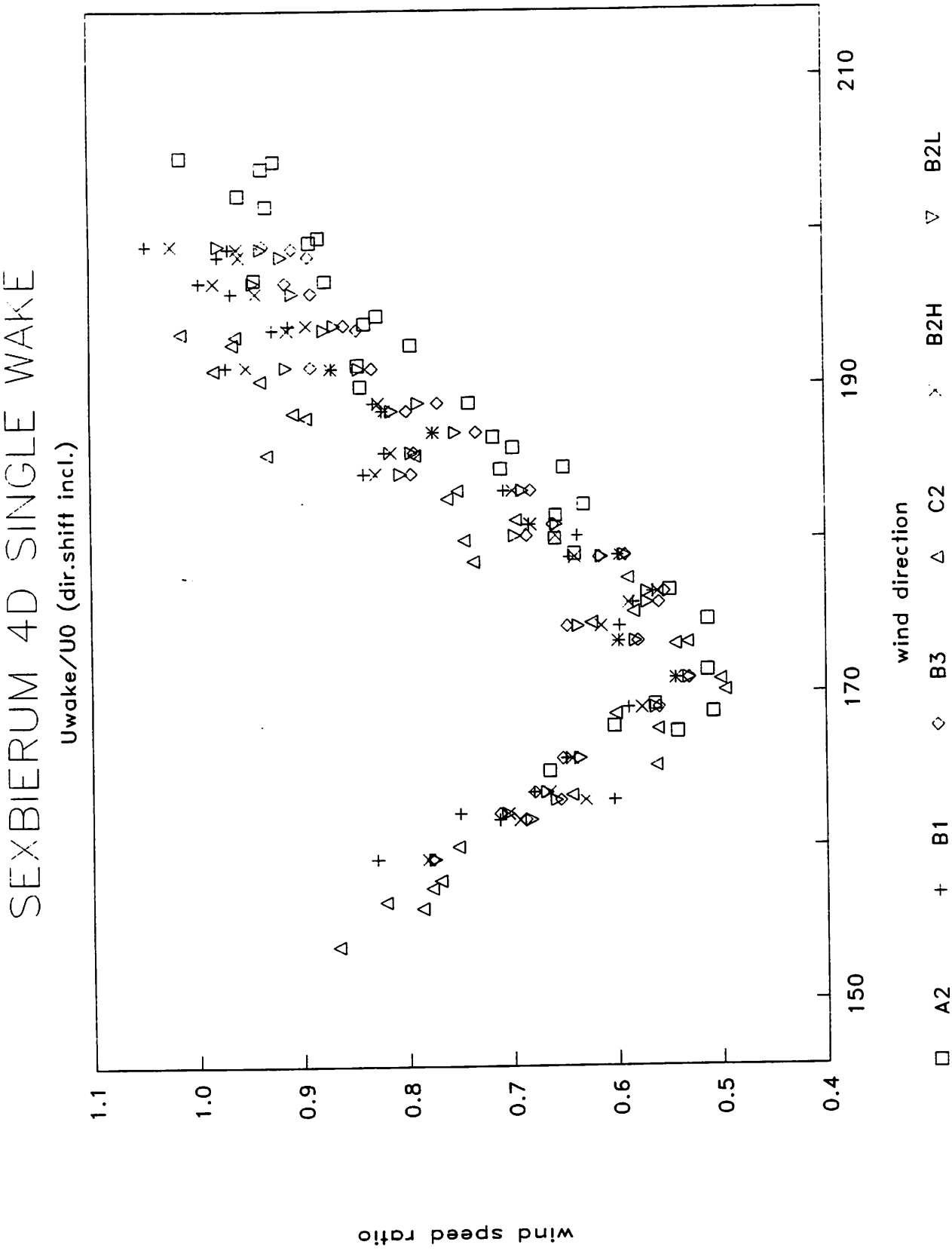
SEXBIERUM 4D SINGLE WAKE
Uwake/U0 (dir.shift incl.)
wind speed ratio
1.1
1.0
0.9
0.8
0.7
0.6
0.5
0.4
150
170
190
210
wind direction
A2
B1
B3
C2
B2H
B2L

Fig 2

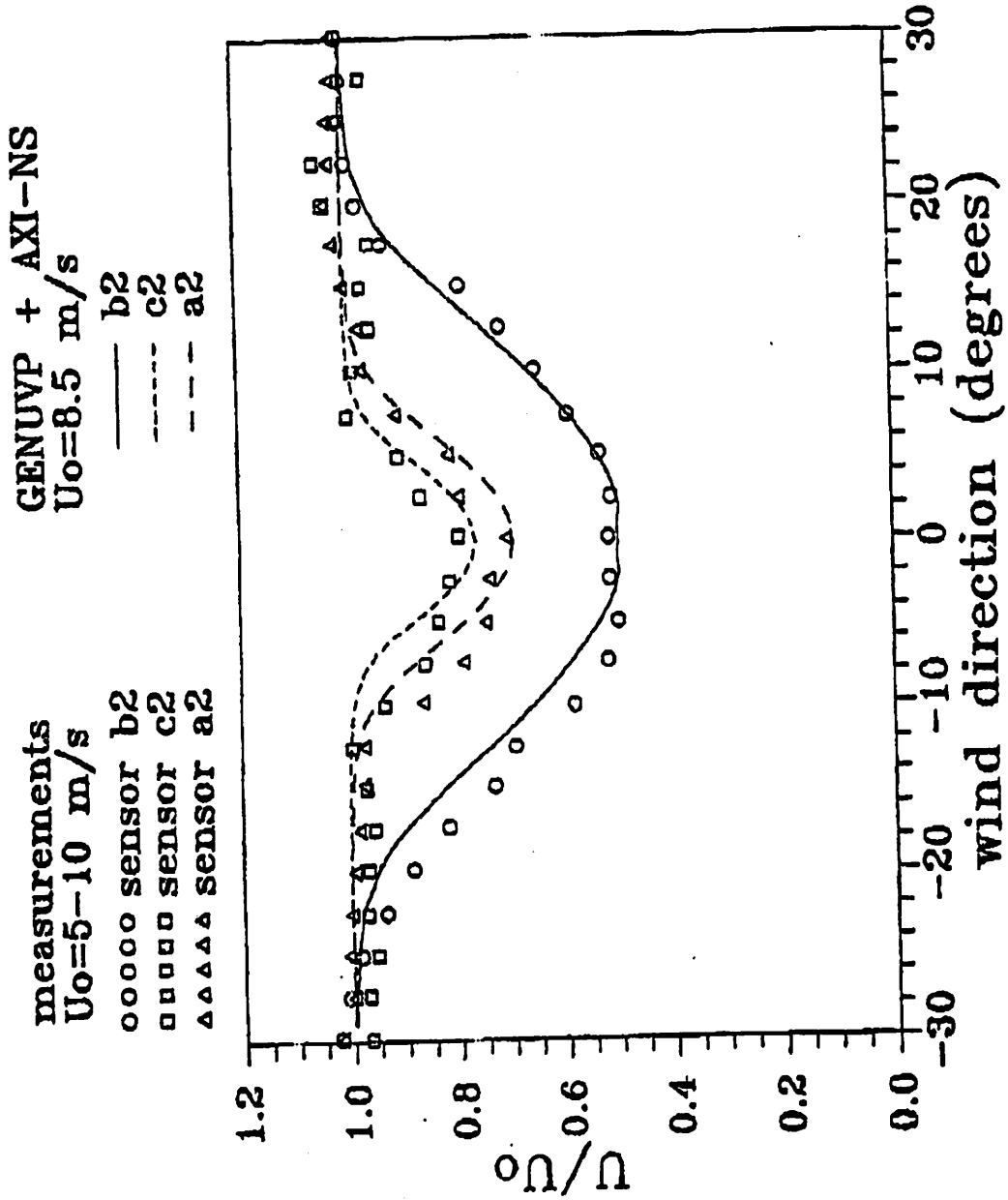
GENUVP + AXI-NS
Uo=8.5 m/s
b2
c2
a2
measurements
Uo=5-10 m/s
sensor b2
sensor c2
sensor a2
U/Uo
wind direction (degrees)
1.2
1.0
0.8
0.6
0.4
0.2
0.0
-30
-20
-10
0
10
20
30

Fig 3

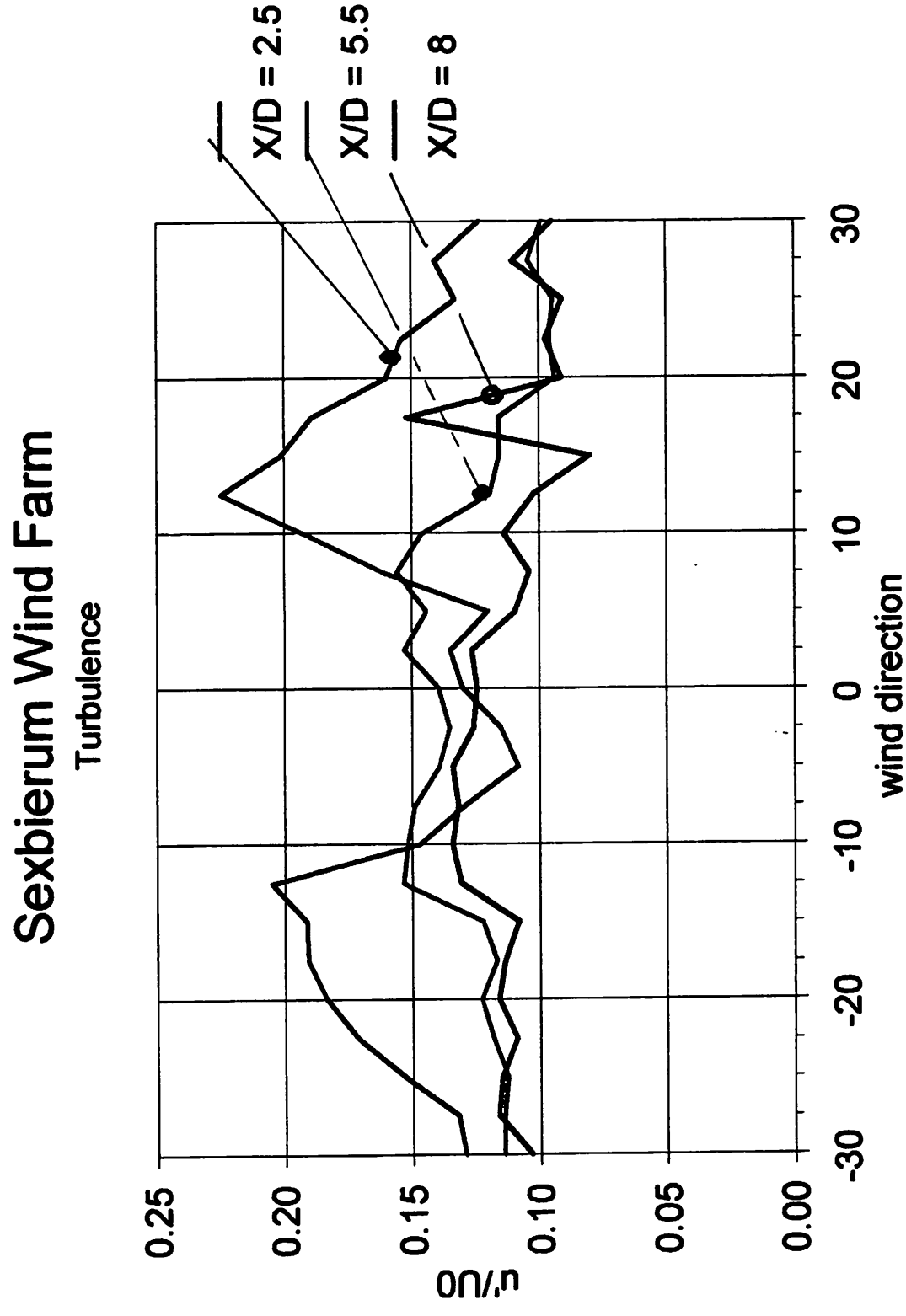
Sexbierum Wind Farm
Turbulence
X/D = 2.5
X/D = 5.5
X/D = 8
u'/Uo
0.25
0.20
0.15
0.10
0.05
0.00
-30
-20
-10
0
10
20
30
wind direction

Fig 4

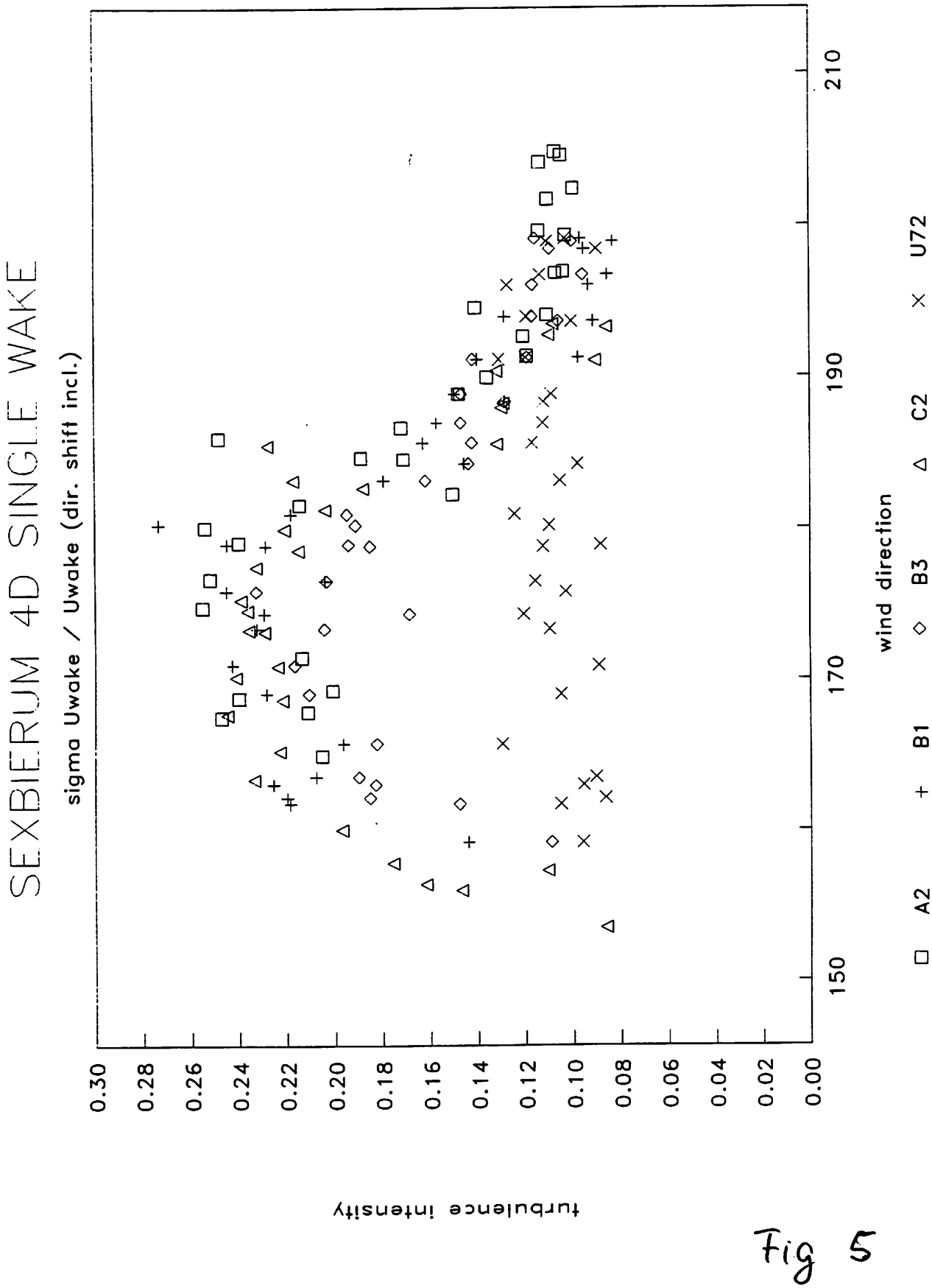
SEXBIERUM 4D SINGLE WAKE
sigma Uwake / Uwake (dir. shift incl.)
turbulence intensity
0.30
0.28
0.26
0.24
0.22
0.20
0.18
0.16
0.14
0.12
0.10
0.08
0.06
0.04
0.02
0.00
150
170
190
210
wind direction
A2
B1
B3
C2
U72

Fig 5

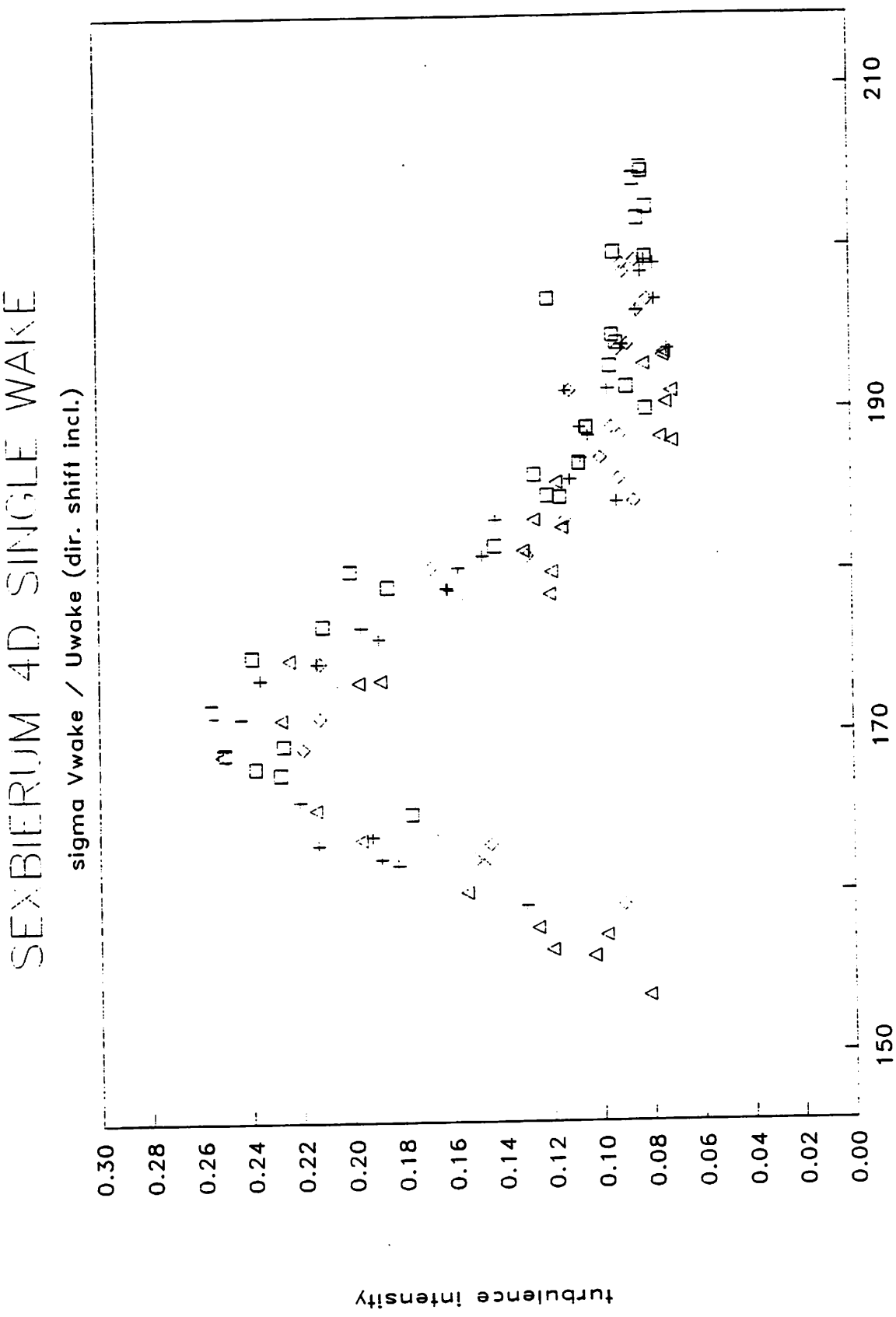
SEABIERUM 4D SINGLE WAKE
sigma Vwake / Uwake (dir. shift incl.)
turbulence intensity
0.30
0.28
0.26
0.24
0.22
0.20
0.18
0.16
0.14
0.12
0.10
0.08
0.06
0.04
0.02
0.00
150
170
190
210
wind direction
A2
B1
B3
C2

Fig 6

Sexbierum Wind Farm

Turbulent kinetic energy

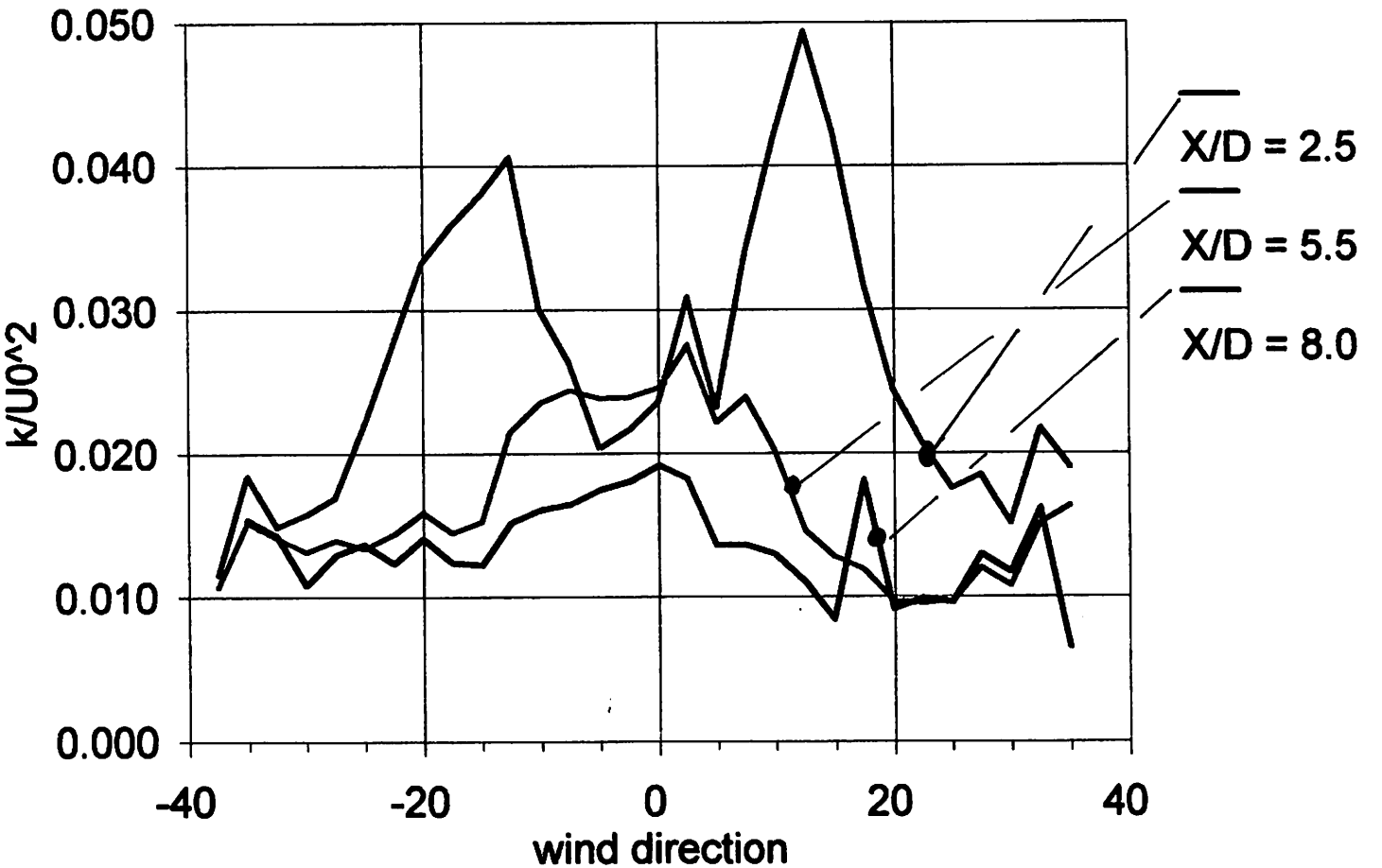

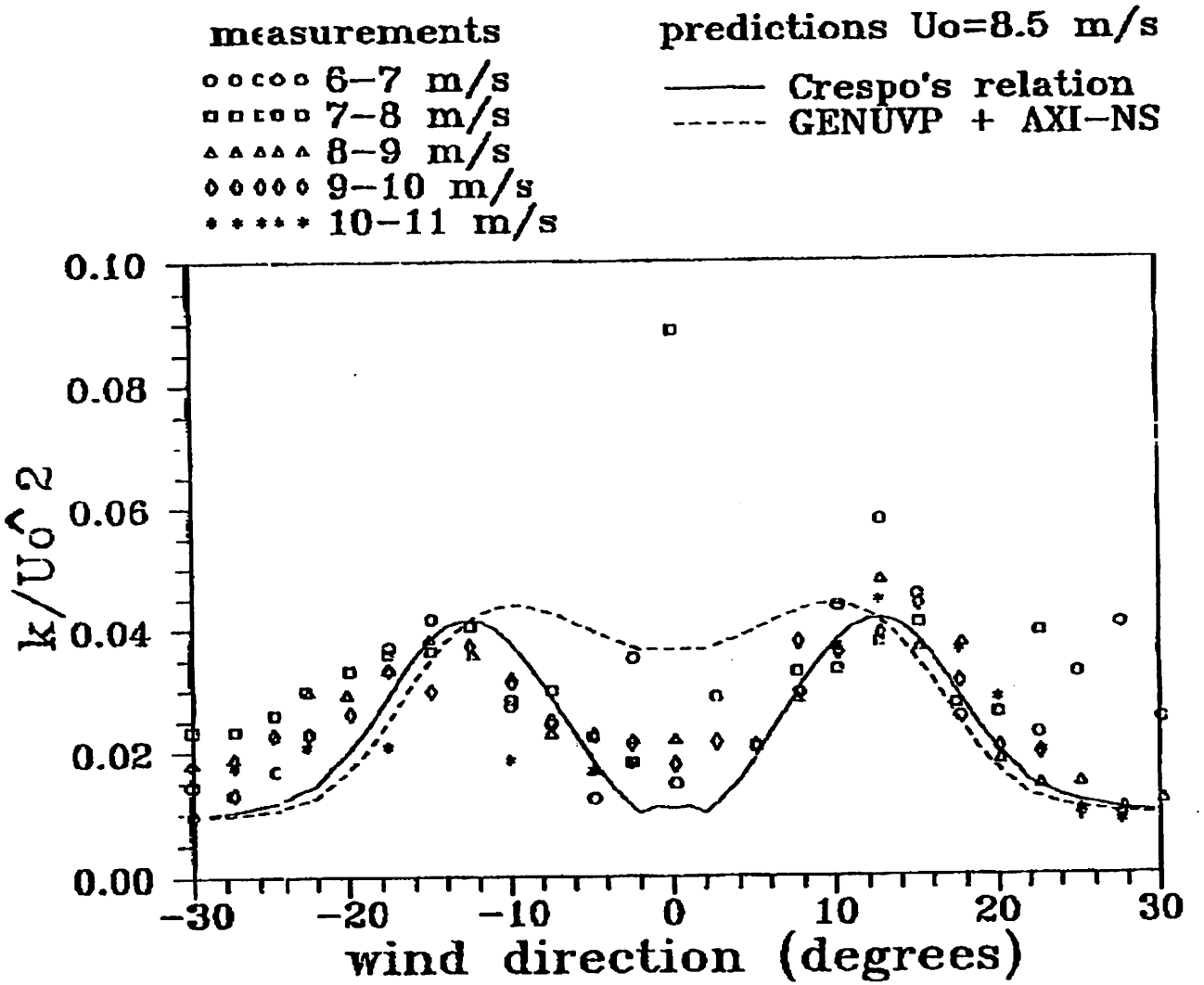
measurements
6–7 m/s
7–8 m/s
8–9 m/s
9–10 m/s
10–11 m/s
predictions Uo=8.5 m/s
Crespo's relation
GENUVP + AXI–NS
0.10
0.08
0.06
0.04
0.02
0.00
k/Uo^2
−30
−20
−10
0
10
20
30
wind direction (degrees)

Fig 8

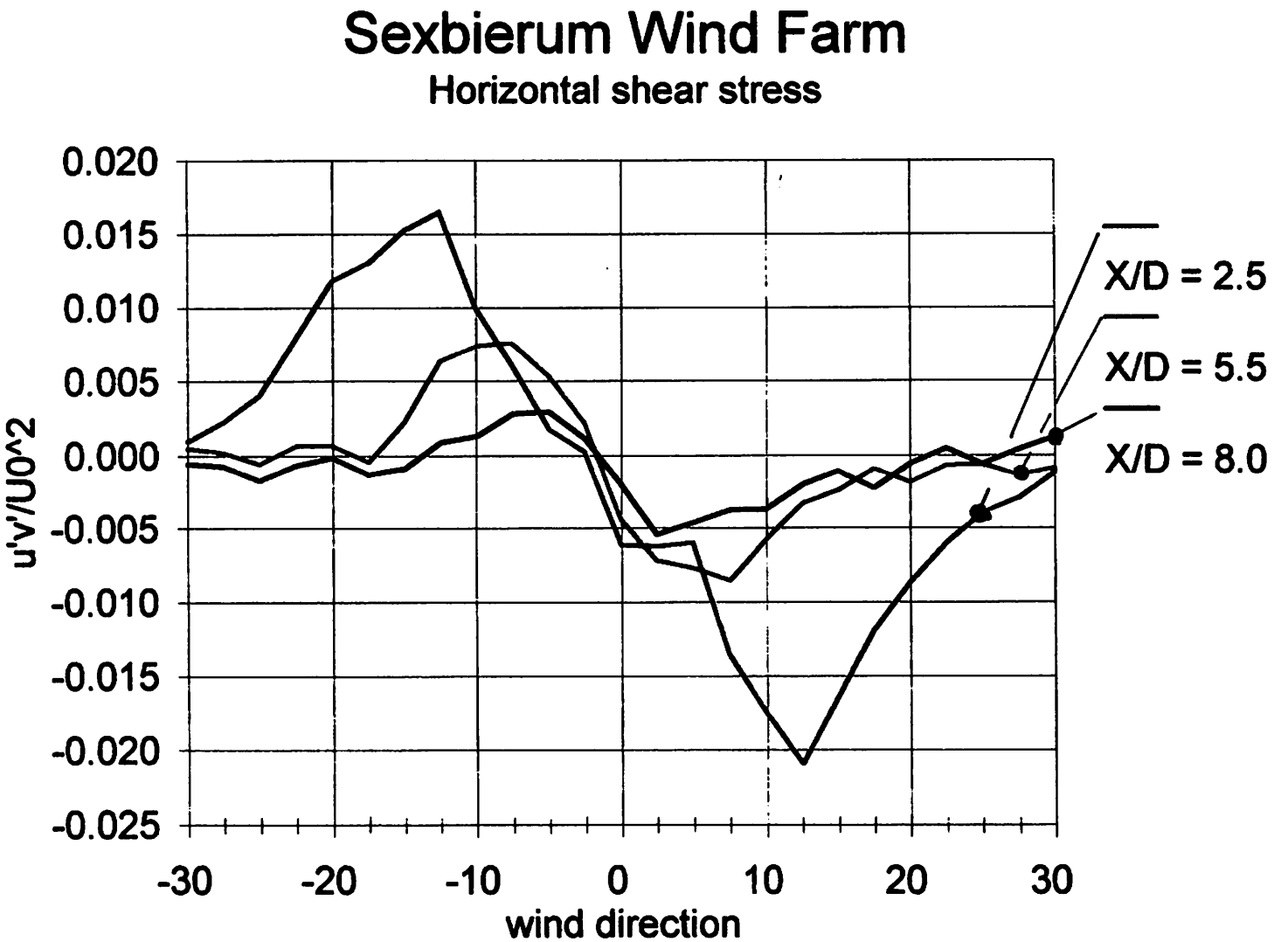
Sexbierum Wind Farm
Horizontal shear stress
0.020
0.015
0.010
0.005
0.000
-0.005
-0.010
-0.015
-0.020
-0.025
u'v'/U0^2
-30
-20
-10
0
10
20
30
wind direction
X/D = 2.5
X/D = 5.5
X/D = 8.0

Fig 9

Sexbierum Wind Farm

Vertical shear stress (X/D =2.5)

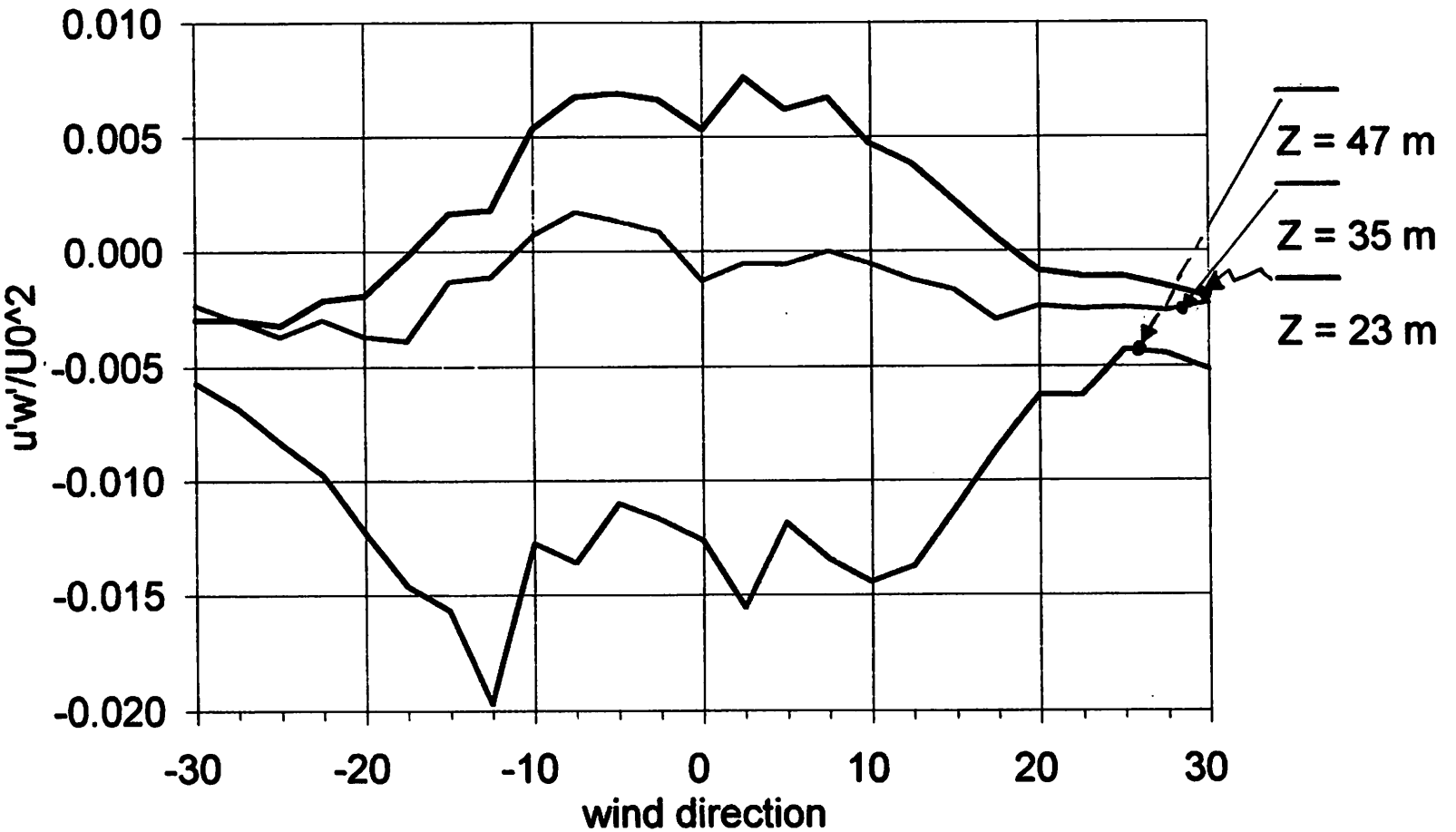

Fig 10

Results
Shear stress u'w'

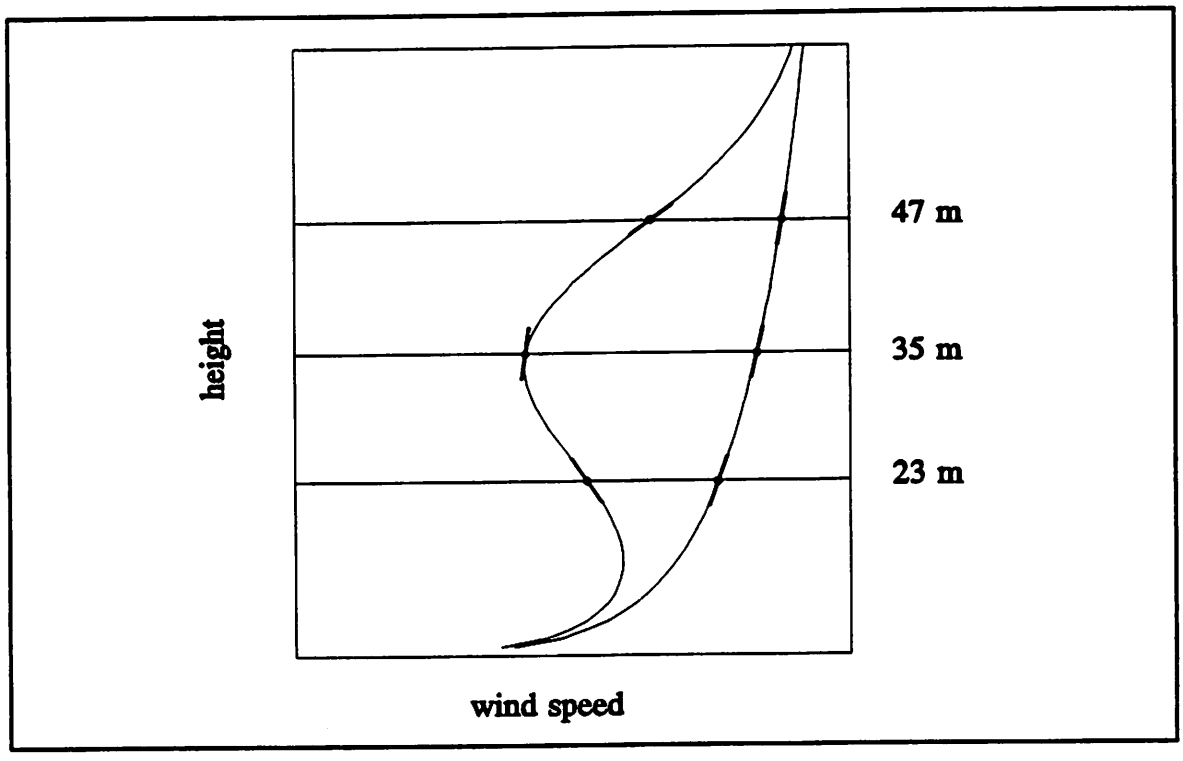

Fig. 11

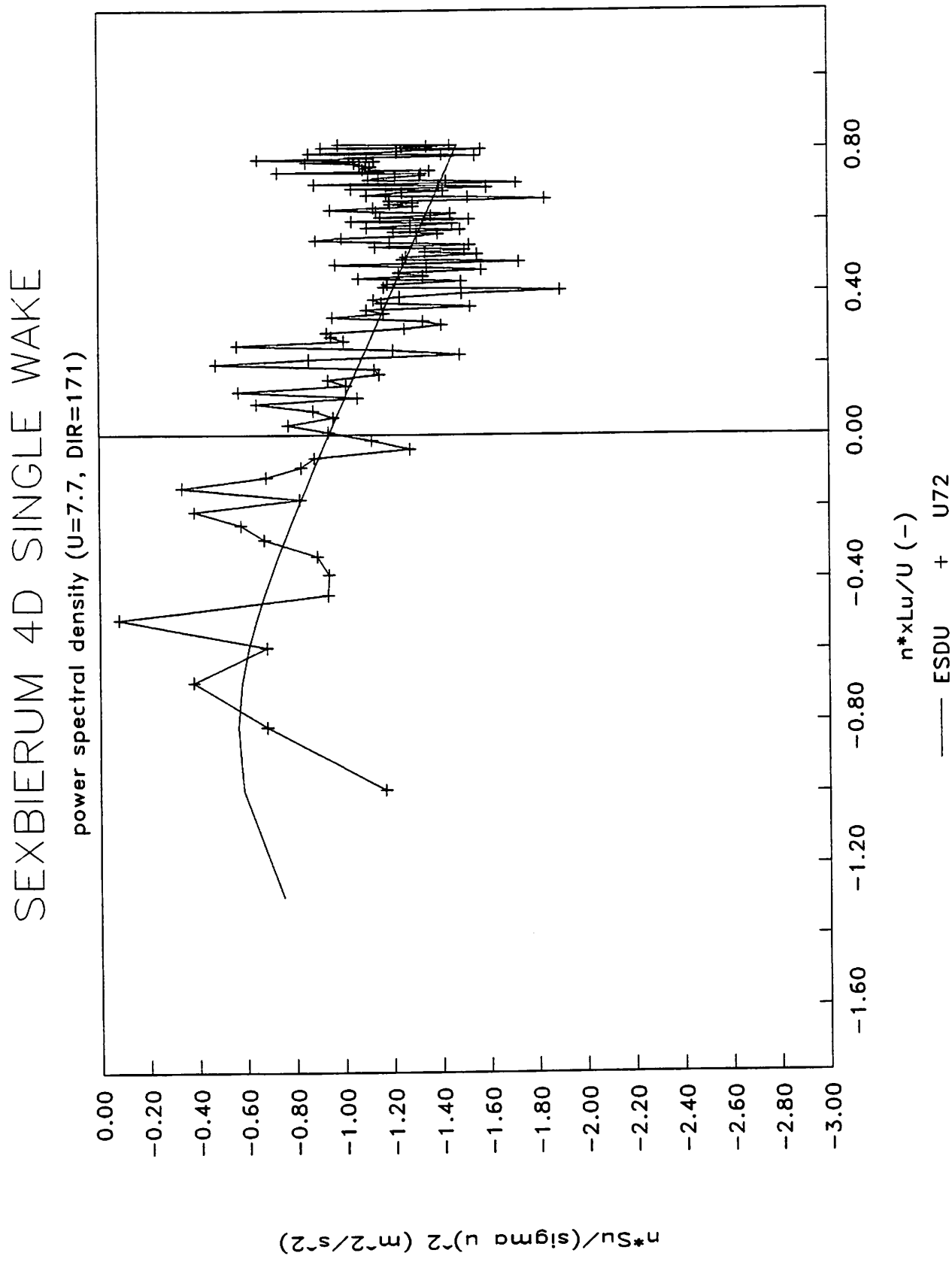
SEXBIERUM 4D SINGLE WAKE
power spectral density (U=7.7, DIR=171)
n*Su/(sigma u)^2 (m^2/s^2)
0.00
-0.20
-0.40
-0.60
-0.80
-1.00
-1.20
-1.40
-1.60
-1.80
-2.00
-2.20
-2.40
-2.60
-2.80
-3.00
-1.60
-1.20
-0.80
-0.40
0.00
0.40
0.80
n*xLu/U (-)
ESDU + U72

Fig 12

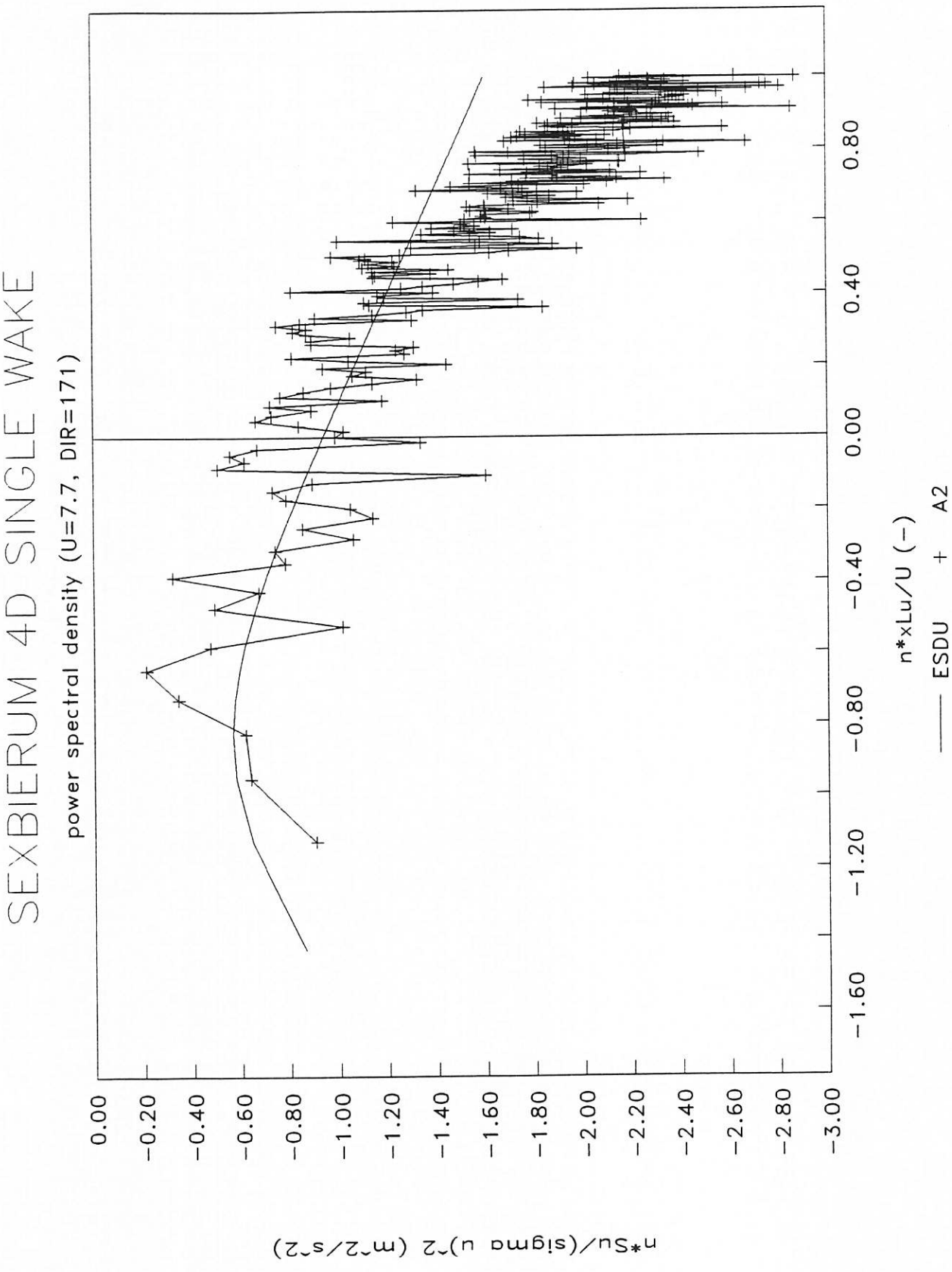
SEXBIERUM 4D SINGLE WAKE
power spectral density (U=7.7, DIR=171)
n*Su/(sigma u)^2 (m^2/s^2)
0.00
-0.20
-0.40
-0.60
-0.80
-1.00
-1.20
-1.40
-1.60
-1.80
-2.00
-2.20
-2.40
-2.60
-2.80
-3.00
-1.60
-1.20
-0.80
-0.40
0.00
0.40
0.80
n*xLu/U (-)
ESDU
A2

Fig 13

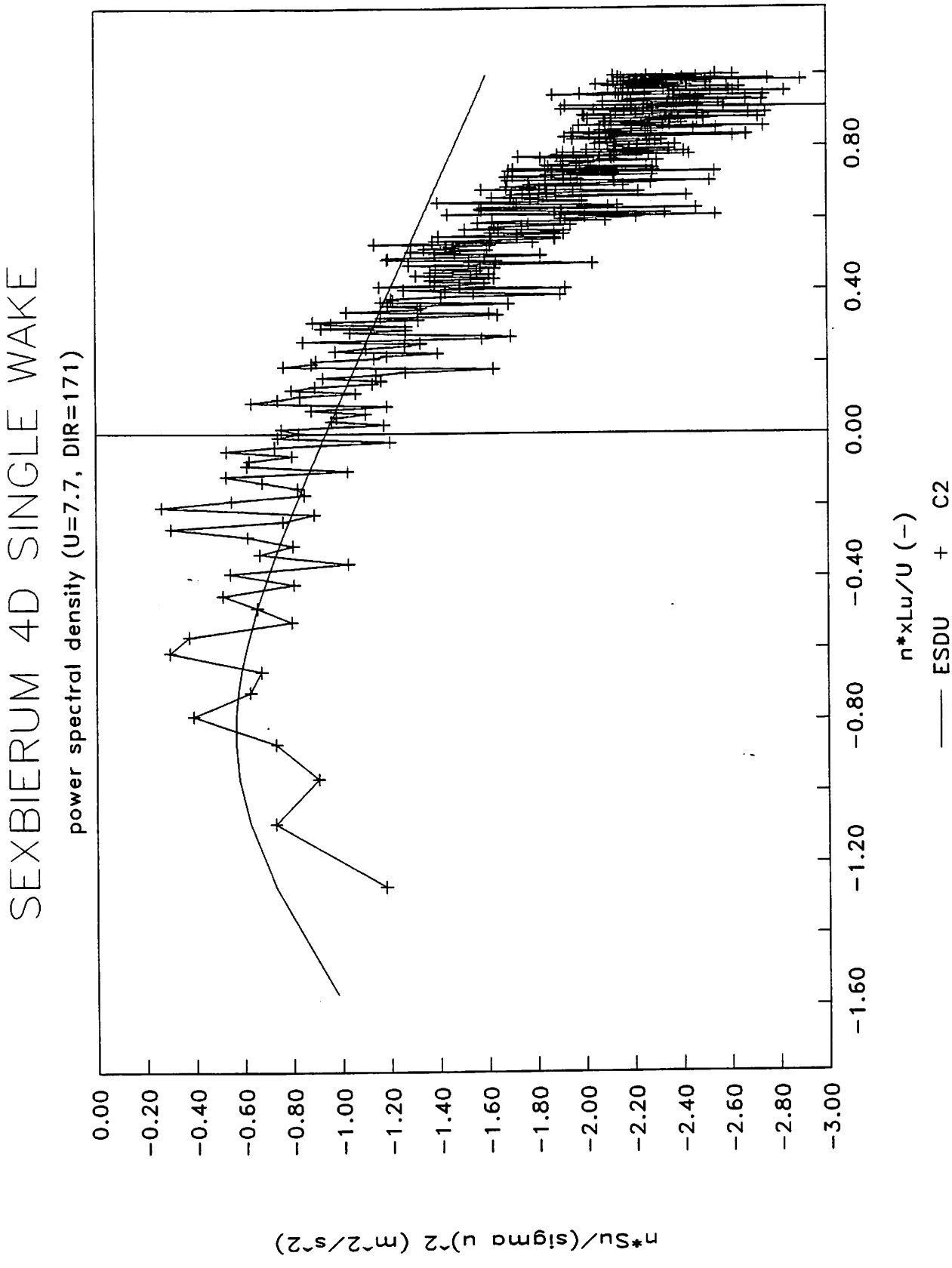
SEXBIERUM 4D SINGLE WAKE
power spectral density (U=7.7, DIR=171)
n*Su/(sigma u)^2 (m^2/s^2)
0.00
-0.20
-0.40
-0.60
-0.80
-1.00
-1.20
-1.40
-1.60
-1.80
-2.00
-2.20
-2.40
-2.60
-2.80
-3.00
0.80
0.40
0.00
-0.40
-0.80
-1.20
-1.60
n*xLu/U (-)
ESDU + C2

Fig 14

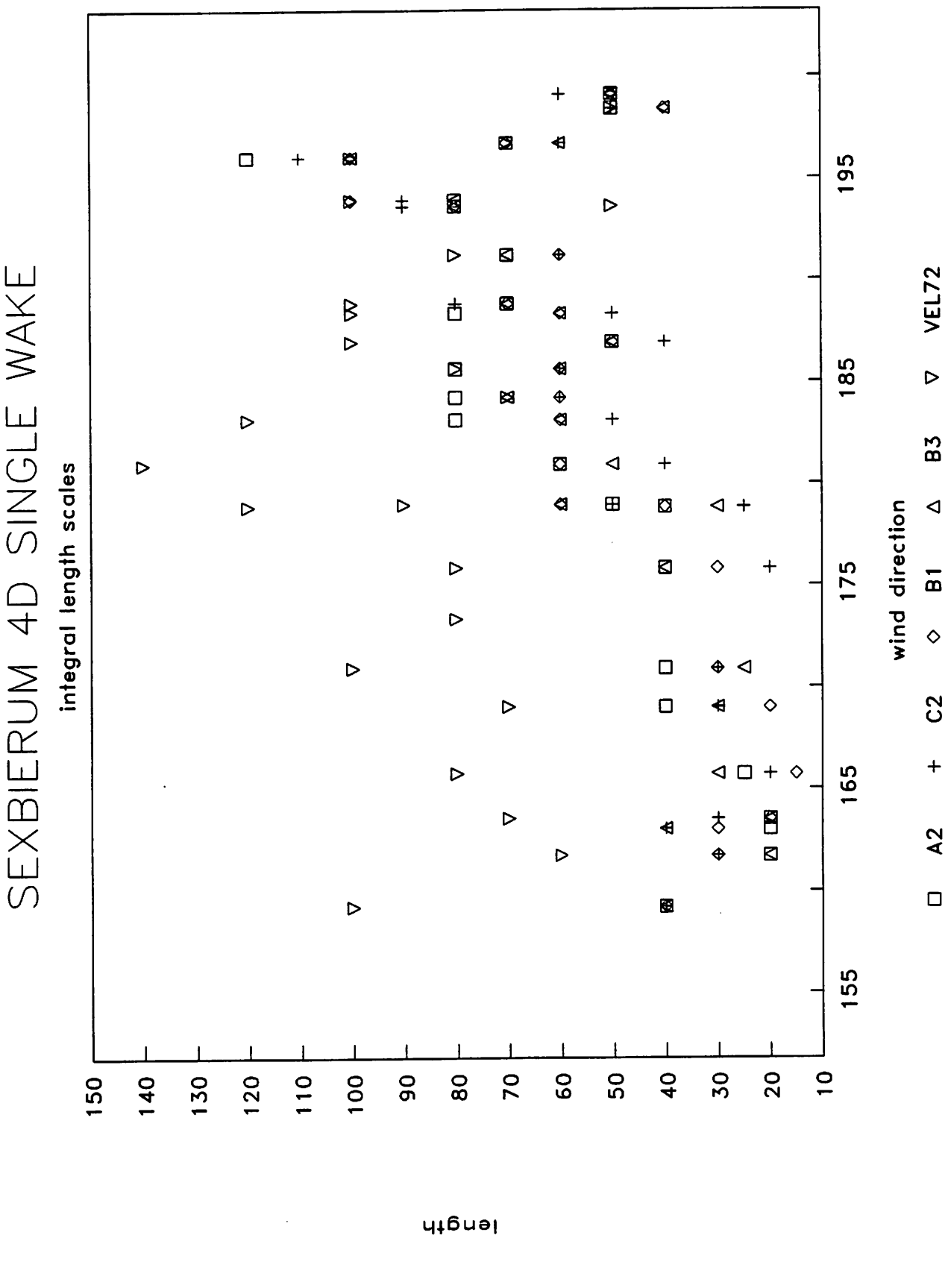
SEXBIERUM 4D SINGLE WAKE
integral length scales
length
150
140
130
120
110
100
90
80
70
60
50
40
30
20
10
155
165
175
185
195
wind direction
A2
C2
B1
B3
VEL72

Fig 15

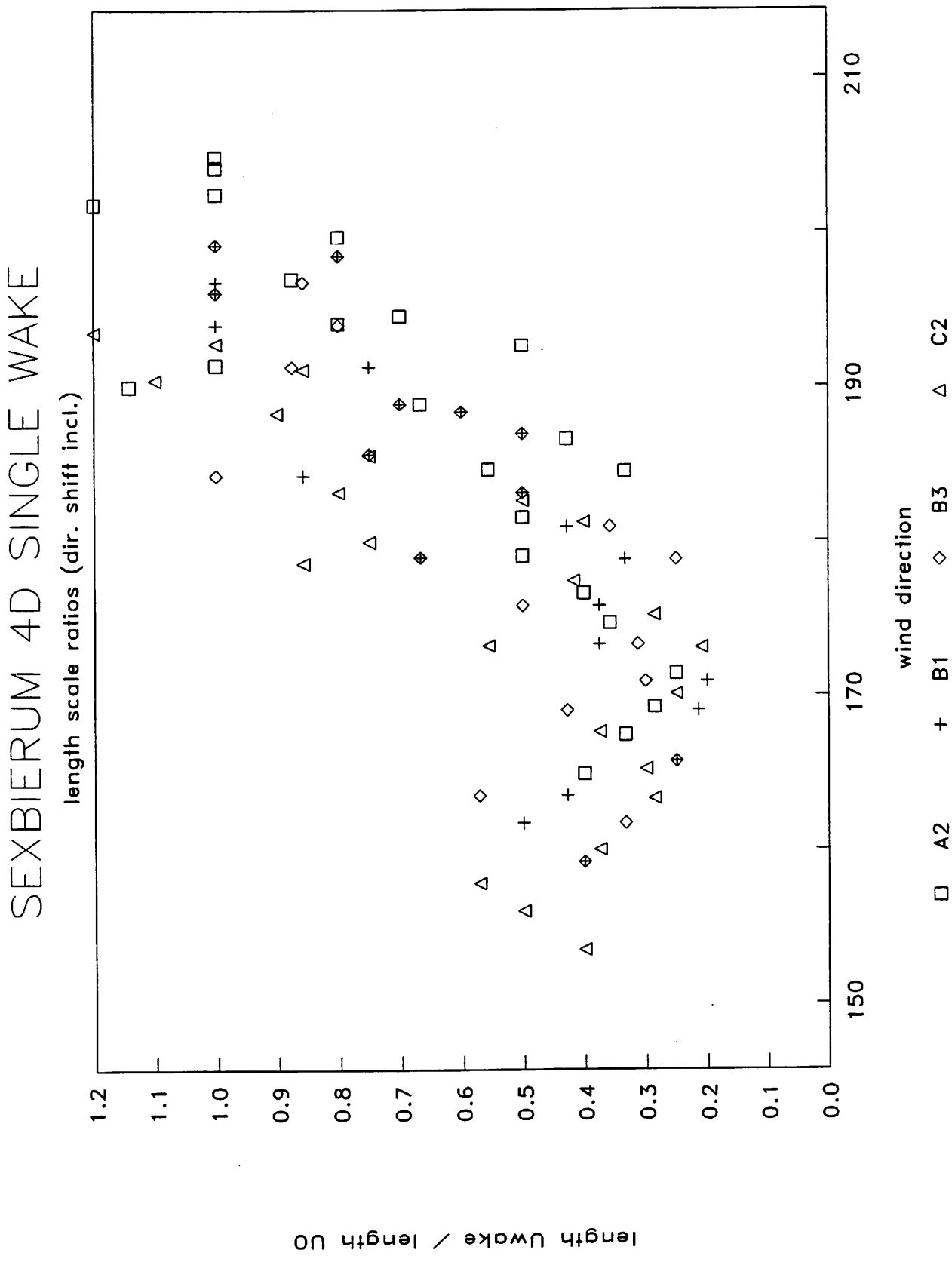
SEXBIERUM 4D SINGLE WAKE
length scale ratios (dir. shift incl.)
length Uwake / length U0
1.2
1.1
1.0
0.9
0.8
0.7
0.6
0.5
0.4
0.3
0.2
0.1
0.0
150
170
190
210
wind direction
A2
B1
B3
C2

Fig. 16

Wake measurements at Alsvik, Sweden

by

Mikael Magnusson
and
Ann-Sofi Smedman
Department of Meteorology
Box 516
S-785120 Uppsala
Sweden

1. INTRODUCTION.

For large scale exploitation of wind energy it will be necessary to site wind turbines not only in flat coastal areas but also in rough inhomogeneous terrain. In order to maximize the use of costly land with a suitable wind resource, wind turbines will also be put together in wind parks, where they will interact with each other.

All this is bound to create potential problems in terms of excessive loads on the turbines. The purpose of this investigation is to study blade loads of a stiff wind turbine working in the wake of another turbine and to express these loads in terms of basic and relatively easily measured parameters. The model is intended to be used in siting investigations. So far the model has only been tested for stand-alone turbines without wakes.

A time simulation model ,VIDYN (Ganander, 1989), has been used to separate the effect on loading from two meteorological factors; turbulence intensity and wind shear. The bending moment can thus be calculated from measurements of σ_u/U and $\Delta U/U$ (Smedman, 1992).

$$(\sigma_m/M)^2 = (C_1 \cdot I_a) + (C_2 \cdot (\Delta U/U)_a)^2$$

where M = mean flap moment, m = fluctuating flap moment, U = mean wind speed, ΔU = difference in mean wind speed over the rotor, $I_a = (\sigma_u/U)_a$ = turbulence intensity in the ambient air, $C_1 \sim C_2 \sim 1$, a = ambient air.

The model has been tested for two turbines. The result for the Näsudden turbine (Smedman, 1992) is showed in Figure 1 and for the Alsvik turbine number 4 (see below) in Figure 2 (Smedman, 1993). The measured and calculated mean flap moments are about the same but the scatter are large. In Figure 3 a comparison between a measured and a calculated time series is shown. Again the mean values are about the same but the variation is much larger in the calculated one.

The turbulence intensity and $\Delta U/U$ can be expressed as a function height (z), roughness (z_0) and stability (Ri).

I the wake behind a turbine the mean wind speed is reduced and the turbulence intensity is increased. This will create an added wind shear and an added turbulence intensity, which magnitudes will decrease with distance. Thus I_{add} and $(\Delta U/U)_{add}$ can be expressed as a function of z, Ri, the lateral distance y and the down wind distance x.

2. THE SITE.

The Alsvik wind farm consists of four Danwin 23/180 kW machines situated only ca 50 m from the shoreline on a very flat coastal strip on the west coast of the island Gotland in the Baltic, Figure 4. The turbines are three-bladed, with a diameter of 23 m and hub height of 30 m. They are stall-regulated and have a rated power of 180 kW each. Wind speed and direction are measured at 8 heights on two 54 m-towers and the temperature profile on mast 1 (see Figure 4). The distance between turbines T1 and T4 is 9.6D (D = turbine diameter), between T2 and T4 4.2D and between T3 and T4 6.1D. For a large wind direction sector mast 1 will thus measure the undisturbed wind and mast 2 wakes at the three different distances.

The data set used in this investigation is collected during a period of two years, June 1990 - July 1992. For calculations of velocity deficits 1-minute averages are used and for 'added turbulence' estimates 30-minutes averages (see Magnusson, 1993).

3. VELOCITY DEFICIT.

In order to identify wake influences on mast 2 the difference in wind speed at different heights between the two masts, divided by the wind speed measured on mast 1, $\Delta U_a /U$ has been evaluated.

$$\Delta U/U_a = (U_a - U_{wake})/U_a$$

where U_a = ambient wind speed, U_{wake} = wind speed in the wake and both are measured at the same height.

The atmospheric stability has been expressed as the Richardsson number

$$Ri = g/T_0 \cdot ((\partial\Theta/\partial z)/(\partial U/\partial z)^2)$$

where g = acc. of gravity, Θ = mean potential temperature and T_0 = a reference temperature.

Figure 5. shows the velocity deficit at the center line as a function of stability for the three distances. As can be seen from the figure the deficit increases with increasing stability and the rate of increase is largest during stable conditions. The deficit decreases as expected with distance.

Figures 6 (a, b and c) give the vertical profiles of the velocity deficit for stable and unstable conditions and for the three distances. During unstable stratification the wake is wider than in stable air but the peak value is lower compared to the stable one. The explanation is of course that mixing is more efficient during unstable conditions.

The lateral deficit profiles are shown in Figures 7 (a, b and c) for different stabilities and distances. The influence of stability is the same as for the vertical profiles in Figure 6 and the lateral extent of the wake grows with distance.

Combining Figures 6 and 7 will give cross sections of the wake for different stabilities and distances. In Figure 8 cross sections at the distance 4.2D are shown for unstable (a) and stable (b) stratification. The same is shown for 6.1D in Figure 9 and for 9.6D in Figure 10. Both in stable and unstable air the wake tends to rise a little with distance. This can be attributed to the combined effect of vorticity generated by the turbine and the vertical wind shear. The wake will also move slightly to the left, probably an effect of convergence, when the wind encounter the island. During stable stratification the wake will be tilted because of the large wind shear in the ambient air.

In analogy with dispersion of air pollution the wake has been described by a Gaussian distribution, using mirroring at the surface. The result is shown in Table 1. Comparison between measured and calculated vertical and lateral

velocity deficit profiles are made in Figures 11 and 12 for both stable and unstable conditions. The agreement is fairly good but the peak values are somewhat underestimated.

4. ADDED TURBULENCE INTENSITY.

The increase of turbulence in the wake has been expressed as 'added turbulence', which is defined as

$$I_{add} = \frac{((\sigma_u^2)_w - (\sigma_u^2)_a)^{-1/2}}{U_a}$$

In Figure 13 a the lateral profiles of added turbulence intensity are shown for the two stability classes at the distance 4.2D (a) and 9.6D (b). In the first figure (a) two separate maxima can be detected with a minimum at the center line. This is a result of maximum wind shear at about 0.4D off the center line, which will increase the production of turbulence at that point. At the distance 9.6D the turbulent mixing in unstable air has 'smeared out' the maxima, while they are still noticeable in stable air. The corresponding vertical profiles are plotted in Figures 14 (a and b). No distinct maxima can be seen in the vertical profiles, which can be attributed to the more intense vertical mixing. From the Näsudden site wake measurements at a shorter distance (2.1D) show distinct maxima also in the vertical profiles (Högström et al 1988).

Again combining the vertical and lateral profiles will result in contour plots for the added turbulence in the wake (Figures 15 a and b).

5. CONCLUSIONS.

Analysis of the velocity deficit and added turbulence in the wake behind a single wind turbine at Alsvik show how important atmospheric stability is

for the structure and propagation of the wake.

6. REFERENCES.

Ganander,H., 1989: 'Importance of yaw system of two bladed HAWT, practical and theoretical results.' Proc. European Wind Energy Conf. and Exhibition, Glasgow, July 10-13, 779-782.

Högström,U.,D.N.Asimakopoulos,H.Kambezidis,C.G.Helmis and A.Smedman: 1988, 'A field study of the wake behind a 2 MW wind turbine'. Atmospheric Enviroment, 22, 803-820.

Magnusson,M., 1993: 'Atmospheric stability effects on turbine wakes'. Proc. European Wind Energy Conf. and Exhibition, Travemünde, 8-12 Mars.

Smedman,A., 1992: 'calculations of dynamic wind turbine blade loads from simple meteorological data'. Wind Engineering, Vol 16, No 4, 195-212.

Smedman,A., 1993: 'Estimates of dynamic wind turbine loads from meteorological data. Proc. European Wind Energy Conf. and Exhibition, Travemünde, 8-12 Mars.

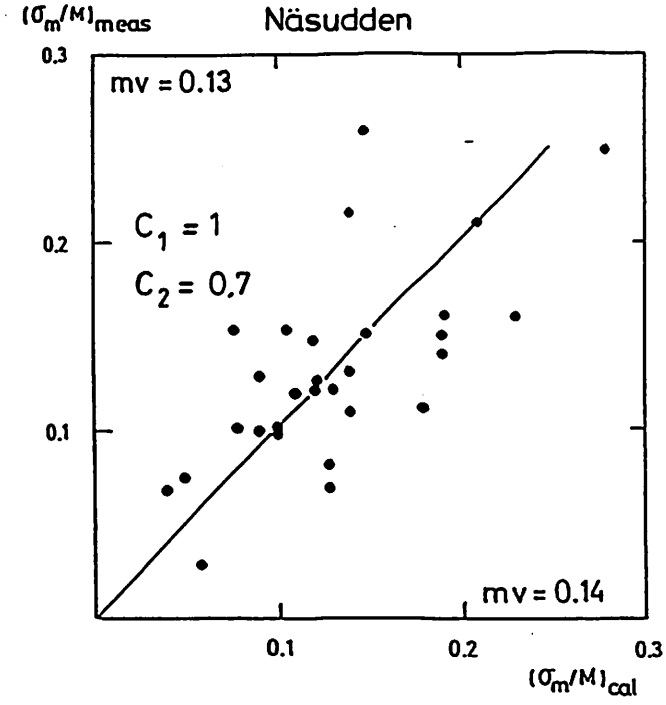

Fig 1

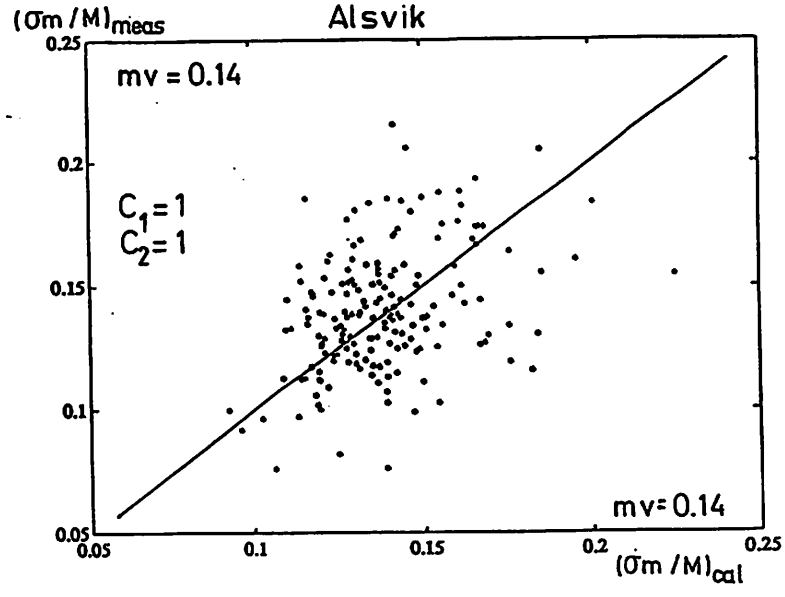

Fig 2

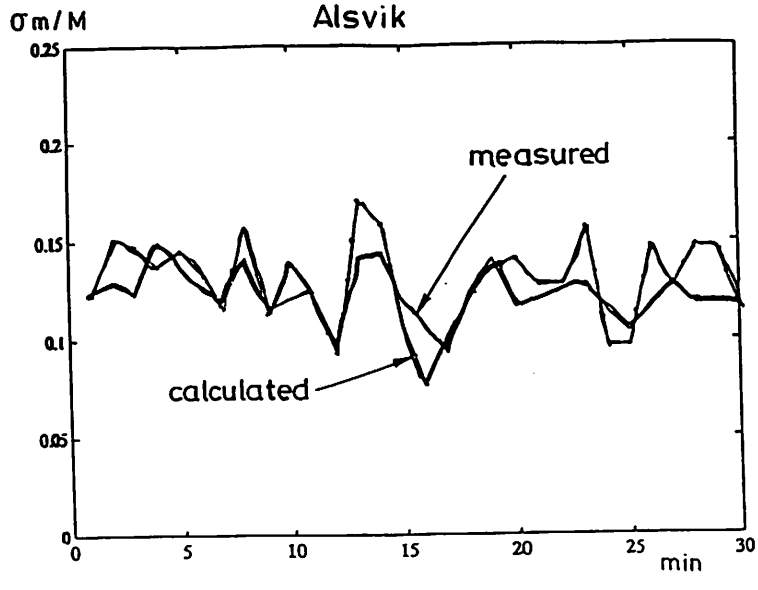

Fig 3

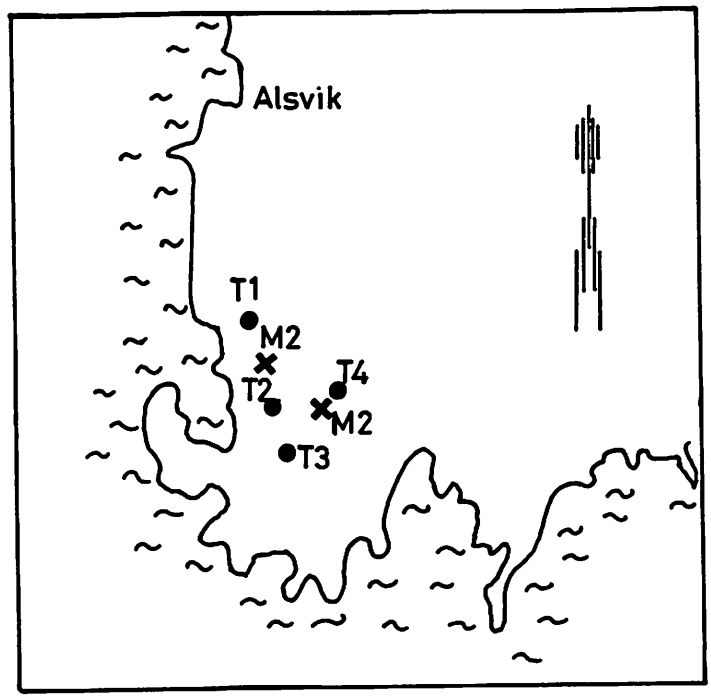
Alsvik
T1
M2
T2
T4
M2
T3

Fig 4

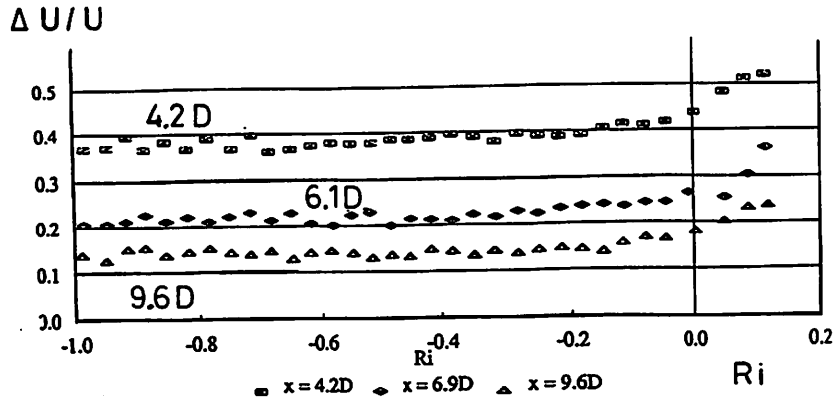
ΔU/U
0.5
0.4
0.3
0.2
0.1
0.0
4.2 D
6.1D
9.6 D
-1.0
-0.8
-0.6
-0.4
-0.2
0.0
0.2
Ri
Ri
x = 4.2D
x = 6.9D
x = 9.6D

Fig 5

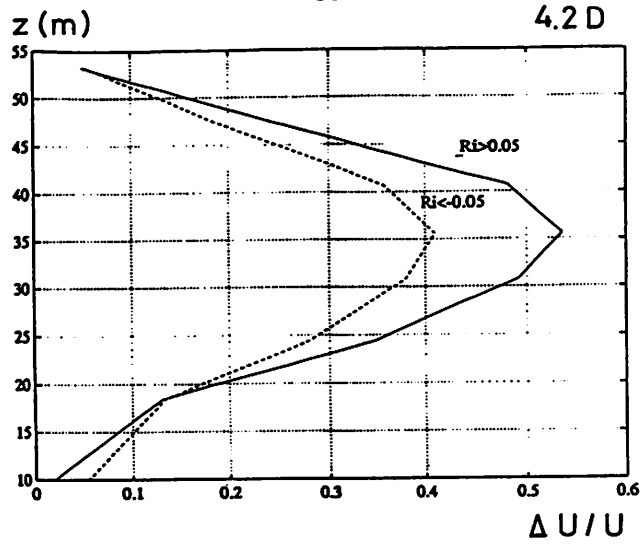

Fig 6a

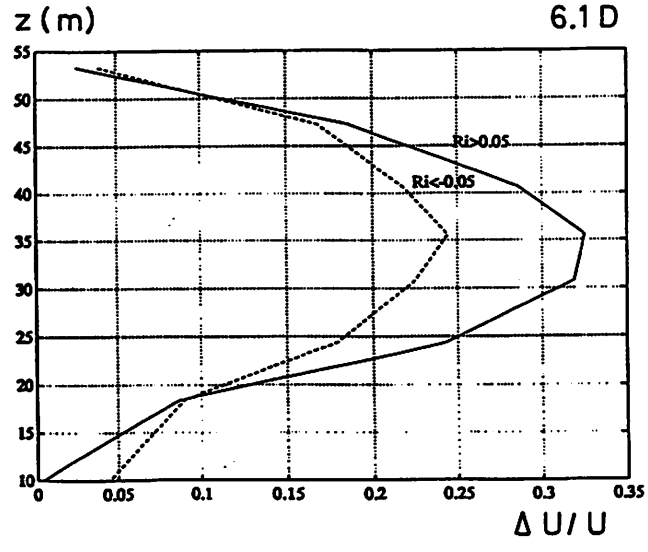

Fig 6b

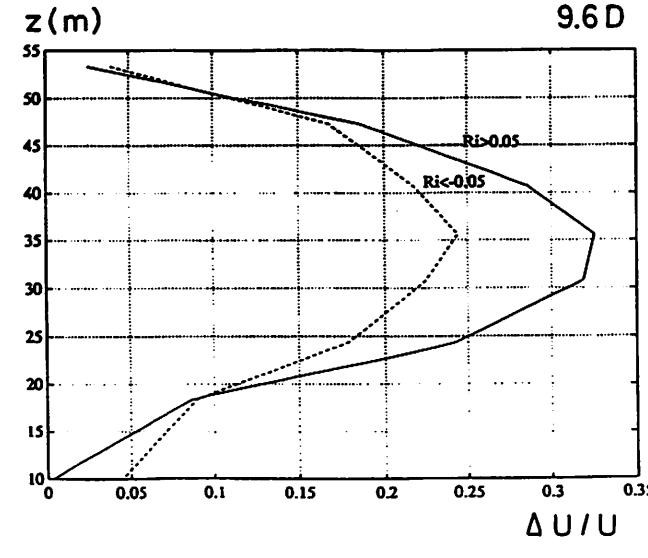

Fig 6c

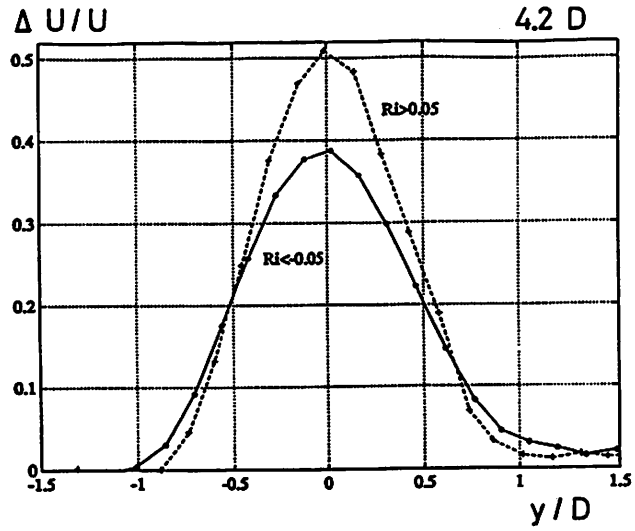

Fig 7a

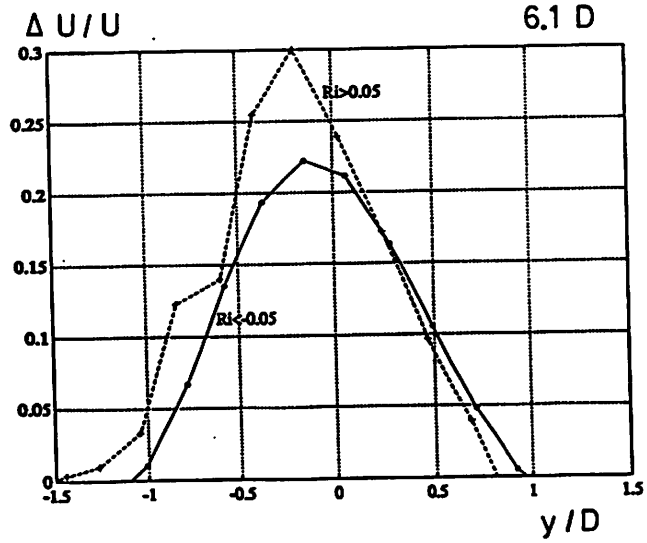

Fig 7b

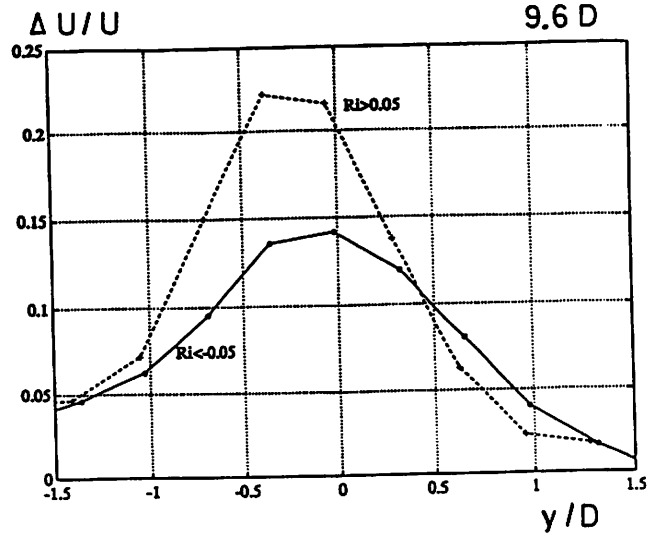

Fig 7c

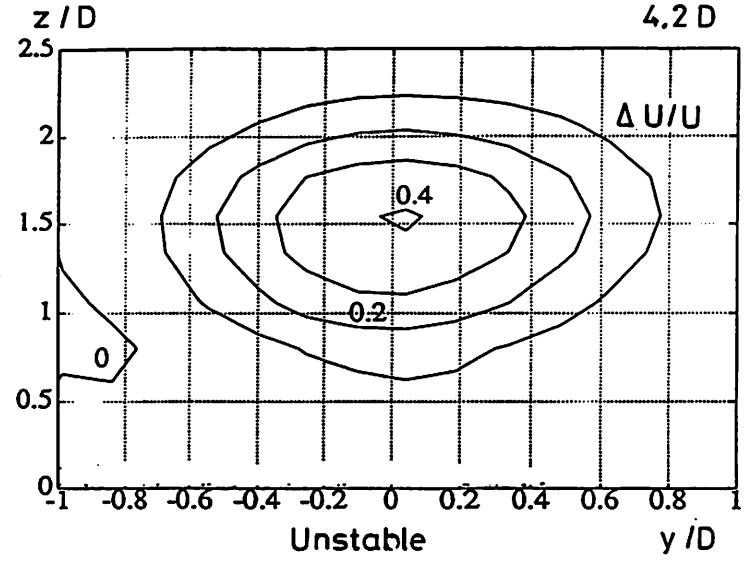
z / D
4.2 D
2.5
2
1.5
1
0.5
0
Δ U/U
0.4
0.2
0
-1 -0.8 -0.6 -0.4 -0.2 0 0.2 0.4 0.6 0.8 1
Unstable
y /D

Fig 8a

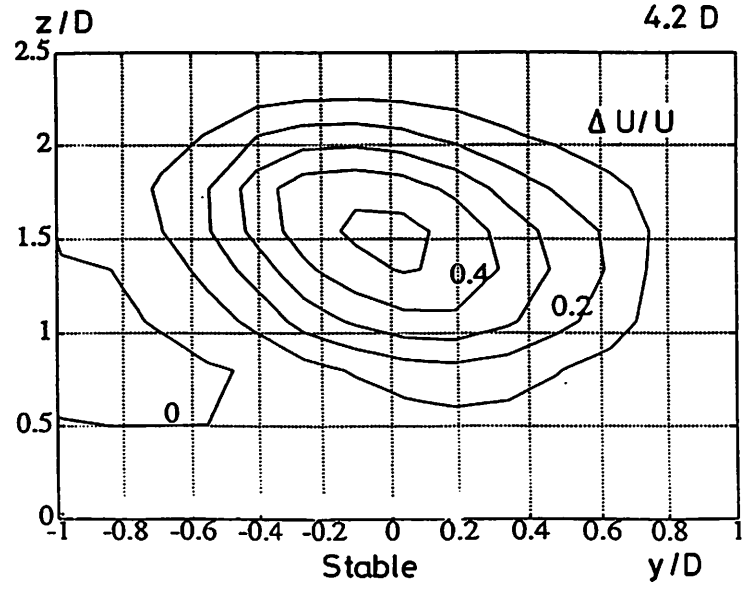
z / D
4.2 D
2.5
2
1.5
1
0.5
0
Δ U/U
0.4
0.2
0
-1 -0.8 -0.6 -0.4 -0.2 0 0.2 0.4 0.6 0.8 1
Stable
y /D

Fig 8b

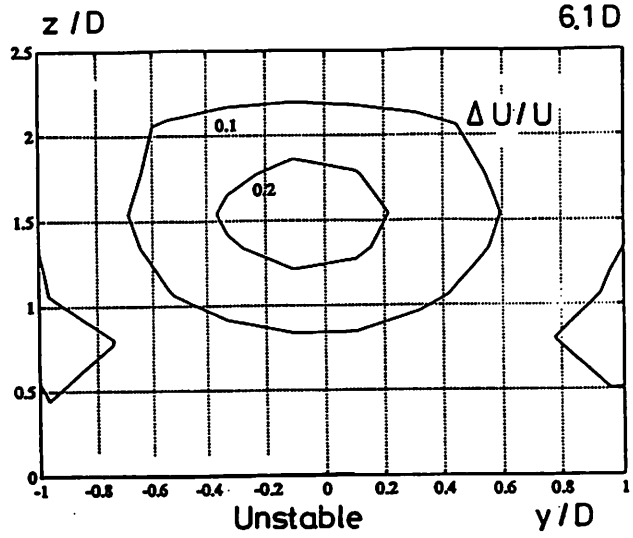
z /D
6.1 D
ΔU/U
0.1
0.2
2.5
2
1.5
1
0.5
0
-1
-0.8
-0.6
-0.4
-0.2
0
0.2
0.4
0.6
0.8
1
Unstable
y/D

Fig 9a

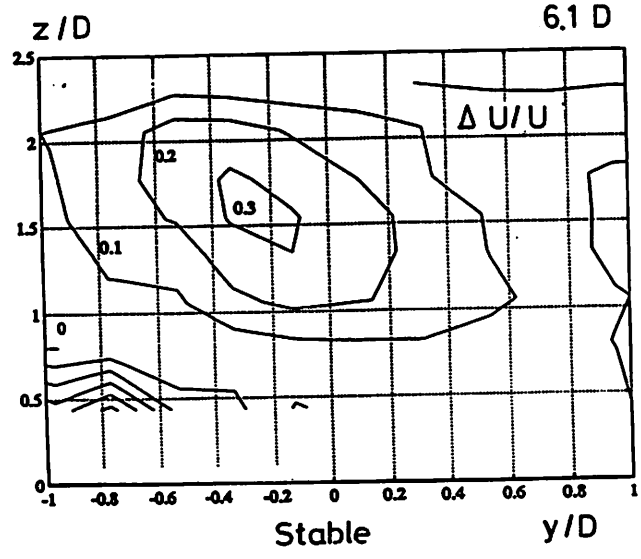
z /D
6.1 D
ΔU/U
0.2
0.3
0.1
0
2.5
2
1.5
1
0.5
0
-1
-0.8
-0.6
-0.4
-0.2
0
0.2
0.4
0.6
0.8
1
Stable
y/D

Fig 9b

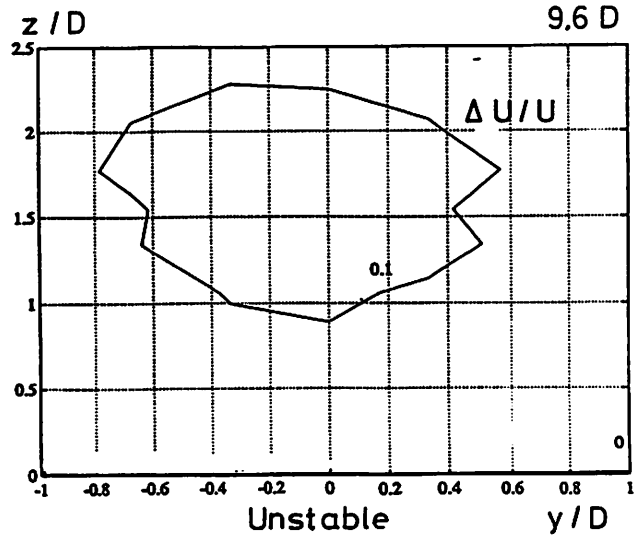

Fig 10 a

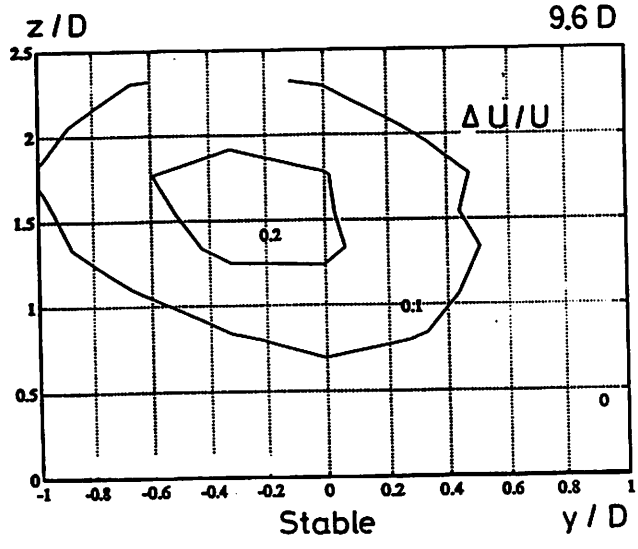

Fig 10 b

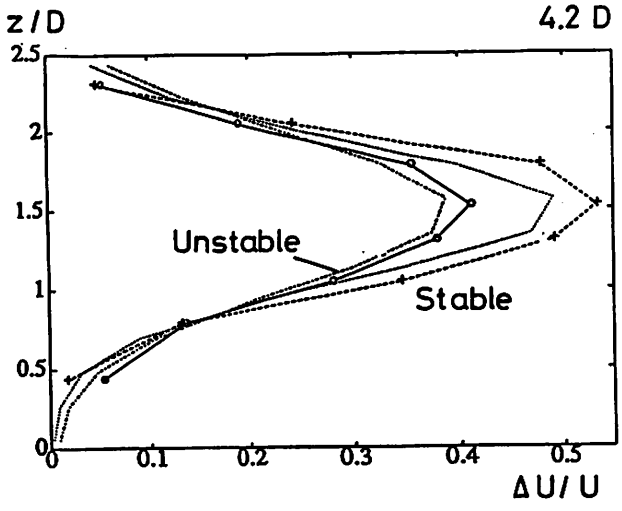
z / D
4.2 D
2.5
2
1.5
1
0.5
0
Unstable
Stable
0
0.1
0.2
0.3
0.4
0.5
ΔU/U

Fig 11

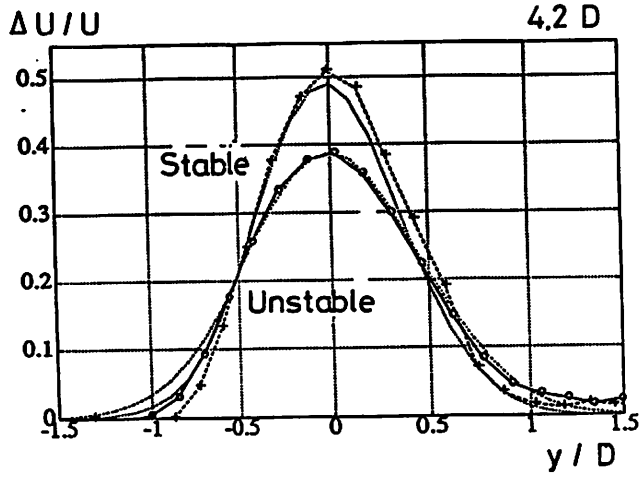
ΔU/U
4.2 D
0.5
0.4
0.3
0.2
0.1
0
Stable
Unstable
-1.5
-1
-0.5
0
0.5
1
1.5
y / D

Fig 12

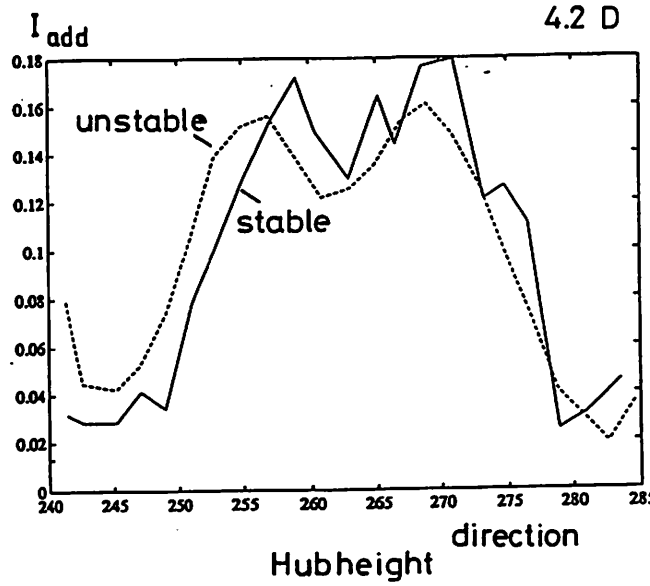

Fig 13a

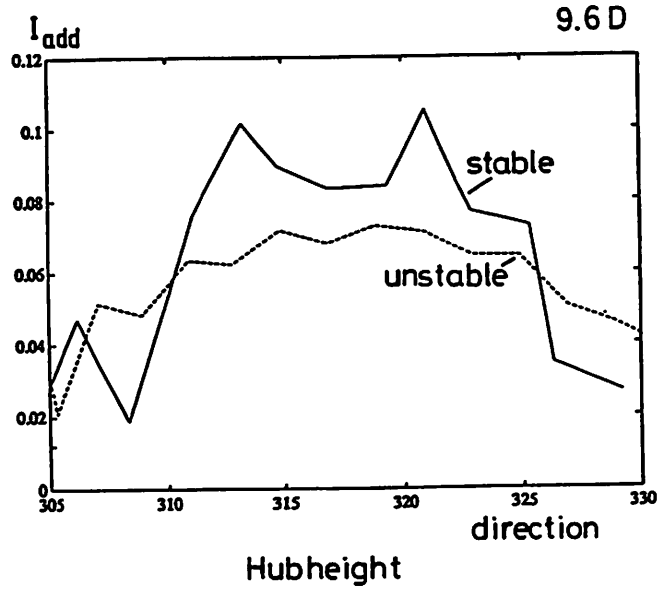

Fig 13b

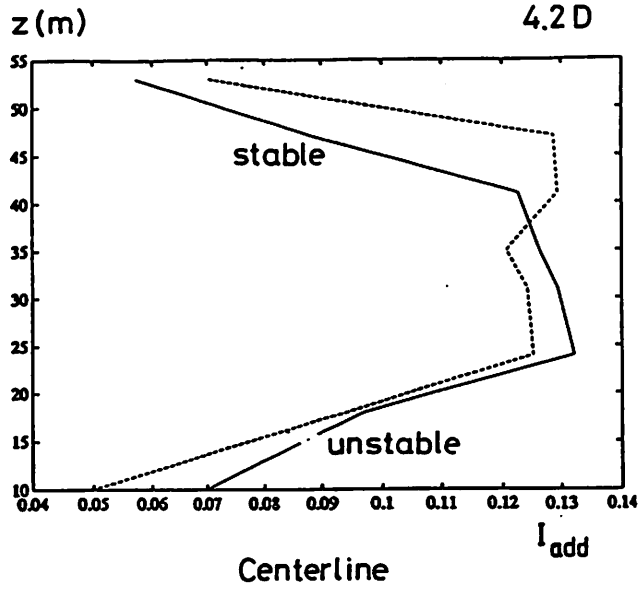

Fig 14a

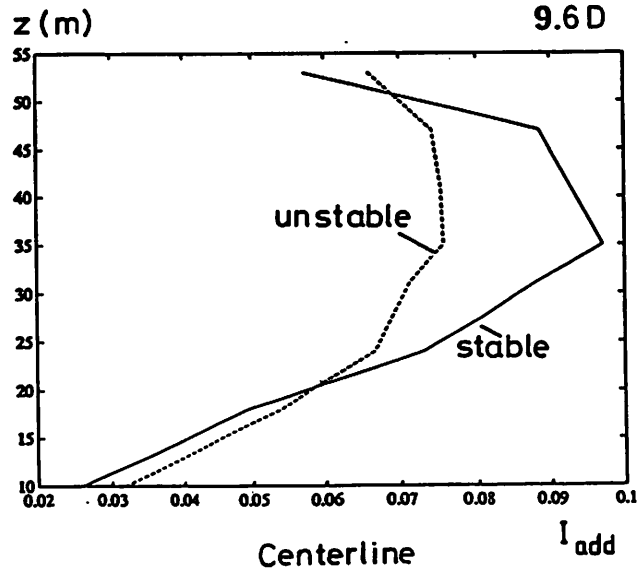

Fig 14b

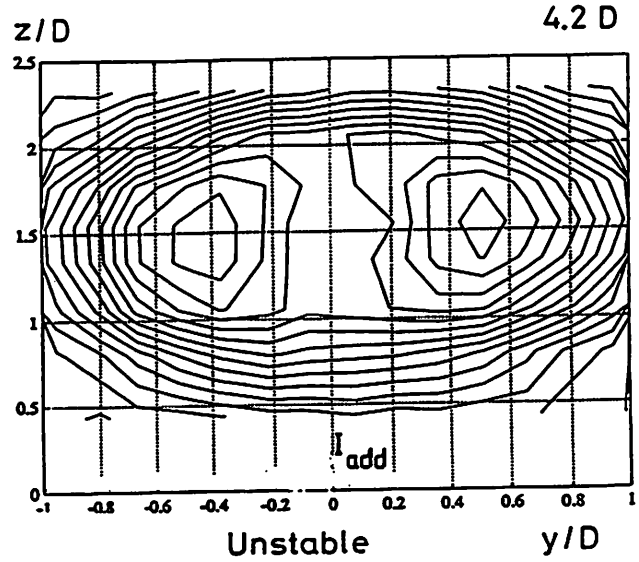

Fig 15a

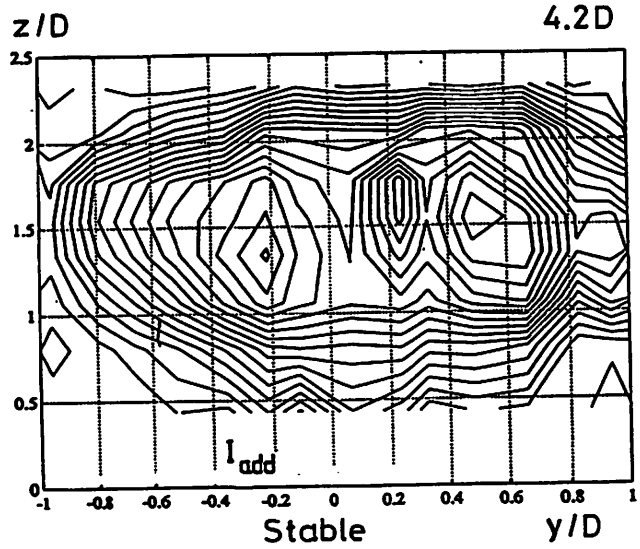

Fig 15b

Table 1.

$$dU/U(x,y,z)=A(x/D)*\exp(-((y-y_c)/D)^2/2\sigma_y^2)*$$
$$(\exp(-((z-z_c+B)/D)^2/2\sigma_z^2)+$$
$$+\exp(-((z+z_c+B)/D)^2/2\sigma_z^2)$$

Coeff.	Stable cases	Unstable cases
z_c	$0.12\ln(x/D)+1.32.$	$0.12\ln(x/D)+1.32.$
y_c	$-0.32\ln(x/D)+0.42$	$-0.154\ln(x/D)+0.21$
σ_y	$0.19\sqrt{x/D}$	$0.22\sqrt{x/D}$
σ_z	$0.21\sqrt{x/D}$	$0.24\sqrt{x/D}$
$A(x/D)$	$2.33(x/D)^{-1.053}$	$2.36(x/D)^{-1.235}$
B	$7*(y-y_c)$	0

IEA-Topical expert meeting: Increased Loads in Wind Farms Gothenburg, Sweden 3-4 may 1993

Measurements of wake effects in the Alsvik wind farm.

Presented by: Jan-Åke Dahlberg, FFA

Purpose of measurements:

* Map the load situation for turbines operating in the wake of another turbine

Short descriptions to presented view graphs (enclosed) are given in the following:

1 The four turbines at the Alsvik wind farm. Turbine no 4, behind the line, is equipped with sensors to enable measurements of loads in the blade roots as well as in the tower. The distances to the upstream wind turbine, depending on the wind direction, are 5, 7 & 9.5*D. The site is flat and homogeneous and the prevailing wind direction is from the south-west.

2 Distribution of turbulence intensity at the Alsvik site. The average turbulence intensity, expressed as the standard deviation of wind speed within the 1-min average, is about 5%.

3 Sensor equipment in turbine 4 at Alsvik.

4 List of channels recorded at the site.

The data acquisition system has been built up with a PCM equipment from J&R and a Macintosh computer with a data acquisition program Lab View. Time series of data are recorded continuously from the four turbines (Unit 1-4) and from the two meteorological towers M1 and M2. The measurements are interrupted during 5 minutes every 3 hours to transfer data to the storage media (an exabyte tape). The tape containing app. 1Gbyte of data is replaced once every week.

The signals according to Table 1 (see appendix) are recorded with a samplings frequency of 31.25 Hz. Since some signals (HUB and ACC) are

doubled the samplings frequency for these are 62.5 Hz. The signals according to Table 2 (see appendix) are recorded with samplings frequency of 2 Hz. All signals in Table 1 (except for POW4) are passing through a filter with a cut off frequency of 37.5 Hz. There are no filters for the signals in Table 2.

The evaluation of data from Alsvik are carried out at FFA using Fortran software in a VAX/VMS environment.

All the measured signals are evaluated and stored in a database. This database or catalogue contains 72 quantities. Each quantity is stored as a 1 minute average values. Also the standard deviation, maximum and minimum value during each minute are stored.

5 Standard 180-minute plot from the evaluation process.

Graph #	Content:
1 2	The two upper graphs are showing the wind speed and standard deviation (shaded area at the bottom) from 3 heights (upper tip, hub & lower tip) in the two met. masts
3	The third graph shows the nacelle and wind directions. When the wind direction lies within any of the shaded areas, turbine no 4 are influenced by a wake.
4	The fourth graph shows the power output from the four turbines.
5	The fifth graph shows the flap and edge moment. The solid curve shows the mean value and the shaded area indicates the standard deviation ($\pm\sigma$) of the moment.
6	Graph six shows some signals from the tower.

Observations from the graphs:

The wind speed is about 10 m/s and the wind direction are changed from 260° to 220° during the 180 minutes. During the 0 to 70 minute period turbine 4 operates in the wake of turbine 2 (5 D). The power loss is significant as well as the increase in load variations which can be seen both for the edge and the flap moment.

6 Scatter plot of flap moment standard deviation (1-minute) as function of wind direction. Based on 13 500 1- min values. Solid curve

shows mean values of the flap moment standard deviation sorted with the method of bins.

7 Time and polar plot of flap moments during 5 revolutions for various positions in the wake. The highest load variations occur when the turbine is operating partly in the wake. This can clearly be seen from the polar plot. On the left peak the polar curve is shifted to the right whereas on the right peak the polar curve is shifted to the left.

8+9 Plot of flap moment standard deviation (1-minute) as function of wind direction and plot of relative power as function of wind direction. The highest load variations occur when the turbine is operating partly in the wake. In these positions the relative power is reduced to about 50% whereas the power is reduced to 30% when the turbine is operating on the centre line of the upstream turbine.

10 Time and polar plots of flap and edge moments during 5 revolutions. Undisturbed operation in a relatively high wind shear situation. The flap moment is slightly higher when the blade is passing the upper half of the revolution. The standard deviation of flap moment is about 3 kNm or 10 % of the mean flap moment.

11 Time and polar plots of flap and edge moments during 5 revolutions. Partial wake operation with the same wind conditions as in the previous graph. The standard deviation of flap moment in this case is 9 kNm or 40-50% of the mean flap moment.

12 Time and polar plots of flap and edge moments during 5 revolutions. Operation conditions: Wind speed at hub height close to stall wind speed and a relatively high wind shear. The highest flap moments occur when the blades are passing the lower half of the revolution. When the blades are passing the upper half of the revolution the flap moments are about 50 % of the flap moments that occur on the lower half. An explanation could be that the flow on the blades are partly separated (stalled) when the blades are passing the upper highly windy half of the revolution. This kind of operation creates the highest load cycles seen so far at the Alsvik wind farm. Also the edge moments are high during these wind conditions. Edge load cycles of more than occur very frequent. An Edge moment of 50 kNm exceeds the highest load cycle that occur during a stop sequence.

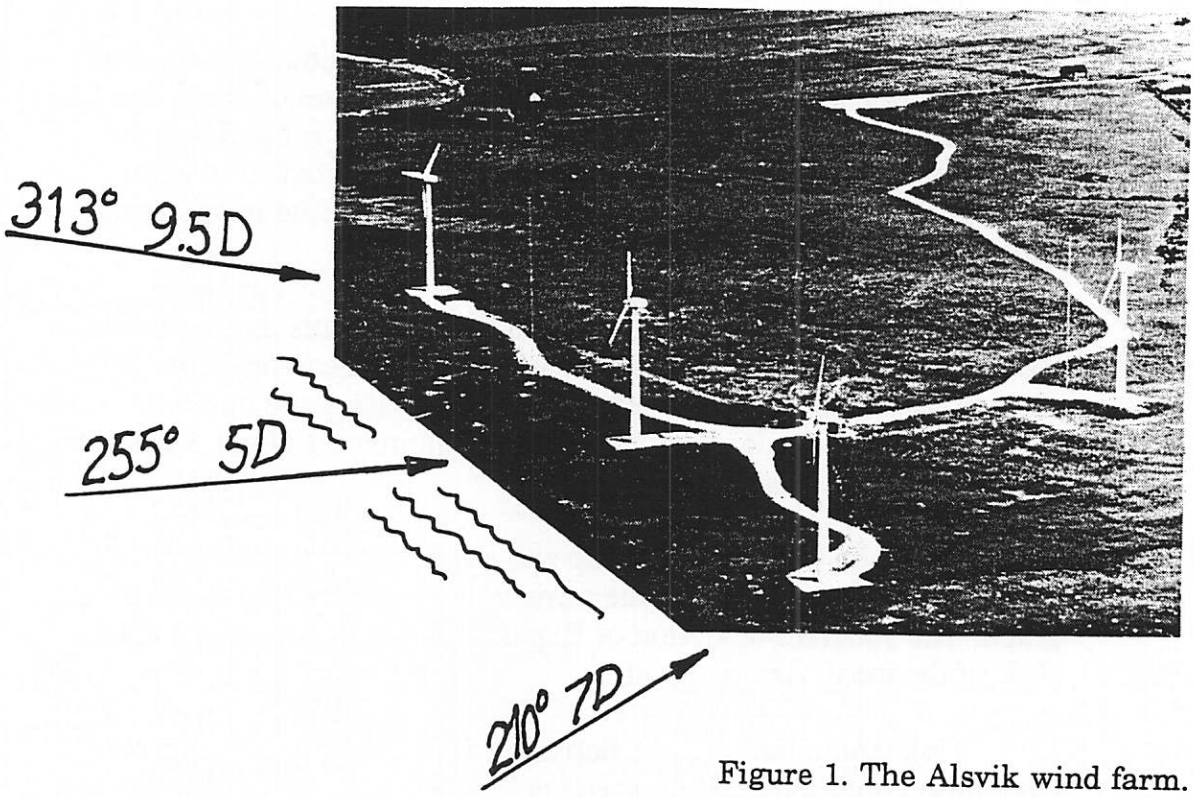

Figure 1. The Alsvik wind farm.

View graph no 1

13:23 1-OCT-92

Distribution of turbulence intensity
0.5 % bin width, 1 min average values
Total number of values: 41860

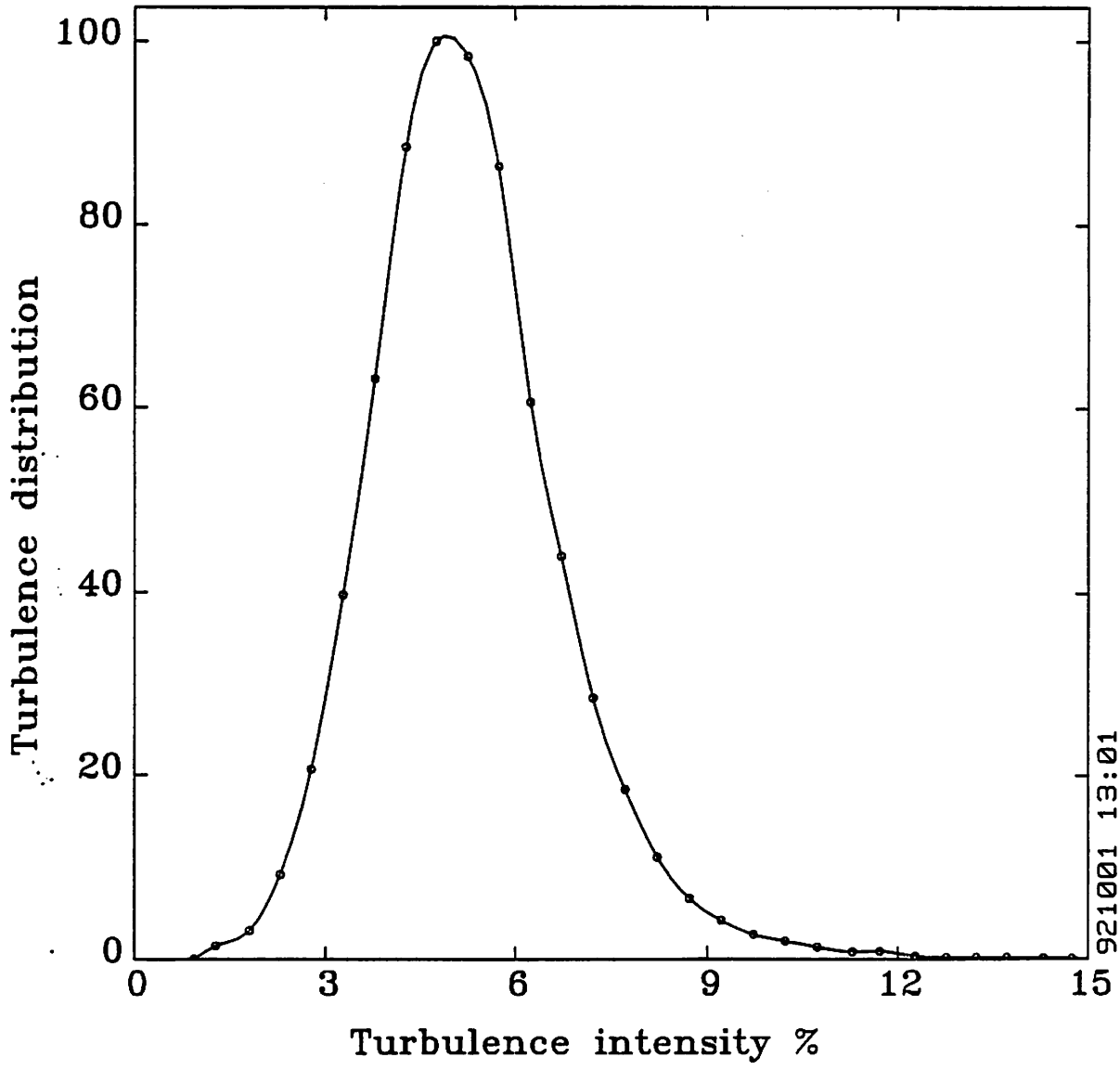

View graph no 2

Sensor Equipment in Turbine 4 at Alsvik

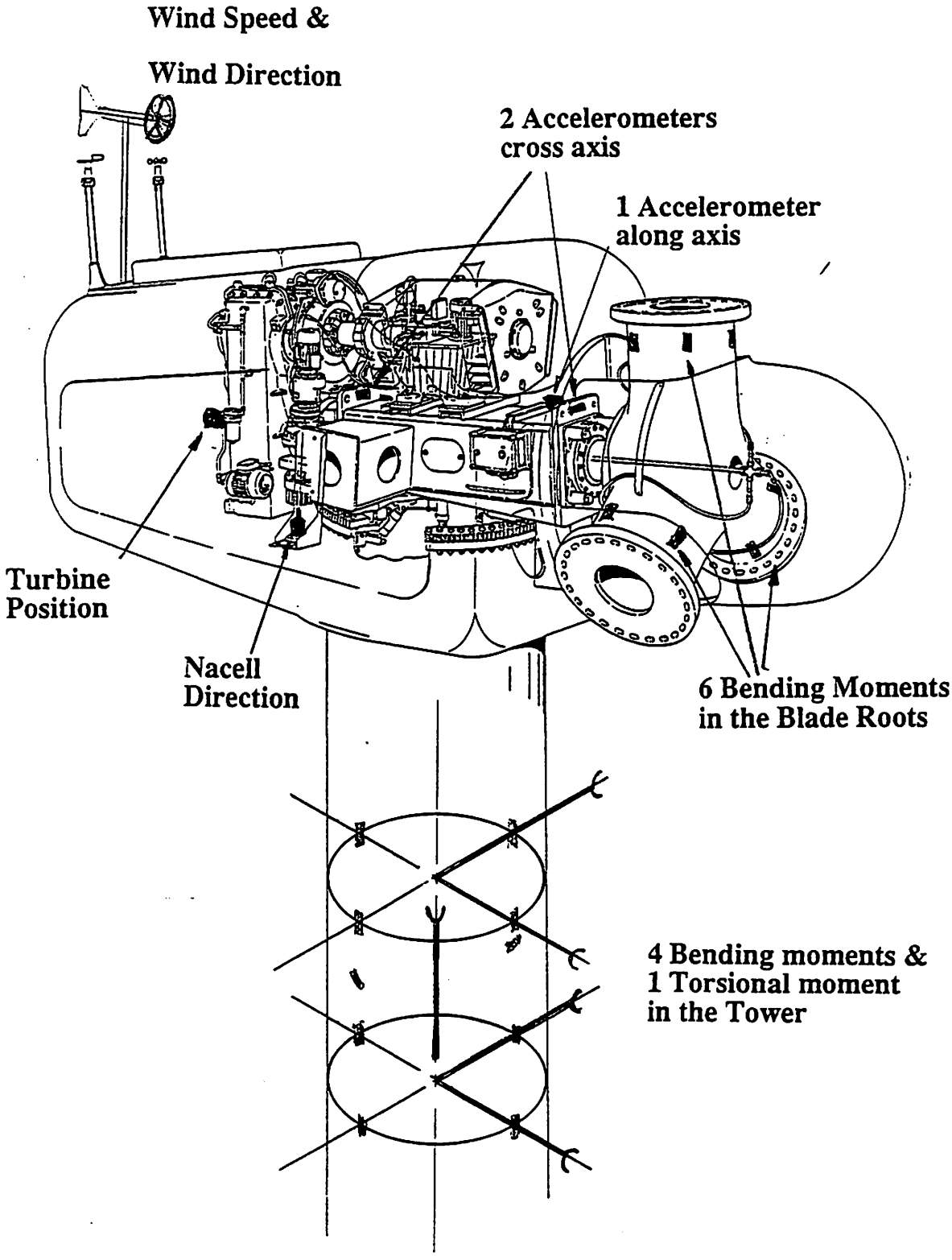

View graph no 3

List of Channels recorded with 31.25 Hz sampling rate/channel			
Ch	**Name**	**Quantity**	**Description**
1	HUB1	Moment	Bending, in the root of blade 1
2	HUB2	Moment	Bending, in the root of blade 1, (90° to HUB1)
3	HUB3	Moment	Bending, in the root of blade 2
4	HUB4	Moment	Bending, in the root of blade 2, (90° to HUB3)
5	HUB5	Moment	Bending, in the root of blade 3
6	HUB6	Moment	Bending, in the root of blade 3, (90° to HUB5)
7	ACC2	Accel.	of the nacell (front) cross the turbine shaft
8	ACC3	Accel.	of the nacell (rear) cross the turbine shaft
9	ACC1	Accel.	of the nacell along the turbine shaft
10	TOW1	Moment	Bending, lower level
11	TOW2	Moment	Bending, upper level
12	TOW3	Moment	Bending, lower level (90° to TOW1)
13	TOW4	Moment	Bending, upper level (90° to TOW2)
14	TOW5	Moment	Torzional, upper level
15	NACPOS	Angle	Nacelle direction
16	TURBAN	Angle	Azimuthal rotor angle
17	HUB1	Moment	Bending, in the root of blade 1
18	HUB2	Moment	Bending, in the root of blade 1, (90° to HUB1)
19	HUB3	Moment	Bending, in the root of blade 2
20	HUB4	Moment	Bending, in the root of blade 2, (90° to HUB3)
21	HUB5	Moment	Bending, in the root of blade 3
22	HUB6	Moment	Bending, in the root of blade 3, (90° to HUB5)
23	ACC2	Accel.	of the nacell (front) cross the turbine shaft
24	ACC3	Accel.	of the nacell (rear) cross the turbine shaft
25	ACC1	Accel.	of the nacell along the turbine shaft
26	TOW1	Moment	Bending, lower level
27	D+	Voltage	Dummy bridge from the hub
28	D-	Voltage	Dummy bridge from the hub
29	VREF	Voltage	Voltage reference signal
30	POW4	Power	Power from Unit 4
31	NACWD	Angle	Wind Direction on top of nacell
32	NACWS	Wind speed	Wind Speed on top of nacell

View graph no 4

List of Channels recorded with 2 Hz sampling rate/channel					
Ch.	Name	Quantity	Description		
33	WS11	Wind speed	Mast 1, level 2.8 m		
34	WS12	Wind speed	Mast 1, level 9.9 m		
35	WS13	Wind speed	Mast 1, level 18.4 m		
36	WS14	Wind speed	Mast 1, level 24.4 m		
37	WS15	Wind speed	Mast 1, level 30.8 m		
38	WS16	Wind speed	Mast 1, level 35.6 m		
39	WS17	Wind speed	Mast 1, level 40.7 m		
40	WD11	Wind direct.	Mast 1, level 2.8 m		
41	WD12	Wind direct.	Mast 1, level 9.9 m		
42	WD13	Wind direct.	Mast 1, level 18.4 m		
43	WD14	Wind direct.	Mast 1, level 24.4 m		
44	WD15	Wind direct.	Mast 1, level 30.8 m		
45	WD16	Wind direct.	Mast 1, level 35.6 m		
46	WD17	Wind direct.	Mast 1, level 40.7 m		
47	WS21	Wind speed	Mast 2, level 4.9 m		
48	WS22	Wind speed	Mast 2, level 10.0 m		
49	WS23	Wind speed	Mast 2, level 18.4 m		
50	WS24	Wind speed	Mast 2, level 24.4 m		
51	WS25	Wind speed	Mast 2, level 30.8 m		
52	WS26	Wind speed	Mast 2, level 35.5 m		
53	WS27	Wind speed	Mast 2, level 40.6 m		
54	WD21	Wind direct.	Mast 2, level 4.9 m		
55	WD22	Wind direct.	Mast 2, level 10.0 m		
56	WD23	Wind direct.	Mast 2, level 18.4 m		
57	WD24	Wind direct.	Mast 2, level 24.4 m		
58	WD25	Wind direct.	Mast 2, level 30.8 m		
59	WD26	Wind direct.	Mast 2, level 35.5 m		
60	WD27	Wind direct.	Mast 2, level 40.6 m		
61	POW1	Power	Power from Unit 1		
62	POW2	Power	Power from Unit 2		
63	POW3	Power	Power from Unit 3		
64	POW4	Power	Power from Unit 4		

View graph no 4

FFA 930125 20:51 110 930115_105711

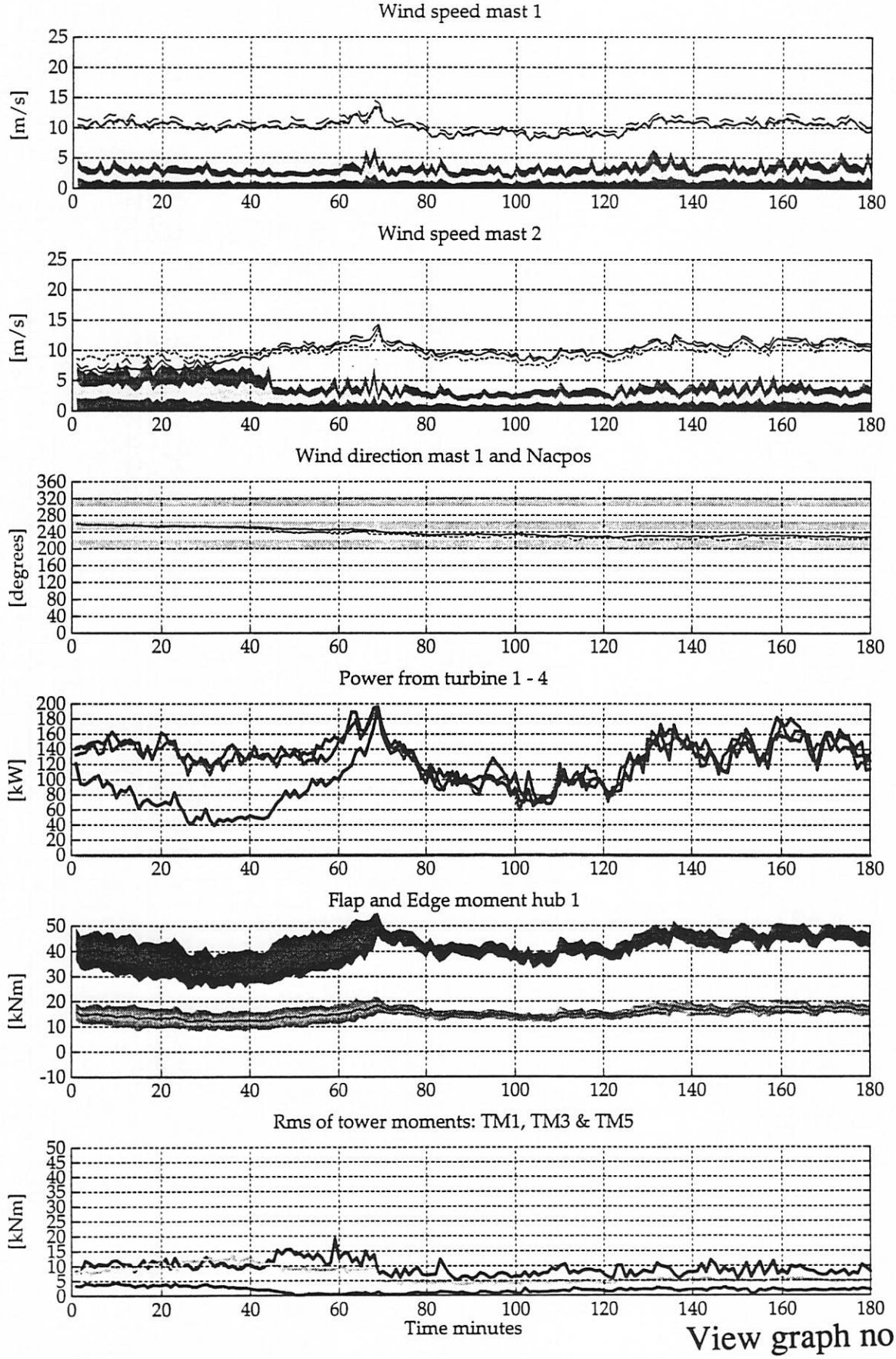

View graph no 5

Scatter of Flap moment standard deviation as function of wind direction. Wind speed range 6–9 m/s, turbulence intensity range 4–8 % and wind shear range 0–1 m/s. Solid curve shows the mean values of the flap moment standard deviation sorted with the procedure "method of bins".

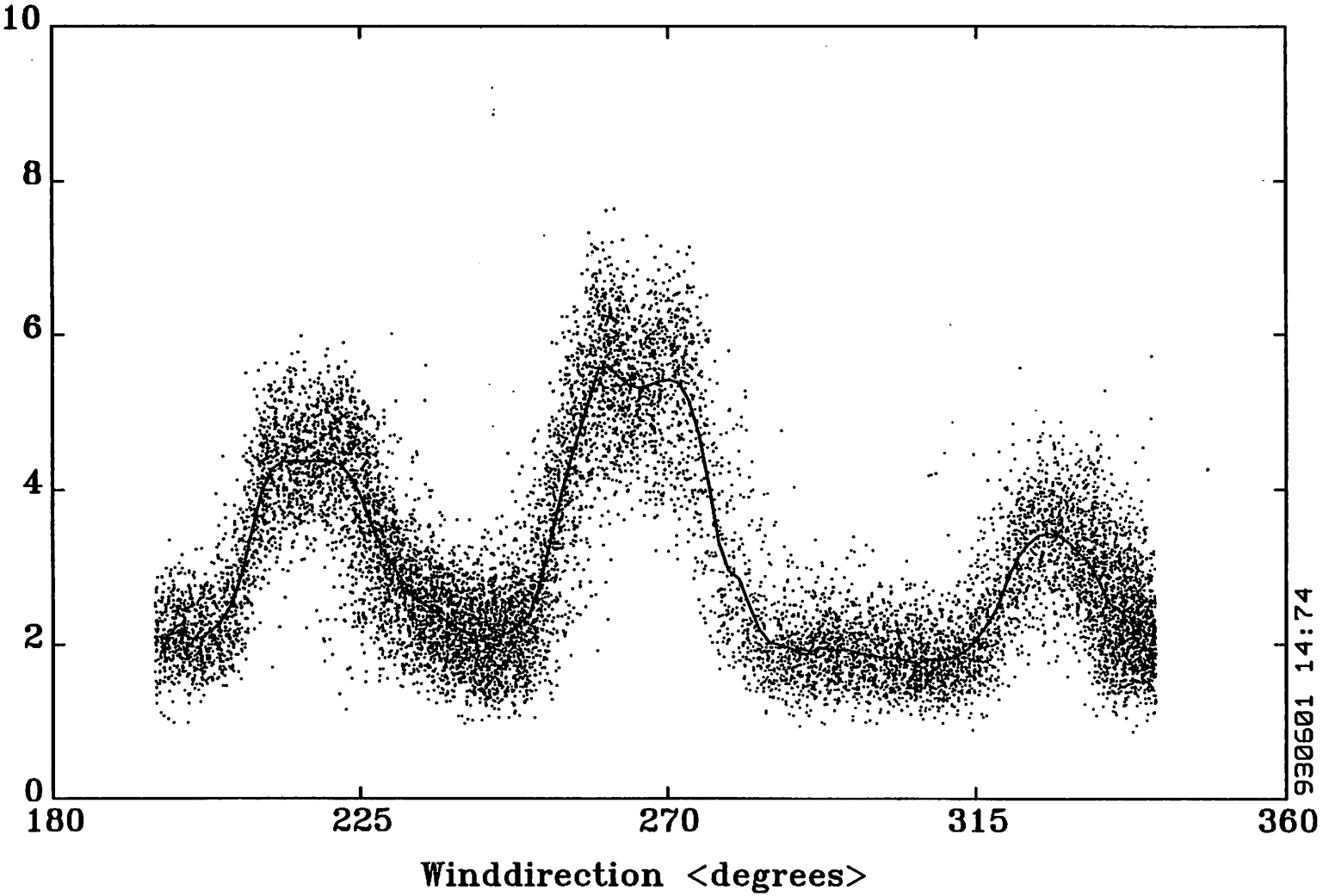

View graph no 6

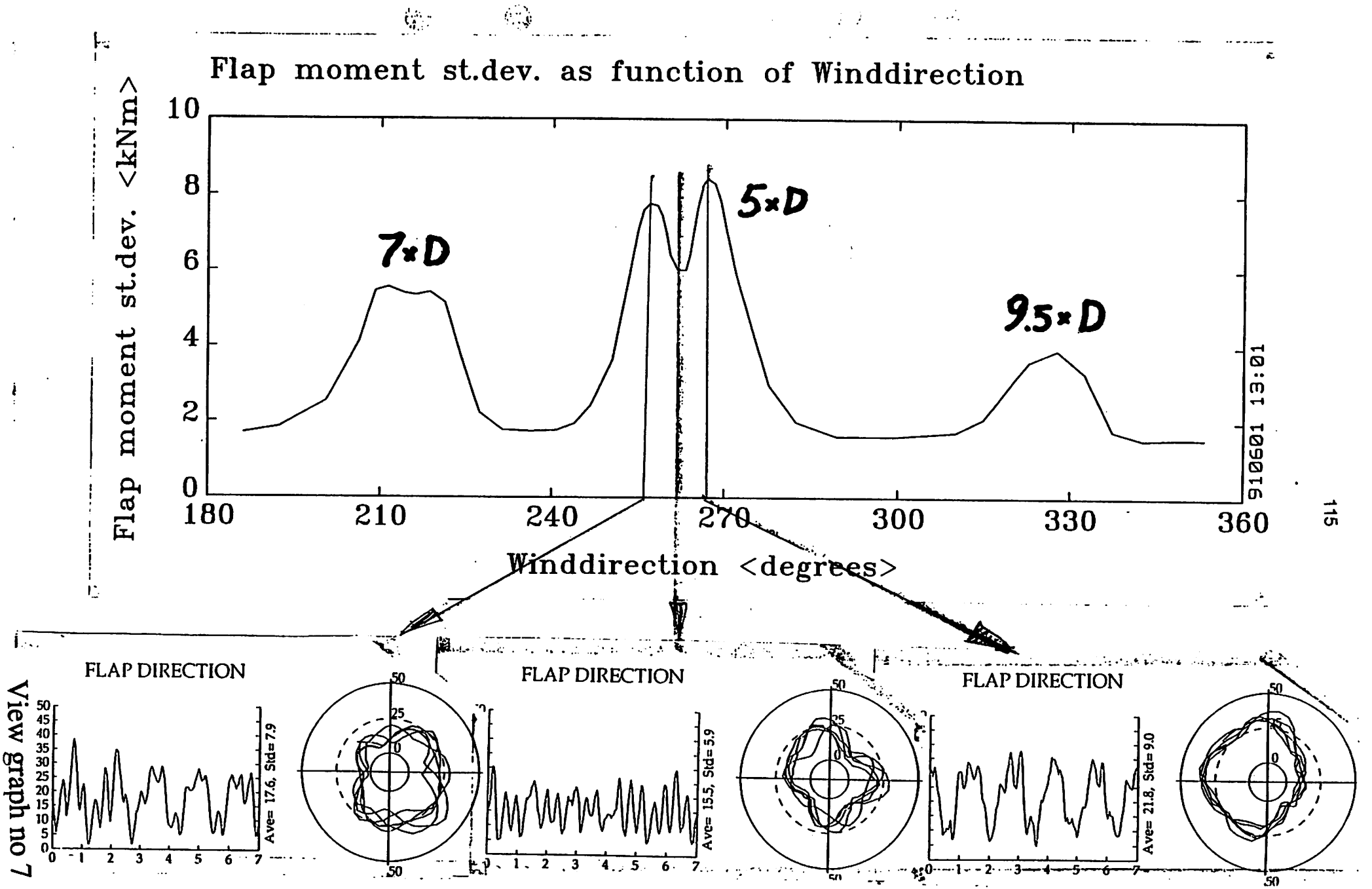
Flap moment st.dev. as function of Winddirection
Flap moment st.dev. <kNm>
10
8
6
4
2
0
180
210
240
270
300
330
360
7×D
5×D
9.5×D
910601 13:01
115
Winddirection <degrees>
FLAP DIRECTION
Ave= 17.6, Std= 7.9
FLAP DIRECTION
Ave= 15.5, Std= 5.9
FLAP DIRECTION
Ave= 21.8, Std= 9.0
View graph no 7

23-JAN-92

FLAP MOMENT VARIATIONS AS FUNCTION
OF WINDDIRECTION
5xD, 8-10 m/s, low turbulence,
wake2.pass

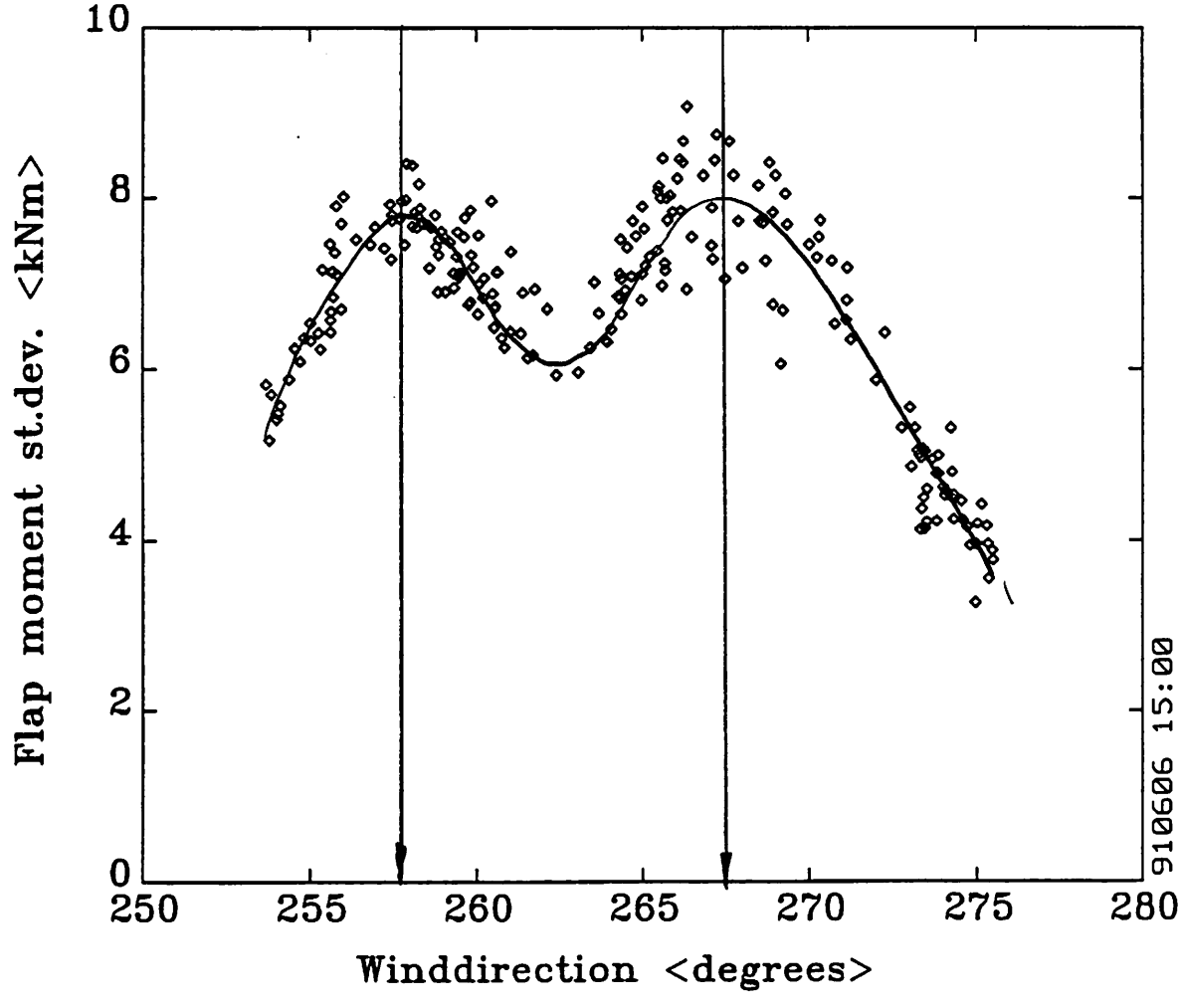

View graph no 8

23-JAN-92

RELATIVE POWER AS FUNCTION OF WIND DIRECTION
5xD, 8-10 m/s, low turbulence,
wake2.pass

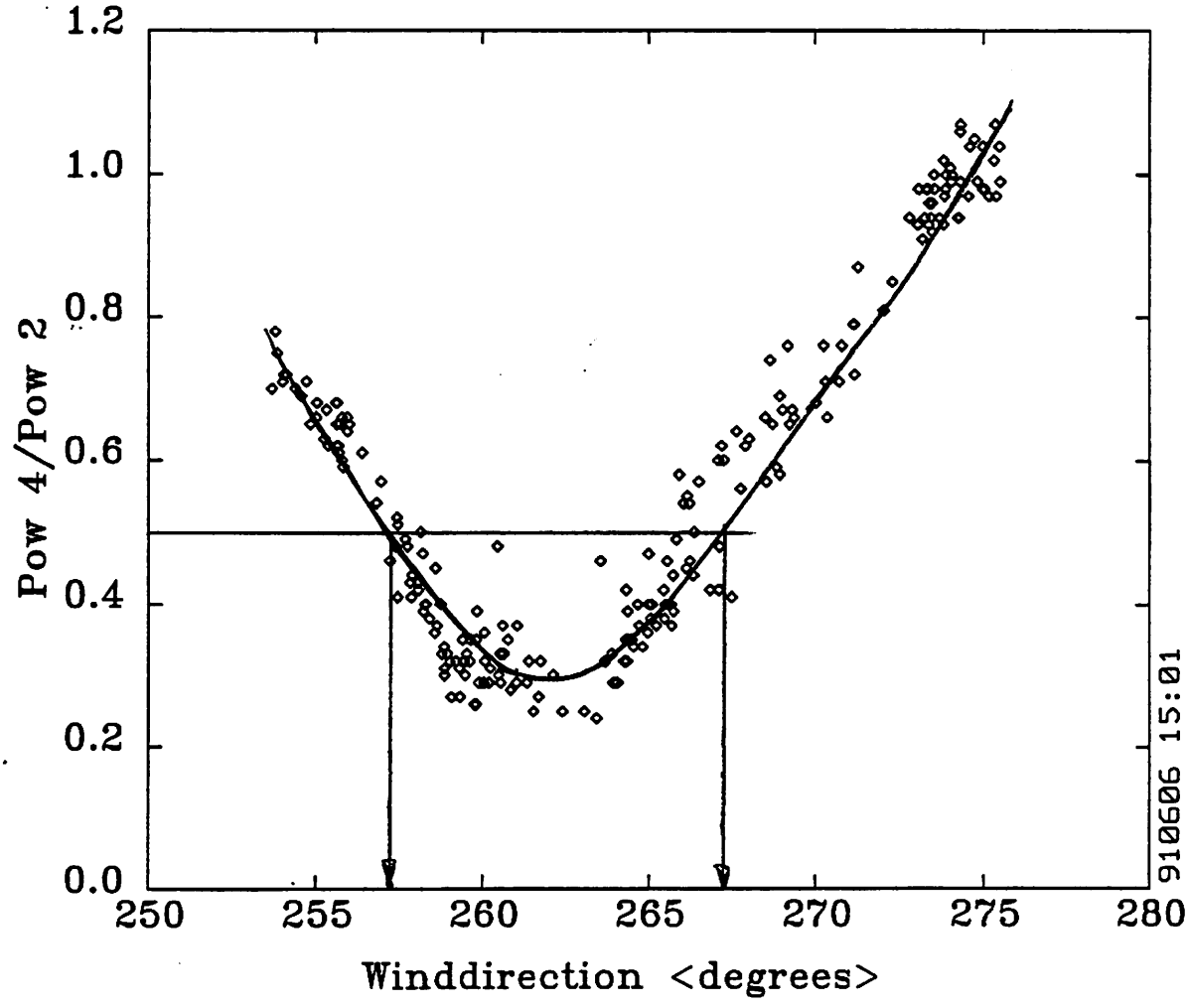

View graph no 9

FFA 900919 17:55 BENDIN(MOME. T IN THE BLADE ROOTS S quence ..00 (160 min), file: 900429_224543

Wind direction in mast 1 and mast 2: 281.4, 279.5

	Mast 1:	Mast 2:
Wind speed average and st.dev at top level:	11.7 0.1	11.0 0.6
hub level:	10.2 0.2	6.9 0.7
bottom level:	8.5 0.2	7.4 0.3

Power output from : Unit 1= -0.5
Unit 2= 118.7
Unit 3= 117.7
Unit 4= 124.8

FLAP DIRECTION

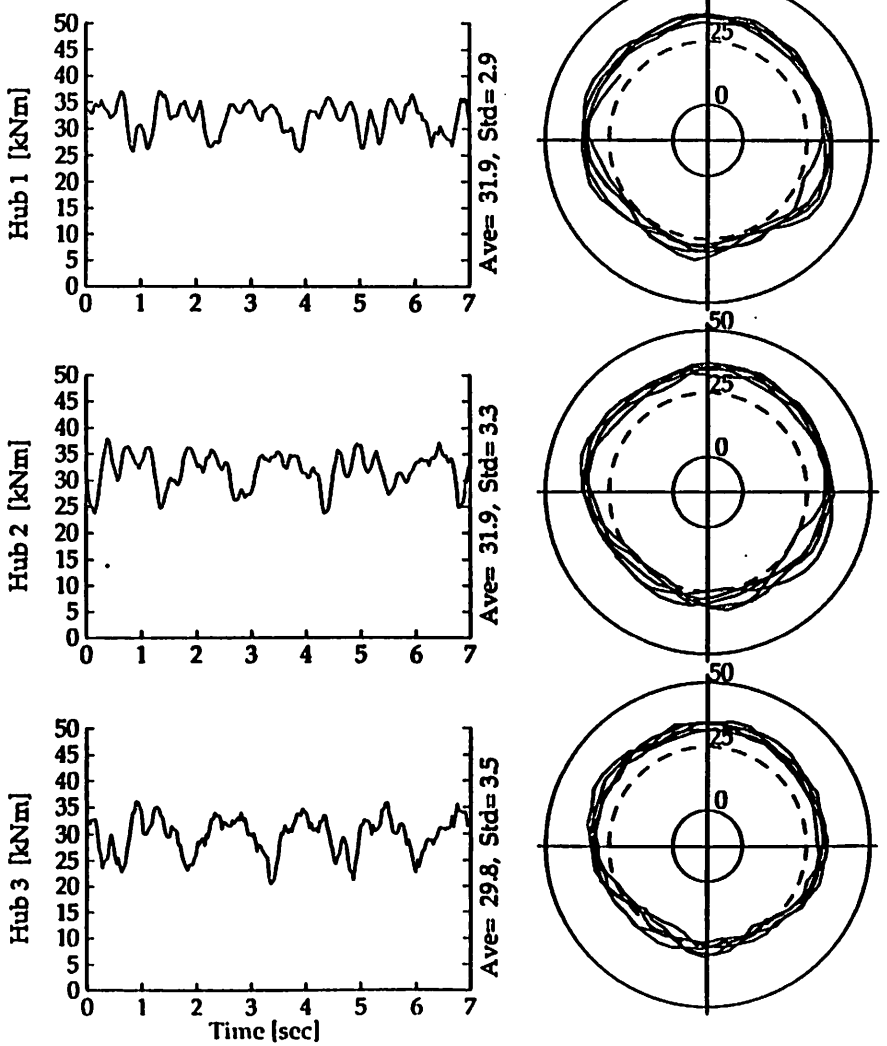

EDGE DIRECTION

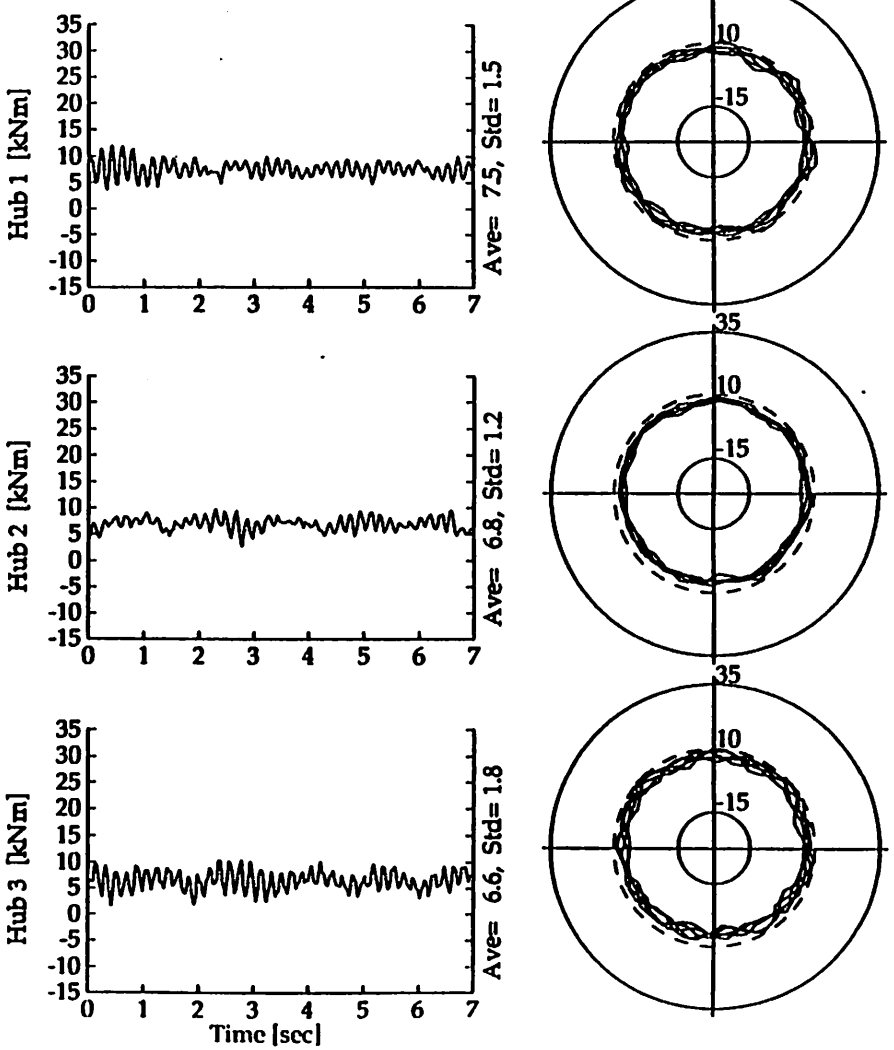

View graph no 10

FFA 900919 17:55 BENDING MOMENT IN THE BLADE ROOTS Sequence 000 (67 min), file: 900429_224543

Wind direction in mast 1 and mast 2: 271.0, 273.5

	Mast 1:	Mast 2:
Wind speed average and st.dev at top level:	11.3 0.2	5.1 0.4
hub level:	10.1 0.3	5.6 0.6
bottom level:	8.9 0.3	6.8 1.3

Power output from : Unit 1= -0.8
Unit 2= 114.6
Unit 3= 108.2
Unit 4= 61.5

FLAP DIRECTION

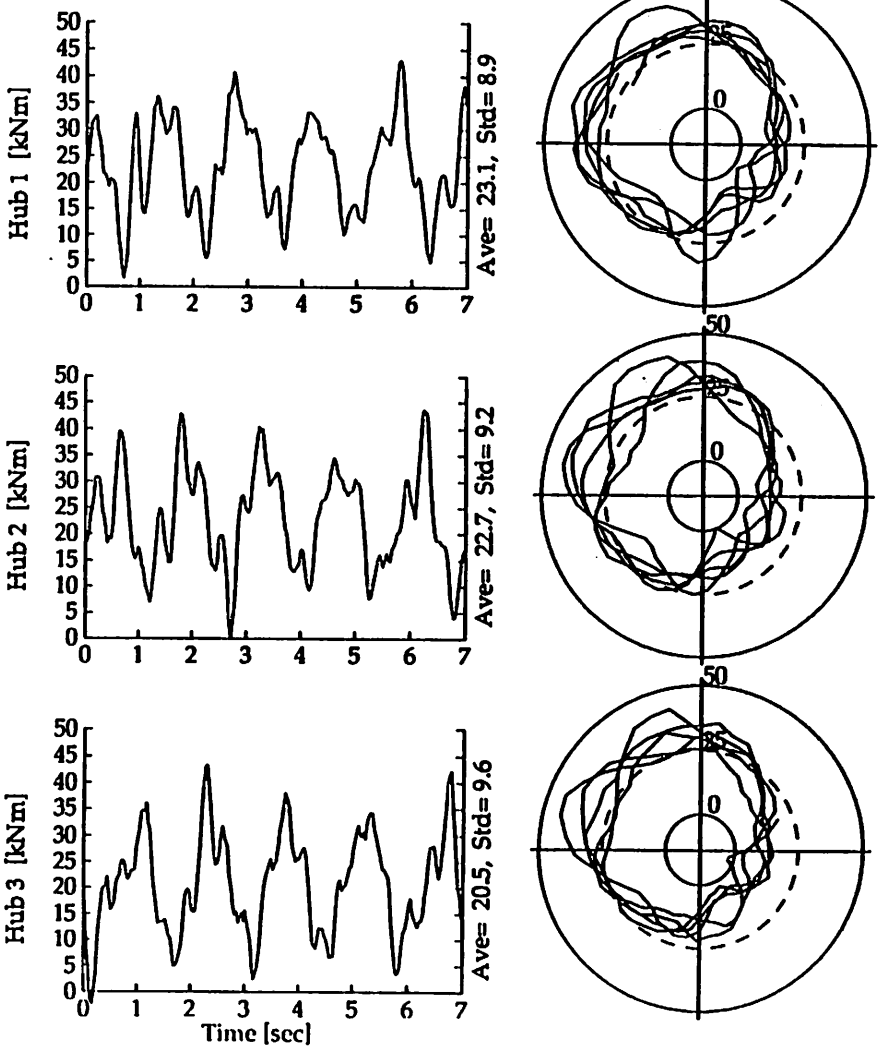

EDGE DIRECTION

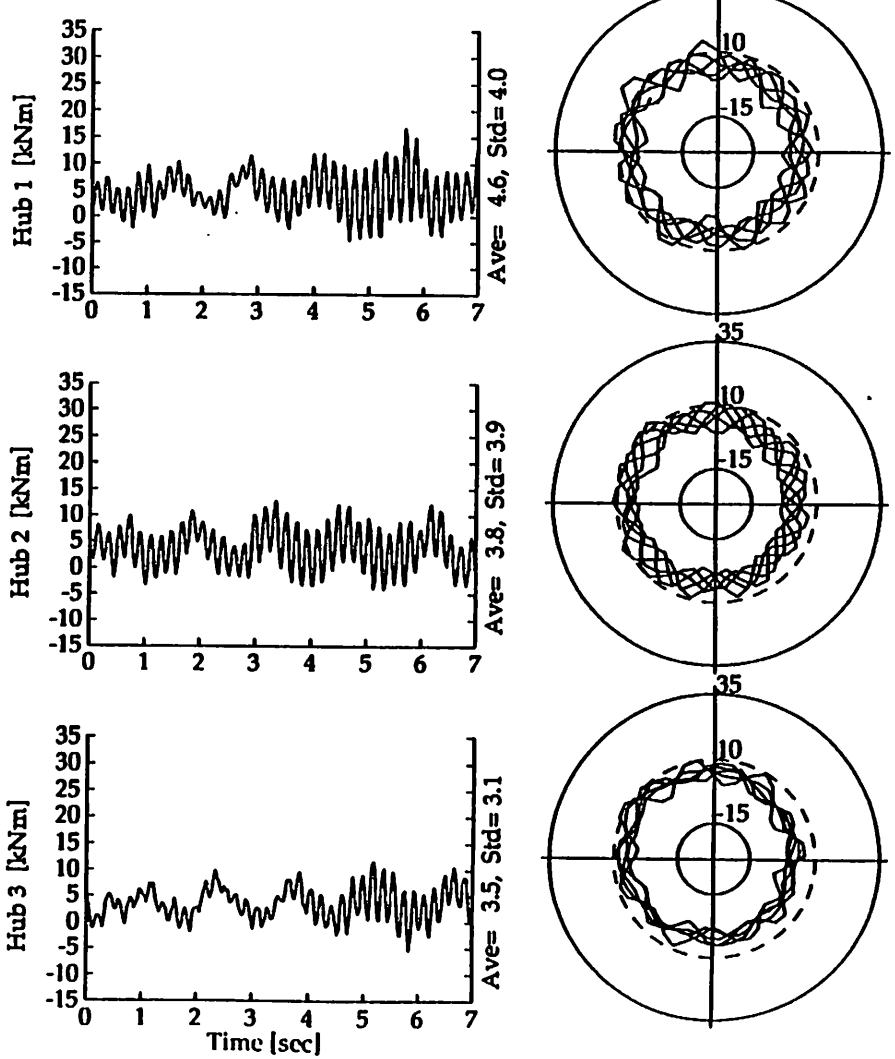

View graph no 11

FFA 911213 17:07 BENDING MOMENT IN THE BLADE ROOTS Sequence 433 (58 min), file: 900915_151833

Wind direction in mast 1 and mast 2:	5.2,	15.3	
	Mast 1:	Mast 2:	Power output from :
Wind speed average and st.dev at top level:	14.2 2.2	15.1 1.2	Unit 1= 176.8
hub level:	13.5 1.9	13.9 1.2	Unit 2= 171.5
bottom level:	12.8 1.6	12.7 0.9	Unit 3= -0.5
			Unit 4= 165.6

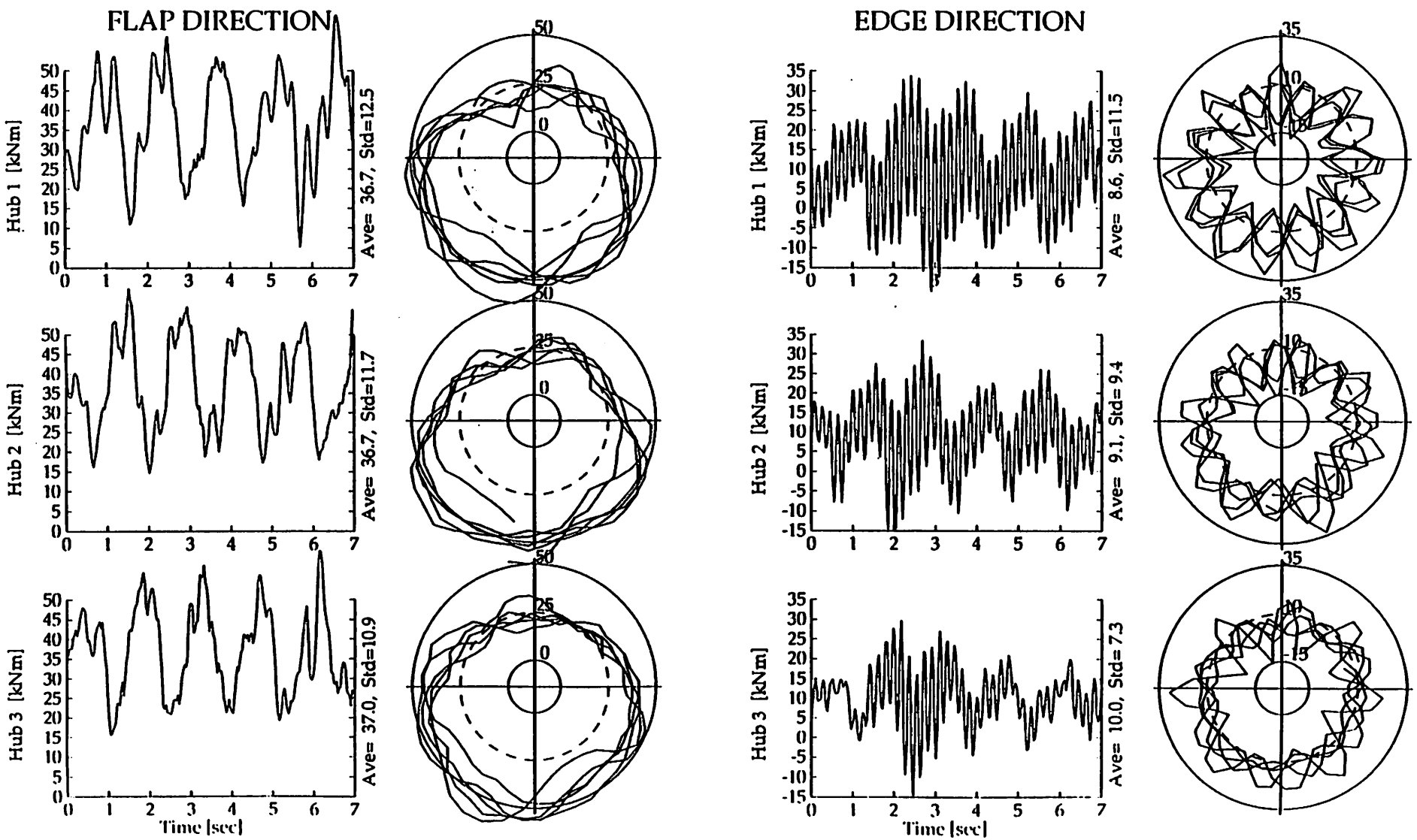

View graph no 12

Flap-load spectra for different situations in the Alsvik windfarm

Maria Poppen, The Aeronautical Research Institute of Sweden

1 Introduction

This study is based on measurements in the Alsvik windfarm. The wind farm is described in the previous paper. The measurements have also been described in [1] and [2].

2 Method

To evaluate the data to establish load spectrum, the time signals are rain-flow-counted. The algorithm used is described in IEA Recommended practises [3]. The amount of available data is large and to find the interesting situations is very time consuming. All time signals have been evaluated once to establish the catalogue described above. It was a requirement to use the data in the catalogue to develop the fatigue spectra. This was important especially since different situations were to be identified.

It was decided to check if a simple method could reconstruct the cycles with the highest amplitudes of each minute from the stored 1 minute values of the flap bending moment. To check the relevance of such a method, typical events were chosen. These events were wake situations and undisturbed steady wind from the sea.

The one minute values provide mean value, standard deviation for that minute, maximum peak value and minimum through value. From this information it is at least possible to reconstruct the most severe cycle during that minute, namely the cycle from the minimum through to maximum peak (or the opposite order). Only taking into account this cycle from each minute will give not give the needed accuracy. A simple algorithm to reconstruct cycles was then looked for.

The base for this algorithm was studies regarding the distribution of cycles in the time signals and how the distribution was connected to the mean value, standard deviation, maximum peak and minimum through, which the catalogue provides.

After some tests, which can be regarded as curve fitting, a simple algorithm which gives 9 cycles was chosen. Each minute contains cycles at three different load levels, dependent on mean value, maximum peak,

minimum through and standard deviation. The result with this algorithm is shown in figure 1. The solid lines represent the rain-flow-count results on the signal reconstructed using this algorithm. The same algorithm is used for both the undisturbed and the wake operation.

In figure 2 the flap moment standard deviation is shown as function of wind direction and wind speed. The line represents the mean line through the one minute flap moment standard deviation values. From this diagram the three different wake situations are clearly separated from the operation in undisturbed wind. The variations are substantially higher in the wakes than in between the wakes, where the variations are more stable.

It is not obvious what width that should be regarded as the width of the wake. A wider wake will give a lower mean flap moment variation over the entire wake but it will also result in a higher percentage of time when the turbine is operating in a wake. Between the 5 diameter and 7 diameter wakes the flap moment variation does not decrease to a level that is low and stable enough to be regarded as "undisturbed". The different wake distances must be compared to an undisturbed situation, and here the wind direction between 5 and 9.5 diameters was chosen to be used as this reference. The different wind direction intervals that were used to establish the different load spectra are shown in Figure 2.

The load spectra for the four different operations are shown in figure 3. These spectra contain only measurements from operation in wind speeds between 4-14 m/s, no starts or stops are included. Neither is operation during stall wind speeds or operation in extreme turbulent wind. These last two operation modes will be discussed below.

The four different spectra are clearly separated, with the spectrum for 5 diameters as the most severe spectrum and the undisturbed wind flow as the least severe, as expected. What might be a little surprising is that even a wake as far as 9.5 diameters will cause substantially higher fatigue loads. It is important to remember that this includes nothing but a running turbine below stall wind speed. Taking into account also other operation modes, e.g. starts and stops, high wind speeds etc., will decrease these differences.

3 Influence of turbulence intensity

An investigation of the influence of turbulence intensity was also performed. In order to have enough data points one wind interval was chosen, 6-8 m/s. Three different intervals of turbulence intensity were chosen, 0-4 %, 4-8 % and 8-12 %. The turbulence intensity is here defined as the standard deviation of the wind speed during the minute divided by the mean wind speed during that minute. The wind speed is measured at hub height in mast 1.

In figure 4 the influence of level of turbulence is shown for the undisturbed operation. Here the most severe spectrum is as expected that of the highest level of turbulence. In figure 5 the influence of level of

turbulence is shown for the operation in a 5D wake. Here the highest level of turbulence results in the least severe spectrum. This can be explained by the mixing of air in to the wake which will reduce the influence of the wake.

4 Application on a more general configuration

To be able to get an idea about how important it is to account for wake effects a study on a more general configuration than the Alsvik configuration was performed. The chosen configuration is an offshore site where the turbines are placed in star shaped clusters. One turbine is placed in the centre and six turbines in a circle around the centre. This means that the turbines will form equilateral triangles with the same distance between all the involved turbines.

Again four spectra were evaluated, one for 5D between the turbines, one with 7D, one with 9.5D and one spectrum for a single turbine for reference. The distribution of wind direction is supposed to be even around the entire wind rose. In these spectra wake operation and undisturbed operation are put together to simulate the actual loading of the blades. The configurations are shown in Figure 6. The disturbed sector is assumed to be as shown by the striped area. The sector width is chosen according to Figure 2. When the wind is blowing from the directions between the wakes where the wind has low turbulence intensity it is supposed to be undisturbed operation. From Figure 2 it is obvious that the wake will influence a larger sector, which means that the differences between the calculated spectra for a turbine in a cluster and a single standing turbine will be larger if a wider wake was chosen. The effect of the wake will therefore be of at least of this significance.

The base for this study is the same as for the other spectra; flap moment, 4-14 m/s, the same wind speed distribution as the Alsvik wind farm had during the time the measurements were performed, no starts and stops. The spectra are shown in Figure 7. The spectrum for a 5D cluster shows significantly higher loads than the spectrum for a single turbine.

For an offshore siting the level of turbulence intensity and the wind gradients will be of about the scale used in this study. The spectra can therefore be considered as being realistic.

5 Comparisons with other types of operation

The type of operation mentioned so far is only normal running conditions. In reality other types of operation may cause load cycles of higher amplitudes. These operation modes will also be less often which means that the number of cycles from these modes will be lower. A full spectrum will have to use the real distribution between the different modes, here no such evaluation is performed. A comparison and a discussion about the

different shapes of the spectra for two other operation modes are presented.

To compare the severity of the wake situations with other types of situation two special conditions were studied. One spectrum was derived using only wind directions from a sector from land where the wind first passes a small forest before it reaches the rotor disc. The surrounding terrain is flat with bushes and trees in groups. The trees are up to 5 meters high. The closest trees are about 100 meters away. The terrain can be regarded as a typical agricultural area, with bushes and trees and flat land. The mean values for wind speed and turbulence can unfortunately not be determined. A guess, based on measurements in other wind directions, would be a factor of two to three higher turbulence intensity compared to open sea. The mean wind speed is lower than from the sea, the difference may only be guessed to maybe 1-2 m/s less than from the sea.The other spectrum contains only load cycles from operation around stall wind speed. Here the wind speed interval 14-16 m/s was chosen. In this interval parts of the rotor disc have wind speeds above stall when other parts will have wind below stall. This will cause high load cycles as the turbine blade will go between these two modes during more or less each revolution.

In Figure 8 the spectrum for winds from the forest is compared to the spectra for stall wind speeds and the full wind speed interval, 4-14 m/s, for the wake situations and the undisturbed situation. The number of cycles is normalised so that each situation occurs the same amount of time in order to make comparisons possible.

From these figures it is clear that the operation mode with the turbine running in the "wind from forest" sector and in the stall wind speed interval will cause the most severe spectra when normalised. But wind speeds around stall are not very common which means that a realistic distribution of wind speeds would give a less pronounced difference, as the accumulated number of cycles for this mode would be less than for example maybe a wake operation mode. The number of cycles for the forest case will be dependent on the site. From Figure 8 it is clear that if the terrain is complex, with trees, bushes and hills, the effect of wakes will be small compared to the effect of the terrain.

6 Conclusions

The influence of wakes on the load spectrum is important to take into account. Especially for offshore sites where the surrounding terrain does not give high load cycles due to high turbulence intensity. This study shows that also wakes from 9.5 diameters distance give significantly higher loads.

Comparisons with other types of operation show that complex terrain may be severe enough to diminish the influence of wakes. This is of course dependent on the terrain and the distribution of wind in different directions.

7 References

[1] Dahlberg J. Å., Poppen M., Thor S. E., Load/Fatigue Effects on a Wind Turbine Generator in a Wind Farm, EWEC '91, Amsterdam, 1991.

[2] Poppen M., Dahlberg J. Å., Fatigue loads on wind turbine blades in a wind farm, FFA TN 1992-21, 1992.

[3] Expert group study on recommended practices for wind turbine testing and evaluation, 3. Fatigue Characteristics, 1984.

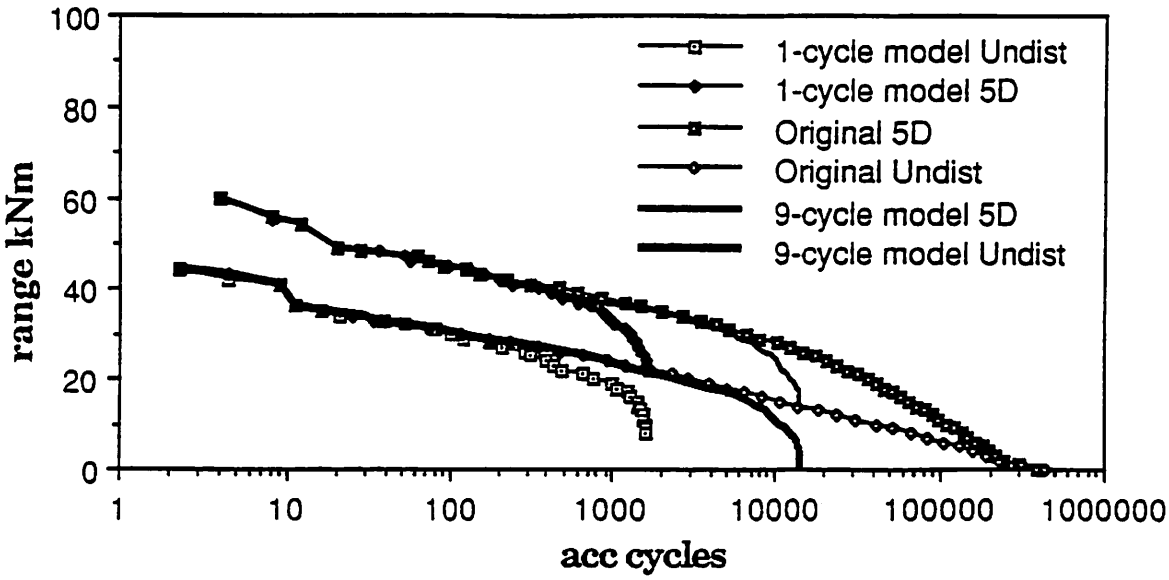

Figure 1. Comparison between results from time signal and more complex model.

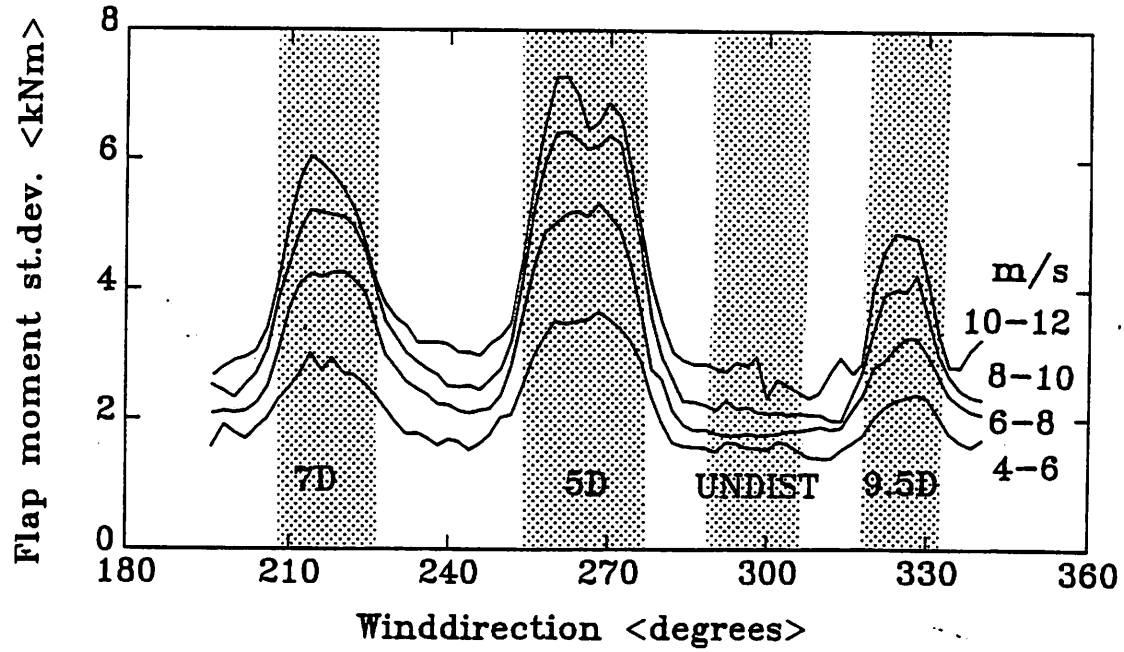

Figure 2. Flap moment standard deviation as function of wind direction and wind speed

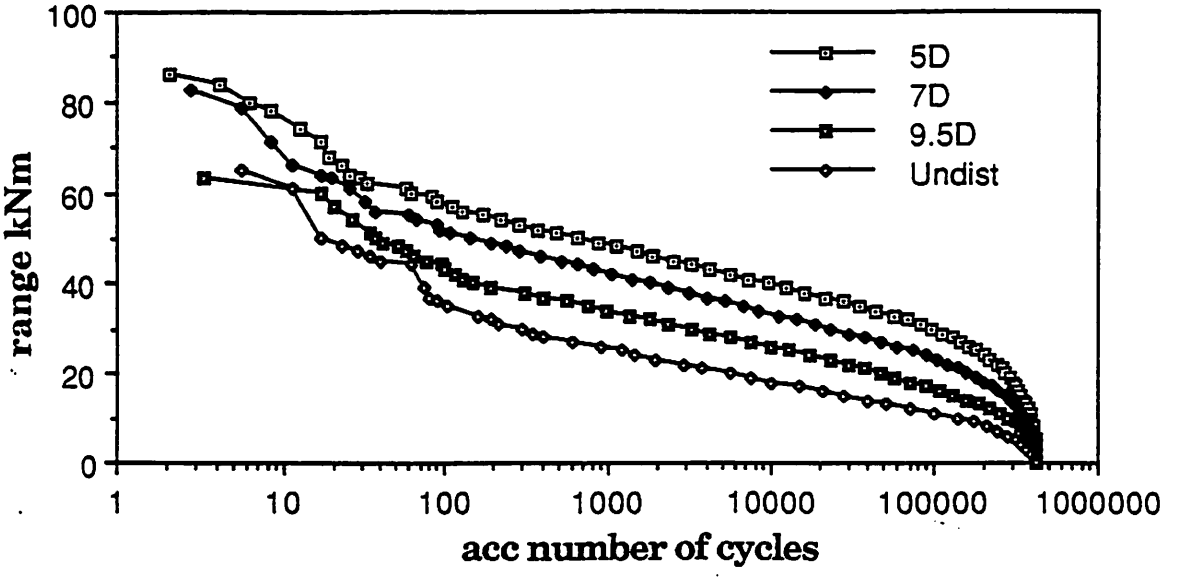

Figure 3. Load spectra for the wind speed interval 4-14 m/s.

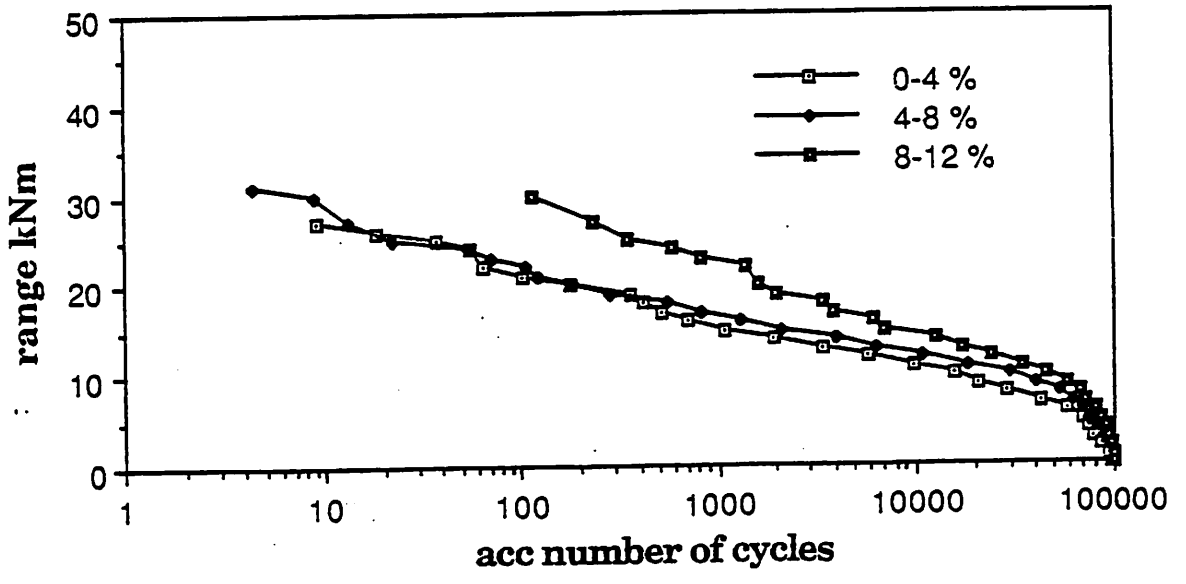

Figure 4. Load spectra for different levels of turbulence intensity for the undisturbed operation.

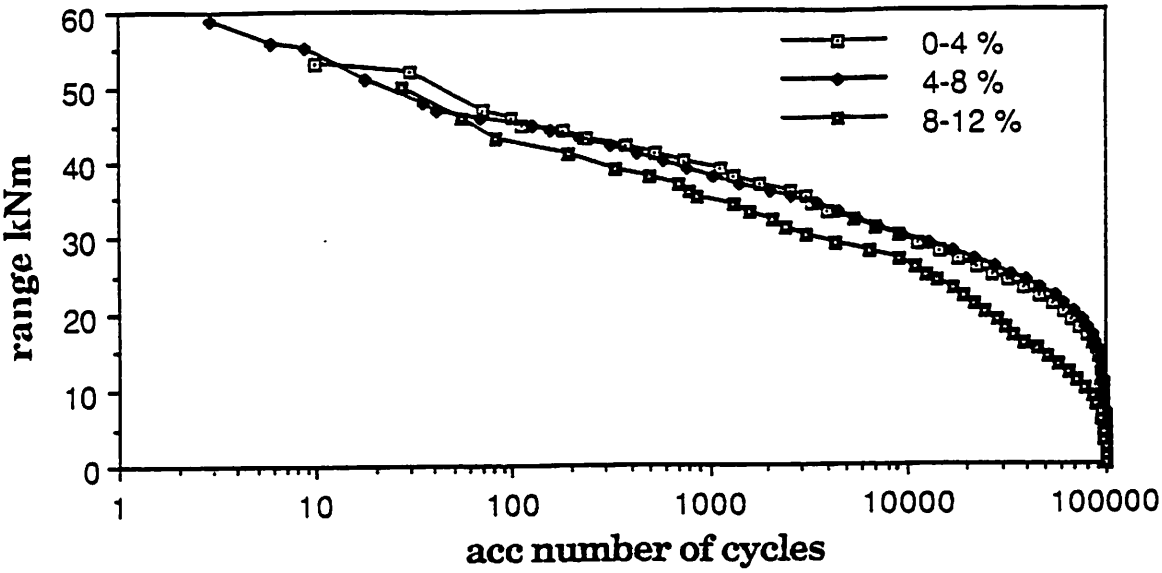

Figure 5. Load spectra for different levels of turbulence intensity for 5D wake operation.

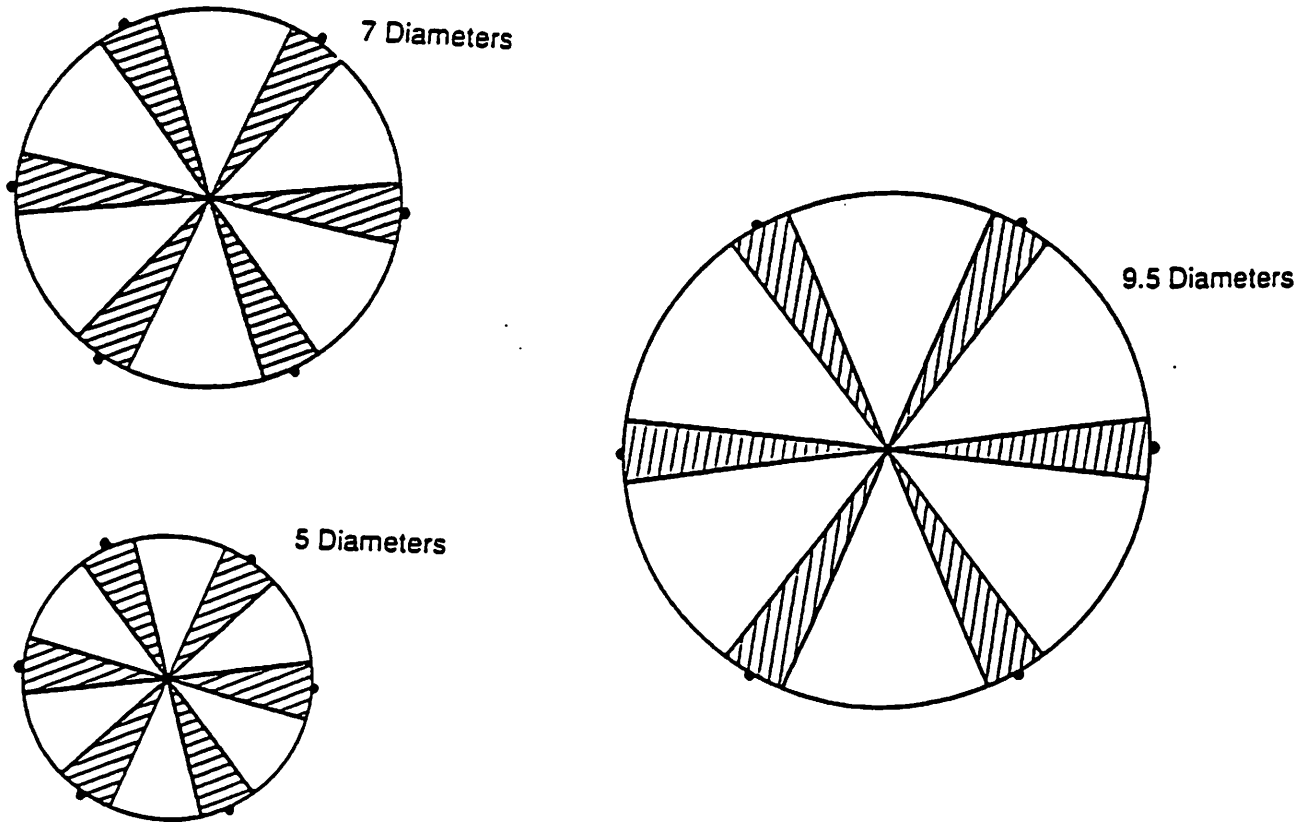

Figure 6. Wind turbine clusters with three different turbine distances.

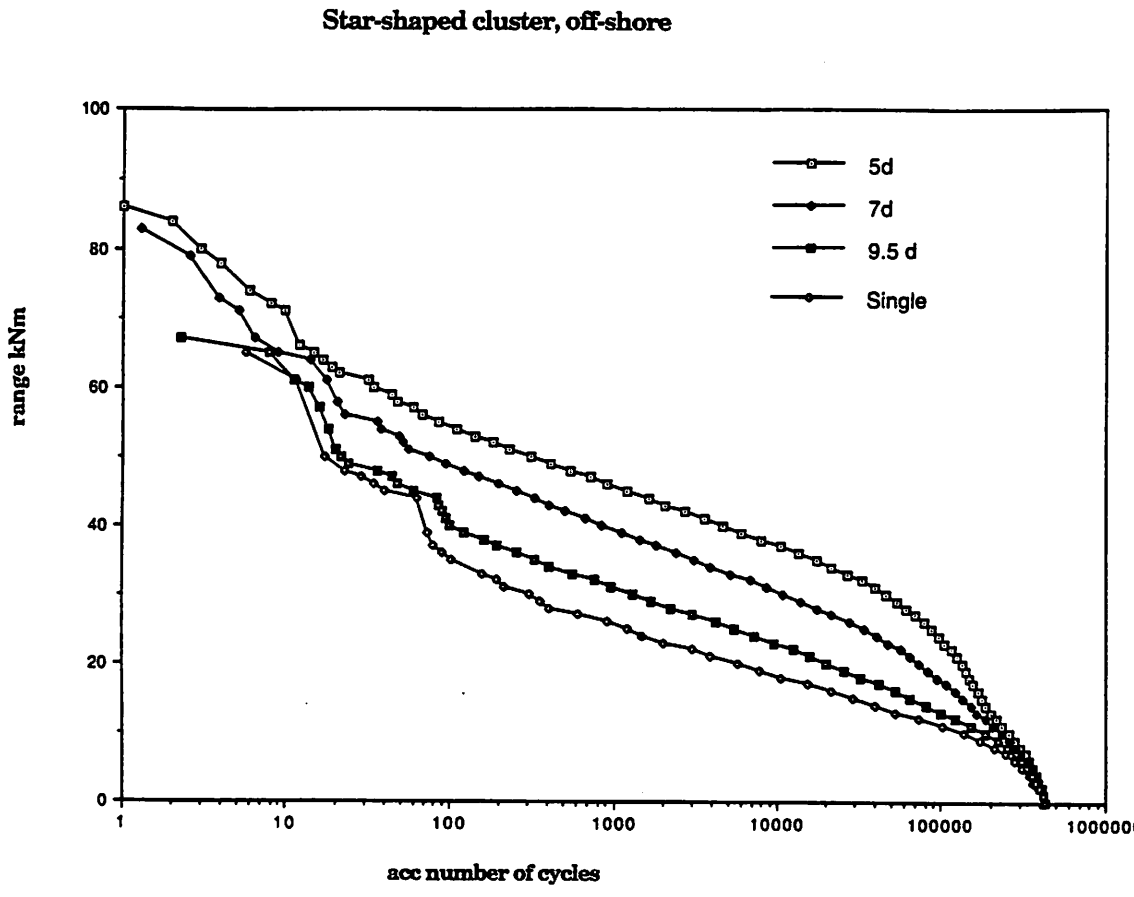

Figure 7. Load spectra for star shaped clusters.

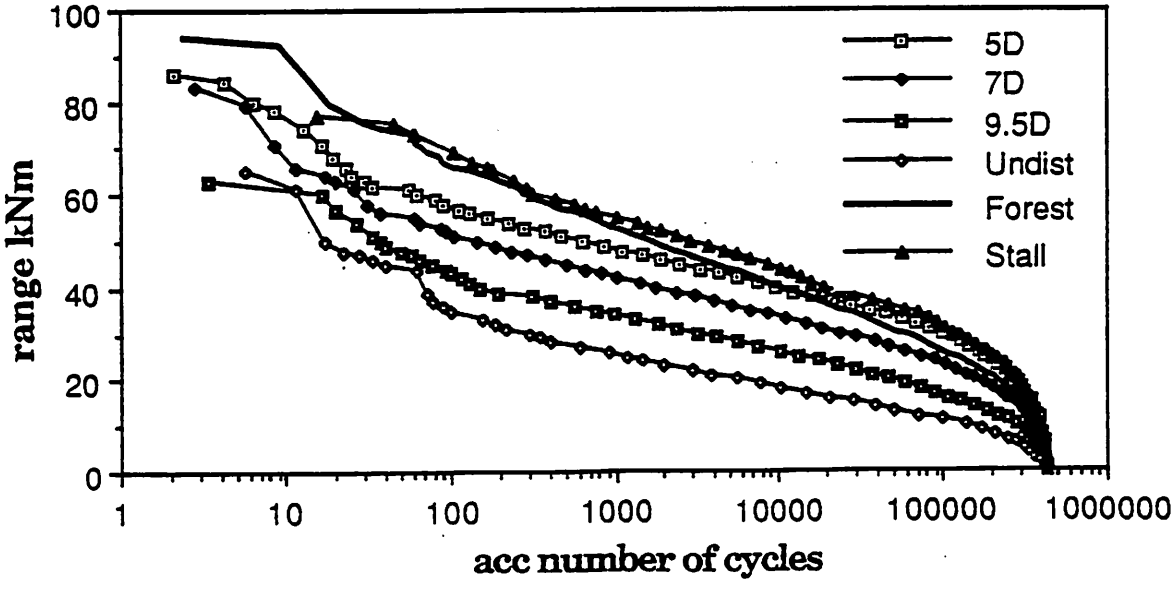

Figure 8. Load spectra for 4-14 m/s compared to higher turbulent wind operation and stall wind speed.

IEA-Expert Meeting on:
Increased Loads in Wind Power Stations
Gothenburg, Sweden, May 3-4 1993

MONITORING FATIGUE LOADS ON WIND TURBINES USING CYCLE COUNTING DATA ACQUISITION SYSTEMS

Henry Seifert

DEWI Deutsches Windenergie-Institut, Germany

- MAIN OBJECTIVES

- Investigate the influence of WT-configuration and site parameter on fatigue loads
- Create a sound basis of statistically approved data
- Help to develop a monitoring method for fatigue loads of large scale WT

MONITORING FATIGUE LOADS USING CYCLE COUNTING FIELD COMPUTER

H. Seifert, H. Söker
Deutsches Windenergie-Institut (DEWI)
D-2940 Wilhelmshaven, Ebertstr. 96
Germany

ABSTRACT: Fatigue loads on components of wind turbines are commonly determined on the basis of short time sequences. However, recording raw data is time consuming and expensive. As an alternative, the presented project suggests long term fatigue load monitoring using on-line cycle counting methods. In parallel meteorological data of the site and operational data of the wind turbines have to be recorded in order to be correlated with the obtained fatigue load spectra.

In order to determine the rotor blade load spectra of wind turbines operating in a wind farm, on-line cycle counting data acquisition systems (DAS) were installed on the hubs of two 300kW pitch controlled wind turbines. Under the prevailing wind direction one of the turbines operates in undisturbed flow, whereas the other turbine operates in wake flow. An independent data logger for meteorological and operational data assessment was installed in the utilities substation. Despite some problems during commissioning of the DAS this paper presents first results. It is planned to monitor the fatigue loads for at least one year.

1. INTRODUCTION

As in any industrial application, the duration of a wind turbine's life is a key parameter for the evaluation of its economic potential. Assuming a life span of 20 years, components of the turbine have to withstand a number of load cycles of up to 10^8. Such high numbers of load cycles pose high demands on the fatigue characteristics of both, the used materials and the construction. However, the specific features of these fatigue loads are mostly unknown yet and can be expected to vary with the type of turbine and the site of operation. Measurements have to be carried out in order to adopt and verify load assumptions for different wind turbine configurations and different sites. Improved load assumptions will be of great importance for the development of the next generation of larger scale wind turbines.

2. METHOD OF APPROACH

Fatigue loads on components of wind turbines are commonly determined by applying cycle counting methods on short time sequences of the respective loads [1]. The resulting frequency distributions of the load cycles are extrapolated and combined according to long term operation statistics in order to obtain an amplitude spectrum. This fatigue load spectrum forms the input data for life time calculations. However, recording raw data requires data acquisition systems with high expenditure of costs and man power. Only a limited number of time sequences may be evaluated and rare events like extreme wind speeds, high gusts and fast changing wind directions may not be recorded at all. As an alternative, the presented project suggests long term fatigue load monitoring using on-line cycle counting methods. Thus compilation of a cost effective, easy to handle and reliable data acquisiton system (DAS) capable of on-line data reduction is the primary task when following this approach. The second objective is to evaluate the fatigue loads on the blade roots of two wind turbines operating in a wind farm. Under the prevailing wind direction one of the turbines operates in undisturbed flow, whereas the other turbine operates in wake flow. On each turbine strain gauges are mounted in half bridge configuration to measure bending moments at the blade root in edgewise and flapwise direction. The signals are sampled and reduced on line employing the Rainflow counting algorithm. The data are stored as frequency distributions of the counted load cycles in form of matrices.

In parallel, meteorological data of the site and operational data of the wind turbine have to be recorded in order to be correlated with the derived fatigue load spectra. For this purpose an independent data logger and a meteorological tower were installed in the wind farm.

Both data acquisition systems are read out once a month. It is planned to obtain load spectra of edgewise and flapwise blade root bending moments as well as the corresponding meteorological and operational statistics for a time span of at least one year.

Two 300 kW wind turbines in the windfarm of Hamswehrum, a small village in the northern part of Lower Saxony, are equipped with data acquisition systems. The wind farm is commercially operated by the local utility EWE (Energieversorgung Weser Ems) and consists of 11 ENERCON 33 wind turbines with 33m rotor diameter, variable speed and pitch control. The turbines are positioned in rows of five and six, respectively. Turbine number twelve is the prototype of a new 36m diameter turbine (Figure 1). Under the prevailing wind direction one of the turbines (#7) operates in undisturbed flow whereas the other turbine (#3) operates in wake flow. The prevailing wind direction is depicted on the top of Figure 1.

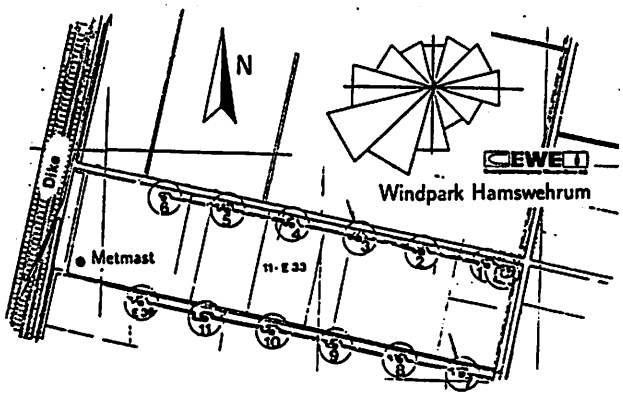

Figure 1: Wind Farm Hamswehrum

3. DATA ACQUISITION SYSTEM

The DAS is made up by two independent subsystems as shown in Figure 2.

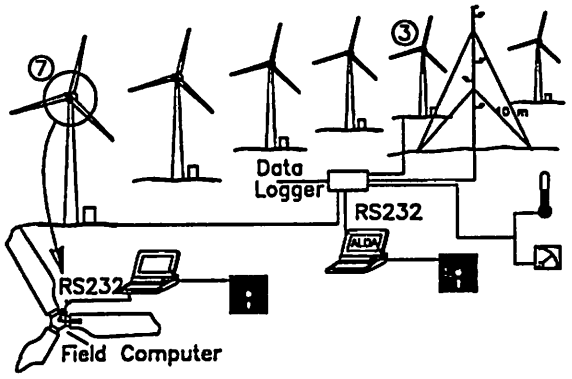

Figure 2: Data Acquisition System

3.1 Field Computer

A commercially available field computer (FC), protected against moisture and rain, is mounted on the rotating hub of each of the observed wind turbines. Each system is equipped with two strain gauge modules. These modules supply and sample two strain gauge brigde circuits and are calibrated to measure bending moments in edgewise and flapwise direction. The sampling rate is set to 100 Hz. On each channel's signal the FC performs Peak-Valley and Rainflow counting and stores the results as frequency distributions of the counted load cycles in form of matrices. The FC are read out via RS232 communication link to a laptop computer. The data are checked directly on the turbine, making it possible to detect faults immediately. A modem connection to the telephone line may be an option in the future.

The FC's external energy supply system is battery buffered and is fed from the grid through slip rings. The slip rings are divided into two parts for assembly on already operating turbines and transmit safety extra-low voltage.

3.2 Ground data logger

The meteorological data i.e. wind speed at heights of 18m and 42m, wind direction at 42m, temperature, and air pressure as well as the operational data such as power output, rotor speed and status signals are recorded by the ground data logger (GDL). They are sampled at a rate of 1Hz. The samples are then stored as 10-min-averages and corresponding standard deviations. They are evaluated with commercially available software which is developed and maintained by DEWI. Figure 3 shows an example for the evaluation of the wind speed at 42m height. The percentage of in wake operation of the two turbines is determined from the wind direction evaluation.

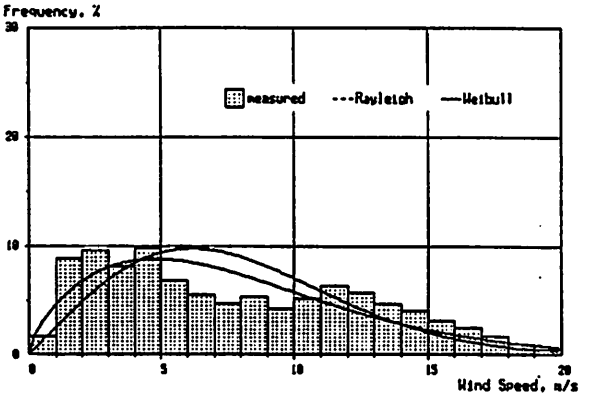

Figure 3: Frequency Distribution of Wind Speed at a Height of 42m

The advantages of the presented DAS are comparably low costs of the hardware and automatic operation combined with a rather quick evaluation of the data.

3.3 Calibrations

The measured bending moments are calibrated with the moment calculated from the blade mass and its centre of gravity. In order to ensure reliability of data, time sequences of the signals are recorded while the turbine is rotating slowly. The range between the extrema of that time sequence can be related to the blade bending moments and a possible zero drift can be detected. Recording these time sequences is part of the procedure when reading out data wich is done once a month.

3.4 First experiences

Laboratory tests of the field computers led to satisfying results. However, after the first in field test they were found damaged, obviously due to electrostatic discharge. In cooperation with the FC's manufacturer an improved, additional electrostatic shielding concept was developed and a special "bleed-off" circuitry is now used when establishing the communication link. In addition a special proceedure was defined for data read out.

The following in field test started promising. Reading out the data from turbine #7 after six days gave the expected results. At this point the second FC was installed on turbine #3 and the test was started. Three days later the data were read out again. This time the FC of turbine 7 presented good results on both channels whereas the FC on turbine #3 delivered good results on the flapwise channel only.

A month later, the next attempt to retreive data from the two FC turned out to be rather disappointing: The system of turbine #7 was damaged again, presumably

due to a lightning stroke and the system on turbine #3 offered bad results on the edgewise channel, because its plug was corroded. Thus, the most pressing work in the near future is to improve the reliability of the DAS.

On the other hand, the GDL proved to be more reliable. It operated since installation without any failure.

4. FIRST RESULTS

A preliminary evaluation was performed on the recorded data in order to give an idea of the nature of the results that can be expected. From turbine #7 data were taken after six days and again after nine days of typical operation i.e. the turbine was operating without failure and the wind speed stayed in the turbine's range of operation. The data of the six days measurement were extrapolated to be equivalent to a period of time of nine days and compared to the nine days measurement. Figure 4 and Figure 5 show the Rainflow matrices of the nine days measurement.

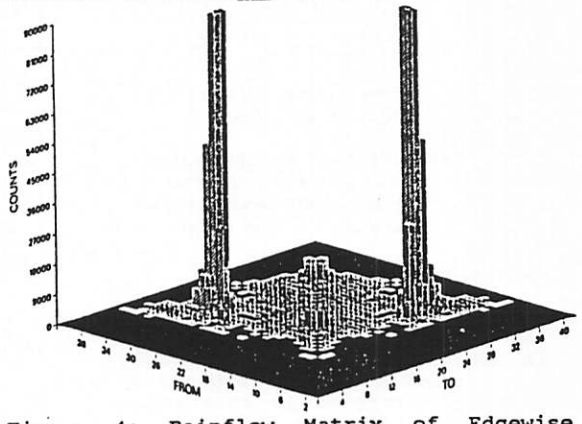

Figure 4: Rainflow Matrix of Edgewise Bending Moment (Turbine #7)

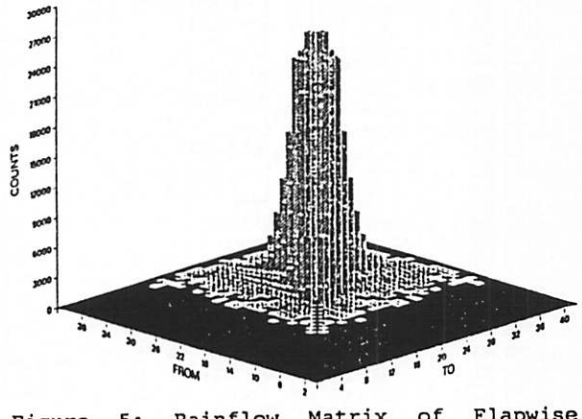

Figure 5: Rainflow Matrix of Flapwise Bending Moment (Turbine #7)

The edgewise bending moment is dominated by the deterministic gravity load of the rotating blade having a relatively high mass. On the other hand the flapwise bending moment shows the expected stochastic behaviour due to the wind speed fluctuations. This is clearly confirmed by the obtained amplitude spectra which were choosen in order to facilitate the comparison (see Figure 6).

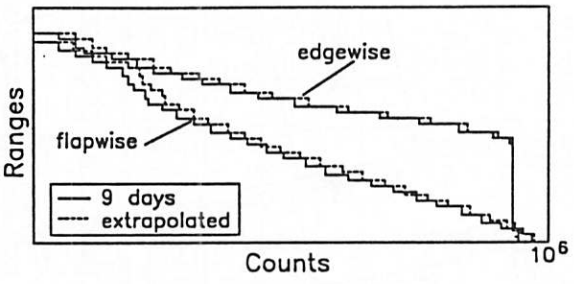

Figure 6: Amplitude Spectra (Turbine #7)

Each pair of curves depicts the extrapolated spectrum and the spectrum of nine days continuous measurement. The differences between the extrapolated curves and the measured curves are of minor influence and can be ignored.

The measurements of the flapwise bending moment of turbine #3 (not calibrated in the same way as on turbine #7 see Figures 7 and 8) over periods of time of three days and 34 days were evaluated in the same way as the data of turbine #7. However, the amplitude spectra now show a tremendous difference between the shapes of the extrapolated and the measured matrix (Figure 9). In that 34 days period the high wind speeds of the January storms were recorded, leading to 10-min-averages of up to 31 m/s.

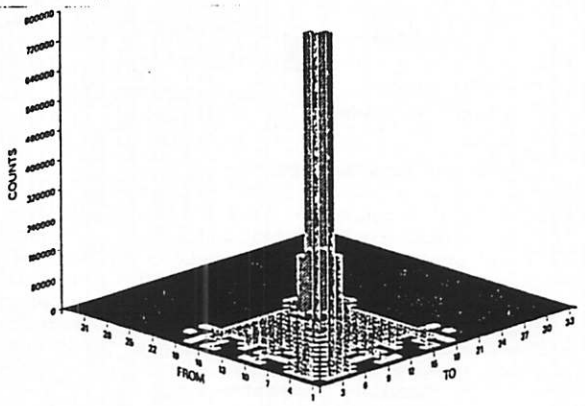

Figure 7: 3 Days Rainflow Matrix of Flapwise Bending Moment (Turbine #3)

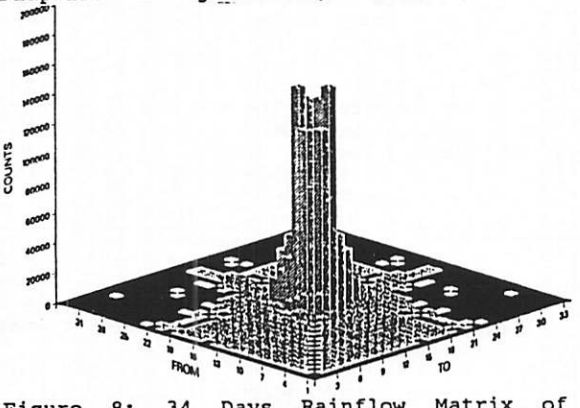

Figure 8: 34 Days Rainflow Matrix of Flapwise Bending Moment (Turbine #3)

The evaluation of the amplitude spectrum reflects this in showing higher amplitudes at lower cycle numbers compared to the extrapolated curve. Also, in the interval between 10^4 to 10^6 the loads are underpredicted by the extrapolated curve.

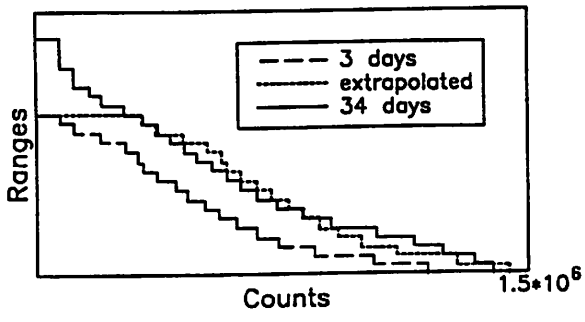

Figure 9: Amplitude Spectra Flapwise Bending Moment (Turbine #3)

Looking at the iceberg model of the lifetime spectrum [2] the stated results seem to be correct.

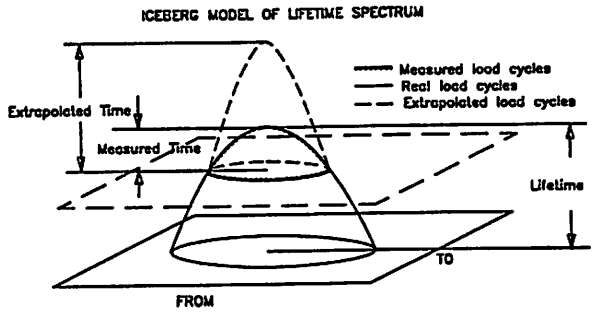

Figure 10: Iceberg Model of Lifetime Spectrum

4. CONCLUSIONS

This first evaluation of the on-line counted Rainflow matrices shows that long time monitoring of fatigue loads can lead to more reliable results at low and high numbers of load cycles. This is especially important for the rotor blades of the next generation of larger wind turbines. It is important to perform such measurements at different turbines in order to improve the load assumptions. Compared to the costs of large scale wind turbines the costs of the proposed monitoring method are marginal, whereas the results can help to save material without diminishing safety.

The next step in the project will be the comparison of load spectra measured at wind turbines of the same type operating in the wind farm. Load spectra are also gathered from a turbine operating at a site with varying turbulence intensity in Greece and at a stall-controlled turbine operating at Alsvik wind farm in Sweden. This is part of a Joule II programme DEWI carries out in cooperation with the Center for Renewable Energy Sources (C.R.E.S.) and the Aeronautical Research Institute of Sweden (FFA).

5. ACKNOWLEDGEMENTS

Although measuring in a commercial wind farm, owned by the local utility EWE, DEWI is allowed to stop the turbines for installation and calibration of the DAS. The authors wish to thank EWE and especially Mr Mentjes who always assists the DEWI staff during their work on the field.

The described measurements are part of a research programme supported by the Commission of the European Communities. The partners are C.R.E.S. in Greece and FFA in Sweden.

REFERENCES

[1] P.H.Madsen et al.(Ed): Recommended Practices for Windturbine Testing and Evaluation: 3.Fatigue Loads, International Energy Agency Programme for Reasearch and Development on Wind Energy Conversion Systems 2nd Ed. Paris (1990).

[2] T.Haberle, T.Kramkowski, H.Söker: Ermittlung von Ermüdungslasten: Rohdatenauswertung oder direkte Datenreduktion?, Proceedings DEWEK'92 Conference, Deutsches Windenergie-Institut Ed. Wilhelmshaven (1992) 71.

Frequency Distribution

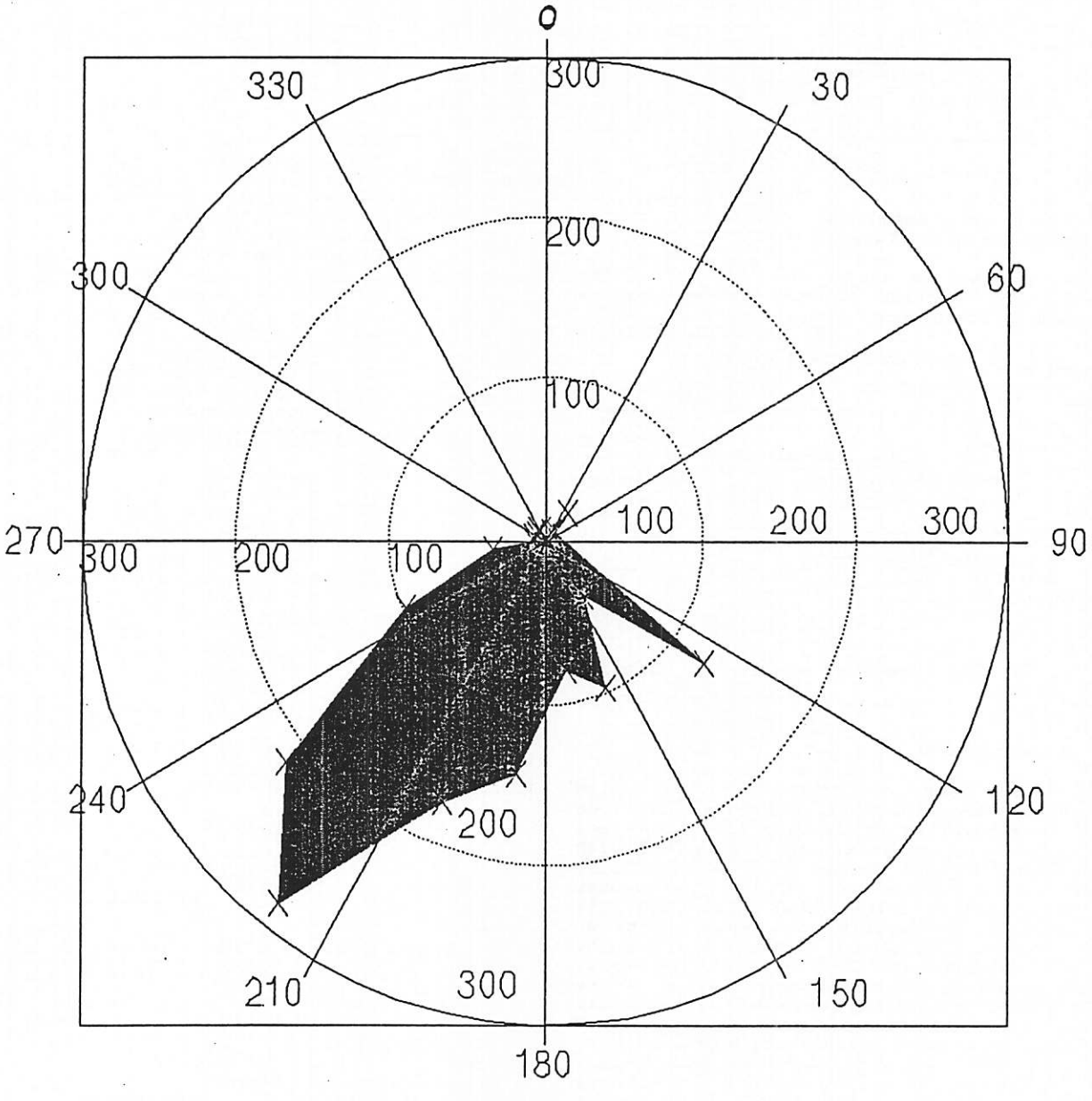

Wind Direction, deg

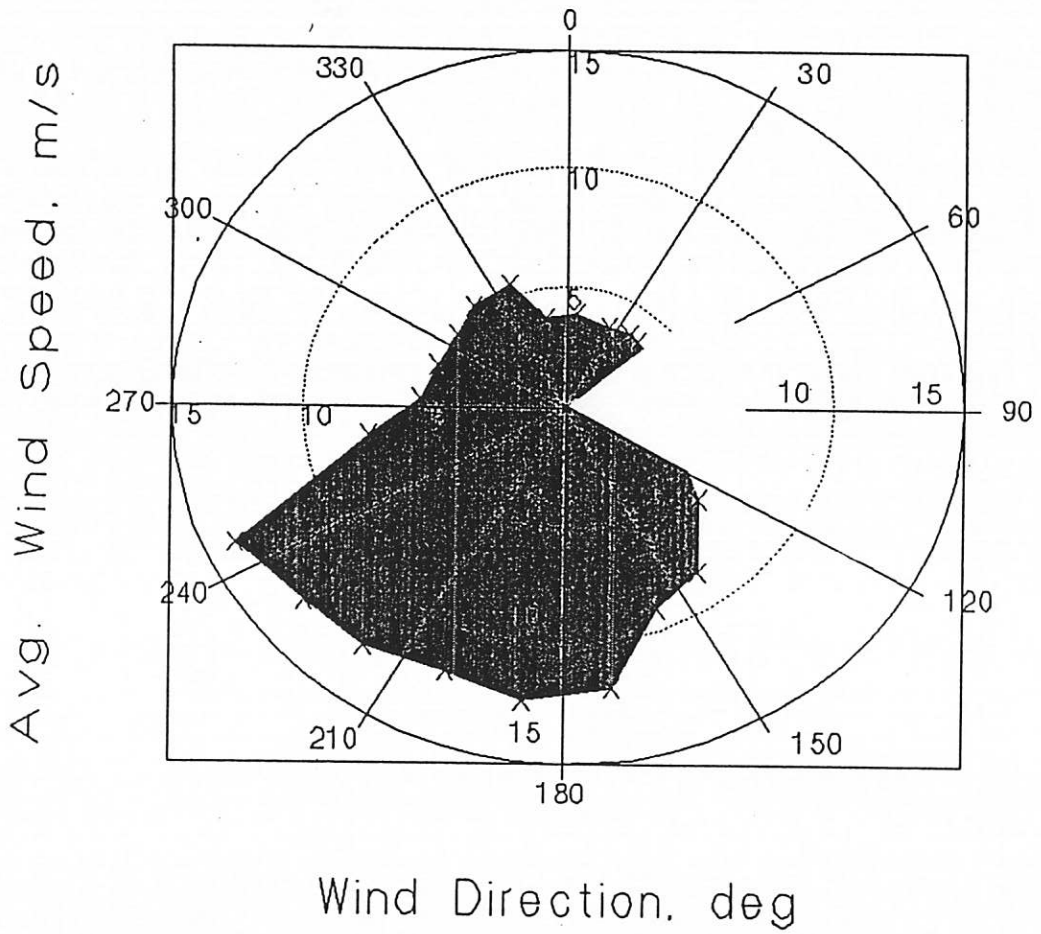
Wind Farm Hamswehrum
Meteorological Data, JAN 1993
Avg. Wind Speed, m/s
Wind Direction, deg
0
30
60
90
120
150
180
210
240
270
300
330
5
10
15

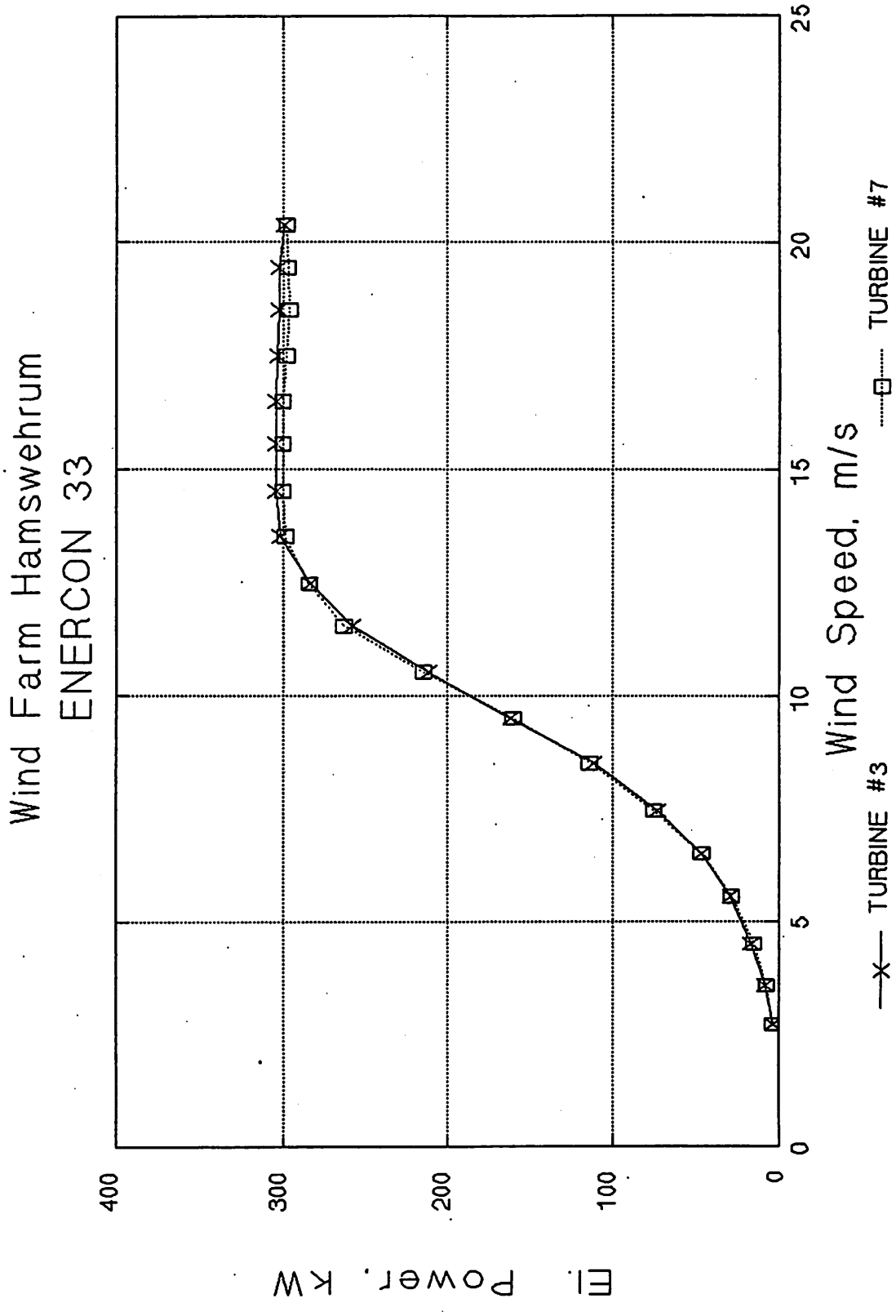
Wind Farm Hamswehrum
ENERCON 33
El. Power, kW
400
300
200
100
0
0
5
10
15
20
25
Wind Speed, m/s
TURBINE #3
TURBINE #7

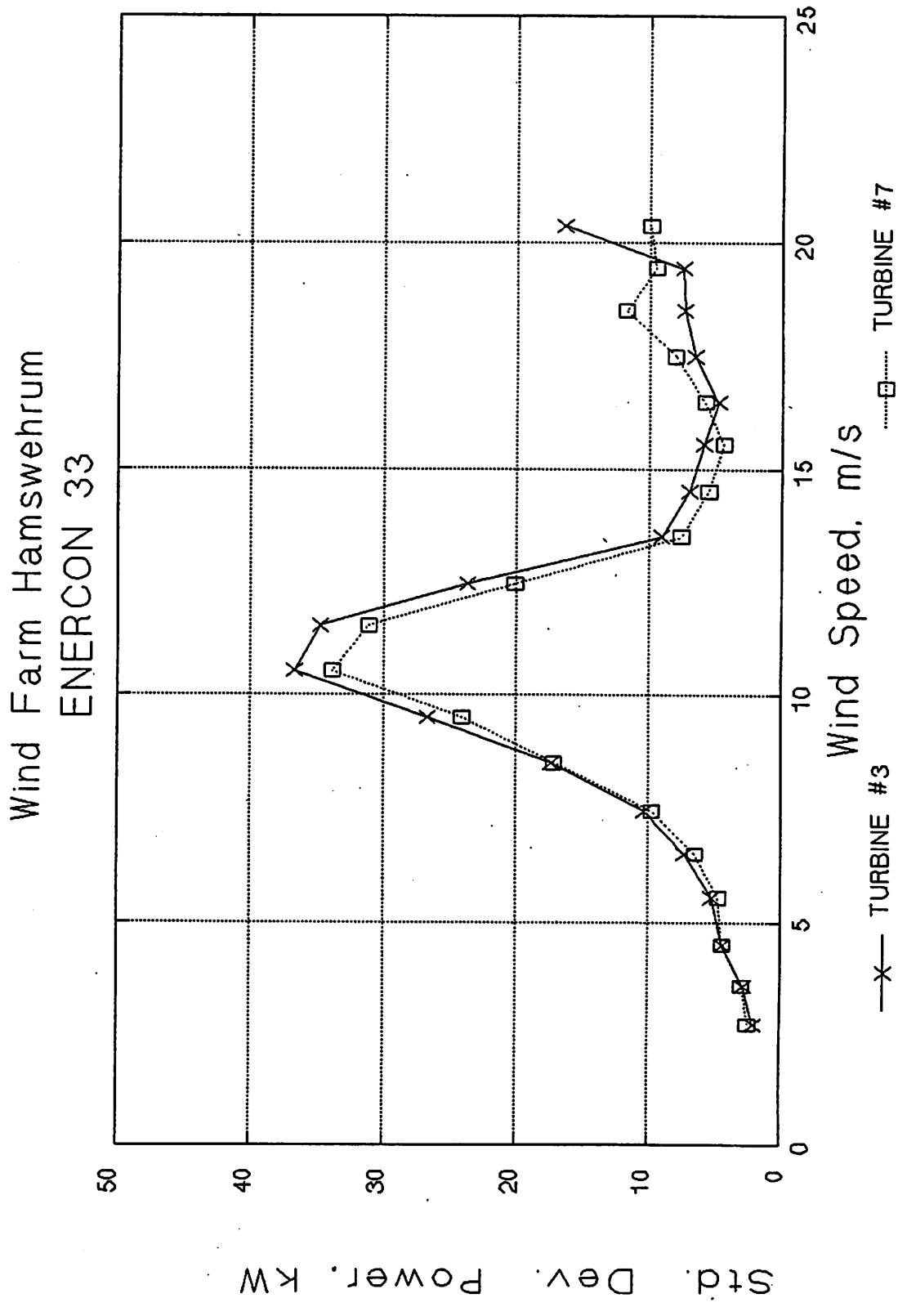
Wind Farm Hamswehrum
ENERCON 33
Std. Dev. Power. kW
0
10
20
30
40
50
0
5
10
15
20
25
Wind Speed, m/s
TURBINE #3
TURBINE #7

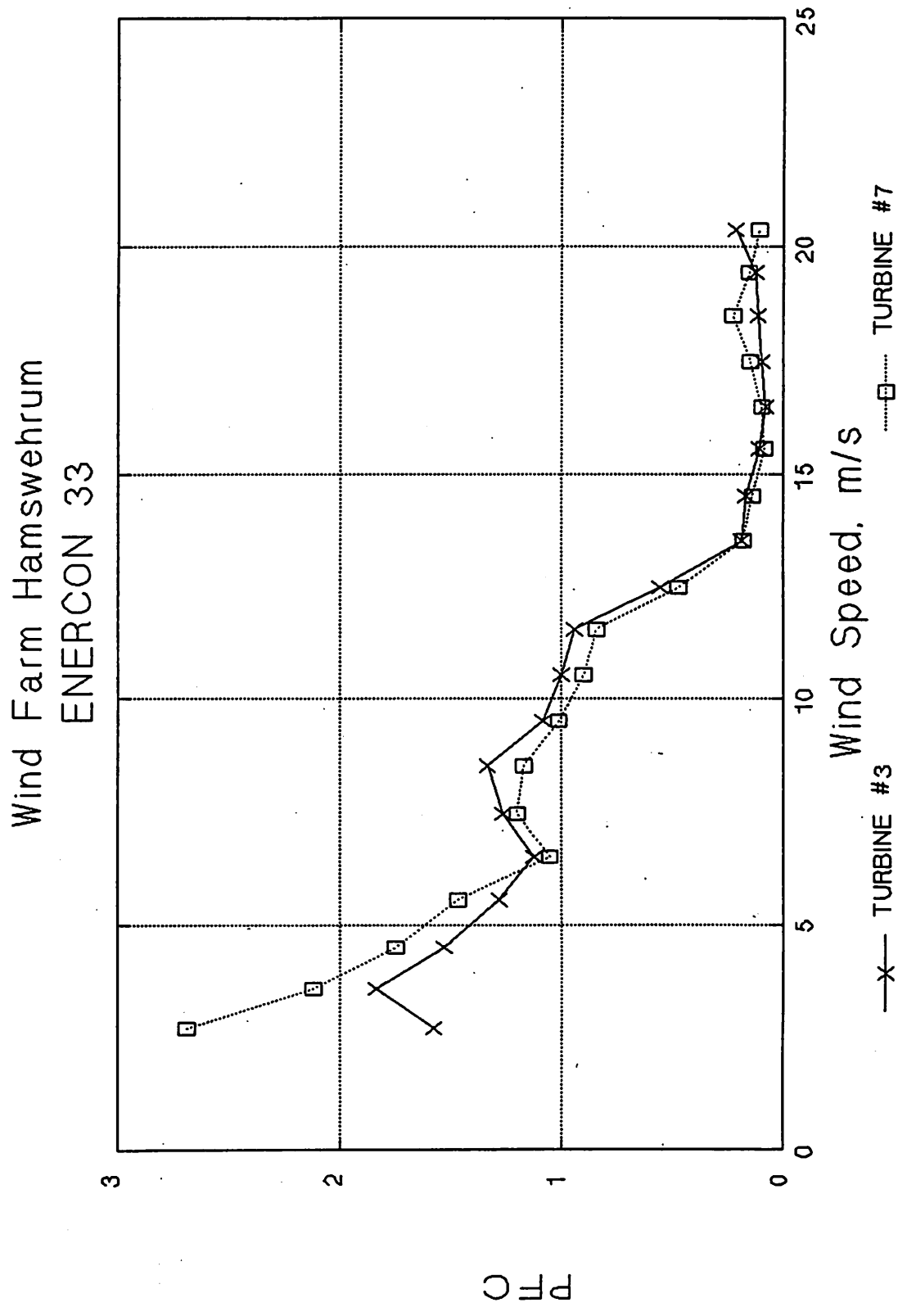
Wind Farm Hamswehrum
ENERCON 33
PTC
3
2
1
0
0
5
10
15
20
25
Wind Speed, m/s
TURBINE #3
TURBINE #7

Measurement and Modelling of the Wind Field Structure in Wind Farms

Axel Albers*, Hans Georg Beyer, Marius Schild, Annette Schomburg,
Wolfgang Schlez, Hans-Peter Waldl, Ubbo de Witt*

Carl von Ossietzky Universität Oldenburg,
Dept. of Physics, Renewable Energy Group,
D-2900 Oldenburg, Germany
FAX + + 49 441 798 − 3326

**Deutsches Windenergie Institut ,*
D-2940 Wilhelmshaven, Germany
FAX + + 49 4421 4808 − 43

We report on the results and current work of a measuring program concerning wake effects. Measurements of the mean velocity field and the turbulence characteristics in the wake flowfield of single wind turbines are performed with meteorological masts and a SODAR equipment. The results of the single wake measurements of mean wind speed are compared to the Ainslie model. Turbulence measurements are presented.

Introduction

At the Deutsches Windenergie Institut (DEWI) and the Carl von Ossietzky Universität Oldenburg, a comprehensive measurement program is carried out in cooperation to improve the database of full scale wind farm effects.

Measurements of the mean velocity field and the turbulence characteristics in the wake flowfield of single wind turbines are performed. Two different wind turbine types, a *ENERCON 16* (rotor diameter (D) 16m) and a *ENERCON 33* (rotor diameter 33m) are analyzed. Both turbines are operated with variable rotational speed.

The goal of these investigations is to gain more detailed information on the performance of standard models for the prediction of wake velocity and turbulence. The results of the turbulence analyzes will be compared to measurements which are in progress at several *ENERCON 33* in an other wind farm (/Seifert/).

In addition, the application of the SODAR equipment for estimating the turbulence in the flow will be tested. The experience gained with the models will be used for a computer code for calculating the farm efficiency and for optimizing wind farms.

Single Wake Measurements

Norddeich Fledderweg, *ENERCON 16*

Wake velocity measurements are performed at a 55 kW *ENERCON 16* wind turbine (diameter 16.2 *m*, hubheight 22.4 *m*) which is stall regulated and operating at variable rotational speed. The turbine is sited in a small straight line wind farm Norddeich/Fledderweg (5 × 55 *kW*, sited at a distance of approximately four rotor diameters) at the North Sea Coast.

The wind velocity was measured at in total three meteorological masts (Fig. 1). One is sited at two rotor diameters upwind from the turbine in the prevailing wind direction, measuring the undisturbed wind velocity and direction at hub height and at the upper and lower edge (hubheight ± rotor radius) of the rotor disk.

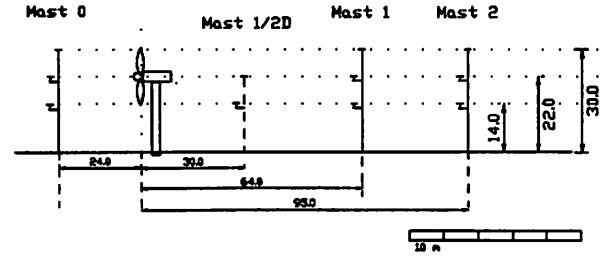

Figure 1 Arrangement of turbine *ENERCON 16* and masts

For one measuring campaign, an additional mast was sited at a distance of two rotor diameters behind the turbine. It was equipped with anemometers at hub height and at the height of the lower edge of the rotor disk.

In a second period, two masts were used for registering the wake wind speed at a distance of four and six rotor diameters form the wind turbine. These masts have the same equipment as the free mast.

For all wind measurements, standard cup anemometers are used. The time resolution of the data recording was one minute respectively one second for selected time periods.

Mean Wake Flow

The data sets gained with this setup are used for an extended test of the Ainslie wake model (/Ainslie/). Fig. 3 and Fig. 4 show the mean wind speed (base : one minute averages) measured in the wake flow at hub height and at height of the lower edge of the rotor disc at the three masts as a function of wind direction (□). All values are normalized to the free wind speed and classified with respect to wind direction bins. Mean free wind speed during this measuring period was about 8 m/s. The wind speed is reduced to about 40 % at two diameters behind the rotor and recovers with increasing distance to the rotor to 70% (4 D) and 80% (6 D).

At one edge of the wake, the wind speed is higher then the undisturbed velocity for a certain range of the wind direction. This effect is supported by former measurements of the farm efficiency (/Beyer89/) which shows the same phenomenon. Unfortunately the respective wind directions are not covered by the data gained with mast $2D$.

In the same figure, calculations with the Ainslie model /Ainslie/ are presented (△). The model is based on the solution of the axial-symmetric reynolds equation. Using the boundary condition proposed by Ainslie the equations are solved applying the /PDE/PROTRAN/ code. The calculations predict a slightly higher wind speed over the whole range of wind directions. They are in total in a reasonable accordance with the measured wind speed values except for the plot at 2 D at the lower rotor edge. Here, the minimum of the wake is distinctly shifted relative to the expected wake axis.

It should be noted that the model calculations are based on a $c_t(windspeed)$-characteristics of the wind turbine calculated by the (measured) rotational speed and the thrust coefficient $c_t(\lambda)$ characteristics supported by the blade manufacturer. A measurement of the rotor thrust by registering the wind turbine tower root bending moment is in progress but not finished yet. So, a more certain comparison between calculated and measured wind speed values can be expected in the near future.

Norddeich Marschweg, *ENERCON 33*

Measurements of the near wake flowfield of a larger turbine are performed at a single wind turbine of type ENERCON E-33. (see Fig. 2)

The upwind mast is equipped with two cup-anemometers, mounted at hubheight and at 10 meters height. The downwind mast is installed at a distance of 2 rotor diameters. It is equipped with three cup-anemometers, mounted at hubheight and at height of the upper and lower rotor tip. In addition the wind vector is registered at hubheight with one ultra sonic anemometer with a high time resolution. The measurements of the wind speeds and characteristic turbine quantities are recorded with a time resolution of 1 second.

As for the smaller turbine the wind speed time series will be analyzed with respect to the wind direction and compared to the predictions of the Ainslie model. Up to now, the gained measured values are not extensivly evaluated yet.

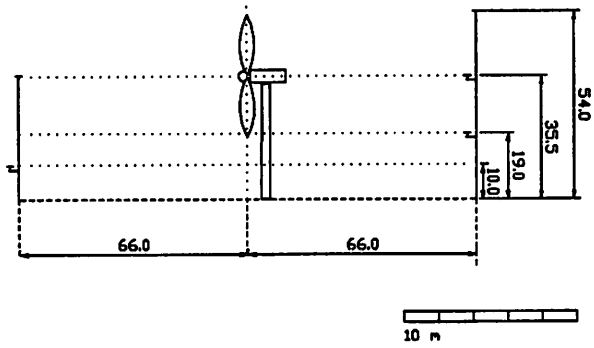

Figure 2 Arrangement of turbine *ENERCON 33* and masts

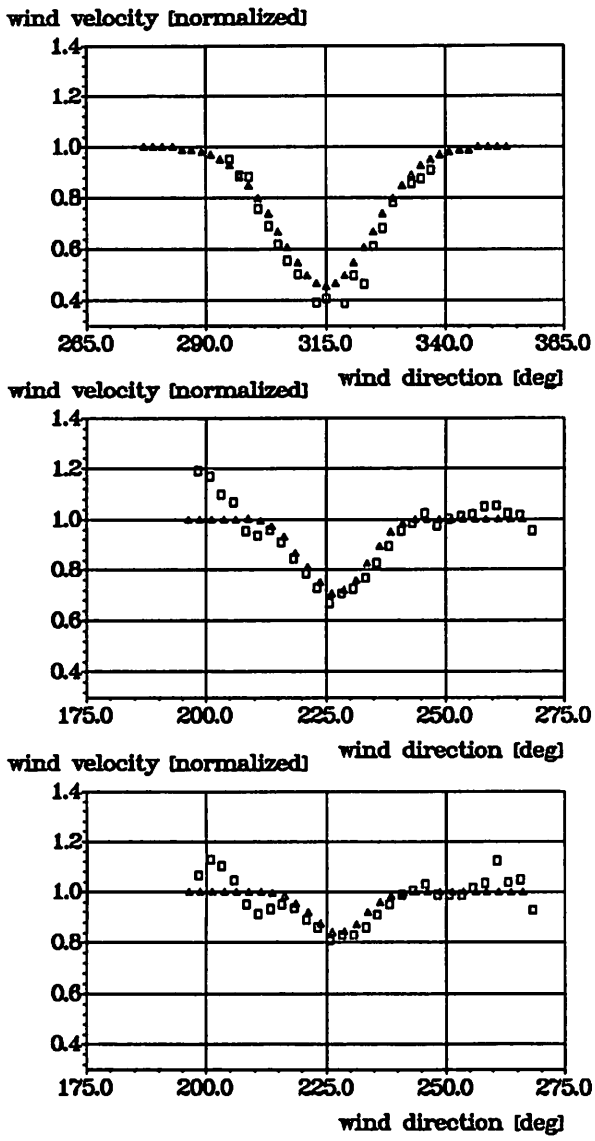

Figure 3 Horizontal profile of the wake velocity (normalized to the free wind speed) at hub height versus wind direction. Distance to the rotor: 2 D (upper), 4 D (middle), 6 D (lower figure). Measured (□) and calculated (△) values.

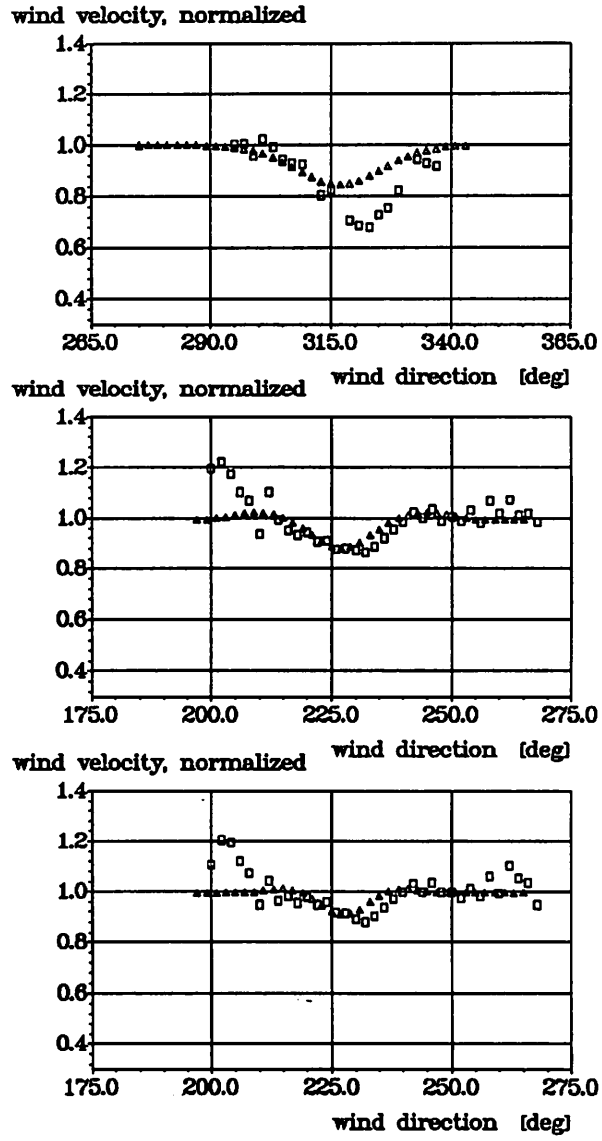

Figure 4 same as Fig. 3, at height of the lower edge of the rotor disc

Sodar Measurements

To gain more detailed information about the vertical profile in the wake flow, measurements where performed at the *ENERCON 16* site with a SODAR developed at the Carl von Ossietzky Universität . Fig. 5 shows the arrangement of the SODAR antenna relative to the wind turbine. The profiles of wind velocity were gained for a maximum height of 40 *m*.

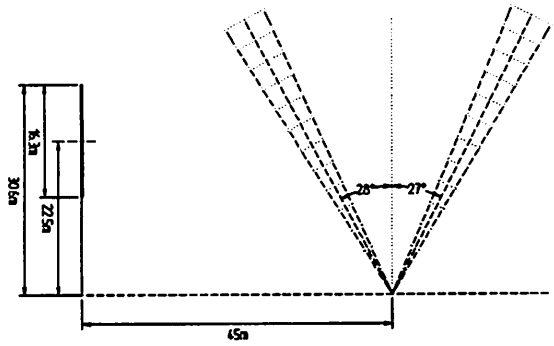

Figure 5 Arrangement of the SODAR and the wind turbine

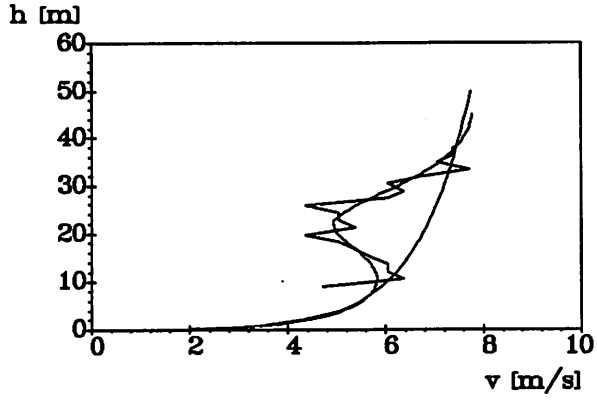

Figure 6 Vertical profile of the normalized wake wind speed from a SODAR measurement (height versus wind speed). Measured and calculated (Ainslie+log. profile, smooth curve) values. The right smooth curve gives the used free stream logarithmic wind profile.

Fig. 6 shows the result from a measurement with a distance of approx. 3 rotor diameters between the wind turbine and the SODAR beam at hubheight.

Additional to the measured values, the undisturbed vertical wind profile (calculated, logarithmic) and the prediction with the Ainslie model are plotted. The Ainslie model produces a axisymmetric wake profile. To take into account the vertical wind profile in the boundary layer, it is suggested to superimpose a logarithmic profile to the wake model calculations. Here the velocity deficit of the wake flow and the wind speed change in the profile relative to the reference height of the rotor hub are added. The comparison with the model calculations (/Ainslie/ + logarithmic profile) supports this quite simple assumption.

Turbulence in the Wake

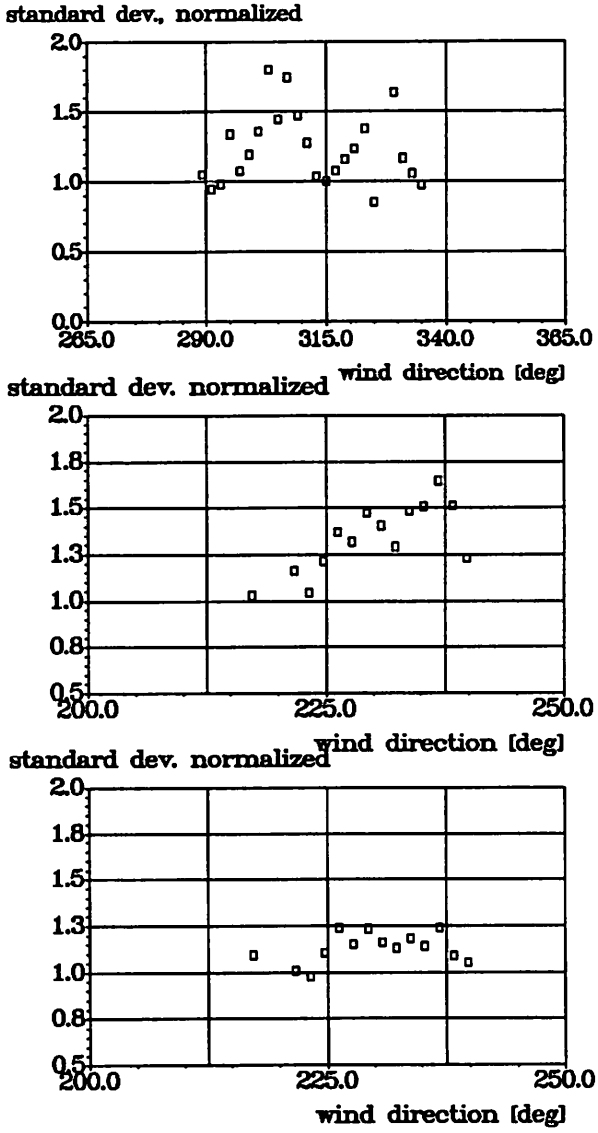

Figure 7 Horizontal profile of the standard deviation in a part of the wake flow of the *ENERCON 16*-turbine. The values are given for a distance of 2 *D* (upper), 4 *D* (middle) and 6 *D* (lower figure). The center of the wake is at approx. 225° resp. 315° for the upper figure.

On the basis of wind speed data registered with a time resolution of one second the standard deviation of the wind speed fluctuations in the free and the wake flow are analyzed. To allow an detailed investigation of the cross flow structure of the turbulence the standard deviations are calculated for one minute time intervals. These calculations are performed for the measurements at the *ENERCON 16* turbine. Figure 9 shows the standard deviation in the wake flow normalized to the free flow value as a function of wind direction. The results for the 4D and 6D masts are given. In addition

the profile for the normalized mean wind speed is given for orientation in the upper plot. Unfortunately only one half of the wake is covered by the wind direction in this measuring period.
The turbulence in the wake flow at 4 D is increased up to 150% compared to the undisturbed flow. At 6 D, the turbulence is lower, but it a increase to 130% still remains at this distance from the rotor.
At the same site, the vertical turbulence profile was gained with the SODAR equipment. Fig. 8 shows the profile of the standard deviation of the wake flow normalized to the standard deviation of the undisturbed flow. The figured values were gained from one ten minute measuring period.

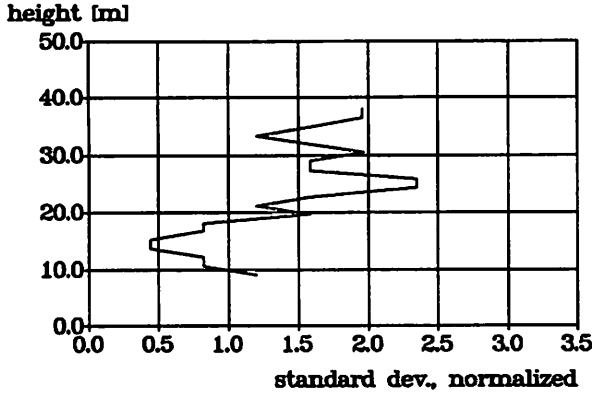

Figure 8 Vertical profile of the normalized standard deviation in the wake flow, measured with the SODAR

Acknowledgement

Part of this work is funded by the german BMFT and the utilities Energieversorgung Weser-Ems AG, Hamburger Electricitäts-Werke AG, and Schleswag AG. We are grateful to the coworkers of the Stadtwerke Norden and to the farmers Mr. Martens and Mr. Wübbens for supporting our work.

References

/Ainslie/ J.F. Ainslie, Calculating the Flowfield in the Wake of Wind Turbines, Journal of Wind Engineering and Industrial Aerodynamics, 27, 1988, 213–224

/Jensen/ N.O. Jensen,A Note on Wind Generator Interaction, RisøNational Laboratory, Risø, 1983

/Beyer89/ Beyer et al, Operational Behaviour of a Small Straight Line Wind Farm, EWEC'89, Glasgow 1989

/Seifert/ H. Seifert, Monitoring Fatigue Loads using cycle counting Field Computer, ECWEC Travemünde 1993

/Schomburg/ A. Schomburg, Use of a Mini-SODAR for Investigation of Turbulence in a Wind Farm, ECWEC Travemünde 1993

/PDE/PROTRAN/ IMSL, 1986

AERONAUTICAL RESEARCH INSTITUTE OF SWEDEN
Sven-Erik Thor

NOTES TAKEN DURING IEA EXPERT MEETING ON INCREASED LOADS IN WIND POWER STATIONS, "WIND FARMS" Gothenburg Sweden 3-4 of May 1993

PARTICIPANT

The expert meeting gathered 17 participants from USA, The Netherlands, Denmark, Germany, England and Sweden. List of participants is enclosed in the end of this document.

PRESENTATIONS

All participants made presentations relevant to the subject of the meeting. A documentation of the presentations will be published shortly by the KFA Jülich.

At the meeting measurements from several wind parks were presented. Three presentations showed result based on measurements in the USA. Compared to European wind farms these farms are much larger and also situated in very complex terrain. In these wind farms the influence of wakes were more or less neglectable, which could also be anticipated as the terrain itself causes high turbulence.

Several participants presented calculations and measurements from the Sexbierum wind farm. The increase in loads is not significant for turbine distances of 8 diameters or more. The loads in the primary shafts are substantially larger for operation in a wake, this could be due to the control system. There is a on-going activity to compare the measurements from Sexbierum and Norreaker with simulations as well as with wind tunnel experiments. Also meteorological measurements at Sexbierum was presented. Calculations of the length scale of the wind caused large discussions.

Three participants from Sweden presented data from the Alsvik wind farm. A large data base has been stored, which contains time signals and 1 minute mean values, from more than two years of measurements. This farm is situated in smooth terrain at the shore line of the Baltic Sea. In this farm the largest influence of wakes has been shown, probably due to the very low turbulence in the wind from the sea. It was also shown that it is important to study the meteorological conditions, stable, neutral or unstable stratification. At Alsvik the influence of wake on the flap moment load spectrum is significant also as far away as 9.5 diameters.

The two participants from Germany made presentations about measuring techniques. A cycle counting monitoring box is used to monitor the rain flow counted cycles at the Hamswehrum wind park. The presentation stressed the problem of making the extrapolation of the data which usually is a couple of days to be valid for a full life time. The other presentation covered the use of SODAR measurements for wind turbines. A discussion followed which stressed the fact that this technique is not giving accurate data for higher wind speed, >10 m/s.

After the presentation there was a general discussion covering the topics of the meeting.

SUMMARY

A summary of the discussions on the second day is made below and in the enclosed pages at the end of this document. The bullets below is our extract of the conclusion that can be drawn from the discussion.

* The participants proposed to arrange this type of meeting on a regular basis.

* List of wind farms where measurements have been carried out would be of great help for researchers in this area.

* The development of design tool which accounts for wind farm operation is currently under development, but verification still lacks.

* Measurements in wind farms have till now been carried out on machines with rigid hub. Measurements on other hub types and concepts is vital for further development of wind turbines not only for operation in wind farms.

* Large spread in results. Some results does not show any influence of operation in wind farms and others show large increase in loads.

* Better knowledge of wind models is required.

* Better understanding of the parameters which are influencing the design of wind turbines is required.

* It is necessary to account for wind farm operation when designing wind turbines.

AERONAUTICAL RESEARCH INSTITUTE OF SWEDEN
Sven-Erik Thor

* **Concept: how to minimise loads by using relevant design solutions**

Thor
Asked for designs which are more suitable for wind farm operation.

Holley
It is not necessarry to skilja between wind farm designs and stand alone designs. All machines have to be designed to operation in a wind farm.

Tindal
Mentioned that Garrad & Hassan had made a theoretical study to investigate the difference between fixed and teetered hub configurations. Reduced loads with a teeetered hub were reported from that study. The effect of partial wake was not included in the study.

Pedersen
Would it be a good idea to have a database with mesured results from wind farm operation.

Schepers
In favour of the idea.

Thor
Not in favour of the idea.

Holley
Doubtful to the idea, but proposed to have a list of relevant litterature in the area.

Seifert
Proposed to have a list of wind farms where measurements have been carried out.

* **Computational methods, tools and philosophy**

Pedersen
Some tools are available, but more development is required.

Beyer
More knowledge is required, especially on the effect of multiple wakes.

* **Meteorological description of wakes, relevant for wind turbine design**

Smedman
More knowledge is required to understand the wind behaviour.
Is in favour of this type of meetings.

* **Presentation of new measurements, preferably on comparisons on flexible and rigid turbines**

Tindal
Informed about the two wind farms in England with teetered hubs. Measurements will be carried out.

Seifert

Proposes to carry out "black box" measurements on many different machines in order to get more information on different machines.

AERONAUTICAL RESEARCH INSTITUTE OF SWEDEN
Sven-Erik Thor

CHRONOLOGICAL SUMMARY OF DISCUSSON

The discussion was focused on the topics in the introductory note for the expert meeting. In the following text is a summary of what was said during the discussion is made.

* The necessity to account for increased loads in the design

The answer is generally speaking yes.

Seifert
Is there a minimum distance between turbines which can be used in the design recommendations? No support for that idea was shown.
Asked for more results from measurments on different tyes of turbines: stall, pitch and variable rpm.

Holley
The effect of operation in a wind farm ranges from negligable to significant.

Schepers
There is a lot of parameters that influence the design.

* Better guidelines that account for loads in wind farms

Tindal
Is in favour of verifying the IEC figures of turbulence 17% to account for the wind farm operation.

Holley
There is a need for good and parametric tools for the design of turbines in general. What parameters is affecting the design.

Tindal
Means that we already have the tools today. But how do we use them in the design process.

Seifert
It is both a question of safety and economics when designing turbines for operation in windfarms.

Kelley
What loads are causing the fatigue damage in wind farm operation. It is still an issue to know which parameters that drives the loads and the design.

Frandsen
We do not speak of different designs for operation for stand alone and wind farm operation. It is rather a continous development of the wind turbine.

Proposed to make different categories of wind turbines.

Holley
The outcome may be that there will be a special class in the IEC TC 88 standards for wind farm operation.

AERONAUTICAL RESEARCH INSTITUTE OF SWEDEN
Sven-Erik Thor

LIST OF PARTICIPANTS IN IEA EXPERT MEETING ON
INCREASED LOADS IN WIND POWER STATIONS, "WIND FARMS"
Gothenburg Sweden 3-4 of May 1993

Andrew Tindal	Garrad & Hassan Coach House, Folleigh Lane, Long Ashton, Bristol, England +44 275-394360
Ann-Sofie Smedman	Meteorological Dept Uppsala Univ. Box 516, 751 21 Uppsala, Sweden +46 18 54 2792
Frits Verheij	TNO Environmental and Energy Research PO Box 342, 7300 AH Apeldoorn, The Netherlands
Bernard Bulder	ECN PO Box 1755, ZG Petten, The Netherlands +31-22464102, fax +31-22463212
Gerard Schepers	ECN PO Box 1755, ZG Petten, The Netherlands +31-22464102, fax +31-22463212
Hans Georg Beyer	University of Oldenburg Dept of Physics D 2900 Oldenburg
Pantelis Vionis	CRES 19 th Maratonos Str., GR-19009, Pikerimi, Greece
Henry Seifert	DEWI Ebertstraße 96, 2940 Wilhelmshaven, Germany +49 4421 4808 12, fax -43
Neil Kelley	NREL Wind Techn Div., 1617 Cole Blvd, Golden, Co 80401, USA +1 303 231 1274, fax +1 303 231 1199
Bill Holley	US Wind Power Inc. 6952 Preston Ave, Livermore, California 94550, USA +1 510 455 6012, fax +1 510 443 3995
Sten Frandsen	Risø National Lab Dept of Met. and Wind Energy, 4000 Roskilde, Denmark +45 42 371212, fax +45 46755619
Kenneth Thomsen	Risø National Lab Dept of Met. and Wind Energy, 4000 Roskilde, Denmark +45 42 371212, fax +45 46755619
Maribo Pedersen	Technical Uiversity of Denmark Dept of Fluid Mech, 2800 Lyngby, Denmark +45 45932711, fax +45 42882421

Sven-Erik Thor
FFA
Box 11021 161 11 Bromma Sweden
+46 8 634 13 70

Jan-Åke Dahlberg
FFA
Box 11021 161 11 Bromma Sweden
+46 8 634 13 36

Maria Poppen
FFA
Box 11021 161 11 Bromma Sweden
+46 8 634 10 08

Ingemar Carlén
Chalmers University of Technology
Inst. of marine structural eng., 412 96 Göteborg, Sweden
+46 31 7721492, fax +46 31 7723699

IEA-Implement Agreement R+D WECS - Annex XI
Topical Expert Meetings

1. Seminar on Structural Dynamics, Munich, October 12, 1978
2. Control of LS-WECS and Adaptation of Wind Electricity to the Network, Copenhagen, April 4, 1979
3. Data Acquisition and Analysis for LS-WECS, Blowing Rock, North Carolina, Sept. 26-27, 1979
4. Rotor Blade Technology with Special Respect to Fatigue Design Problems, Stockholm, April 21-22, 1980
5. Environmental and Safety Aspects of the Present LS WECS, Munich, September 25-26, 1980
6. Reliabiltiy and Maintenance Problems of LS WECS, Aalborg, April 29-30, 1981
7. Costings for Wind Turbines, Copenhagen November 18-19, 1981
8. Safety Assurance and Quality Control of LS WECS during Assembly, Erection and Acceptance Testing, Stockholm, May 26-27, 1982
9. Structural Design Criteria for LS WECS, Greenford, March 7-8, 1983
10. Utility and Operational Experiences and Issues from Mayor Wind Installations, Palo Alto, October 12-14, 1983
11. General Environmental Aspects, Munich, May 7-9, 1984
12. Aerodynamic Calculational Methods for WECS, Copenhagen, October 29-30, 1984
13. Economic Aspects of Wind Turbines, Petten, May 30-31, 1985
14. Modelling of Atomospheric Turbulence for Use in WECS Rotor Loading Calculation, Stockholm, December 4-5, 1985
15. General Planning and Environmental Issues of LS WECS Installations, Hamburg, December 2, 1987
16. Requirements for Safety Systems for LS WECS, Rome, October 17-18, 1988
17. Integrating Wind Turbines into Utility Power Systems, Herndon (Virginia), April 11-12, 1989
18. Noise Generationg Mechanisms for Wind Turbines, Petten, November 27-28, 1989
19. Wind Turbine Control Systems, Strategy and Problems, London, May 3-4, 1990
20. Wind characteristics of Relevance for Wind Turbine Design, Stockholm, March 7-8, 1991
21. Elektrical Systems for Wind Turbines with Constant or Variable Speed, Göteborg, October 7-8, 1991

22. Effects of Environment on Wind Turbine Safety and Performance, Wilhelmshaven, June 16, 1992
23. Fatigue of Wind Turbines, Golden (Colorado), October 15 - 16, 1992
24. Wind Conditions for Wind Turbine Design, RisÝ, April 29 - 30, 1993
25. Increased Loads in Wind Power Stations, "Wind Farms", Göteborg, May 3 - 4, 1993
26. Lightning Protection of Wind Turbine Generator Systems and EMC Problems in the Associated Control System Milan, March 8-9, 1994

Note: Nr. 26 to be published by Technical University of Denmark